

D3.2 – Safety precautions in train configuration and brake application

Planned date of deliverable: 30/06/2018

Submission date: 05/07/2018

Responsible of this Deliverable – Mats Berg, KTH

Reviewed: Y

Document status		
Revision	Date	Description
1	4/12/2017	Table of Contents
2	7/3/2018	Demonstrator part
3	6/6/2018	Longer train pneumatics (two locos)
4	21/6/2018	Final report for TMT review
5	4/7/2018	Final version approved by TMT and submitted on EC portal

Project funded from the European Union's Horizon 2020 research and innovation programme		
Dissemination Level		
PU	Public	X
CO	Confidential, restricted under conditions set out in Model Grant Agreement	
CI	Classified, information as referred to in Commission Decision 2001/844/EC	

Start date of project: 01/11/2016

Duration: 20 months

REPORT CONTRIBUTORS

Name	Company	Details of Contribution
Maria Marsilla and Rafael Gisbert	Stadler Rail Valencia	Link to Task 3.1 on traction and braking scenarios
Stefano Melzi	Politecnico di Milano (POLIMI)	Brake pneumatics simulations and analyses
Daniel Jobstfinke	Technische Universität Berlin (TUB)	1D longitudinal train dynamics simulations and analyses
Visakh V Krishna and Mats Berg	KTH Royal Institute of Technology (KTH)	3D analysis of derailment risk at longitudinal compressive forces and curves. General parts.
Andrea Demadonna	UNIFE	Quality check and submission

EXECUTIVE SUMMARY

In Europe operation of long freight trains, say up to 1500 m, is of interest to increase the transport capacity and cost efficiency. However, not using an electric wire along the freight train will generally result in traction and braking commands that are not synchronous for the different locomotives respectively vehicles. Together with heterogenous train configurations this can cause large longitudinal coupler forces which in turn can lead to train disruption or derailment.

This challenge is faced in DYNAFREIGHT WP3 together with WP5 of the member project FFL4E, and can be seen as a continuation of the EU project MARATHON. In the present work, Task 3.2, a methodology to analyse this issue has been formulated and extensive simulations have been carried out for two main applications, the first one being closely linked to a planned FFL4E demonstrator.

It is assumed from Task 3.1 that the locomotives of the freight trains are not physically coupled but are communicating via radio. This is the basis in the formulation of traction and braking scenarios, at nominal and degraded conditions, in Task 3.1 which has provided input to Task 3.2.

The braking pneumatics, 1D longitudinal dynamics (actual coupler forces) and 3D derailment analysis (tolerable coupler forces) are then key elements in the work of Task 3.2. For in particular long trains there are many possible heterogenities in the train configuration: wagon types, running gear design, coupler design, brake block material, brake rigging efficiency, brake regime, brake performance dependent on payload, actual payload and actual position of each wagon in the train. The second (third etc) locomotive can also be put in different positions. Further, the trains run at different (initial) speeds and negotiate different track layouts with gradients and horizontal curves.

This complex parameter space has been systematically analysed in Task 3.2 and the main safety precautions that should be taken in long-train operation are found as:

- Operation in very tight S-curves should be avoided
- Long and torsionally flexible wagons should be avoided
- Buffers with high energy dissipation should be chosen
- Empty wagons should be avoided, but if not possible they should be positioned at the end of the train and anyway not between two fully loaded wagons
- The brake performance of each wagon should be proportional to its weight, including the payload. Replacement of current load devices might be necessary.
- Introducing a third locomotive may mitigate the situation.
- Other actions to decrease, or ideally remove, the unsynchronous application of brake cylinder pressures of the train vehicles should be investigated.

Further work on long trains is foreseen in the upcoming Shift2Rail project FR8RAIL II.

ABBREVIATIONS AND ACRONYMS

Abbreviation etc	Description
1D	One-Dimensional
3D	Three-Dimensional
BC	Brake Cylinder
BP	Brake Pipe
CI	Cast Iron brake block
DBV	Distributor Brake Valve
DOF	Degree Of Freedom
DPS	Distributed Power System
FALNS	Wagon type
FFL4E	Future Freight Locomotives For Europe
G	Braking regime
K	Type of composite brake block
KSB	Type of buffer (Keystone)
LCF	Longitudinal Compressive Force
LL	Braking regime ("Long Locomotive")
LL	Type of composite brake block
LTD	Longitudinal Train Dynamics
LTF	Longitudinal Tensile Force
LTS	Longitudinal Train Simulator
MARATHON	MAke RAil The HOpe for protecting Nature
MBP	Main Braking Pipe
MBS	Multi-Body Simulation
P	Braking regime
QGO	Type of buffer (Also known as 4G)
SGGNSS	Wagon type
UIC	International Union of Railways

TABLE OF CONTENTS

Report Contributors	2
Executive Summary.....	3
Abbreviations and Acronyms	4
Table of Contents	5
List of Figures	9
List of Tables	15
1. Introduction.....	17
2. Methodology	19
2.1 Train configuration	19
2.2 Traction and braking scenarios	20
2.3 Pneumatics simulations	20
2.3.1 Model of the main braking pipe.....	20
2.3.2 Brake distributor model.....	24
2.3.3 Implementation of braking support logic	26
2.4 1D simulations (actual forces).....	26
2.4.1 General simulation setup.....	26
2.4.2 Vehicle models	27
2.4.3 Brake, resistance and friction models	28
2.4.4 Coupler model.....	32
2.4.5 Graphical representation	32
2.4.6 Result analysis	34
2.5 3D simulations (tolerable forces).....	36
2.5.1 UIC Code 530-2 Propelling test	36
2.5.2 Simulation methodology	38
2.5.3 Modelling	42
2.5.4 Buffer angle concept.....	44
2.6 Actual vs. tolerable forces	46
2.7 Conclusions and safety precautions.....	47
3. First application: Present-day coal train operation.....	48
3.1 Train configuration	48
3.2 Traction and braking scenarios	48

3.3 Pneumatics simulations	52
3.3.1 Nominal condition.....	54
3.3.2 Degraded condition	59
3.4 1D simulations (actual forces).....	67
3.5 3D simulations (tolerable forces): FALNS 121 & FALNS 183	72
3.5.1 Running gear: Link suspension bogie	73
3.5.2 Sensitivities of individual heterogeneities.....	74
3.5.3 Stochastic studies	82
3.6 Actual vs. Tolerable Forces.....	84
3.7 Conclusions and safety precautions.....	85
4. Second application: trains up to 1500 m long.....	86
4.1 Introduction.....	86
4.2 Pneumatics simulations	87
4.2.1 Train compositions and overall results.....	88
4.2.2 Results for scenario 202.....	95
4.2.3 Simulations with two slave locos.....	96
4.3 1D Simulations (Actual forces)	100
4.3.1 Modelling of the SGGNSS80 wagon.....	100
4.3.2 Methodology of the result analysis.....	100
4.3.3 Assessment of stopping distances.....	104
4.3.4 General trends of LCF and LTF results.....	105
4.3.5 LCF and LTF results of trains with random individual load statuses.....	107
4.3.6 Comparison of 1D simulations results with 3D limit values (SGGNSS)	110
4.3.7 Comparison of 1D simulations results with 3D limit values (FALNS).....	114
4.3.8 Simulations with two slave locomotives	118
4.3.9 Further analysis of simulation results with two slave locomotives	123
4.3.10 Stretch braking	125
4.4 3D SIMULATIONS (TOLERABLE FORCES).....	127
4.4.1 Flat wagons: SGGNSS80	127
4.4.2 Flat wagons - Tolerable LCF	128
4.4.3 FALNS121-SGGNNS80-FALNS121	131
4.4.4 SGGNSS80-FALNS121-SGGNNS80	134

4.4.5 Effect of adjacent wagons.....	135
4.5 Conclusions and precautions	136
5. Overall conclusions and safety precautions	138
References.....	140
Appendix A: Pneumatics validation.....	142
Model validation.....	142
Emergency braking	142
Maximum service braking	144
Venting of main braking pipe from different positions	145
Refilling of main braking pipe	146
Appendix B: Results of pneumatics for trains up to 1500 m	148
FALNS with two locos	148
FALNS 750 m, scenario 103	149
FALNS 750 m, scenario 106	151
FALNS 1000 m, scenario 103	152
FALNS 1000 m, scenario 106	153
FALNS 1250 m, scenario 103	155
FALNS 1250 m, scenario 106	156
FALNS 1500 m, scenario 103	157
FALNS 1500 m, scenario 106	159
SGGNSS with two locos	160
SGGNSS 750 m, scenario 103	161
SGGNSS 750 m, scenario 106	162
SGGNSS 1000 m, scenario 103	163
SGGNSS 1000 m, scenario 106	165
SGGNSS 1250 m, scenario 103	166
SGGNSS 1250 m, scenario 106	167
SGGNSS 1500 m, scenario 103	169
SGGNSS 1500 m, scenario 106	170
FALNS with three locos	171
FALNS 1000 m, scenario 103	172
FALNS 1000 m, scenario 106	172

FALNS 1250 m, scenario 103	172
FALNS 1250 m, scenario 106	173
FLANS 1500 m, scenario 103	173
FALNS 1500 m, scenario 106	173
SGGNSS with three locos.....	174
SGGNSS 1000 m, scenario 103	175
SGGNSS 1000 m, scenario 106	175
SGGNSS 1250 m, scenario 103	175
SGGNSS 1250 m, scenario 106	176
SGGNSS 1500 m, scenario 103	176
SGGNSS 1500 m, scenario 106	176
Appendix C: Comparison of 1D simulation results with limit values.....	177

LIST OF FIGURES

Figure 1: Flow chart of methodology for longitudinal train dynamics	19
Figure 2: Lumped parameter model of main braking pipe for a single vehicle.....	21
Figure 3: Model of the entire main braking pipe	21
Figure 4: Pressure drop in main braking pipe (a); corresponding pressure command signal to brake cylinder	25
Figure 5: Pressure build-up in brake cylinder.....	25
Figure 6: Interaction between the MATLAB tool and the MBS software	27
Figure 7: Topologies of the locomotive base model (left), wagon base model (middle) and coupler base model (right)	27
Figure 8: Exemplary characteristics of friction materials	29
Figure 9: Braked weight percentage, braked weight and stopping distance for FALNS 121 wagon with LL brake blocks and auto-continuous device	31
Figure 10: Braked weight percentage, braked weight and stopping distance for FALNS 121 wagon with cast iron brake blocks and manual load device.....	31
Figure 11: Exemplary hysteresis function for two buffers in series	32
Figure 12: Graphical representation of models	32
Figure 13: 1D multi-body oscillator.....	33
Figure 14: Schematic train path within the initial system	33
Figure 15: Exemplary standard result diagram.....	35
Figure 16: Exemplary parameter variation of total wagon mass.....	36
Figure 17: UIC 530-2 Track layout [10]	37
Figure 18: UIC-530-2 Train configuration [10].....	37
Figure 19: Simulation set-up in the GENSYS environment	39
Figure 20: Heterogeneities w.r.t. 3D simulations. Example: Demonstrator train case	40
Figure 21: Approaching heterogeneities in three-dimensional simulations	41
Figure 22: Simulation model in GENSYS for 3D derailment analysis	42
Figure 23: Torsionally flexible carbody in GENSYS	43
Figure 24: Transition function for points in between loading and unloading [12].....	44
Figure 25: Coupler angle calculation [17].....	45
Figure 26: Coupler angles through an S-curve.....	45
Figure 27: Coupler angles through circular curve.....	46
Figure 28: FALNS wagons for coal train operation in Germany [18].....	48

Figure 29: Time histories of pressure in main braking pipe (a) and braking cylinders (b) for scenario 101	54
Figure 30: Pressure in main braking pipe (a) and braking cylinders (b) as function of time and wagon position for scenario 101.....	55
Figure 31: Time histories of pressure in main braking pipe (a) and braking cylinders (b) for scenario 102	55
Figure 32: Time histories of pressure in main braking pipe (a) and braking cylinders for scenario 103	56
Figure 33: Time histories of pressure in main braking pipe (a) and braking cylinders for scenario 104.....	57
Figure 34: Pressure in main braking pipe as function of time and wagon position for scenario 101 (a) and 104 (b)	57
Figure 35: Pressure braking cylinders as function of time and wagon position for scenario 101 (a) and 104 (b)	58
Figure 36: Time histories of pressure in main braking pipe (a) and braking cylinders (b) for scenario 105	58
Figure 37: Time histories of pressure in main braking pipe (a) and braking cylinders for scenario 106	59
Figure 38: Time histories of pressure in main braking pipe (a) and braking cylinders (b) for scenario 202	60
Figure 39: Time histories of pressure in main braking pipe (a) and braking cylinders (b) for scenario 203	61
Figure 40: Time histories of pressure in main braking pipe (a) and braking cylinders (b) for scenario 204	61
Figure 41: Time histories of pressure in main braking pipe (a) and braking cylinders (b) for scenario 205	62
Figure 42: Time histories of pressure in main braking pipe (a) and braking cylinders (b) for scenario 206	63
Figure 43: Time histories of pressure in main braking pipe (a) and braking cylinders (b) for scenario 206 assuming maximum service braking from the slave loco.....	64
Figure 44: Time histories of pressure in main braking pipe (a) and braking cylinders (b) for scenario 207; no reaction from master loco.....	65
Figure 45: Pressure in main braking pipe (a) and braking cylinders (b) as function of time and wagon position for scenario 207; no reaction from master loco.....	65
Figure 46: Time histories of pressure in main braking pipe (a) and braking cylinders (b) for scenario 207; maximum service brake applied by master loco.....	66
Figure 47: Time histories of pressure in main braking pipe (a) and braking cylinders (b) for scenario 207; emergency brake applied by master loco.....	66

Figure 48: Dependency of LCF on traction behaviour in scenario 202	68
Figure 49: Procedure of parameter variations for scenario 202.....	69
Figure 50: Trains taken from simulation in scenario 202 for simulation in other scenarios (indicated with red dots)	70
Figure 51: LCF values for nominal and varied trains in selected scenarios	71
Figure 52: Influence of gradients on LCF values.....	71
Figure 53: Wagon key geometry parameters [10]	73
Figure 54: Bogie-type 665 [21].....	73
Figure 55: Simulation cases and nomenclature. Fill and no-fill indicate fully loaded and empty cases respectively.....	74
Figure 56: Tolerable LCF values: Comparison for different buffers, wagon arrangements and payload	75
Figure 57: Tolerable LCF values: Comparison between curvatures (QGO buffer)	77
Figure 58: Tolerable LCF values: Comparison between gradients (QGO buffer)	78
Figure 59: Comparison of Tolerable LCF between rigid and torsionally flexible wagon cases w.r.t maximum coupler angle (φ_{12max}): Red: rigid; Blue: flexible; Dashed line: S190M10; Solid line: S150M10.....	80
Figure 60: Tolerable LCF vs. buffer angle difference trends for m1e1 and m0e0 configurations. Buffer 1- QGO; Buffer 2- KSB	81
Figure 61: Tolerable LCF vs. buffer angle difference trends for mixed wagon configurations (m0e1 and m1e0).....	81
Figure 62: Heterogeneities covered in stochastic simulations. (F- Fully loaded, H- Half loaded and E- Empty wagon)	83
Figure 63: Results: Stochastic investigation sorted by payload distribution.....	83
Figure 64: Actual vs. Tolerable forces - Demonstrator train	84
Figure 65: Schematic of a train with two locos	88
Figure 66: Time required to complete a pressure drop of at least 1.5 bar in MBP in all wagons [s]; trains with FALNS wagons.	92
Figure 67: Time required to reach at least 99% of maximum pressure in braking cylinders of all wagons [s]; trains with FALNS wagons.	93
Figure 68: Time required to complete a pressure drop of at least 1.5 bar in MBP in all wagons [s]; trains with SGGNSS wagons.	94
Figure 69: Time required to reach at least 99% of maximum pressure in braking cylinders of all wagons [s]; trains with SGGNSS wagons.....	95

Figure 70: 750m-long train (SGGNSS), slave loco 25%, scenario 202. Time histories of pressure drop in the main braking pipe (a); time history of pressure gradient in the main braking pipe for the slave loco (b)	96
Figure 71: Schematic of a train with three locos.....	97
Figure 72: 1000 m FALNS train with one slave loco: time histories of pressure drop in MBP and pressure build-up in BC for the slowest and fastest wagon (a); time required to obtain a pressure drop of 1.5 bar in MBP and to reach 99% of maximum pressure in BC.	98
Figure 73: 1000 m FALNS train with two slave locos: time histories of pressure drop in MBP and pressure build-up in BC for the slowest and fastest wagon (a); time required to obtain a pressure drop of 1.5 bar in MBP and to reach 99% of maximum pressure in BC.	99
Figure 74: FALNS wagons: time required to complete a pressure drop of 1.5 bar in MBP and time required to reach 99% of the maximum pressure in BC (b).....	99
Figure 75: SGGNNS wagons: time required to copmlete a pressure drop of 1.5 bar in MBP and time required to reach 99% of the maximum pressure in BC (b).	100
Figure 76: Exemplary LCF analysis - method 1	101
Figure 78: Exemplary LCF analysis – method 2.....	103
Figure 78: Stopping distances from 100 km/h in cases 103 and 106	104
Figure 79: Maximum LCF values vs. total train mass.....	105
Figure 80: Maximum LCF values for FALNS trains	106
Figure 81: Maximum LCF values for SGGNSS trains	107
Figure 82: LCF values of mass and buffer/draw gear variations for the SGGNSS train.....	108
Figure 83: LTF values of mass and buffer/draw gear variations for the SGGNSS train	109
Figure 85: LCF/LTF values of 1000 m SGGNSS train with 220 m S-curve radius and without empty wagon in loaded trains	111
Figure 86: LCF/LTF values of 1250 m SGGNSS train with 220 m S-curve radius and without empty wagon in loaded trains	112
Figure 87: LCF/LTF values of 1000 m SGGNSS train with 190 m S-curve radius and empty wagon in loaded trains	113
Figure 88: LCF/LTF values of 1000 m FALNS train with 220 m S-curve radius and no empty wagon in loaded trains	115
Figure 89: LCF/LTF values of 1250 m FALNS train with 220 m S-curve radius and no empty wagon in loaded trains	116
Figure 90: LCF/LTF values of 1000 m FALNS train with 190 m S-curve radius and empty wagon in loaded trains	117
Figure 91: LCF/LTF values of 1000 m SGGNSS train with two slave locomotives, 220 m S-curve radius and empty wagon in loaded trains	119

Figure 92: LCF/LTF values of 1000 m FALNS train with two slave locomotives, 220 m S-curve radius and empty wagon in loaded trains	120
Figure 93: LCF/LTF values of 1250 m FALNS train with two slave locomotives, 220 m S-curve radius and without empty wagon in loaded trains	121
Figure 94: LCF/LTF values of 1500 m FALNS train with two slave locomotives, 220 m S-curve radius and without empty wagon in loaded trains	122
Figure 94: MBP pressure, brake cylinder pressure, and LCF values for 1000 m FALNS train with two slave locomotives in case 103	123
Figure 95: MBP pressure, brake cylinder pressure, and LCF values for 1000 m FALNS train with two slave locomotives in case 106	124
Figure 96: Primitive model of the train with two different load statuses of the front and the rear part	124
Figure 97: Emergency brake application of a 750 m FALNS train with load status “half-loaded” and an initial velocity of 30 km/h	126
Figure 98: Emergency brake application of a 750 m FALNS train with load status “half-loaded” and an initial velocity of 30 km/h with ‘stretch braking’	127
Figure 99: SGGNSS80 [22]	128
Figure 100: Simulation model for SGGNSS80	129
Figure 101: Heterogeneity (Barrier wagons: FALNS121)	131
Figure 102: Heterogeneity (Barrier wagons: SGGNSS80)	134
Figure 103: Tolerable LCF: Combination of contrasting wagon classes	136
Figure 104: 500m-long train, emergency braking; (a): time histories of pressure drop in the main braking pipe and pressure build-up in the braking cylinders for first and last vehicle; (b) time histories of pressure build-up in 9 braking cylinders along the train.....	142
Figure 105: 750m-long train, emergency braking; (a): time histories of pressure drop in the main braking pipe and pressure build-up in the braking cylinders for first and last vehicle; (b) time histories of pressure build-up in 9 braking cylinders along the train.....	143
Figure 106: 1000m-long train, emergency braking; (a): time histories of pressure drop in the main braking pipe and pressure build-up in the braking cylinders for first and last vehicle; (b) time histories of pressure build-up in 9 braking cylinders along the train.....	143
Figure 107: 1200m-long train, emergency braking; (a): time histories of pressure drop in the main braking pipe and pressure build-up in the braking cylinders for first and last vehicle; (b) time histories of pressure build-up in 9 braking cylinders along the train.....	144
Figure 108: 500m-long train, maximum service braking; (a): time histories of pressure drop in the main braking pipe and pressure build-up in the braking cylinders for first and last vehicle; (b) time histories of pressure build-up in 9 braking cylinders along the train.....	144

- Figure 109: 1000m-long train, maximum service braking; (a): time histories of pressure drop in the main braking pipe and pressure build-up in the braking cylinders for first and last vehicle; (b) time histories of pressure build-up in 9 braking cylinders along the train.....145
- Figure 110: 1500m-long train, maximum service braking commanded by two locos; (a): time histories of pressure DBV controls; (b) time histories of pressure drop in MBP in several positions along the train.....146
- Figure 111: 1500m-long train, refilling of the braking pipe; (a): time histories of pressure DBV controls; (b) time histories of pressure drop in MBP in several positions along the train..147

LIST OF TABLES

Table 1: Track design parameters	44
Table 2: Nominal Scenarios - Demonstrator cases	50
Table 3: Degraded Scenarios - Demonstrator cases	51
Table 4: Scenarios involving pneumatic braking for nominal condition.....	52
Table 5: Scenarios involving pneumatic braking for degraded condition	53
Table 6: Results for nominal condition of the 530 m long train	67
Table 7: Results for degraded condition of the 530 m long train	67
Table 8: Summary of results for altered versions of scenario 202	68
Table 9: Bogie pivot length, Buffer to Buffer distance and Buffer length of the two wagons	72
Table 10: Tolerable LCF values: Comparison for different buffers, wagon arrangements and payloads (S150M6)	75
Table 11: Tolerable LCF values: Comparison between curvatures (QGO buffer).....	76
Table 12: Tolerable LCF values: Comparison between gradients (QGO buffer).....	77
Table 13: Tolerable LCF values for critically loaded cases with torsionally flexible carbodies ...	79
Table 14: Tolerable LCF values for nominally loaded cases with torsionally flexible carbodies .	79
Table 15: Comparing Tolerable LCF values of rigid and torsionally flexible carbody cases (Cases 2 and 3 are FALNS183 and FALNS121 respectively)	80
Table 16: Derailment mode examination.....	82
Table 17: Parameters considered for simulations of trains longer than 500 m operating with two locos. (f= fully loaded, h= half loaded, e= empty)	87
Table 18: Train compositions for trains with FALNS wagons	89
Table 19: Train compositions for trains with SGGNSS wagons.....	90
Table 20: Time required to complete a pressure drop of at least 1.5 bar in MBP in all wagons [s]; trains with FALNS wagons.	91
Table 21: Time required to reach at least 99% of maximum pressure in braking cylinders of all wagons [s]; trains with FALNS wagons.	92
Table 22: Time required to complete a pressure drop of at least 1.5 bar in MBP in all wagons [s]; trains with SGGNSS wagons.	93
Table 23: Time required to reach at least 99% of maximum pressure in the braking cylinders of all wagons [s]; trains with SGGNSS wagons.	94
Table 24: Parameter considered for simulations of trains longer than 750 m operating with three locos. f= fully loaded, h= half loaded, e= empty.....	96
Table 25: Train compositions for trains with FALNS wagons.	97

Table 26: Train compositions for trains with SGGNSS wagons.....	97
Table 27: SGGNSS80 attributes	128
Table 28: Tolerable LCF for critically loaded wagon cases with QGO buffers (SGGNSS80x3).....	129
Table 29: Tolerable LCF for critically loaded wagon cases with Keystone buffers (SGGNSS80x3)	130
Table 30: Tolerable LCF for nominally loaded wagon cases with QGO buffers (SGGNSS80x3)	130
Table 31: Tolerable LCF for nominally loaded wagon cases with Keystone buffers (SGGNSS80x3)	131
Table 32: Tolerable LCF for critically loaded wagon cases with QGO buffers (FALNS121-SGGNSS80-FALNS121).....	132
Table 33: Tolerable LCF for critically loaded wagon cases with Keystone buffers (FALNS121-SGGNSS80-FALNS121).....	132
Table 34: Tolerable LCF for nominally loaded wagon cases with QGO buffers (FALNS121-SGGNSS80-FALNS121).....	133
Table 35: Tolerable LCF for nominally loaded wagon cases with Keystone buffers (FALNS121-SGGNSS80-FALNS121).....	133
Table 36: Tolerable LCF for critically loaded wagon cases with QGO buffers (SGGNSS80-FALNS121-SGGNSS80).....	134
Table 37: Tolerable LCF for nominally loaded wagon cases with QGO buffers (SGGNSS80-FALNS121-SGGNSS80).....	135

1. INTRODUCTION

For extensive rail freight transportation, one action to improve its capacity and efficiency is to run long trains. From an European perspective this typically means running freight trains longer than 800-900 m. However, there are technical challenges associated with long-train operation.

During traction (acceleration) the longitudinal tensile coupler forces can be significant, in particular if all locomotives are positioned in the front of the train. This might cause coupler breakage and thus loss of train integrity and safety risks.

During braking (retardation) the longitudinal compressive coupler forces can become very large, especially when the braking is applied only from the front and when the braking signal is propagating slowly by the pneumatics through the main braking pipe. This issue is further emphasized when payload-dependent braking devices of the wagons do not fully match the payloads in question and when the brake blocks are of different materials. The large compressive forces may cause derailment when the train negotiates curves, in particular tight S-curves with radii such as 150 m, 170 m, etc.

DYNAFREIGHT WP3 is devoted to different aspects of operation of long freight trains. In particular Task 3.1 and the present task, Task 3.2, are closely related assuming that the locomotives of the trains are not physically connected but use radio communication. It is also assumed that the traditional (P) UIC braking pneumatic system is used, thus electrically controlled pneumatic (ECP) braking is not introduced. Moreover, all couplers are assumed to consist of side buffers and central screw couplers.

The work in these two DYNAFREIGHT tasks is carried out in collaboration with that of WP5 in the Shift2Rail member project Future Freight Locomotive for Europe (FFL4E). This joint work can be seen as a continuation of the work in the European project MARATHON [1], in which some of the DYNAFREIGHT WP3 partners participated.

Given the specifications defined in Task 3.1 of radio communication and traction&braking scenarios of long-train operation, the objective of Task 3.2 is to address the challenges indicated above and provide safety precautions when operating long freight trains. The Task 3.2 work rests on simulations, verified by measurements, and are split in three parts: braking pneumatics, 1D longitudinal dynamics and 3D derailment risk analysis. The pneumatics result is an important input to the 1D simulations, whose result in terms of longitudinal compressive forces (LCFs) is compared with tolerable LCFs found in the 3D analysis.

In this D3.2 report Chapter 2 describes in more detail the simulation methodology adopted, the simulation tools that have been further developed and some verifications against measurements. The first application, suggested by the FFL4E WP5 partners and consisting of an existing coal train operation with two locomotives (front+rear), is then simulated in Chapter 3. In Chapter 4 longer and more heterogeneous freight trains are

studied with the second locomotive at different positions. Some simulations have also been carried out with three locomotives assuming that the second and third locomotives give identical traction/braking commands, see Chapter 4.

Last but not least, Chapter 5 gives guidelines for long-train operation with respect to safety precautions in train configurations (locomotive positions, wagon types, coupler performance, brake block material, payloads), traction and braking scenarios, and track layout (gradients, horizontal curves).

2. METHODOLOGY

Investigations of safety risks of long-train operation involve many input parameters, even if restricted to train integrity and derailment as indicated in the previous chapter. The present methodology is illustrated in Figure 1 and is explained in more detail in this chapter.

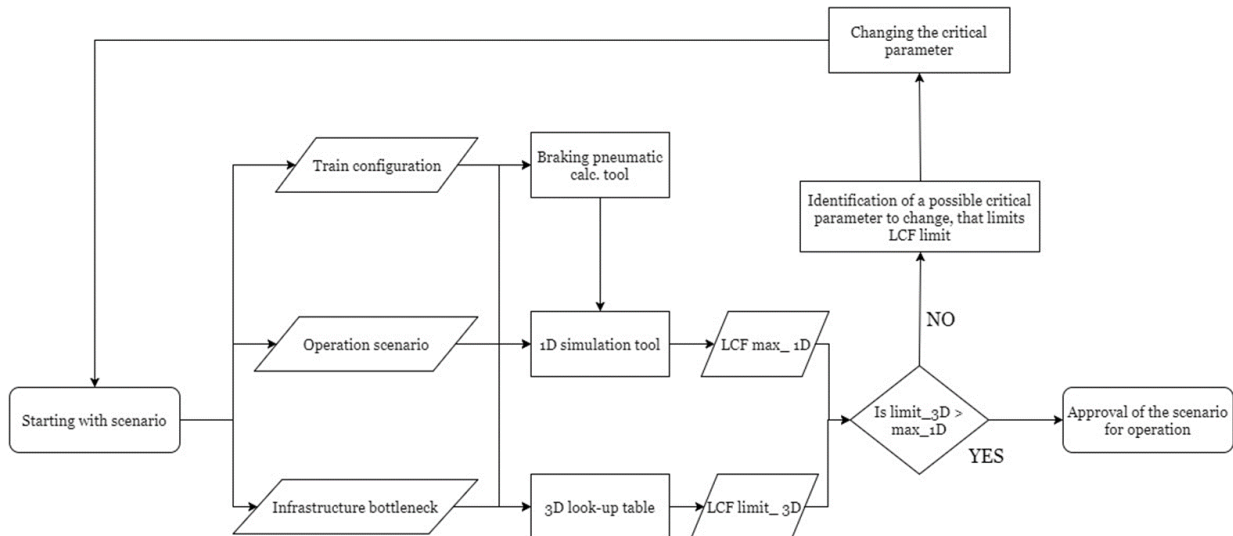


Figure 1: Flow chart of methodology for longitudinal train dynamics

2.1 TRAIN CONFIGURATION

In general a long freight train consists of many wagon types with litera such as FALNS, Hbis, Oms etc. For each litera there are still parameters that vary, mainly:

- Wagon length and tare weight
- Running gear design
- Coupler design (buffer and draw gear, incl. plays)
- Brake block material
- Brake rigging efficiency
- Brake regime (G, P, etc)
- Brake performance dependent on payload
- Actual payload (in tonnes)
- Actual position in train.

Although the locomotives of the train are usually of the type, the position of the second (etc) locomotive is generally not in the front of the train.

In all, long freight trains can be configured in millions of ways and the safety risk significantly depends on the actual train configuration.

In the present work extensive parameter studies have been done to identify the most important parameters so as to reduce the number of train configurations in each application. The methodology is developed by starting with a fairly homogenous train configuration and then going towards more heterogeneous configurations, including trains of up to 1,500 m in length.

2.2 TRACTION AND BRAKING SCENARIOS

For a given train configuration, the next question is how the train operates. The train speed is important but in the present context the applied traction/braking is even more important since the longitudinal train dynamics is in focus here.

DYNAFREIGHT Task 3.1 and Task 3.2 together with FFL4E partners have studied various traction and braking scenarios of long freight trains assuming that the first (master) loco gives commands to the second (slave) loco through radio communication. The Task 3.1 work is documented in Deliverable D3.1 [2]. Two sets of scenarios can be distinguished (see Table 2 and Table 3):

- Nominal condition (the radio communication is working properly)
- Degraded condition (radio communication is lost for a number of seconds)

The scenarios will greatly influence the traction/braking force time histories, including the timing of the force applications between different vehicles of the train in question.

The braking forces are also largely dependent on the pneumatics performance of the train and the friction forces induced at the wheel tread – brake block interface. The braking pneumatics methodology is described in the section below, followed by 1D longitudinal dynamics (actual coupler forces) and 3D derailment analysis (tolerable compressive coupler forces).

2.3 PNEUMATICS SIMULATIONS

2.3.1 Model of the main braking pipe

The brake model developed by POLIMI to describe the dynamics of compressed air inside the main braking pipe, is a lumped parameter model; the main braking pipe (MBP) is divided into several sections, each one characterized by an equivalent electric scheme. For validation details, refer Appendix A. According to this model, fluid internal friction is reproduced by resistance elements, fluid mass is represented through inductance elements and fluid compressibility is modelled with the capacitance elements. Figure 2 shows the scheme used to discretize the main braking pipe of a single vehicle.

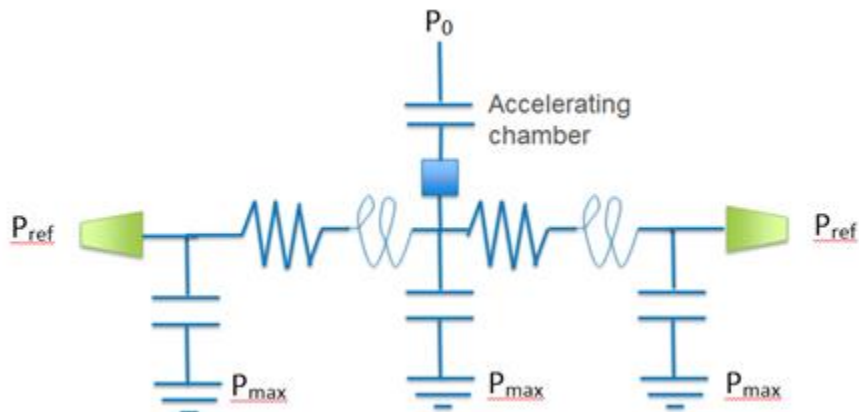


Figure 2: Lumped parameter model of main braking pipe for a single vehicle.

As presented in Figure 2, the MBP of the single vehicle is divided into two sections. The pipe presents also two openings at the extremities allowing venting of the pipe itself; a boundary condition P_{ref} is imposed at the pipe extremities to simulate venting or refilling of the pipe itself. P_{max} represents the nominal pressure inside MBP when braking is not applied and P_0 is the atmospheric pressure (1 bar, absolute).

Each vehicle is also characterized by an accelerating chamber, an element of the brake distributor which is supposed to be at the centre of the vehicle.

When several vehicles are joined together, the model of the MBP is simply derived by connecting in series several models of the same kind. As shown in Figure 3, the pipe can be vented at the extremities or in a generic position along the trainset. $P_{ref,i}(t)$ are boundary conditions, function of time, that can be applied to the model to simulate venting or refilling of the main braking pipe.

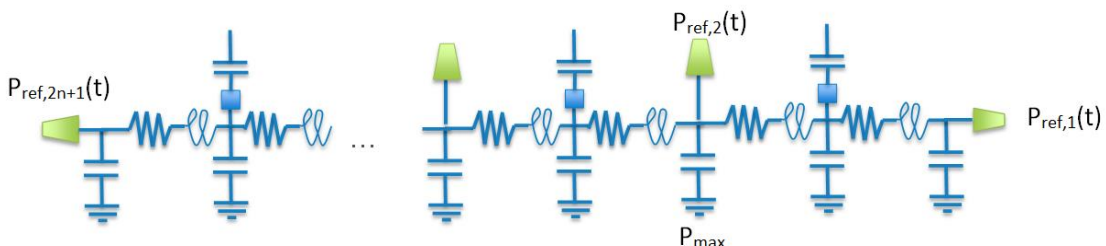


Figure 3: Model of the entire main braking pipe

Each venting valve is characterized by a reference pressure determined by the corresponding DBV control. Different reference pressure values could be thus defined; this allows for example to perform an emergency braking from the train head and a

simultaneous maximum service braking commanded by a second loco in a different position along the train. It is also possible to perform re-filling of the MBP from one point and a simultaneous emergency braking from another, to simulate a possible malfunction of the remote controls.

Altogether, the equivalent electrical circuit for n vehicles is characterized by $2n+1$ unknowns represented by the pressures in the nodal points. A system of $2n+1$ non-linear differential second-order equations can be implemented and solved numerically to determine the time histories of pressures at nodal points.

Values for lumped parameter model

Resistance

The resistance of the equivalent electric circuit is representing the internal friction of the fluid. The resistance of a section of the main braking pipe was estimated according to the model proposed in [3]. In particular, the pressure drop across a segment of pipe of length l is given by:

$$\Delta p = \lambda \rho \frac{w^2}{2} \frac{l}{D} \quad (1)$$

where

- λ is the dimensionless friction coefficient;
- w is the fluid average speed (1D flow);
- ρ is the fluid density;
- D is the pipe diameter.

The fluid average speed is related to the mass flow-rate G by:

$$G = \rho \frac{\pi D^2}{4} \cdot w \quad (2)$$

The fluid speed is thus given by:

$$w = \frac{1}{\rho} \frac{4G}{\pi D^2} \quad (3)$$

Combining Equation (1) with Equation (3), the pressure drop across the section of the main braking pipe can thus be expressed as function of the volumetric flow rate as:

$$\Delta p = \lambda \frac{\rho L}{2D} \frac{16}{\rho^2 \pi^2 D^4} G^2 = \lambda \frac{8l}{\rho \pi^2 D^5} G^2 \quad (4)$$

The dimensionless friction coefficient λ is a function of the Reynolds number Re :

$$Re = \frac{4G}{\pi D \mu} \quad (5)$$

The air viscosity μ is estimated using the empirical relationship:

$$\mu = \left(1.84 - \frac{300 - T}{300} \right) \cdot 10^{-5} \quad (6)$$

with T in K. Dependence of λ from Re can be expressed through the following formula:

$$\lambda = \frac{1}{\left(2 \log \left(0.5625 Re^{\frac{7}{8}} \right) - 0.8 \right)} \quad (7)$$

The pressure drop across a section of the pipe is thus a function of the fluid density and the mass flow-rate:

$$\Delta p = R(\rho) G^2 \quad (8)$$

where $R(\rho)$ represents the fluid resistance. The value of I used for computing resistance takes into account the length of the vehicle, adding up the length of connections between adjacent vehicles and increasing the value by 7.5% to consider additional resistances due to pipe bends and concentrated pressure losses.

The fluid density ρ is a function of the density ρ_N measured at standard conditions (ANR).

$$\rho = \rho_N \frac{P}{P_N} \frac{T_N}{T} \quad (9)$$

T_N and P_N respectively represent the temperature and pressure at standard conditions. While integrating the equations of main braking pipe, the value of resistance is thus updated at each integration step to consider variation of density.

Inductance

The inductances are used to represent the inertial effects of compressed air. The value of inductance L is simply given by:

$$L = \frac{4l}{\pi D^2} \quad (10)$$

Capacitance

The capacitance is introduced to model the fluid elasticity. The overall capacitance of a vehicle is obtained as:

$$C = \frac{\pi D^2 l}{4} \frac{1}{\hat{R}T} \quad (11)$$

where \hat{R} is the universal gas constant and T is the temperature. Again, the values of capacitances are updated at each integration step as local temperature changes with pressure. The capacitance of the vehicle is distributed over three capacitances (Figure 2); in particular 50% of the total capacitance is assigned to the central capacitor. The remaining 50% is equally divided between the capacitor at the vehicle's extremities.

Venting of main braking pipe

Simulation of venting of the main braking pipe is performed creating a connection between the pipe and a volume at a reference pressure p_{ref} opening one or more nozzles along the pipe. The area of the nozzles depends on the braking maneuver, i.e. larger for emergency braking and smaller for a maximum service braking. Transition of flux from sonic to subsonic is considered when venting the main braking pipe as well as when accelerating chambers activate.

In a similar way it is possible to re-fill the main braking pipe setting as boundary condition, for one or more nozzles, a pressure higher than the one inside the main braking pipe.

2.3.2 Brake distributor model

The model for the brake distributor takes as input the pressure drop in the main braking pipe between in the range 0-1.5 bar. When a pressure drop of 1.5 bar is reached, the braking cylinder develops the maximum braking force.

Figure 4a shows a time history of the pressure in the main braking pipe; Figure 4b plots the corresponding pressure drop with a saturation at 1.5 bar.

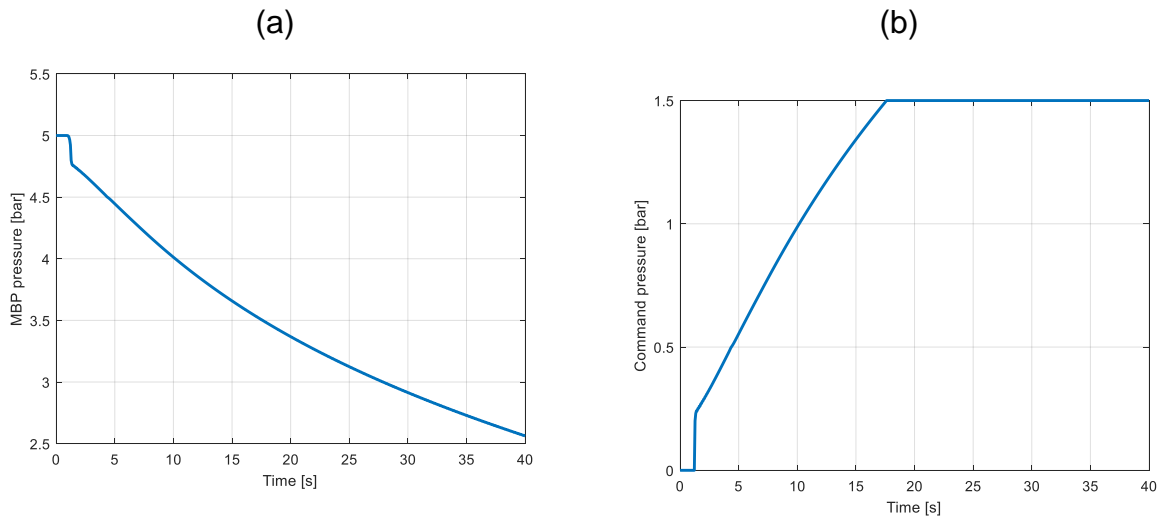


Figure 4: Pressure drop in main braking pipe (a); corresponding pressure command signal to brake cylinder

The signal reported in Figure 4b represents the “command” signal for the brake cylinder. This signal is processed considering the crossing of thresholds associated with the intervention of the first time device, which speeds up the filling of cylinders in the first part of the braking (Figure 5). Once the first time device intervention ends, the pressure build-up follows the gradient associated with the braking regime (P or G) up to a value determined by the pressure drop in the main braking pipe. With a pressure drop of 1.5 bar, the air in the cylinder reaches the maximum pressure and the cylinder will develop the maximum braking force.

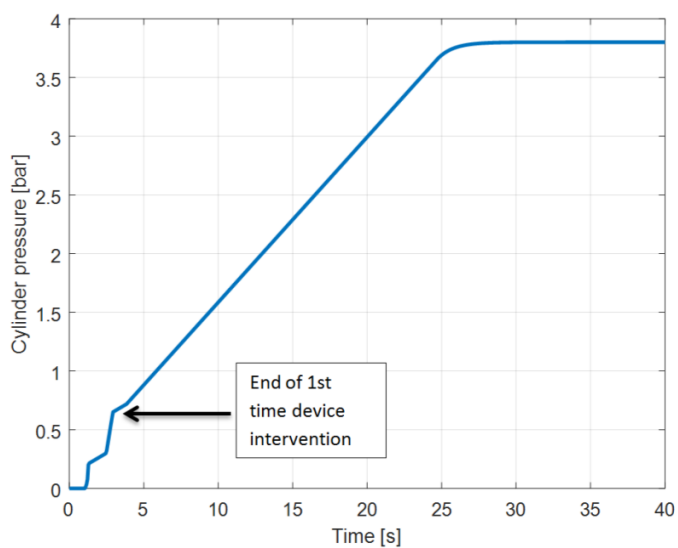


Figure 5: Pressure build-up in brake cylinder.

Accelerating chambers

The accelerating chambers are modelled with a volume of precise value (the volume of accelerating chambers is one of the model inputs) where the nominal pressure is equal to the atmospheric one (P_0) when braking is not activated. As braking is commanded and the pressure inside MBP starts to drop, the nozzles between the main braking pipe and the accelerating chambers are opened and air flows inside their volumes.

2.3.3 Implementation of braking support logic

During the DYNAFREIGHT project, Faiveley Transport (partner of FFL4E) proposed a control logic for the slave loco, allowing to support venting of the main braking pipe in case of radio communication loss. Under normal operating condition, when emergency (or maximum service) braking is commanded by the master loco, the same command is activated by the slave loco(s) given the delay associated with radio transmission. When the radio communication fails and a braking manouevre is commanded by the master loco, the main braking pipe is used to convey the information to the slave loco(s).

According to the control logic developed by Faiveley Transport, the slave loco supports the venting of the main braking pipe according to the following steps;

1. The remote DBV on slave detects a 200 mbar pressure delta drop in 500ms
2. The remote DBV discharges the brake pipe to 4.2bar, applying 0.2bar/s pressure gradient
3. The remote DBV brings BP to 4.2 bar and continues to discharge the BP for 10-15 s. After that Remote DBV is isolated from BP
4. The Remote DBV continues to monitor pressure in the BP
5. If remote DBV detects a further pressure drop of 200 mbar in 500 ms, discharges again the BP to 3 bar (FS brake), applying a 0.2 bar/s pressure gradient and continues to discharge the BP for 10-15 s with BP pressure already achieved 3 bar; then remote DBV is isolated from BP.

This logic was implemented in the present brake model.

2.4 1D SIMULATIONS (ACTUAL FORCES)

2.4.1 General simulation setup

The 1D simulation tool developed by TUB is based on a commercial multi-body simulation (MBS) software (SIMPACK) and a MATLAB tool. The MBS software is used to solve the equations of motion of the 1D train model. The MATLAB tool is used for simulation setup, simulation control, and result evaluation. Figure 6 shows the interaction between the MBS software and the MATLAB tool.

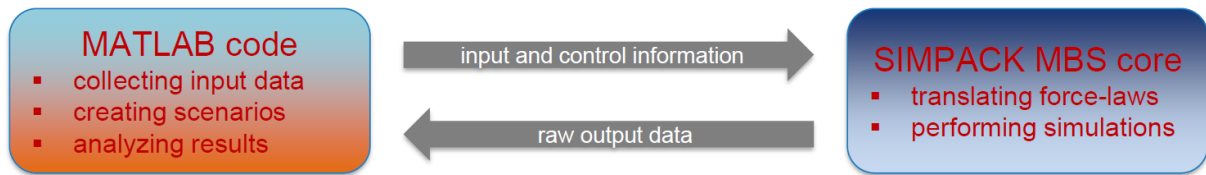


Figure 6: Interaction between the MATLAB tool and the MBS software

2.4.2 Vehicle models

The train model consists of three different base model types. One base model represents a locomotive, the second one a wagon and the third one a standard screw coupler with side buffers. Figure 7 shows the topologies of all three base models.

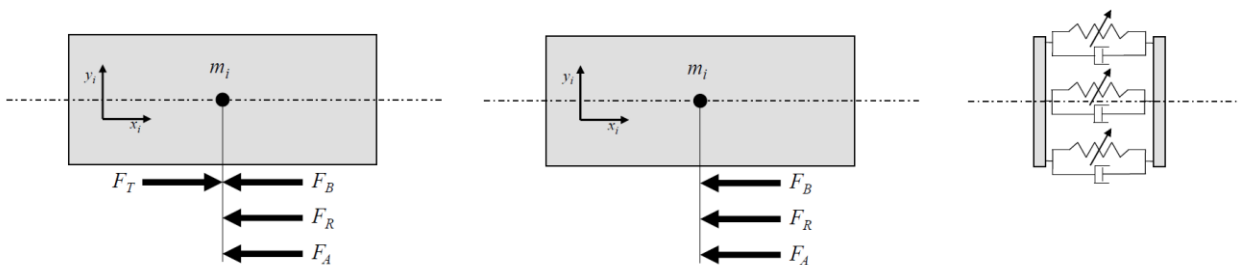


Figure 7: Topologies of the locomotive base model (left), wagon base model (middle) and coupler base model (right)

The locomotive base model consists of one mass m , one force element for traction and regenerative braking F_T , one force element for the friction brake F_B , one force element for rolling resistance F_R , and one force element for aerodynamic resistance F_A . The model does not include any rotational components such as wheelsets or traction motors. However, the kinetic energy of the rotational motion of such elements is added to the longitudinal motion of the locomotive by making use of the following formula:

$$\rho = 1 + \frac{\sum_i \frac{J_i}{r^2}}{m} \quad (12)$$

where ρ is a factor to be multiplied with the total mass m of a vehicle, J_i are the mass moments of inertia of rotating components and r is the wheel radius of a vehicle.

The force element for traction and regenerative braking F_T makes use of the traction force and regenerative braking force characteristic of a locomotive. It takes current speed v , desired relative tractive force (0 to 100%) and adhesion condition as input and applies the available tractive effort. The adhesion condition between wheel and rail can be modelled with either a constant coefficient of adhesion μ or a velocity dependent adhesion law $\mu(v)$ (Curtius-Kniffler):

$$\mu(v) = 0.161 + \frac{27}{v + 158.4} \quad (13)$$

The locomotive models have a mechanism for traction cut-off when the pneumatic brake is applied. The mechanism is activated when a certain pressure drop in the main brake pipe of the locomotive is detected. The tractive effort is then linearly ramped down to zero within one second.

2.4.3 Brake, resistance and friction models

The force element for the friction brake F_B takes the brake cylinder pressure, the maximum normal tread force, the friction material/braking system and the number of brake blocks/brake discs per vehicle as input. The well-known Karwatzki-law is used to determine the effective friction coefficient between brake block and wheel if the vehicle is equipped with cast-iron brake blocks.

A similar law is used for LL brake blocks. This law was determined with measured friction coefficients for the IB116* brake block for 20 and 60 kN tread normal force per wheel. It should be noted that the LL friction law takes the normal tread force per wheel as input whereas the cast-iron friction law takes the normal tread force per brake block as input. Furthermore, it should be noted that the LL friction law considers a linear interpolation of normal forces due to measurement limitations of only two different normal force values being available. This is inconsistent with the supposed nonlinear dependency. However, the two available normal force values are the minimum ('empty' load status / empty wagon) and maximum ('full' load status / 65 % of total mass or above). These conditions are therefore considered as correctly represented. Intermediate loading conditions between the empty wagon and 65 % of total mass in combination with an auto-continuous device may differ. Refer to equation (17).

The friction law for K brake blocks was determined by a similar method as the one for LL blocks. As there were no measured characteristics available, average required values from UIC 541-4 [4] /EN16452 [5] were taken. In case of a disc brake, a constant friction value of 0.37 is taken in accordance to UIC 541-3 [6]. Figure 8 shows exemplary characteristics of different friction materials.

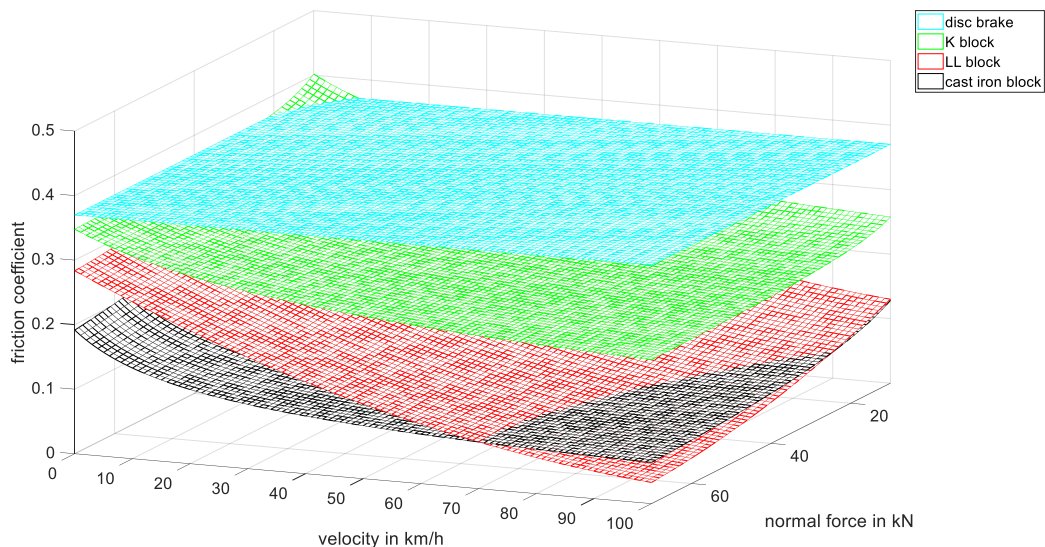


Figure 8: Exemplary characteristics of friction materials

The force element for the rolling resistance F_R makes use of the following formula:

$$F_R = c_R mg \quad (14)$$

where c_R is a vehicle specific coefficient and depends on vehicle type and load status.

The force element for the aerodynamic resistance F_A makes use of the following formula:

$$F_A = c_L (v + v_0)^2 \quad (15)$$

with

$$c_L = 0.5 \cdot c_w A_{nom} \rho_{air} \quad (16)$$

where v_0 is the speed of head wind, c_w is the vehicle specific drag coefficient, A_{nom} is the standard cross-sectional area of a vehicle (10 m^2) and ρ_{air} is the density of air.

The base model of the wagon is very similar to the locomotive model and only misses the force element for traction and regenerative braking. The force element for the friction brake includes the functionality of empty-loaded devices, both manual and auto-continuous ones. In the case of manual empty-loaded devices, the maximum normal tread force is determined by the following formula:

$$F_{B,max} = \begin{cases} F_{B,empty} & , if m < m_{switch} \\ F_{B,laden} & , if m \geq m_{switch} \end{cases} \quad (17)$$

where m_{switch} is the total mass of the wagon where the load status of the vehicle has to be changed. In case of the auto-continuous device, the braked weight percentage of the wagon varies according to [7]. This means that the maximum normal tread force rises proportionally with the mass of the wagon until 65% of the total wagon mass is reached. After this point, the maximum normal tread force stays constant:

$$F_{B,max} = \begin{cases} am + b & , if m < 0.65 m_{max} \\ F_{B,laden} & , if m \geq 0.65 m_{max} \end{cases} \quad (18)$$

with

$$a = \frac{F_{B,laden} - F_{B,empty}}{0.65 m_{max} - m_{empty}}, b = F_{B,empty} - a \cdot m_{empty} \quad (19)$$

In order to check the proper modelling of the friction characteristics, brake mechanics and running resistance, the stopping processes of both a single wagon and trains were simulated. The stopping distance, the resulting braked weight percentage, and the braked weight were then compared to values from data sheets. The methodology is similar to the evaluation of braking performance described in [8]. Figure 9 shows exemplary results for one wagon type with LL brake block and an auto-continuous device. The simulation results match the data sheet values very well for total masses above 58 t. There are some deviations between 24 t and 58 t. This behaviour is most likely the result of the modelling of the friction characteristics of the LL blocks as described earlier. However, the deviations of resulting stopping distances from data sheet values are within a range of approx. -10 %. That means that effective braking forces in this range are slightly too high, thus resulting in slightly increased dynamics. This appears justifiable for the scope of finding critical scenarios with high LCF/LTF values.

Figure 10 shows stopping distance, the resulting braked weight percentage, and the braked weight for a wagon with cast iron brake blocks and a manual load device. The match of simulated values and data sheet values is satisfying.

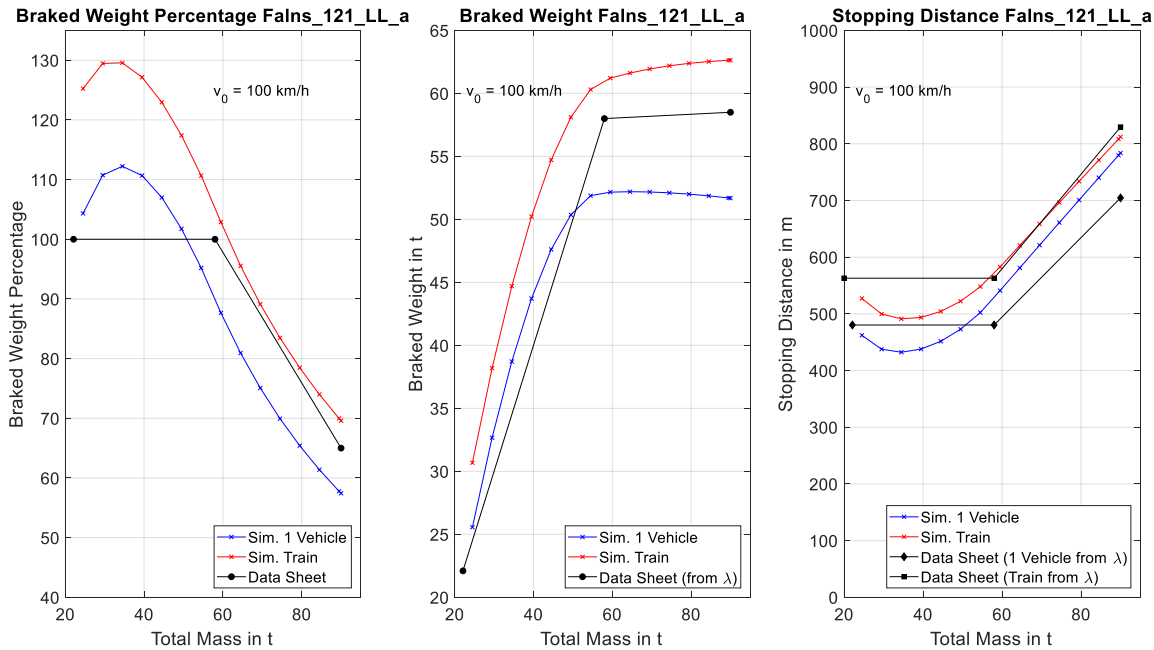


Figure 9: Braked weight percentage, braked weight and stopping distance for FALNS 121 wagon with LL brake blocks and auto-continuous device

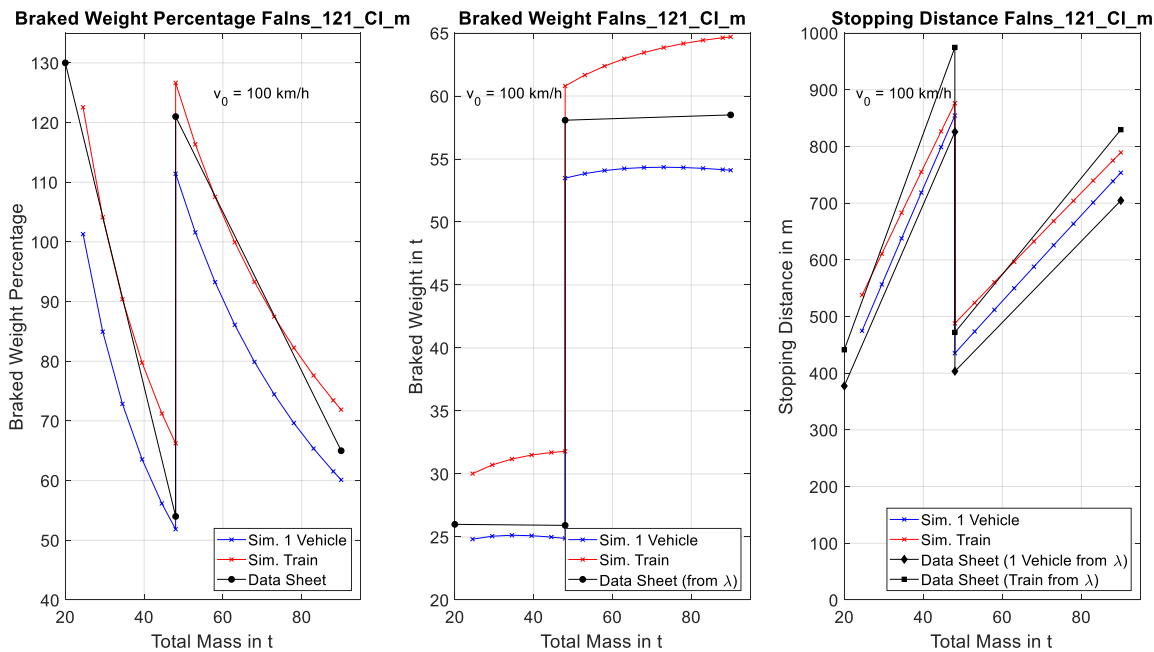


Figure 10: Braked weight percentage, braked weight and stopping distance for FALNS 121 wagon with cast iron brake blocks and manual load device

2.4.4 Coupler model

The base model of the coupler consists of two masses. These are dummy headstocks of the vehicles. They have a mass close to zero and are later coupled to the vehicles with zero degrees of freedom (see Figure 13). A total number of six force elements connect the two headstocks. Two of them represent the two buffers connected in series for both sides right and left. One force element represents the two draw gears of the screw coupler connected in series. All three previous elements make use of a nonlinear hysteresis function, which is defined by an upper and a lower envelope. Figure 11 shows an exemplary hysteresis function used for two buffers in series. The remaining three force elements are linear viscous dampers for the hysteresis elements. They avoid high frequency oscillations with very low amplitude, thus improving computational time.

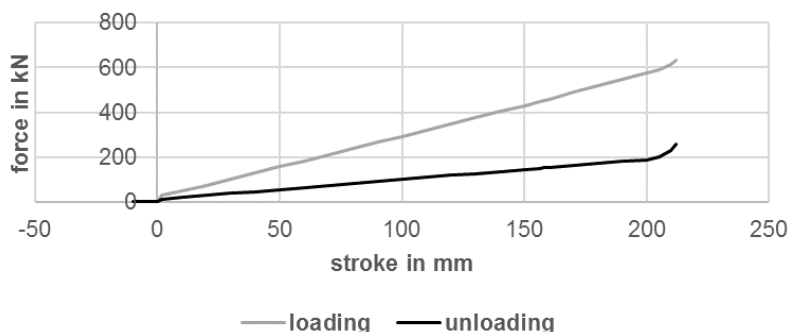


Figure 11: Exemplary hysteresis function for two buffers in series

2.4.5 Graphical representation

All models have a graphical representation for purposes of visualization, as shown in Figure 12. However, this graphical representation is usually neither needed nor used in the simulations.

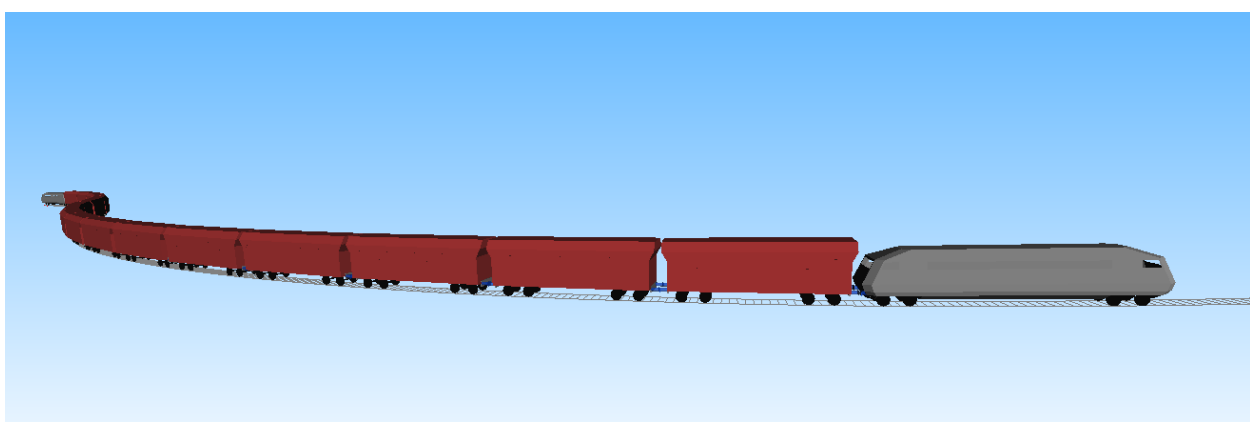


Figure 12: Graphical representation of models

Train and scenario setup

All parameters that define the models (e.g. mass, resistance coefficients, and force element characteristics) are listed in a parameter file and controlled by the MATLAB tool. The entire train setup is also controlled by the MATLAB tool. A train setup consists of a variable number n of vehicles (both locomotives and wagons) and $n-1$ couplers. For every vehicle and coupler in the train, the respective base model is copied into a simulation folder. The parameter lists of the base models are then modified with the actual parameters used in the respective model. All modified models are then connected in a train model. This train model represents a 1D multi-body oscillator as depicted in Figure 13.

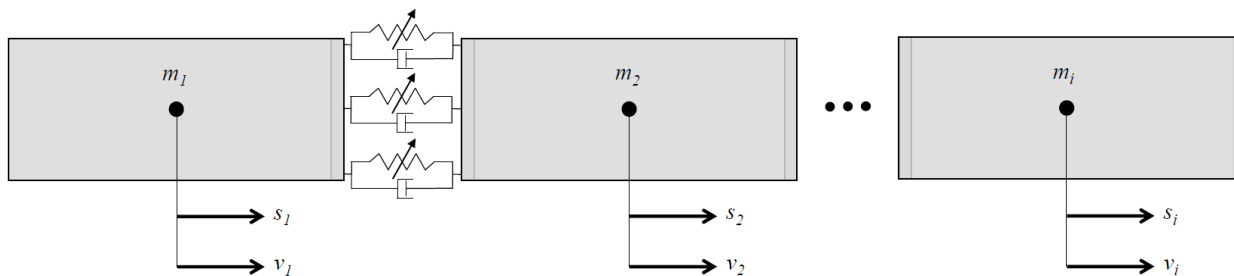


Figure 13: 1D multi-body oscillator

It should be noted that every vehicle in the train has only one degree of freedom. This degree of freedom is the movement along the train's path (s-coordinate). However, this path might generally be three-dimensionally curved within the initial system. In the context of this work, only gradients were used within the 1D simulations, as curves were investigated in the 3D simulations. Figure 14 shows a schematic train path within the initial system.

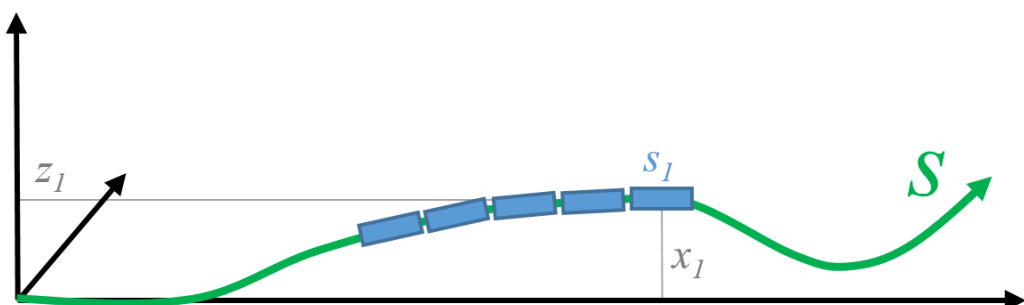


Figure 14: Schematic train path within the initial system

Grades can be defined in the simulation setup in the MATLAB tool. Furthermore, the entire simulation scenario can be defined. A scenario consists, besides other parameters of train setup, of initial velocity, traction behaviour of locomotives (acceleration,

deceleration, constant speed etc.), time of pneumatic brake activation, and time and place of a train disruption. The brake pressure time histories described in the previous section can be shifted to any instant of time within the 1D simulation to enable flexible starting points without the need of individual pneumatic simulations. Some simulation scenarios contain train disruptions. If this function is enabled, the force element representing the screw coupler in the designated vehicle is set inoperable from a designated instant of time on.

2.4.6 Result analysis

After a scenario is completely defined, it is ready to be simulated. The next step after the simulation run is the automatic post-processing of results by the MATLAB tool. The post-processing includes a standard result diagram as shown in Figure 15. This standard result diagram contains the time histories for velocities, stopping distances and traction forces of the individual vehicles in the left column, the actual pneumatic time histories (including eventual shifting) in the middle column, and the resulting time histories of longitudinal compressional forces (LCF) and longitudinal tensional forces (LTF) in the right column. Both LCF and LTF are filtered with a one-second sliding mean filter. The LCF are additionally filtered with a sliding 10-meter minimum filter (see also Section 2.6) in the distance domain, which is commonly used for LCF assessment. The original unfiltered time histories of LCF and LTF are depicted in gray and dashed.

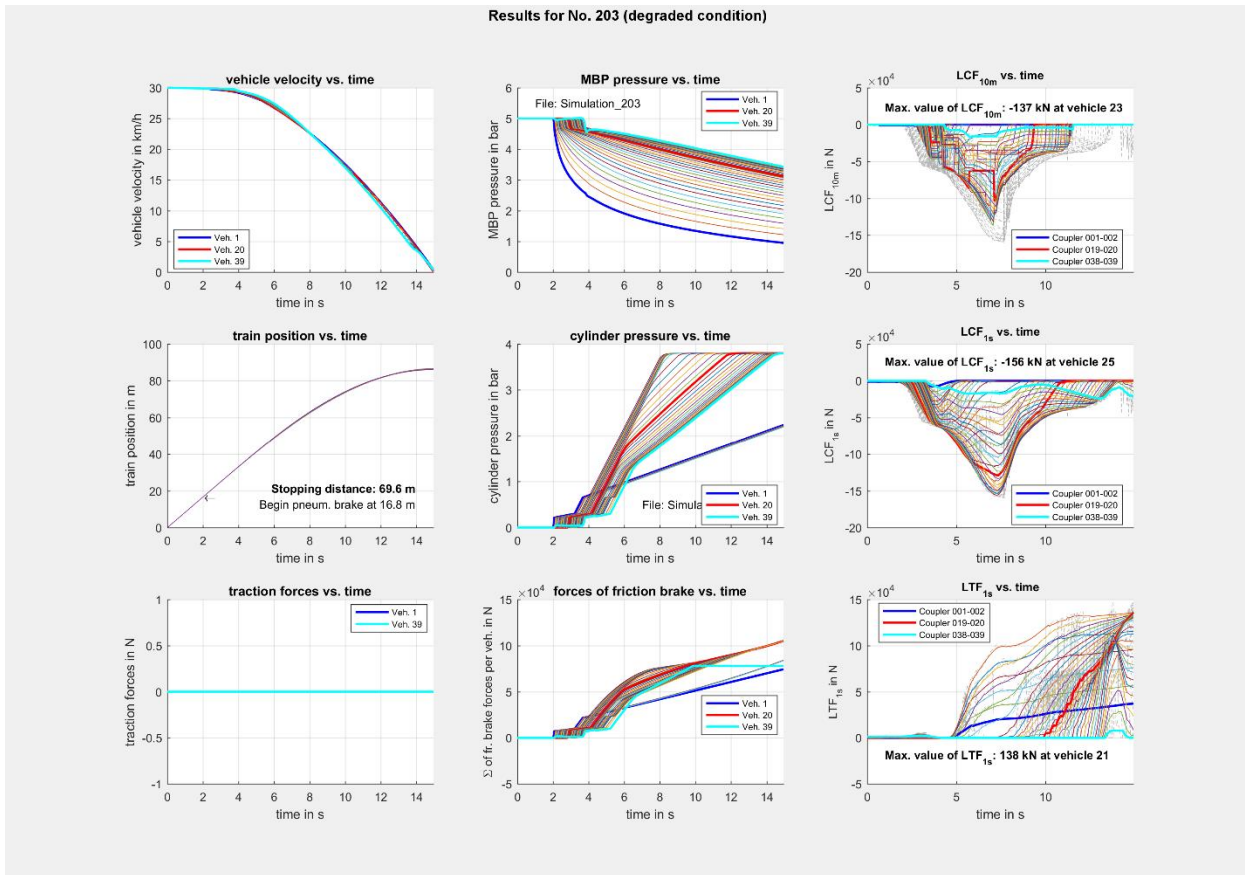


Figure 15: Exemplary standard result diagram

Parameter variations

Simulation scenarios which are defined in an excel table (see Section 3.2) can be automatically simulated in sequence. Furthermore, the MATLAB tool allows for parameter variation within a designated scenario. The example in Figure 16 shows a variation with 50 cases of randomly distributed total masses of the wagons within the range of 85 to 95 tons. The abscissa shows the variations and the ordinate shows the vehicles in the train. Variation number one on the far left is the standard (unvaried) train where each wagon has a nominal total mass of 90 t (vertical green bar). As the weight of the locomotives in the front and in the rear of the train is not varied, it stays at the nominal value of 84 t for all variations (horizontal blue bars).

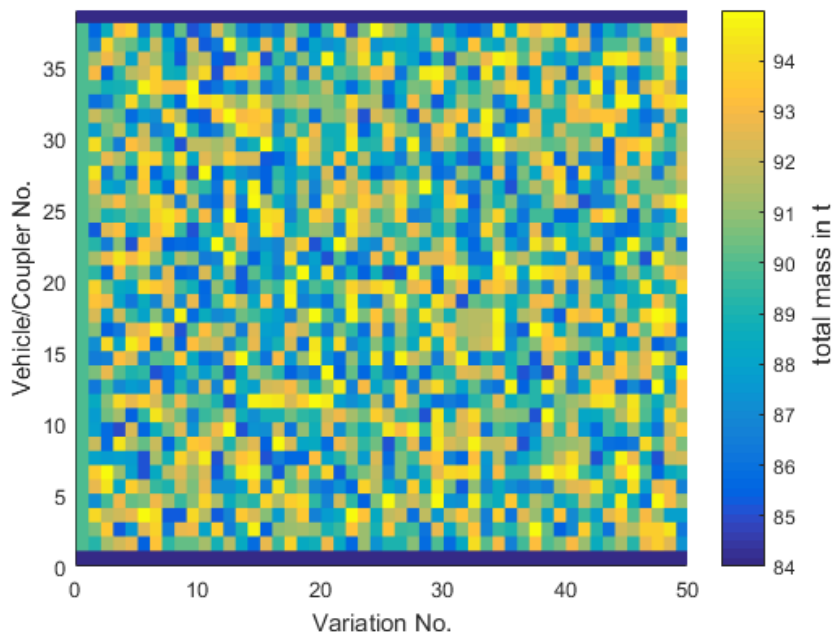


Figure 16: Exemplary parameter variation of total wagon mass

2.5 3D SIMULATIONS (TOLERABLE FORCES)

The three-dimensional simulation tool for the calculation of tolerable LCF values was developed by KTH in the GENSYS [9] simulation environment along with the use of MATLAB for the preprocessing and post processing of the simulation variables. The methodology adopted for three-dimensional simulations is inspired from the tests specified to be conducted for the approval of new wagon as per the UIC 530-2 leaflet that concerns with the running safety of wagons. The testing methodology is described and some initial results for the simulations can be found in [10].

2.5.1 UIC Code 530-2 Propelling test

The UIC 530-2 Code [10] proposes some guidelines and tests to be performed to determine the running safety of wagons in its Appendix G. An important aspect of interest as far as Longitudinal Train Dynamics (LTD) is concerned is the push test, which is explained in detail in the document. The test is conducted to demonstrate the permissible Longitudinal Compressive Force (LCF) through propelling tests. These tests are carried out on a flat S-curve with a radius of 150 m and 6 m of straight track section between the circular sections as described in Figure 17. The standard procedure consists of the wagon being tested kept empty, surrounded by two ‘barrier’ wagons. The specification of the leading and the trailing barrier wagons are described as well. The barrier wagons are then

surrounded by intermediate wagons on each side with a locomotive on one end and a measurement car on the other. The test train configuration can be seen in Figure 18.

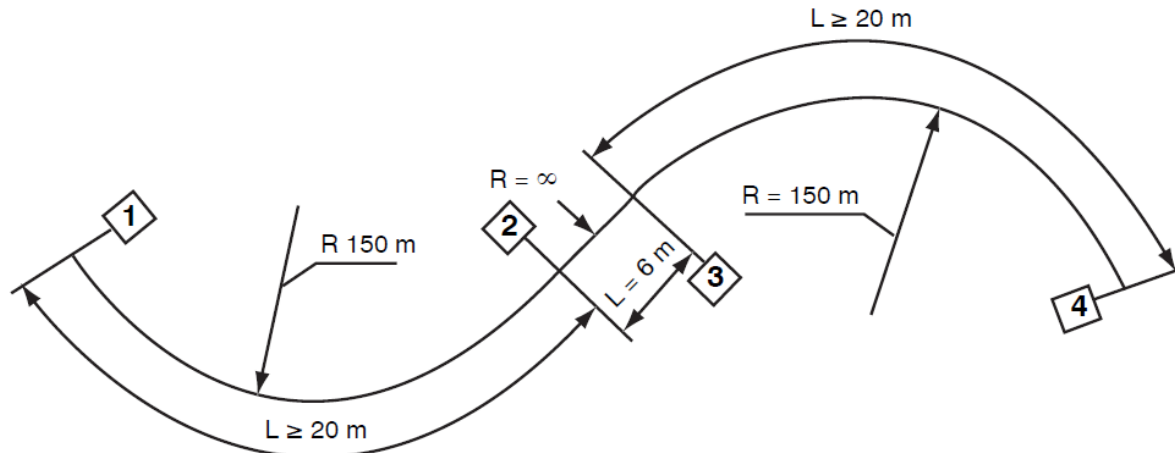


Figure 17: UIC 530-2 Track layout [10]

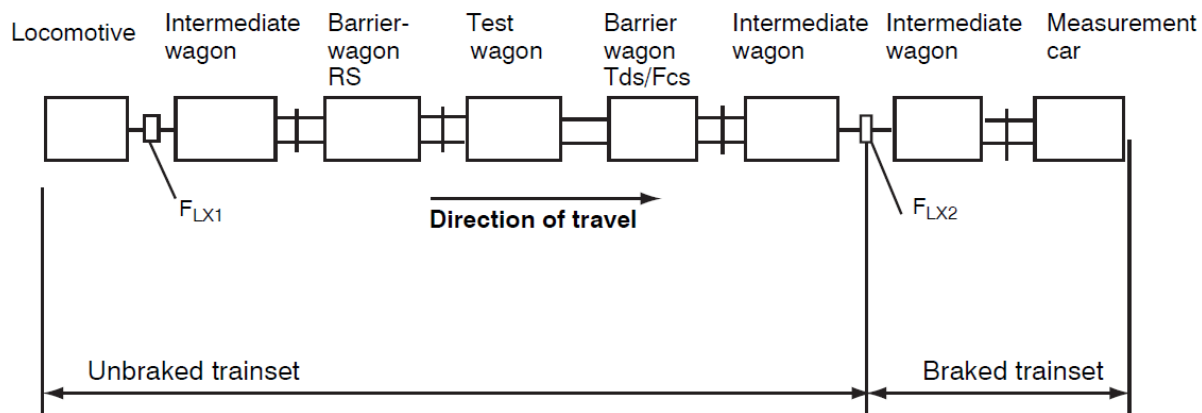


Figure 18: UIC-530-2 Train configuration [10]

The buffer head height difference is to be kept approximately 80 mm between the test wagon (higher) and the barrier wagons (lower) and the surfaces slightly lubricated. The test train hence constructed is then propelled into the S-curve at a speed of 4 to 8 km/h with a constant (static) LCF. The LCF is generated by the propelling locomotive on one end and braking wagons on the other. The torsional stiffness (C_t^*) is measured prior to the test. It is the torsional stiffness of the wagon body which for an angular rotation ϕ that corresponds to the torsional moment ($F \times 2b^*$). The relationship is given by:

$$C_t^* = \frac{2a^* \times 2b^* \times F}{\phi} \quad (20)$$

where $2b^*$ is the lateral distance between the buffers, F is the vertical force and $2a^*$ is the bogie pivot distance. The following parameters are measured during the tests:

- Longitudinal Compressive Force
- Wheel-uplift on all wheels
- Lateral forces on the axle boxes exerted on all the axles
- Deformation of axle guards on all wheels
- Lateral movements of the buffers between the barrier and the test wagons
- Track markers in Figure 17
- Distance covered.

The assessment criteria to decide derailment are:

- Uplift of a non-guided wheel of more than 50 mm over a distance of 2 m.
- Climbing of guided wheels by more than 5 mm.
- Stabilized track stress (lateral forces)

$$H_{\text{lim}(2m)} \geq 25 + 0.6 \times 2Q_0 \text{ [kN]}$$

where Q_0 is the mean vertical force of the wheel on rail.

2.5.2 Simulation methodology

The simulation methodology developed from the UIC standards aims to provide operation-specific (limited to a particular route and train composition) tolerable limits since it is possible to account for multiple scenarios through simulations. As mentioned in the previous subsection, UIC based on-track tests take a lot of time and resources and only cover a limited scenario. The test is wagon-specific and does not take other influencing factors such as adjacent wagons and their buffer types into account. It can be seen from the test conditions that the estimation of permissible LCF is quite conservative in the procedure and may not necessarily reflect the normal operation of freight wagons. The methodology hence cannot be considered as a generalized testing methodology for wagons with heterogeneous compositions or passing through any track geometry. Depending on the kind of train configurations and track conditions, different LCF limits can be calculated. Hence, the conditions of the tests are modified according to the operating conditions while drawing upon certain parts of the methodology from the UIC propelling tests.

Simulation setup

In the current study, the barrier wagons are also taken as loaded wagons of one of the configurations since it would represent the critical case of an empty wagon surrounded by two loaded wagons in the freight train. The running speed is kept at 8 km/h as mentioned in the UIC standard. The buffer height would be the resulting difference in

deflection arising due to loading pattern of the adjacent wagons. The wheel radii are assumed to be same for all the wagons. The UIC 530-2 track (Figure 17) with 30 m of each circular section is chosen. A transition length (not mentioned in Figure 2) is taken as 2 m to avoid computational issues due to the steep change in the track curvature. The derailment criterion used in the simulations is an instantaneous wheel-lift value of 10 mm for all wheels which can be seen as a compromise between the 50 mm limit for non-guided wheels and 5 mm for the guided wheels in the UIC standard [10] as mentioned in the methodology used in MARATHON [1]. Apart from the wheel-lift values, the Prud'hommes criterion was also checked simultaneously.

Such a simulation setup strives to incorporate elements from both the UIC 530-2 methodology's *wagon-based* approach and the more flexible *train-based* approach of various one-dimensional Longitudinal Train Simulators (LTS) such as TrainDy [12], CRE-LTS, etc [13][14] to form a *wagon vicinity-based* approach.

Concept of heterogeneities

In the previous subsection, a brief overview of the UIC 530-2 based testing methodology was presented. The wagon-based approach limits the number of possible operating combinations in terms of the issues that affect the LTD behaviour. This subsection points to the issues that have an influence on the tolerable LCF values from the three-dimensional simulations point of view. The issues related to braking and traction such as braking regimes, brake block materials and traction scenarios are not discussed since they are already utilized in the calculation of the actual forces in one-dimensional simulations and their effects are replaced by the statically applied LCF as seen in Figure 19.

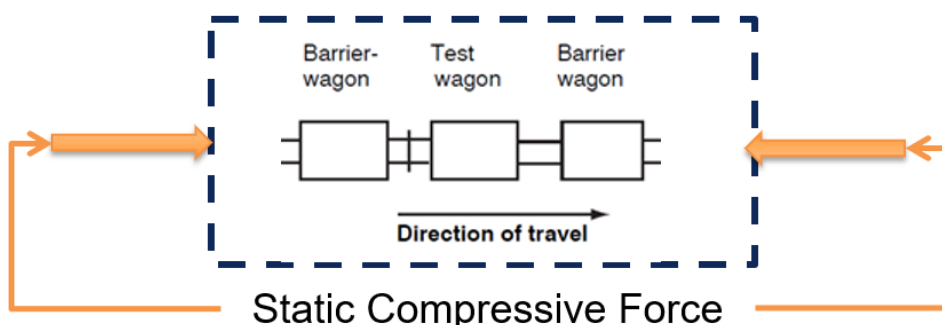


Figure 19: Simulation set-up in the GENSY environment

For the operation of long trains, these issues can be broadly classified into three categories (see Figure 20):

- **Vehicle-based:**

- *Wagon construction:* This refers to the wagon attributes such as bogie-pivot length, buffer overhang lengths, buffer characteristics, etc.

- *Running gear:* This refers to the type of running gear such as Y25, Link suspension bogies , two-axled wagons, etc.
 - *Payload:* This refers to the loading state of the individual wagons and also the pattern amongst the adjacent ones. This could also come under the operation-based category.
- **Infrastructure-based:**
 - *Type of curve:* Track design geometry that includes attributes such as horizontal curve radius, curve shape, cant, etc. Typical infrastructure bottlenecks such as tight S-curves could be quite critical.
 - *Gradients:* Gradients, and especially sags, could limit the tolerable LCF value of the wagons.
 - **Operation-based:**

These are issues with factors from both the infrastructure and the vehicle side which affect inter-wagon interactions rather than a single wagon or applying at a specific infrastructure point. Some of the issues include:

 - *Wagon arrangement:* The order in which different wagons, including their payloads are arranged while building the train.
 - *Locomotive arrangement:* The position of the locomotives along the length of the train.

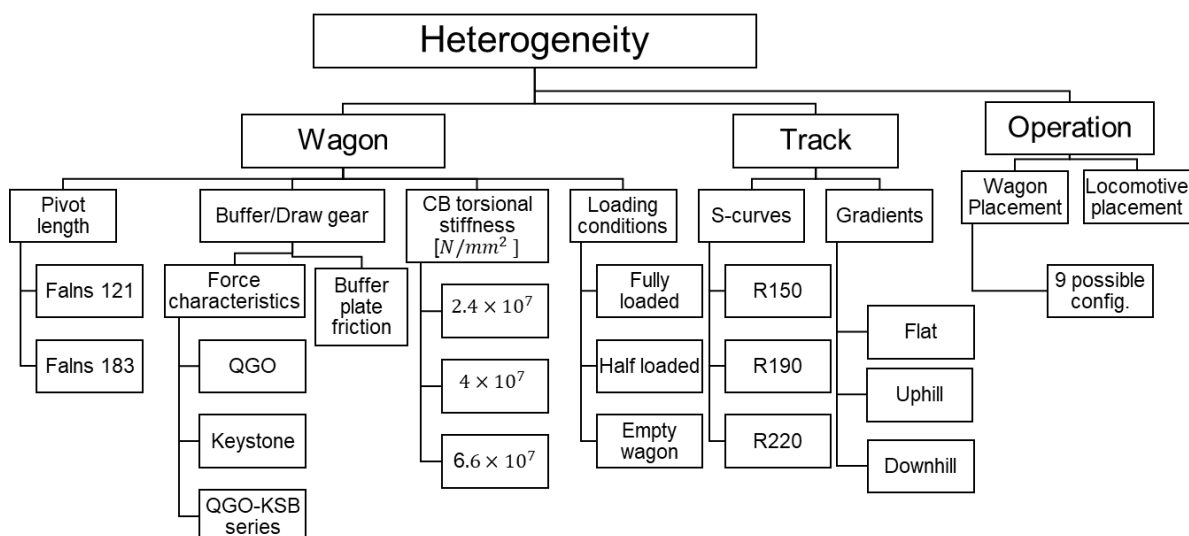


Figure 20: Heterogeneities w.r.t. 3D simulations. Example: Demonstrator train case

The tolerable LCF generally change when one or a combination of the issues above are changed. This is not taken into account by the *wagon-based* approach of the UIC testing methodology. One alternative is to utilize one-dimensional LTS that has a more *train-based* approach.

based approach. Though, it can cover some of the factors such as buffer characteristics, gradients, etc, the derailment occurrence mainly arising due to lateral forces in tight curves would not be covered by the same.

Keeping the computationally demanding nature of such simulations in mind, it is not possible to perform simulations with different combinations of the heterogeneities which could result in millions of cases. Hence, two parallel approaches were formulated (see Figure 21) :

- To first check the sensitivities of the individual heterogeneities on the tolerable LCF.
- To check the variation in the tolerable LCF values for a stochastic variation of multiple heterogeneities.

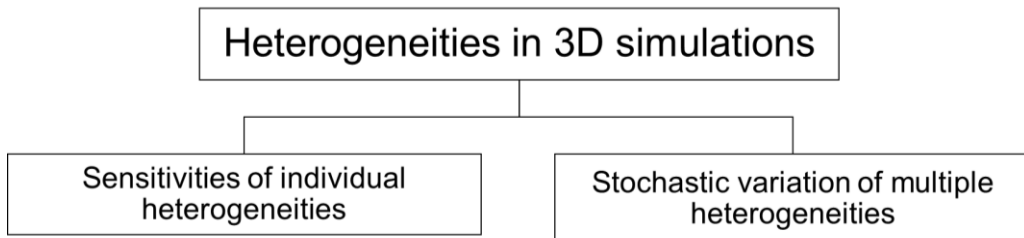


Figure 21: Approaching heterogeneities in three-dimensional simulations

Simulation routine

The LCF limit value for each case is calculated in an iterative process. One property observed throughout the simulation cases was that the wheel-lift values of the wagons for a simulation case increase with increasing LCF. This leads to a reasonable assumption that the wheel-lift w.r.t. the applied LCF is steadily increasing. The goal function is hence to find the minimum LCF value for which the wheel-lift exceeds 10 mm. A halving algorithm is developed for a range of LCF values where the first iteration starts with the upper limit LCF value while the interval is halved in consecutive iterations. The accuracy a of the LCF limit increases with the number of iterations given by:

$$a = \frac{Max - Min}{2^N} \quad (21)$$

where *Max* and *Min* are the higher and lower bound for the LCF range while *N* is the number of iterations.

2.5.3 Modelling

The modelling process of the simulation model has been categorised into three parts: wagon, wagon couplers and track design geometry.

Wagon

The three wagons are modelled as shown in Figure 22 with the notations for the Degrees Of Freedom given by (Refer Figure 22):

- X,Y,Z as translational degrees of freedom.
- φ , χ and ψ as rotational degrees of freedom about X,Y and Z axis respectively.

Wagons are modelled as rigid or torsionally flexible car bodies to examine the effect of car body torsional stiffness. In case of the flexible car body, it is modelled as a lumped element model with two similar mass elements joined at the centre of mass by a force element acting on all the 6 DOF (Figure 23). The force element consists of a torsional stiffness ($C_{T\varphi}$) calculated according to Equation below in the φ direction while very high values of stiffness in the other DOF's (100MNm/rad) [10]. The relation between $C_{T\varphi}$ and C_T^* is derived from and given by:

$$C_{T\varphi} = \frac{C_T^*}{2a^*} \quad (22)$$

where $2a^*$ is the bogie pivot distance.

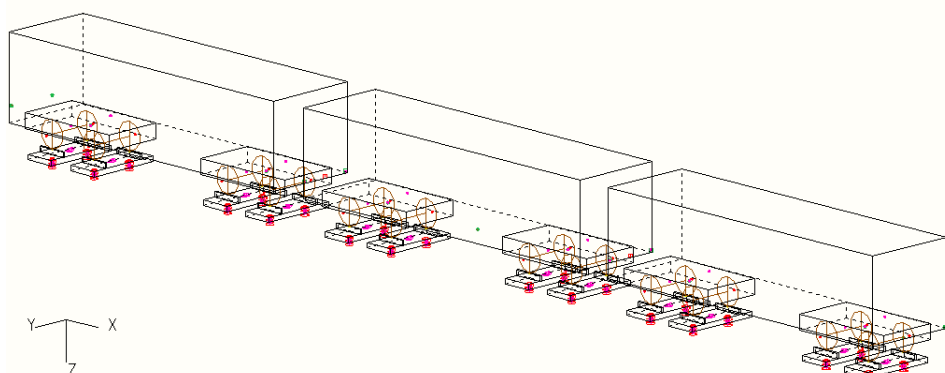


Figure 22: Simulation model in GENSYS for 3D derailment analysis

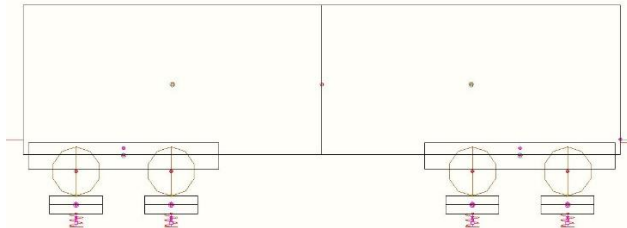


Figure 23: Torsionally flexible carbody in GENSYS

Wagon couplers

The three-dimensional wagon coupling model consists of a draw gear (screw coupler) in the centre, and two buffers and bufferstops, situated each on both the sides of the wagon. The loading and the unloading characteristics of the buffers and the draw gears are modelled in a similar manner but with the forces acting on opposite directions. The vehicle coupler modelling is based on the work of Cantone [12] in the development of the LTS (Longitudinal Train Simulator) TrainDy. The buffers and drawgears are modelled by their force-stroke characteristics, while considering a friction model for damping. When relative speed is in the interval between load velocity (v_{load}) and unload velocity (v_{unload}), the force exchanged is calculated as:

$$F_{long}(x_{rel}, v_{rel}) = c(v_{rel})F_{unload}(x_{rel}) + [1 - c(v_{rel})]F_{load}(x_{rel}) \quad (23)$$

where x_{rel} and v_{rel} are the relative displacement and velocity between the adjoining vehicles respectively. $c(v_{rel})$ as seen in Figure 24 is computed by a third order polynomial to connect the loading and the unloading curves.

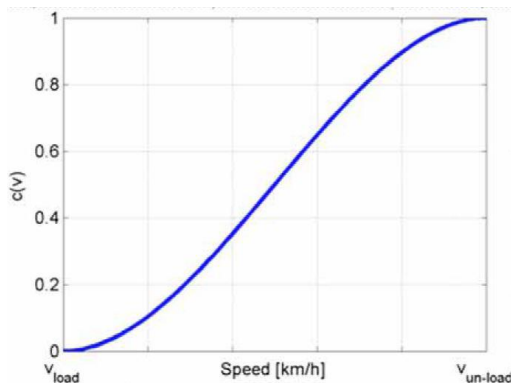


Figure 24: Transition function for points in between loading and unloading [12]

The coupler forces in the lateral and vertical directions are the result of buffer-head friction. The forces are modelled in the form of a sprung block on a two-dimensional friction surface.

Track design geometry

There are two types of tracks used in the present work. Circular track with transition curves and S-shaped curves with sudden transition. The transition curves are modelled with a parabolic variation in both curvature and cant as described in [15]. The track design geometry is elaborated in Table 1.

Table 1: Track design parameters

Curve name	Radius [m]	Transition length [m]	Cant [m]	Additional data
S150M6	150	2	-	Intermediate length = 6 m
S190M10	190	2	-	Intermediate length = 10 m
R300	300	80	0.15	-
R600	600	110	0.12	

2.5.4 Buffer angle concept

Previously, the concept of heterogeneities was discussed, where the simultaneous contribution of the vehicle, infrastructure and operating parameters on the Longitudinal Train Dynamics varies. The coupler angle concept put forward by Simson cf. [16] incorporates the effect of the wagon geometry, adjacent wagon geometries and the curvature at each of the wagon positions (Figure 25). It is used in the calculation of buffer angles, i.e. the angle between the buffers of the adjoining wagons. It is also useful as a tool in the *wagon vicinity-based* approach described in the present simulation setup. The coupler angles along with the angles between the adjacent wagons for different types of curve-sections are illustrated in Figure 26 and Figure 27.

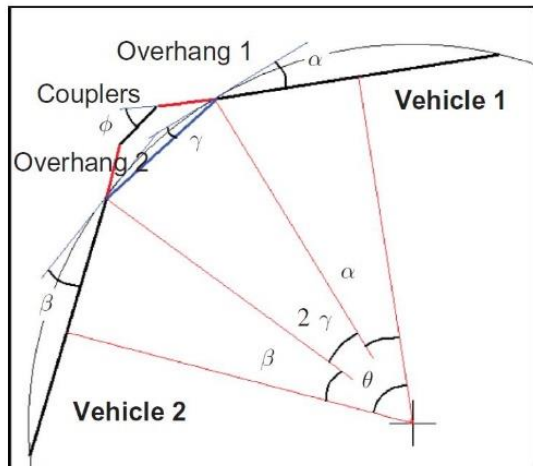


Figure 25: Coupler angle calculation [17]

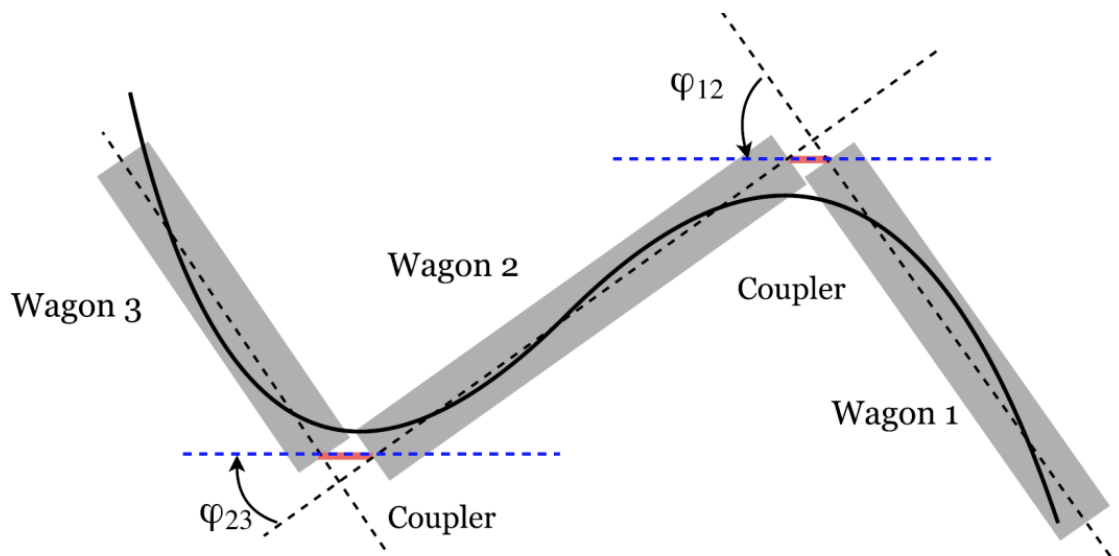


Figure 26: Coupler angles through an S-curve

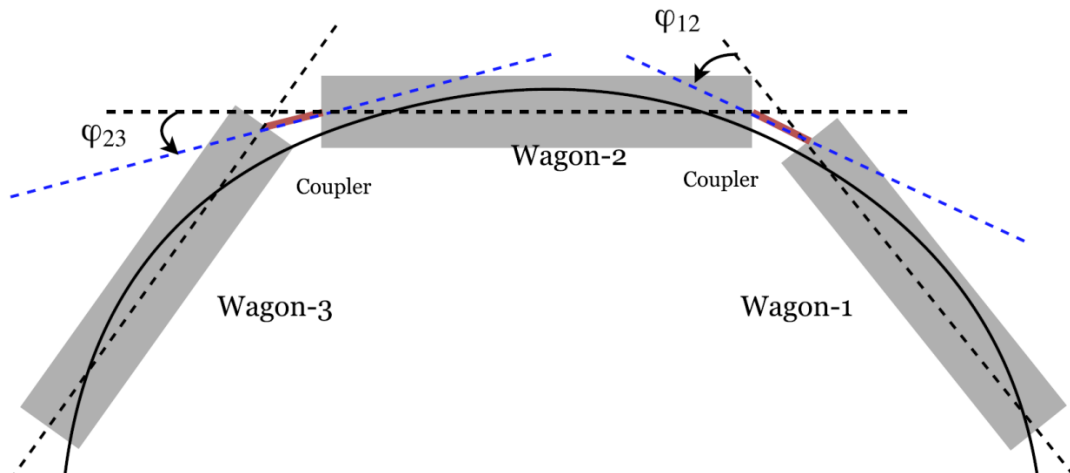


Figure 27: Coupler angles through circular curve

The buffer angles (ψ_{12} , ψ_{23}) and their difference ($\Delta\psi_2$) are calculated from the coupler angles as described in Equations (24),(25) and (26).

$$\psi_{12} = \varphi_{12} + \varphi_{21} \quad (24)$$

$$\psi_{23} = \varphi_{23} + \varphi_{32} \quad (25)$$

$$\Delta\psi_2 = \psi_{12} - \psi_{23} \quad (26)$$

The LCF values for different wagon and track design geometries are plotted against the buffer angle difference ($\Delta\psi_2$).

2.6 ACTUAL VS. TOLERABLE FORCES

This section combines the findings from the individual methodologies seen in the previous Sections 2.3, 2.4 and 2.5. The values of actual compressive forces calculated from Section 2.4 are compared against the tolerable LCF values from Section 2.5. The flowchart in Figure 1 illustrates the same.

For each train configuration, operational scenario and track layout the actual LCFs from the 1D dynamics simulation can be compared against the tolerable LCFs found in the 3D analyses of three-wagon “trains”. The tolerable LCFs is as implied by the push test methodology, a static force whereas the actual LCFs are dynamic in nature. In the comparison it is therefore not reasonable to use the instantaneous values of the actual LCFs but applying a filtering so that they have a certain duration. From the MARATHON work it was found that one-second duration gives feasible quasi-static LCFs that can be compared against the (static) tolerable LCFs. As indicated above one-second sliding mean values of actual LCFs have been used. Also the more traditional ten-metre sliding

minimum values of actual LCFs have been used. In most cases the two filtering methods of the actual LCFs give similar force histories.

In cases where the actual forces exceed the tolerable LCF values, the various sensitivities in the freight wagon system studied in these simulations can provide appropriate measures to make the long-train operation safer.

2.7 CONCLUSIONS AND SAFETY PRECAUTIONS

It is common that for some combinations of train configuration, operational scenario and track layout some of the (filtered) actual LCFs at some point in time exceed the corresponding tolerable LCFs. This assumes the worst possible timing like heavy braking in tight S-curves. If this poor timing cannot be avoided, actions have to be taken on train configuration and/or operational scenario. Another option is that the train is not allowed to run through the tightest S-curves. See also Figure 1 at the beginning of this chapter.

3. FIRST APPLICATION: PRESENT-DAY COAL TRAIN OPERATION

The first application was suggested by the FFL4E WP5 partners (DB, Faiveley Transport, Bombardier Transportation) and is an existing coal train operation on the railway line Mainz-Munich. In this chapter this application is studied with respect to longitudinal dynamics and associated derailment risk in tight curves.

3.1 TRAIN CONFIGURATION

The train in question consists of two locomotives (BR 151 and 187), one in the front and one (pushing) in the rear. Between the locos there are 37 wagons of type FALNS 121 and 183, see Figure 28.



Figure 28: FALNS wagons for coal train operation in Germany [18]

The train is fairly homogeneous and only 530 m long, but was considered a good starting point to evaluate and improve the methodology outlined in the previous chapter.

The heterogeneity of the train is mainly related to two slightly different wagons (length, tare weight), two different payload-dependent brake devices, three different brake block materials, different brake rigging efficiency, two different buffer types and two different draw gear types. When the train runs towards Munich, the wagons are normally fully loaded. But in the 1D simulations some payload variation is included and in the 3D derailment analyses wagons are even left empty (no payload).

Brake regimes (positions) are G and P, plus a so-called LL regime with the front loco and the first five wagons braking in G regime and the other vehicles in P regime.

3.2 TRACTION AND BRAKING SCENARIOS

Today this operation is based on having both locomotives manned with the two drivers communicating over mobile phone. The goal is to have the rear loco unmanned and let the front (master) loco communicate with the rear (slave) loco via radio. The new setup is planned to be demonstrated in late 2018.

As indicated in Section 2.2, two sets of operational scenarios can be defined:

- Nominal condition (the radio communication is working properly)
- Degraded condition (radio communication is lost for a number of seconds)

Based on work in DYNAFREIGHT Task 3.1, the scenarios are described in Table 2 and Table 3.

Table 2: Nominal Scenarios - Demonstrator cases

No.	Config.	DPS party	System/Sub System of interest	Description	Delay of action at							
					BP control of slave active	slave command ded by master	ED/Tract. Force Master	ED/Tract. Force	ramp down time	Suspend ramp down time	Suspend ramp up time	initial slave speed [km/h]
Slave [s]	[kN]	Slave [kN]	slave [s]	slave [s]	slave [s]	slave [s]	[km/h]					
101 VSC1	Slave	Pneumatics	Brake Position	no action	no	-						100
101 VSC1	Master	Pneumatics	Brake Position	Emergency brake. Running train in brake position P	no	-						100
102 VSC1	Slave	Pneumatics	Brake Position	no action	no	-						100
102 VSC1	Master	Pneumatics	Brake Position	Emergency brake. Running train in brake position	no	-						100
103 VSC1	Slave	Pneumatics	Brake Position	LL	no	-						100
103 VSC1	Master	Pneumatics	Brake Position	no action	no	-						100
103 VSC1	Master	Pneumatics	Brake Position	Emergency brake. Running train in brake position	no	-						100
104 VSC1	Slave	Pneumatics	Brake Position	Emergency brake. Running train in brake position P	yes	2						100
104 VSC1	Master	Pneumatics	Brake Position	Emergency brake. Running train in brake position P	yes	2						100
105 VSC1	Slave	Pneumatics	Brake Position	LL	yes	2						100
105 VSC1	Master	Pneumatics	Brake Position	Emergency brake. Running train in brake position	yes	2						100
106 VSC1	Slave	Pneumatics	Brake Position	LL	yes	2						100
106 VSC1	Slave	Pneumatics	Brake Position	G	yes	2						100
106 VSC1	Master	Pneumatics	Brake Position	Emergency brake. Running train in brake position	yes	2						100
106 VSC1	Master	Pneumatics	Brake Position	G	yes	2						100
107 VSC1	Slave	Traction	Max Traction Forces	Accelerate train	yes	2	300					30
107 VSC1	Master	Traction	Max Traction Forces	Accelerate train	yes	2	300					30
108 VSC1	Slave	ED-Brake	Max ED Forces	Decelerate train applying only ED-brake	yes	2	30					30
108 VSC1	Master	ED-Brake	Max ED Forces	Decelerate train applying only ED-brake	yes	2	30					30
109 VSC1	Slave	ED-Brake	Switch Traction/lbrake	Full traction and then switching to emergency	yes	2	30					30
109 VSC1	Master	ED-Brake	Switch Traction/lbrake	Full traction and then switching to emergency	yes	2	30					30

Table 3: Degraded Scenarios - Demonstrator cases

No.	Config.	DPS party	System/Sub System	Hazard	Description (always 2 variants: BP control active or inactive at slave loco)	Delay of action at slave								initial speed [km/h]
						d by master [s]	ED/Tract. Force Master [kN]	ED/Tract. Force Slave [kN]	Suspend time ramp down slave [s]	ramp down time slave [s]	Suspend time ramp down slave [s]	ramp up time slave [s]		
201 VSC1	Slave	Traction	Comm loss		After 2 seconds control of slave loco is suspended for 1 sec. (in total 2+1 seconds no reaction), then traction is ramped down to 0 kN in 5 sec. After reconnection traction control is suspended again for 4 before traction is reestablished within 8 seconds to 300 kN	2	300		1	5	4	8	30	
201 VSC1	Master	Traction	Comm loss		master loco keeps traction	2	300							30
202 VSC2	Master	Traction	Comm loss		At the beginning both locos have full traction for 2 seconds. Traction is ramped down in 5 seconds Then master switches to emergency brake after 2 seconds by venting the brake pipe and comm loss takes place simultaneously for infinite seconds	infinite	300		1	5				30
202 VSC2	Master	Pneumatics	Comm loss		After 2 seconds control of slave loco is suspended for 1 sec. (in total 2+1 seconds no reaction), then traction is ramped down to 0 kN in 5 sec.	infinite								30
202 VSC2	Slave	Traction	Comm loss		slave loco is supporting venting of the brake pipe in iterative steps by checking Delta pressure in brake pipe	infinite	300		1	5				30
202 VSC2	Slave	Pneumatics	Comm loss		Emergency brake mode without venting of brake pipe at slave	infinite								30
203 VSC2	Slave	Pneumatics	DPS control failure		Emergency brake mode	2								30
203 VSC2	Master	Pneumatics	DPS control failure		slave loco is supporting venting of the brake pipe in iterative steps by checking Delta pressure in brake pipe	2								30
204 VSC1	Slave	Pneumatics	Comm loss		Unexpected charging of brake pipe	infinite								30
204 VSC1	Master	Pneumatics	Comm loss		Emergency brake mode	infinite								30
205 VSC1	Slave	Pneumatics	DPS control failure		Emergency brake mode	2								30
205 VSC1	Master	Pneumatics	DPS control failure		Train disruption after first vehicle	2								30
206 VSC1	Master	Pneumatics	Train disruption		Train disruption after first vehicle	2								30
206 VSC1	Slave	Pneumatics	Train disruption		Unexpected discharging of brake pipe in emergency brake mode	2								30
207 VSC1	Slave	Pneumatics	DPS control failure		Master's response ?	2								30

3.3 PNEUMATICS SIMULATIONS

Pneumatics simulations were carried out for a subset of the scenarios presented in Section 3.2; in particular scenarios involving pneumatic braking are presented in Table 4 and Table 5 for nominal and degraded conditions respectively.

Table 4: Scenarios involving pneumatic braking for nominal condition

No.	Config.	System/Sub System	Subject of interest	DPS party	Description	Brake Position	BP control of slave loco active	Delay of action at slave commanded by master [s]
101	VSC1	Pneumatics	Brake Position	Slave	no action	P	no	-
				Master	Emergency brake. Running train in brake position P			
102	VSC1	Pneumatics	Brake Position	Slave	no action	LL	no	-
				Master	Emergency brake. Running train in brake position LL			
103	VSC1	Pneumatics	Brake Position	Slave	no action	G	no	-
				Master	Emergency brake. Running train in brake position G			
104	VSC1	Pneumatics	Brake Position	Slave	Emergency brake. Running train in brake position P	P	yes	2
				Master	Emergency brake. Running train in brake position P			
105	VSC1	Pneumatics	Brake Position	Slave	Emergency brake. Running train in brake position LL	LL	yes	2
				Master	Emergency brake. Running train in brake position LL			
106	VSC1	Pneumatics	Brake Position	Slave	Emergency brake. Running train in brake position G	G	yes	2
				Master	Emergency brake. Running train in brake position G			

Table 5: Scenarios involving pneumatic braking for degraded condition

No.	Config.	System/Sub System	Subject of interest /Hazard	DPS party	Description	Brake Position	BP control of slave loco active
202	VSC2	Pneumatics	Comm loss	Slave	At the beginning both locos have full traction for 2 seconds. Traction is ramped down in 5 seconds Then master switches to emergency brake after 2 seconds by venting the brake pipe and comm loss takes place simultaneously for infinite seconds	LL	yes
				Master	After 2 seconds control of slave loco is suspended for 1 sec. (in total 2+1 seconds no reaction), then traction is ramped down to 0 kN in 5 sec. slave loco is supporting venting of the brake pipe in iterative steps by checking Delta pressure in brake pipe		
203	VSC2	Pneumatics	DPS Control Failure	Slave	Emergency brake mode without venting of brake pipe at slave	LL	yes
				Master	Emergency brake mode		
204	VSC1	Pneumatics	Comm loss	Slave	slave loco is supporting venting of the brake pipe in iterative steps by checking Delta pressure in brake pipe	LL	yes
				Master	Emergency brake mode		
205	VSC1	Pneumatics	DPS Control Failure	Slave	Unexpected charging of brake pipe	LL	yes
				Master	Emergency brake mode		
206	VSC1	Pneumatics	Train Disruption	Slave	Train disruption after first vehicle	LL	yes
				Master	Train disruption after first vehicle		

The following subsections report the main output of the pneumatic simulations for the scenarios considered.

3.3.1 Nominal condition

Scenario 101

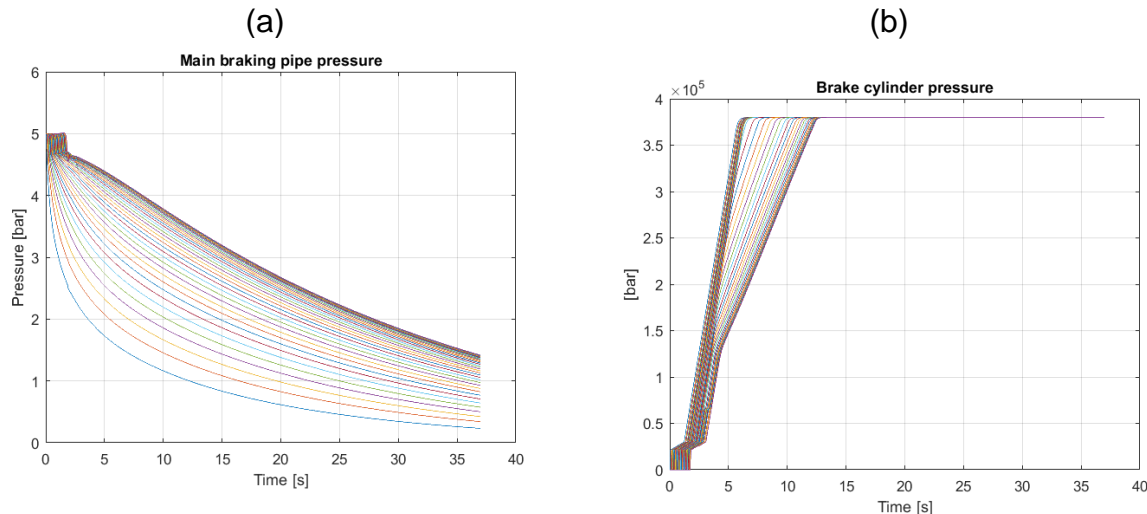


Figure 29: Time histories of pressure in main braking pipe (a) and braking cylinders (b) for scenario 101

Figure 29 shows the time histories of pressure inside the main braking pipe (Figure 29a) and in the braking cylinders (Figure 29b). Each line of the figure represent the time history for a single wagon. The same charts will be presented in the following paragraphs for all the scenarios considered.

Figure 29a shows that almost 12 seconds are required to have a pressure drop of 1.5 bar in the last vehicle. This pressure drop determines the maximum opening of the distributor valve. The maximum pressure in the braking cylinder of the last vehicle is reached after 13 seconds.

Delay in propagation of braking command from the train head (pressure drop) is clearly visible in Figure 30a where the pressure in the main braking pipe is presented using the colour code as function of time and wagon position. The corresponding chart referred to pressure in braking cylinders is reported in Figure 30b.

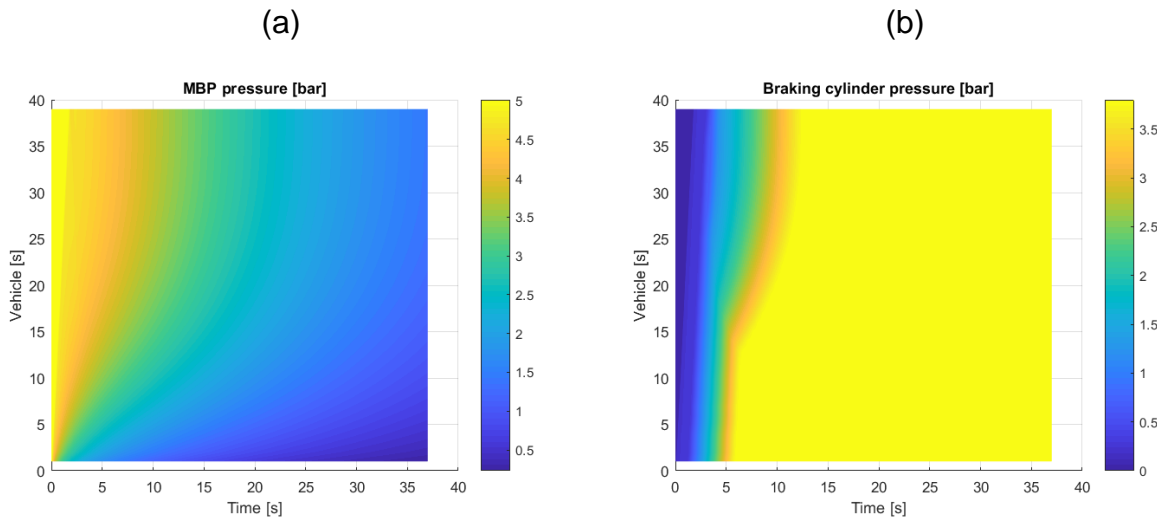


Figure 30: Pressure in main braking pipe (a) and braking cylinders (b) as function of time and wagon position for scenario 101

Scenario 102

Like scenario 101 (see Table 4), this operating condition refers to an emergency braking commanded by the master loco. Figure 31a is identical to Figure 29a since the manoeuvre is the same. Figure 31b puts into evidence the effect of LL braking regime where the master loco and the first five wagons adopt G regime. Maximum pressure in these vehicles is therefore reached after 25 s.

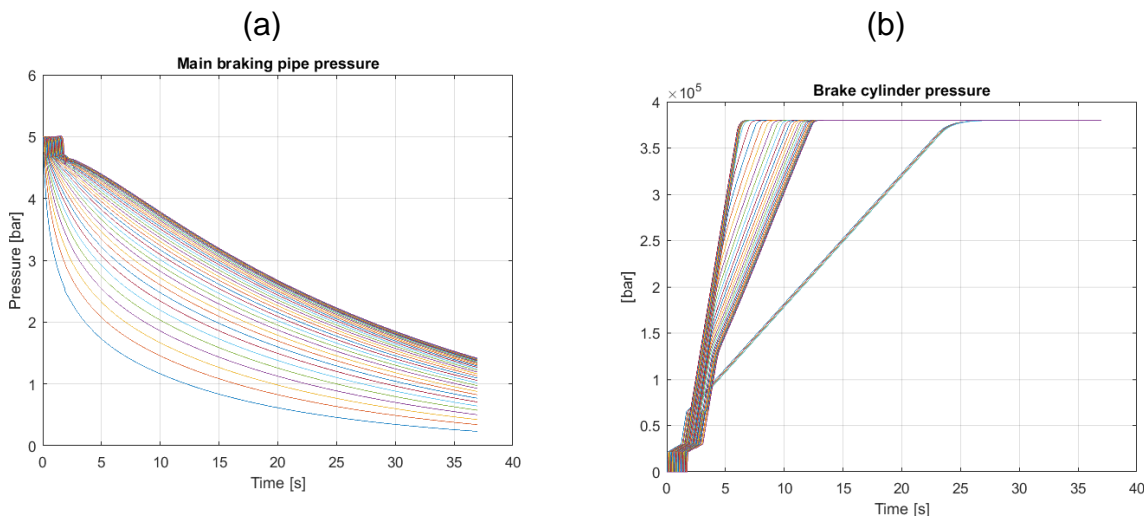


Figure 31: Time histories of pressure in main braking pipe (a) and braking cylinders (b) for scenario 102

Scenario 103

Also scenario 103 refers to an emergency braking commanded by the master loco. For this reason, the time history of pressure inside the main braking pipe doesn't change. Being all the wagons in braking position G, in this case the pressure build-up in the cylinders is delayed and the maximum pressure is reached after 25 s for all the vehicles (Figure 32b).

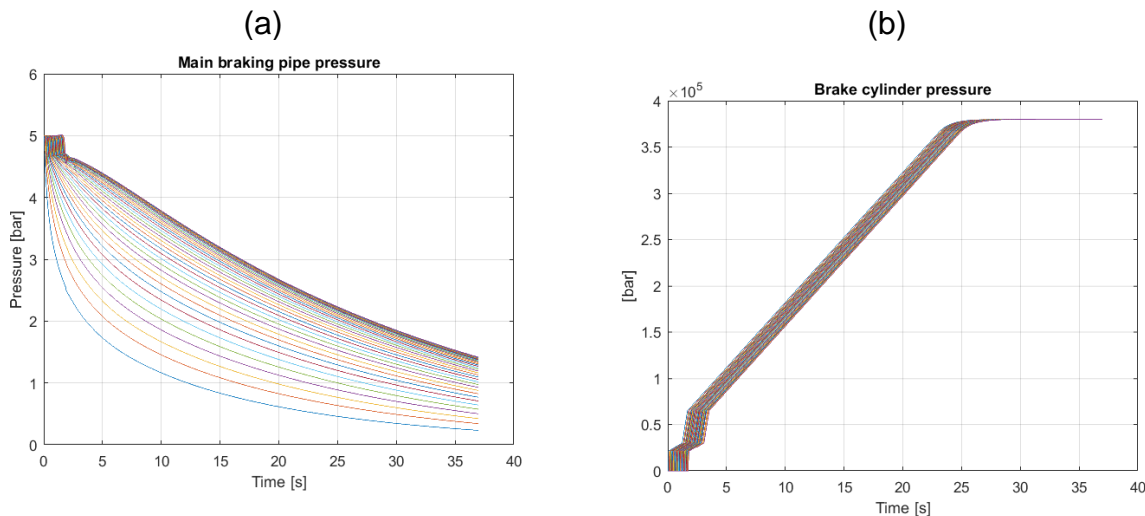


Figure 32: Time histories of pressure in main braking pipe (a) and braking cylinders for scenario 103

Scenario 104

This scenario considers that the slave loco can be commanded by the master loco via radio signals. In particular, it is assumed that the slave loco performs an emergency braking (i.e. by opening the main braking pipe from the rear) with a 2-second delay with respect to the master loco.

Looking at Figure 33a, it is interesting to notice how, in this condition, the time required to get a pressure drop of 1.5 bar on all the wagons is below 6 seconds (compared to the 12 s of scenario 101). In parallel, the pressure build-up in all the braking cylinders can be completed in almost 8.5 s. (Figure 33b)

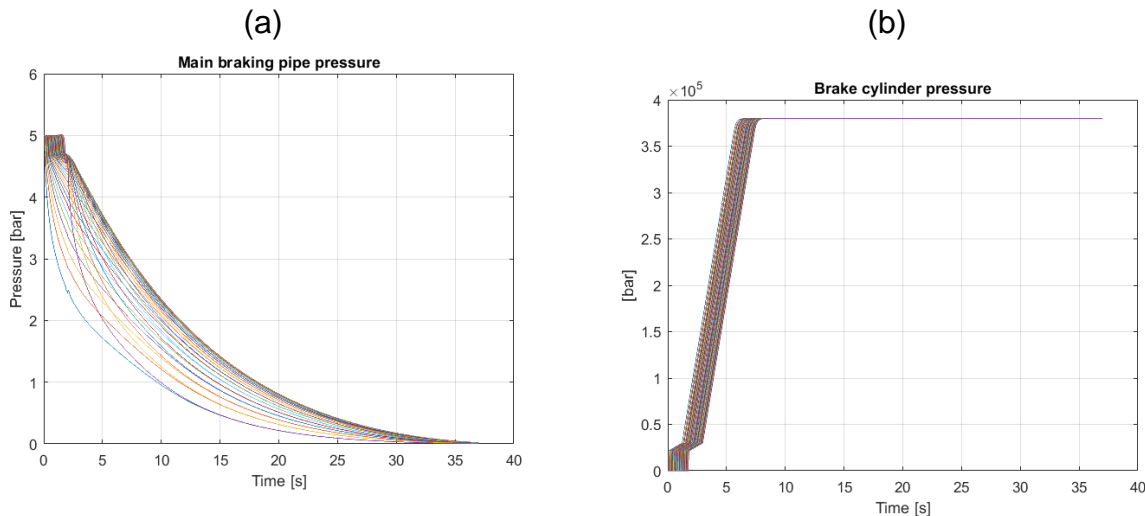


Figure 33: Time histories of pressure in main braking pipe (a) and braking cylinders for scenario 104.

Trying to get a better comparison between scenario 101 and 104, Figure 34 displays with colour code the pressure in main braking pipe (MBP) as function of time and vehicle position. It is easy to notice how the venting from the slave loco allows to drastically reduce the effect of delay in propagation of the braking command.

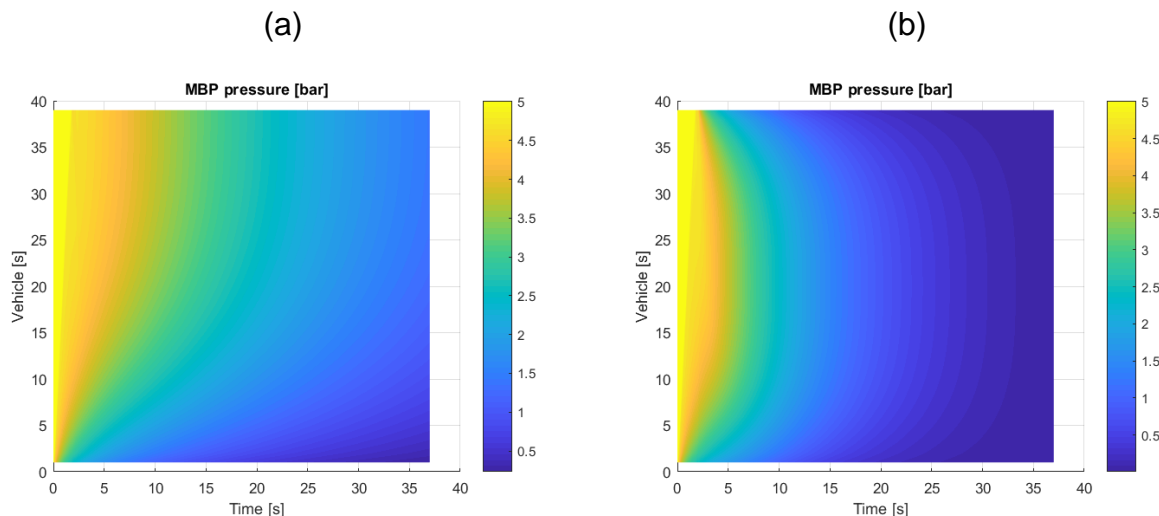


Figure 34: Pressure in main braking pipe as function of time and wagon position for scenario 101 (a) and 104 (b)

The effect of a faster venting produces a faster pressure build-up in braking cylinders, as evidenced in Figure 35.

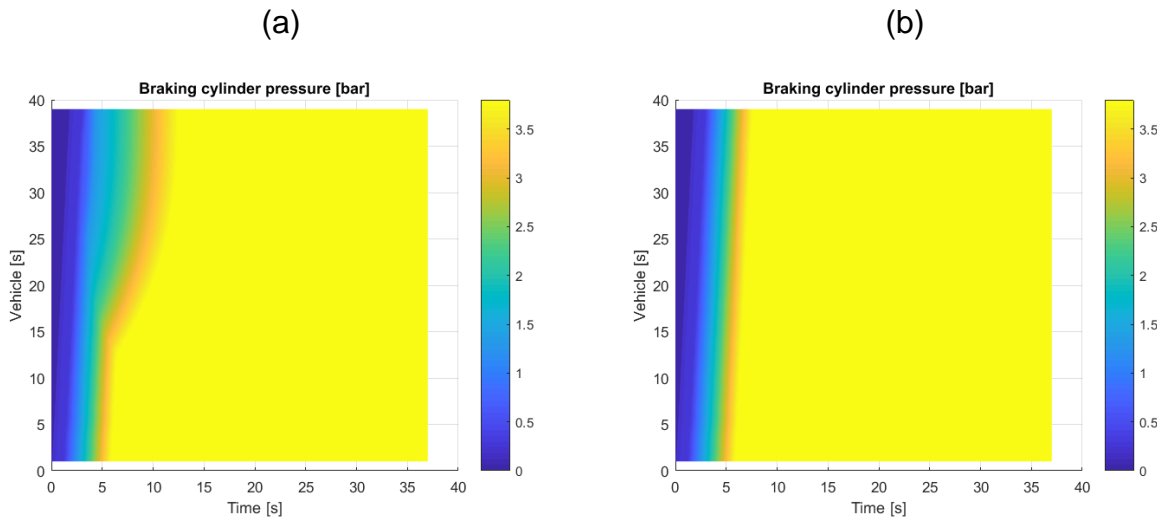


Figure 35: Pressure braking cylinders as function of time and wagon position for scenario 101 (a) and 104 (b)

Scenario 105

This is the same manoeuvre as scenario 104 but an LL braking regime is assumed. The only difference with respect to the previous case is thus associated with the pressure build-up in the cylinders of the master loco and the first five vehicles.

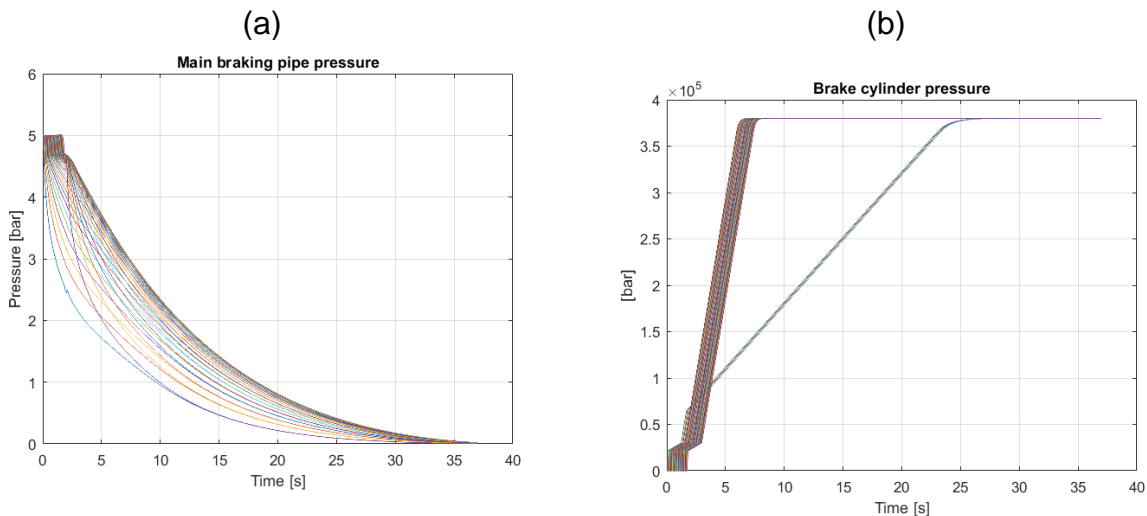


Figure 36: Time histories of pressure in main braking pipe (a) and braking cylinders (b) for scenario 105

Scenario 106

Also scenario 106 is characterised by the same manoeuvre as scenario 104; In this case the braking position is G for all the vehicles. As the dynamics of the pressure build-up is very low compared to the one of the main braking pipe, this condition looks very similar to the one of scenario 103.

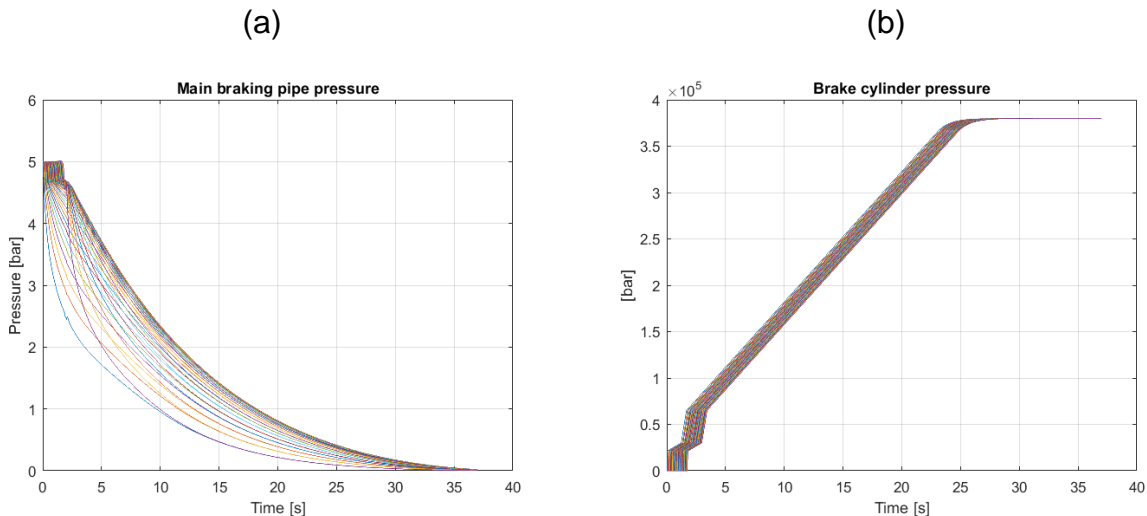


Figure 37: Time histories of pressure in main braking pipe (a) and braking cylinders for scenario 106

3.3.2 Degraded condition

Scenario 202

As far as the pneumatics is concerned, this scenario is characterized by the application of emergency braking from the master loco with a simultaneous communication loss. Braking regime LL is assumed. The slave loco supports the venting of the main braking pipe by monitoring the pressure drop in the pipe itself. The support logic is the one described in 2.3.3, recalled hereafter:

1. The remote DBV on slave detects a 200 mbar pressure delta drop in 500ms
2. The remote DBV discharge the brake pipe to 4.2bar, applying 0.2bar/s pressure gradient
3. The remote DBV brings BP to 4.2 bar and continues to discharge the BP for 10-15s. After that Remote DBV is isolated from BP
4. The Remote DBV continues to monitor pressure in the BP
5. If remote DBV detects a further drop of 200 mbar of delta in 500 ms, discharges again the BP to 3 bar (FS brake), applying a 0.2bar/s pressure gradient and continues to discharge the BP for 10-15s with BP pressure already achieved 3bar; then remote DBV is isolated from BP

Figure 38a reports the time history of pressure drop in main braking pipe clearly showing the behaviour of the slave loco: Four distinct phases can be observed after the first sudden drop. In particular the slave loco controls the pressure gradient up to 4.2 bar; then pressure is kept around 4.2 bar until the threshold on gradient is crossed a second time. Another discharge phase is thus triggered till the pressure in MBP reaches 3 bar. The support from the slave loco allows to reach a pressure drop to 3.5 bar in the last vehicle after 10 s from the braking command activation (which starts at 2 seconds).

Figure 38b refers to the time histories of pressure in the brake cylinders. The control logic has a clear impact over the last wagons. Due to the LL braking regime, the maximum pressure in the master loco and the first 5 vehicles is reached after 25 s from the braking command activation.

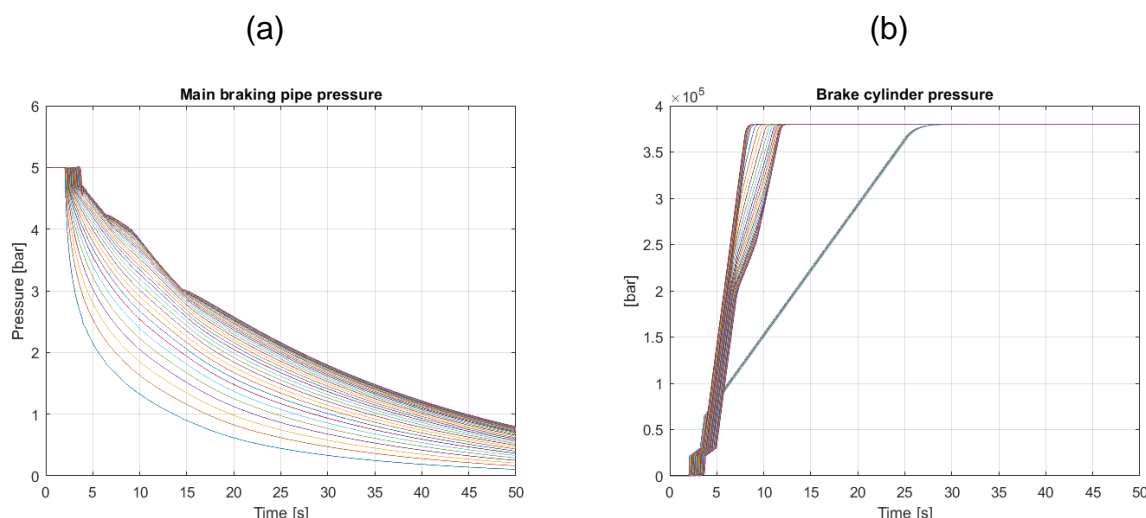


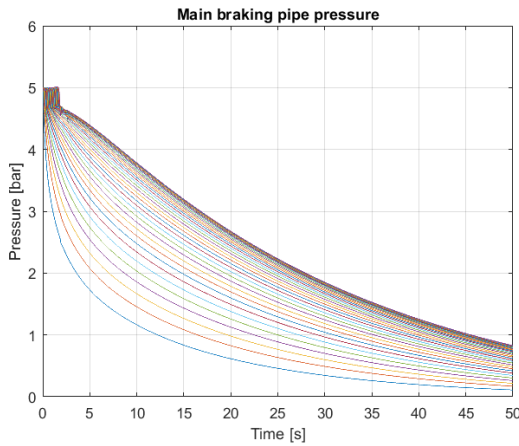
Figure 38: Time histories of pressure in main braking pipe (a) and braking cylinders (b) for scenario 202

Scenario 203

In this case an emergency braking from the master loco is commanded but the slave loco does not react, i.e. no venting of the main braking pipe by the slave loco. Figure 39a reports the time histories of pressure in the main braking pipe; Comparing Figure 39a with Figure 38a put into evidence the effect of the support of venting process from the slave loco also in degraded condition.

Also the comparison between time histories of pressure build-up in cylinders (Figure 38b vs Figure 39b) evidences the benefit of the venting support.

(a)



(b)

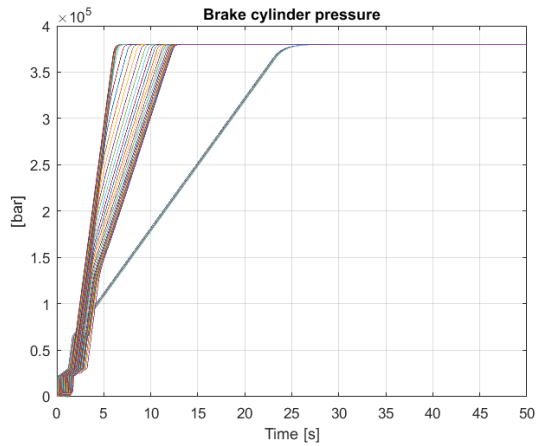
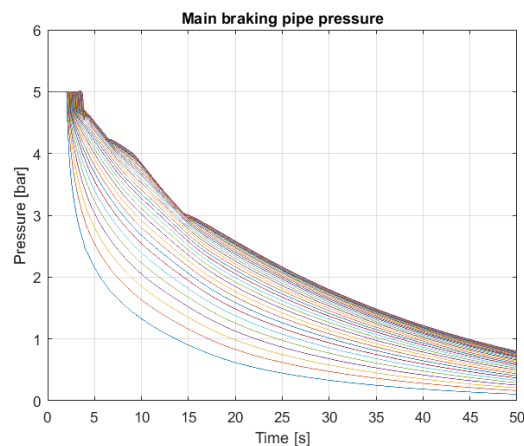


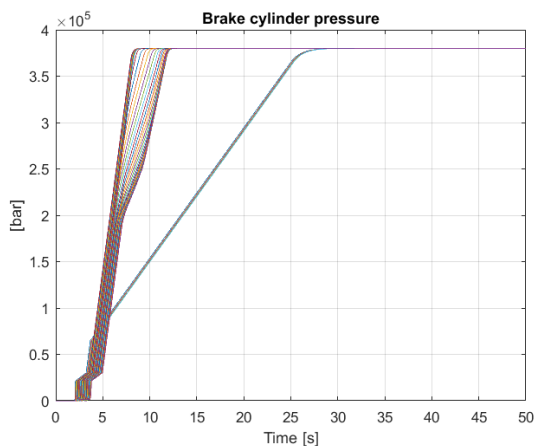
Figure 39: Time histories of pressure in main braking pipe (a) and braking cylinders (b) for scenario 203

Scenario 204

The operating condition of scenario 204 is identical to the one of scenario 201, at least from the pneumatics point of view.



(a)



(b)

Figure 40: Time histories of pressure in main braking pipe (a) and braking cylinders (b) for scenario 204

Scenario 205

In this scenario an emergency braking is commanded from the master loco; a DPS control failure causes the slave loco to refill the pipe instead of venting it. Pressure build-up in the rear vehicles is thus delayed.

As shown in Figure 41a, the time required to reach a pressure drop of 1.5 bar on the last vehicle is around 30 s, compared to 10 s of scenario 202 and to 13 s of 203. As a consequence also the pressure build-up in vehicles is significantly larger (see Figure 41b): the response of the vehicles in G position cannot be distinguished so clearly from the one of the last vehicles.

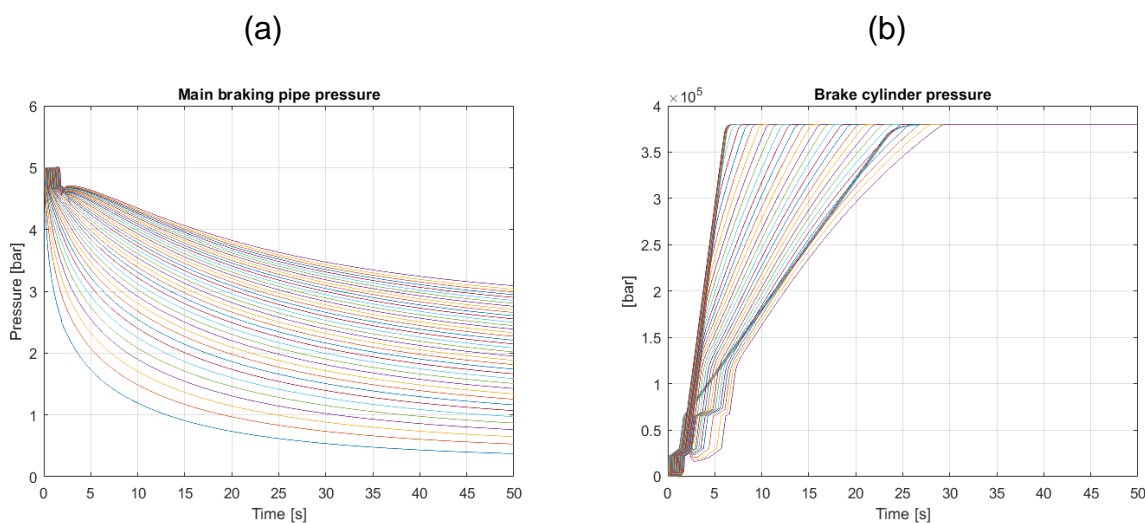


Figure 41: Time histories of pressure in main braking pipe (a) and braking cylinders (b) for scenario 205

Scenario 206

Scenario 206 considers a train disruption after the first vehicle. The rupture of the main braking pipe hose subsequent to this event, causes the venting of the pipe itself at the interface between vehicles 1 and 2. This condition was simulated considering one simulation with the master loco alone and one simulation with the second part of the train alone (i.e. from vehicle 2 to the end of the train). Data were then put together to obtain the time histories of pressure in main braking pipe and in braking cylinders.

Results of Figure 43 are referred to the case where the slave loco does not react to the pressure drop in the main braking pipe; This means that the slave does not support the venting of the main braking pipe from the rear. Figure 43a reveals how the master loco, once detached from the rest of the train, obtains an almost instantaneous pressure drop in the main braking pipe. Despite this, due to the G position, the dynamics of the pressure

build-up in the braking cylinder for the master loco is almost the same as for the first 5 vehicles of the second part of the train (Figure 43b).

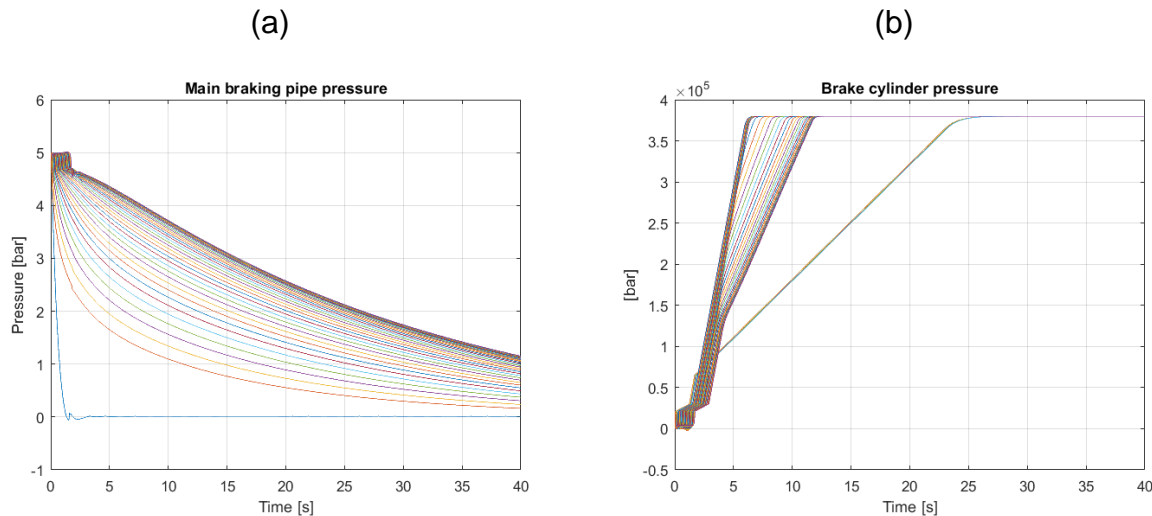


Figure 42: Time histories of pressure in main braking pipe (a) and braking cylinders (b) for scenario 206

In addition, the activation of automatic braking from the slave loco as a consequence of the unexpected pressure drop in the main braking pipe was considered. In particular, it is assumed that when detecting a pressure drop larger than 200 mbar in 0.5 s, the slave loco performs a maximum service braking. The event is triggered as the support logic of venting from the slave loco. In this case the radio communication between master and slave loco is still active; This determines the different strategy adopted by the slave loco. So when the radio communication is off, a pressure drop larger than 200 mbar in 0.5 s triggers the venting support logic according to the process described when discussing scenario 202. When the radio communication is on, like in this case, a maximum service braking is performed.

Figure 43 shows the time histories of pressure drop in main braking pipe and of pressure build-up in braking cylinders, assuming a maximum service braking performed by the slave loco. The effects on the rear part of the train are clearly visible.

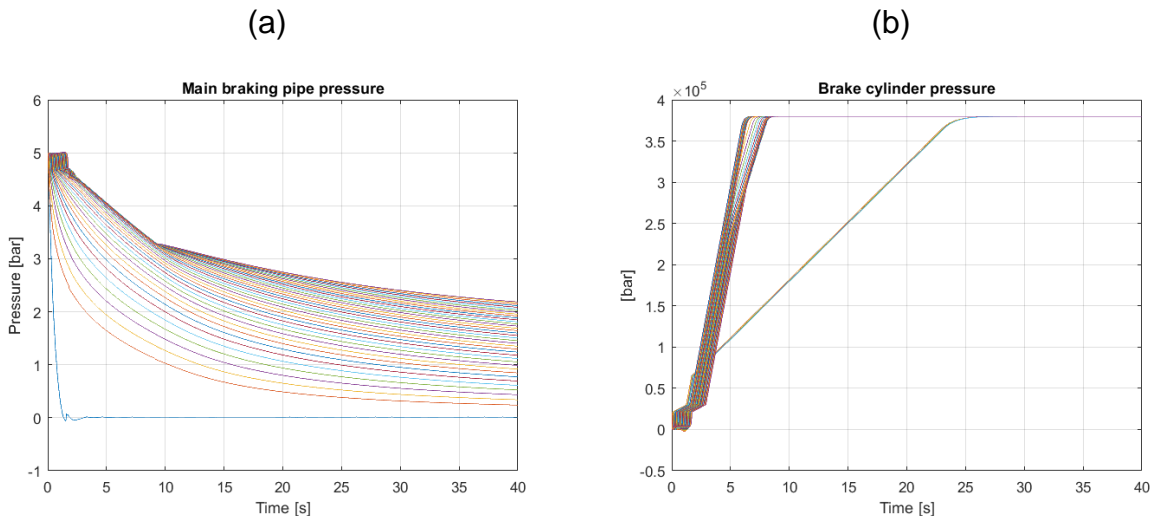


Figure 43: Time histories of pressure in main braking pipe (a) and braking cylinders (b) for scenario 206 assuming maximum service braking from the slave loco

Scenario 207

This scenario considers a malfunction of the DSP control, causing a discharge of the main braking pipe from the slave loco. From the pneumatics point of view, three sub-cases were analysed, assuming:

- No reaction from the master loco
- Maximum service braking applied by the master loco
- Emergency braking applied by the master loco

When a reaction of the master loco is considered, the braking is always triggered by the detection of a pressure drop larger than 200 mbar in 0.5 s in the main braking pipe.

Figure 44 shows the time histories of pressure drop in the main braking pipe and of pressure build-up in the cylinders with no reaction from master loco (first sub-case).

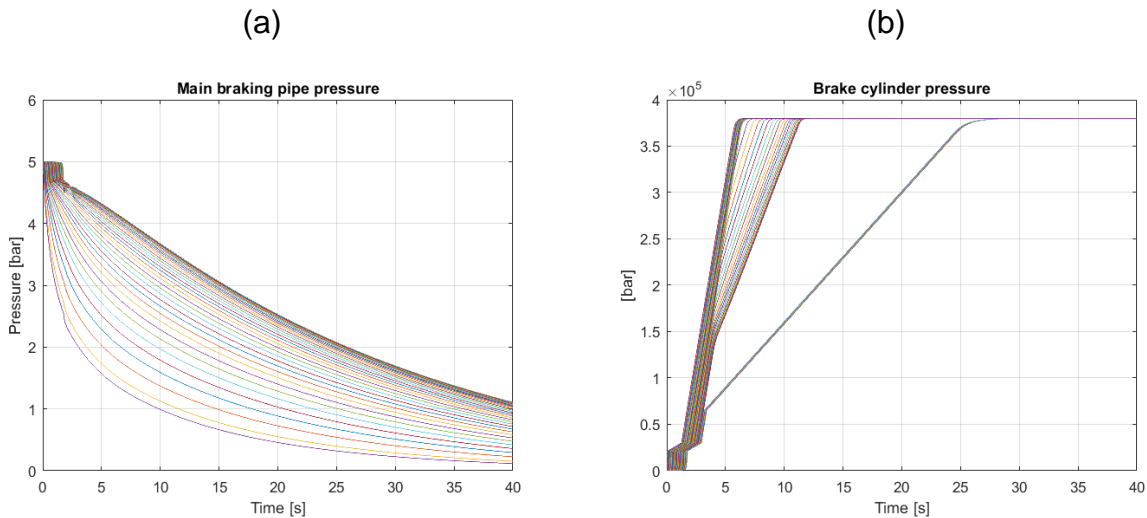


Figure 44: Time histories of pressure in main braking pipe (a) and braking cylinders (b) for scenario 207; no reaction from master loco.

Figure 45a shows with colour code the variation of pressure drop in the main braking pipe as function of time and vehicle position. This allows to notice how the pressure drop starts from the tail of the train. As a consequence pressure build-up develops first in the rear part of the train (Figure 45b).

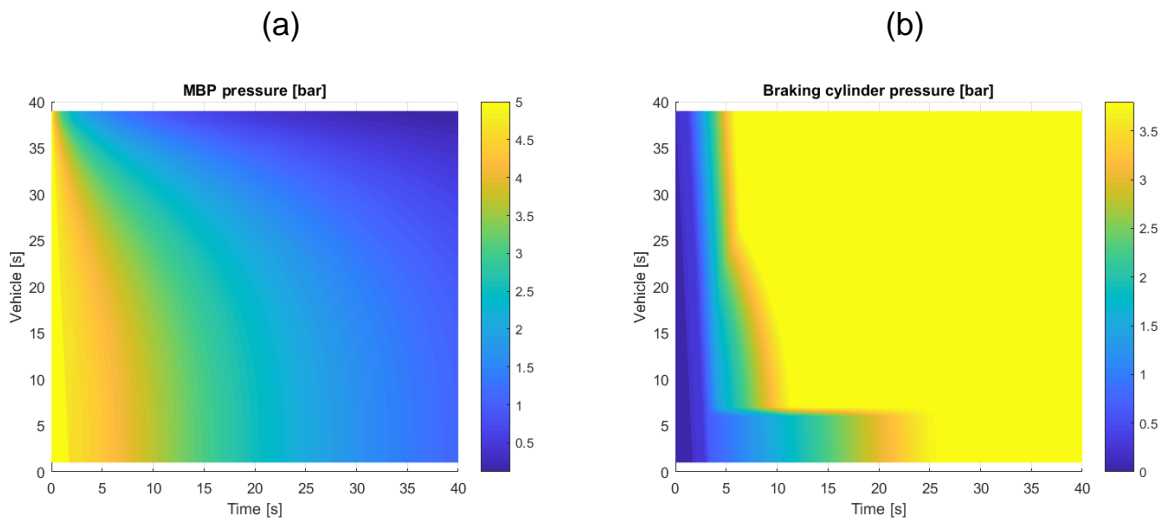


Figure 45: Pressure in main braking pipe (a) and braking cylinders (b) as function of time and wagon position for scenario 207; no reaction from master loco.

Figure 46 refers to the sub-case with the maximum service braking applied from the master loco. Differences in pressure time histories of both braking pipe and cylinders appear.

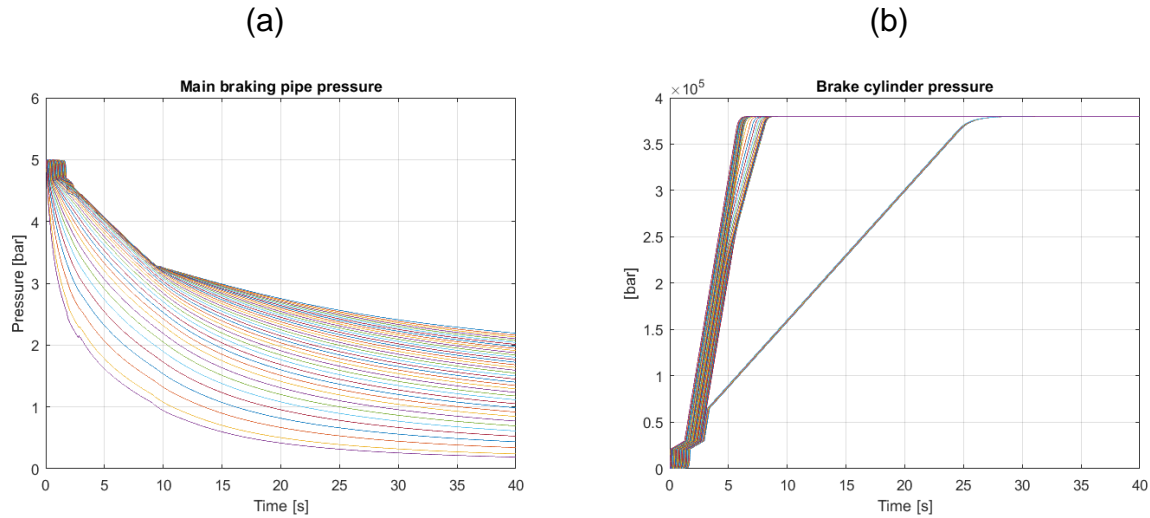


Figure 46: Time histories of pressure in main braking pipe (a) and braking cylinders (b) for scenario 207; maximum service brake applied by master loco.

As last, Figure 47 shows the time histories of pressure drop in the braking pipe and of pressure build up in the cylinders when the master loco performs an emergency braking when detecting an unexpected pressure drop in the main braking pipe.

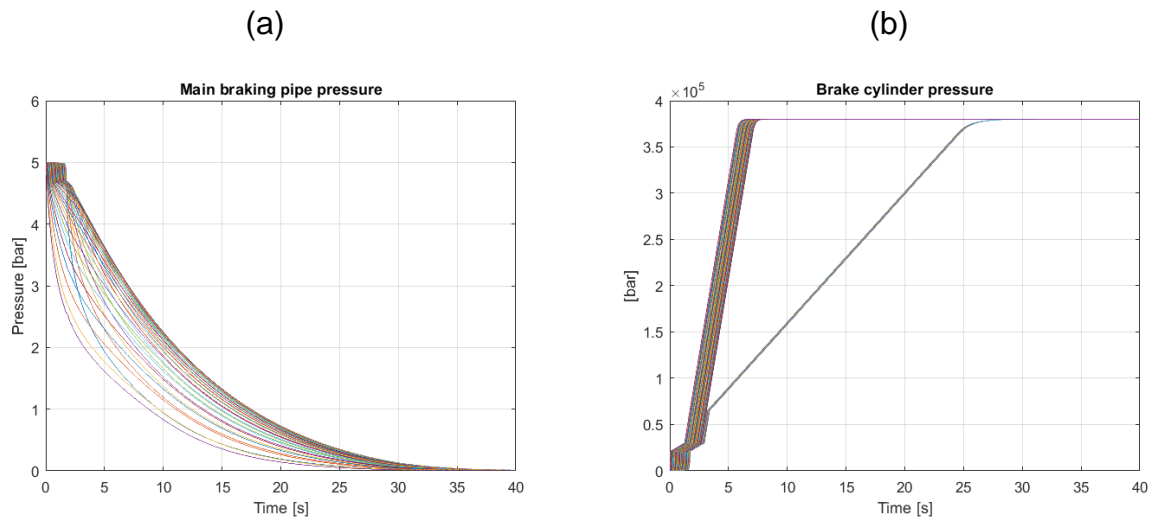


Figure 47: Time histories of pressure in main braking pipe (a) and braking cylinders (b) for scenario 207; emergency brake applied by master loco.

3.4 1D SIMULATIONS (ACTUAL FORCES)

Table 6 and Table 7 show the results of the 1D simulations of the scenarios described in Section 3.2. Table 6 shows the results for the nominal condition of the train. The LCF and LTF values are determined by traction forces (both accelerating and braking) of the two locomotives. The values are all around 300 kN. The LCF and LTF induced by the pneumatic brakes at emergency applications from 100 km/h are all uncritical and comparatively low. The highest values occur in brake regime P, followed by LL and G. The stopping distances behave the other way round. The highest value of 890 m occurs in brake regime G and the lowest of 794 m in brake regime P. The influence of the active venting of the main brake at both master and slave loco is visible only in brake regimes P and LL. This mechanism leads to shorter stopping distances and lower LCF. The behaviour of LTF is heterogeneous.

Table 6: Results for nominal condition of the 530 m long train

Scenario	Max. LCF_1s / kN	at veh.	Max. LTF_1s / kN	at veh.	Max. LCF_10m / kN	at veh.	s_stop / m
101	-142	18	81	11	-143	17	803
102	-81	22	79	25	-83	23	819
103	-62	18	38	38	-63	18	890
104	-107	17	55	7	-108	17	794
105	-73	20	108	18	-74	21	809
106	-62	18	38	38	-63	18	890
107	-299	38	296	1	-284	38	-
108	-297	1	287	38	-290	1	-
109	-290	38	347	27	-286	38	72

Table 7: Results for degraded condition of the 530 m long train

Scenario	Max. LCF_1s / kN	at veh.	Max. LTF_1s / kN	at veh.	Max. LCF_10m / kN	at veh.
201	-300	38	303	1	-288	37
202	-411	20	404	29	-289	23
203	-156	25	138	21	-137	23
204	-126	24	167	11	-98	24
205	-313	25	88	6	-266	26
206	-147	25	115	19	-126	22
207	-27	38	322	15	-12	38

Table 7 shows the results for the degraded condition of the train. Scenario 202 (full traction + communication loss + simultaneous emergency brake application) is the most critical scenario with a maximum LCF value of 411 kN. The second most critical scenario is 205 (accidental filling of main brake pipe from slave during emergency application) with a maximum LCF value of 313 kN. Both scenarios are similar in terms of a delayed deceleration of the rear part of the train.

A train disruption after the first vehicle was investigated in scenario 206. This scenario does not lead to an impact with the given parameters. Even a forced collision after a disruption with alternative initial parameters (higher initial velocity and initial accelerating of only the master locomotive) does not lead to high forces.

Scenario 202 was investigated in more detail as it is the most critical scenario for the first application of the 530 m long coal train. The investigation shows that the delay of traction cut-off of the slave locomotive has a significant influence. This delay consists of two components. The first component is the maximum transmission time of the radio (two seconds) plus the reaction time of the radio to detect a communication loss (one second). The second component is the time for traction cut-off after a communication loss is detected (five seconds). UIC 647 proposes a traction cut-off within five seconds. This value is initially implemented in the locomotive control. UIC 647 addresses the communication between multiple locomotives in a train. However, it does not necessarily consider distributed locomotives within a train. Instead, it more likely considers multiple locomotives which are coupled to each other. Figure 48 shows that the maximum LCF values decrease as the traction cut-off behaviour becomes more similar. A similar behaviour should thus be aspired. The results are summarized in Table 8.

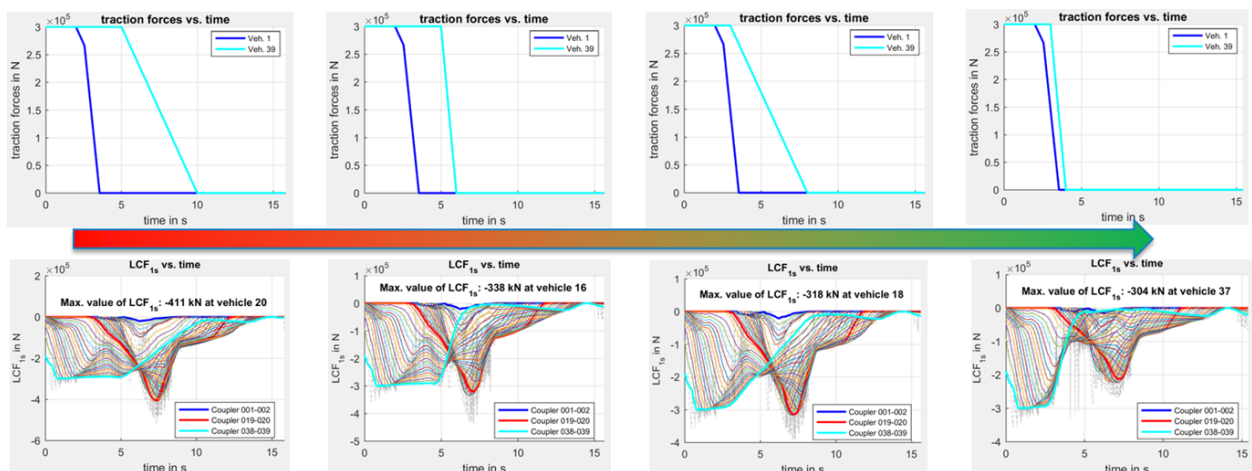


Figure 48: Dependency of LCF on traction behaviour in scenario 202

Table 8: Summary of results for altered versions of scenario 202

Scenario	Max. LCF_1s / kN	at veh.	Max. LTF_1s / kN	at veh.	Max. LCF_10m / kN	at veh.
202	-411	20	404	29	-289	23
202_3_1	-338	16	383	30	-289	38
202_1_5	-318	18	364	28	-288	38
202_1_1	-304	37	311	2	-283	38

It should be noted that the locomotive models have a second mechanism for traction cut-off, which is independent of the radio control. The mechanism is activated when a certain pressure drop in the main brake pipe of the locomotive is detected. At the current state a

pressure drop of at least 1.5 bar is needed to activate this second traction cut-off mechanism. In this case, the traction cut-off happens within one second. The functionality of this mechanism can be observed in the master locomotive in Figure 48 (steep dark blue gradients). However, even for a short train of only 530 m length, it takes more than 10 seconds before a pressure drop of 1.5 bar is reached at the last vehicle of the train (see also Figure 15). This means that a traction cut-off commanded by the radio is faster in this situation.

Besides the variation of traction cut-off behaviour, further parameter variations were performed for scenario 202. The variation included two steps. In the first step, 50 trains were built with a random distribution of all six variants of the FALNS 121 wagon (CI, LL or K blocks, each with either manual or automatic load device). The 50 different trains were then simulated in sequence. The train with the highest LCF values was then taken as basis for 1000 random parameter variations of the following parameters within the given ranges:

- Total mass of wagons (85 t – 95 t)
- Rigging efficiency (0.71 – 0.95),
- Buffers (4g, QGO, KSB)
- Draw gear (540.5-1500, Miner)
- Coupler play (-1 mm – 10 mm)

These 1000 variations were then simulated in sequence and the results sorted by LCF values. Figure 49 shows the entire procedure.

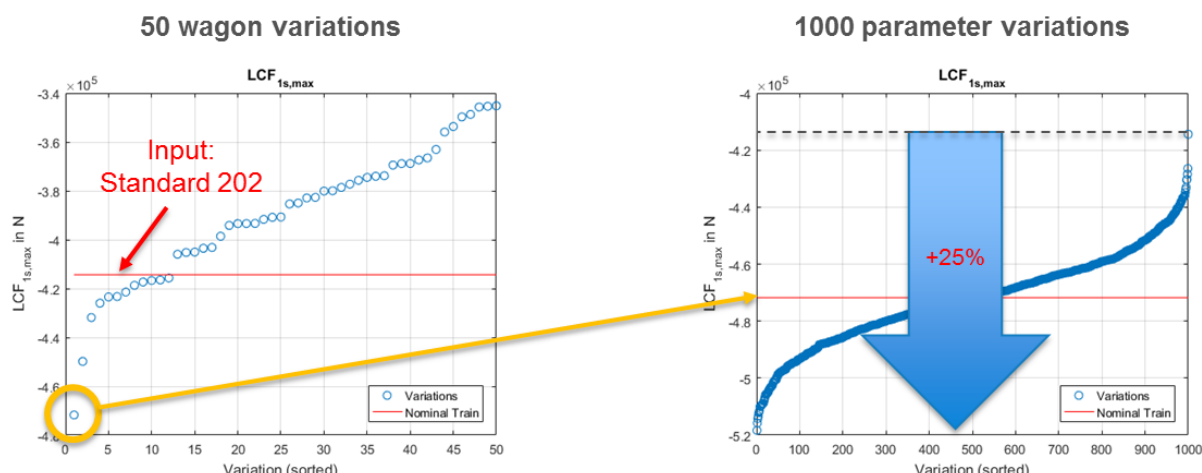


Figure 49: Procedure of parameter variations for scenario 202

The simulation results show that LCF might be up to 25% higher for a train with randomly distributed wagon variants and parameters than for a train with only nominal parameters and only one variant of wagon in scenario 202. To examine the influence of such

variations for other scenarios without having the computational effort of the described procedure, 21 trains (every 50th) of the 1000 variations were selected as indicated with red dots in Figure 50.

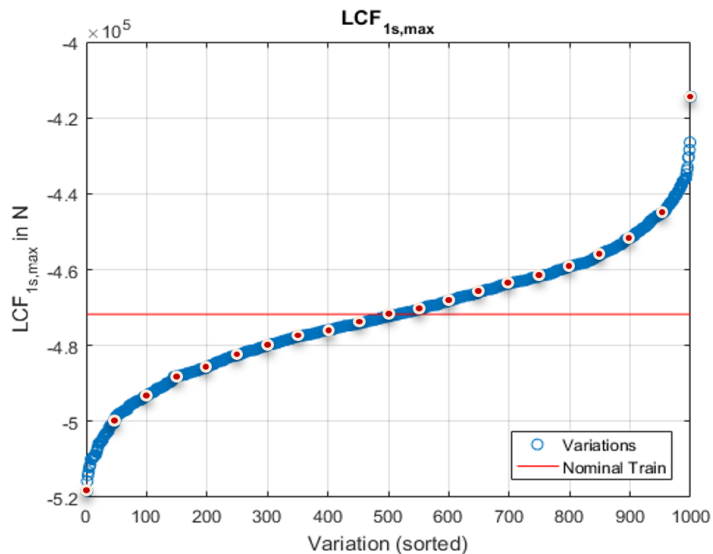


Figure 50: Trains taken from simulation in scenario 202 for simulation in other scenarios (indicated with red dots)

These 21 trains were then simulated for the scenarios 101, 103, 202 and 205. It seems likely that these 21 trains do not represent the entire range of possible results as shown for scenario 202. However, these 21 trains can be considered as very different from each other. They will therefore presumably represent the order of influence that these variations have on the nominal results. Figure 51 shows the nominal values for the mentioned scenarios and the respective maximum and minimum values of the variations on the left side. The right side shows the relative increases of varied scenarios with regard to the standard scenario.

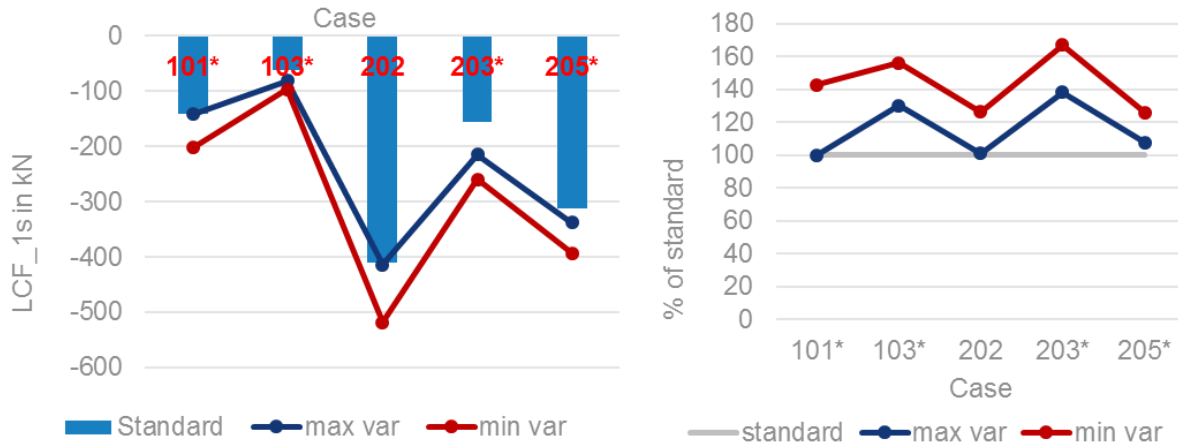


Figure 51: LCF values for nominal and varied trains in selected scenarios

The potential increase of LCF values by factors of up to 1.7 due to variations of parameters should be kept in mind when comparing 1D simulation results (of standard scenarios) with tolerable LCF limits.

The influence of gradients on the resulting LCF has been examined very early on. The results show that gradients, especially sags, have a significant influence on LCF. A particular critical case is a scenario where the pressure build-up of the pneumatic brakes is finished at the same time when the middle of the train is in the bottom of the sag. Figure 52 shows the results for the demonstrator train on different kinds of gradients.

brake regime	result	horizontal track	ascending slope	descending slope	sag
P	LCF_10 m in kN	309	284	317	543
	LCF_max in kN	359	329	356	648
	Δ LCF_10 m	100%	92%	102%	176%
	Δ LCF_max	100%	92%	99%	181%
LL	LCF_10 m in kN	193	172	193	379
	LCF_max in kN	212	198	207	438
	Δ LCF_10 m	100%	89%	100%	196%
	Δ LCF_max	100%	93%	97%	206%
	gradient in 1/1000	0	12.5	-12.5	-12.5 / 12.5
		—	/	\	\\/

Figure 52: Influence of gradients on LCF values

Furthermore, some variations of the gradients suggest that the increase of LCF in sags can be calculated with the static equilibrium of the train within the sag as a first

approximation. However, the 3D simulations identified tight S-curves as the most critical infrastructure (see Section 3.5.3). This type of infrastructure is commonly only found in stations, which are mostly horizontal or almost horizontal. This means that the critical infrastructure and increased LCF due to gradients do not occur at the same position.

Because of this fact and the possibility to superpose the results of trains on horizontal track with the static equilibrium in sags, no further simulations of trains in gradients were conducted.

3.5 3D SIMULATIONS (TOLERABLE FORCES): FALNS 121 & FALNS 183

The two open wagons 'FALNS 121' and 'FALNS 183' are used for transporting coal were chosen in the present application. These are used to transport coal. Link suspension bogies (bogie-type 665) are used as the running gear. The values for Bogie pivot lengths, Buffer to Buffer distances, Buffer lengths of the wagon types are given in Table 9 (see Figure 53).

Table 9: Bogie pivot length, Buffer to Buffer distance and Buffer length of the two wagons

Parameter	FALNS 183	FALNS 121
Bogie pivot length ($2a$) [m]	7.5	7.7
Buffer to Buffer distance ($2L$) [m]	12.54	13.04
Buffer length (b_l) [m]	0.62	0.62
Wheel base length ($2a_b$) [m]	1.8	1.8

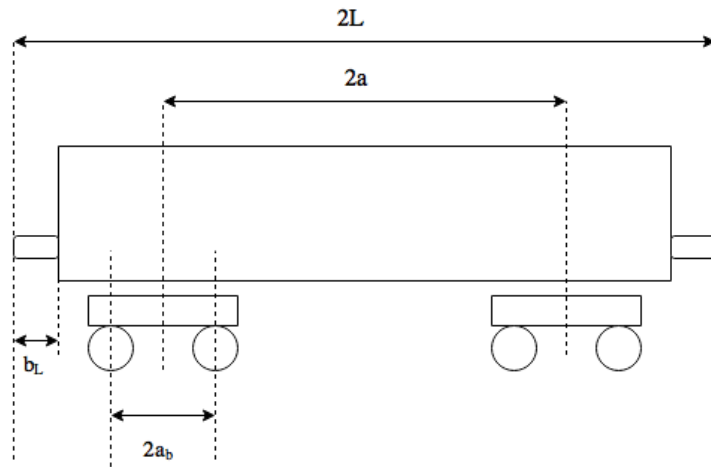


Figure 53: Wagon key geometry parameters [10]

3.5.1 Running gear: Link suspension bogie

The FALNS type wagons are equipped with link-suspension bogies with parabolic leaf springs (bogie-type 665) as shown in Figure 54. The modelling is based on the benchmarked GENSYS model from [19]. The primary suspension consists of leaf springs in the vertical direction and a front and a rear link for the lateral and longitudinal directions. The longitudinal, lateral and vertical suspension is modelled by a friction damper and a linear spring in series, parallel to a linear spring to account for the hysteresis in the suspension characteristic.

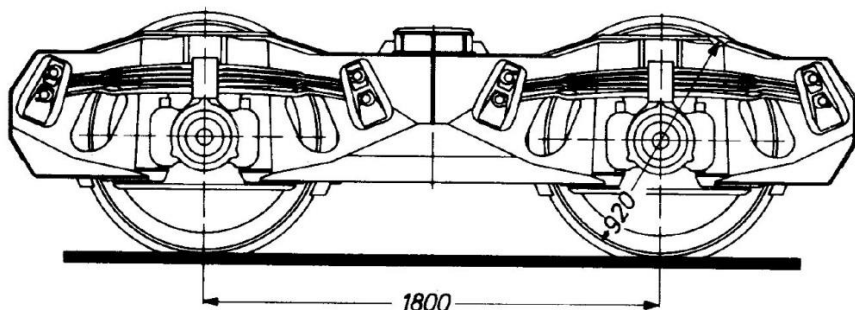


Figure 54: Bogie-type 665 [21]

The secondary suspension consists of a spherical centre pivot and two rigid side bearers. The stiffness of the centre pivot in the translational degrees of freedom is taken to be very stiff. In rotational degrees of freedom, however, friction damping is modelled similar to the

primary suspension. The friction coefficient multiplied by the dynamic normal moment gives the breakout torque (the torque required for rotational sliding). For a carbody in the nominal centre position, the sidebearers are not in contact vertically. A nominal play of 5 mm is allowed beyond which it acts like a bumpstop in the vertical direction. Two standard buffer models, QGO and Keystone buffers are used in the study.

3.5.2 Sensitivities of individual heterogeneities

As described in Section 2.5, the sensitivities of individual heterogeneities on the tolerable LCF values were first checked. The sensitivities are checked in a stepwise manner. At each step, the model complexity is increased and the sensitive parameters are included for the next step of simulations. In the initial step, sensitivities of the *buffer types, wagon arrangements, loading patterns, track radii and gradients* are checked. In this step, the wagons are modelled with rigid car bodies.

Buffer types, wagon arrangements and payload:

The sensitivities arising due to heterogeneities in buffer types, wagon arrangements and payload are checked initially (see Figure 55). Here '*m0e0*' indicates a wagon combination where both middle (empty) and barrier wagons (fully loaded) are of FALNS183 type. QGO and Keystone buffers are denoted by QGO and KSB respectively. The results for the different cases can be seen in Table 10.

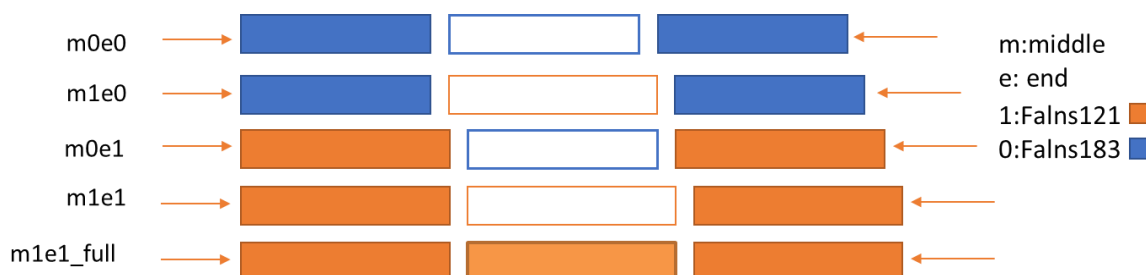


Figure 55: Simulation cases and nomenclature. Fill and no-fill indicate fully loaded and empty cases respectively.

The buffer with higher energy absorption (KSB) increases the static LCF limit significantly as compared to QGO (>85% on average). But when used in combination (QGO - KSB), the LCF limit lies in between that of QGO and KSB buffers, skewed more towards QGO. This could be due to the limited energy absorption at higher deformations by QGO in the combination.

The train with all 'FALNS 183' type wagons (m0e0) have a higher LCF. When longer wagon is placed in between shorter wagons (m1e0), the LCF limit increases by 9% when either QGO or KSB type buffers are used. But it seems to decrease when both QGO and KSB are used in series. When a shorter wagon is placed in between longer wagons

(m0e1), the LCF increases (< 5%) as compared to the case with the train system with all 'FALNS 121' type wagons (m1e1). Overall, there seems to be a trend of decreasing LCF limit values with increasing train lengths. This can be explained by the increasing deviation of the wagon ends from the track centre line with increasing bogie pivot lengths leading to increasing lateral forces.

Table 10: Tolerable LCF values: Comparison for different buffers, wagon arrangements and payloads (S150M6)

Configuration	Buffer-1 (QGO) [kN]	Buffer-2 (KSB) [kN]	Buffer-1-2 [kN]
m0e0	440	880	760
m1e0	480	960	520
m0e1	400	720	480
m1e1	400	680	440
m1e1_full	480	720	-

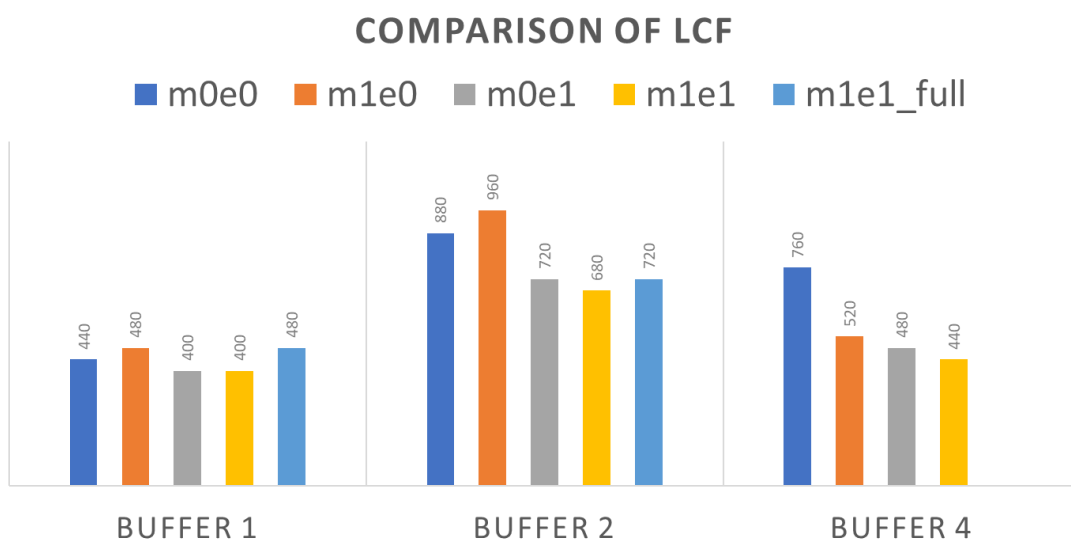


Figure 56: Tolerable LCF values: Comparison for different buffers, wagon arrangements and payload

Most of the cases discussed in above have empty test wagons as proposed in the UIC standard. The difference in loading between the barrier and test wagons resulted in a buffer height difference of about 50 mm. For comparison, the nominal case with all the

three wagons loaded, resulting in equal buffer heights, are checked as well. The critical case w.r.t wagon length (*m1e1_full*) is chosen for the same. There is an increase of 80 and 40 kN respectively for the cases with buffers QGO and KSB respectively as can be seen in Figure 56. This marginal increase despite an additional loading of 65 tons (~637 kN vertical force) points to the high effect of lateral forces on wagon stability in tight curves. Subsequent simulation cases are hence focussed more on the critically loaded cases with QGO buffers.

Curvature and gradients

In this step, the track geometry design is varied beyond the UIC 530-2 based S150M6 track. Circular curves with constant radius of 300 m and 600 m were also checked. The results are given in Table 11. The tolerable LCF values are low for the S-curve with 150 m radius while higher for circular curves. LCF's in the magnitude of 6000-10000 kN rarely occur in long freight train operations and it is also demonstrated by the type of derailment that occurs for these cases. So the circular section with a radius of 600 m is not considered critical. As seen in Figure 57, the derailment occurs due to the lifting of the wagon rather than due to lateral roll-over as was the case for S150. Simulations were also performed by varying the length of the intermediate section of the S-curve between 6 and 10 m. This did not influence the magnitude of tolerable LCF.

Table 11: Tolerable LCF values: Comparison between curvatures (QGO buffer)

Configuration	R300 [kN]	R600 [kN]
m0e0	6200	-
m1e0	6000	-
m0e1	6200	-
m1e1	6000	10860
m1e1_full	7120	11826

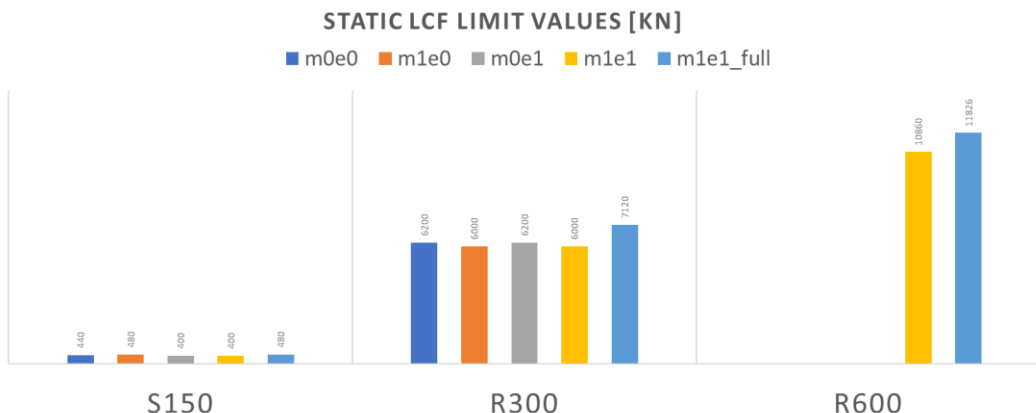


Figure 57: Tolerable LCF values: Comparison between curvatures (QGO buffer)

In cases of challenging gradients, the tolerable LCF could be affected. The circular curve of 300 m radius (R300) and the S-curve of 190 m radius (S190M10) were chosen with wagon combinations m1e1 and m1e1_full to study the effect of gradients because of the lower tolerable LCF seen in the previous subsections. Two gradient cases were modelled with steep ascent and descent of 10/mille respectively and compared with the tolerable LCF of the corresponding horizontal track case. An additional case of 98.5 mm cant excess was also checked for the circular track section. The tolerable LCF's are listed in Table 12.

The gradients do not have a significant effect on values obtained for a horizontal track irrespective of the type of horizontal curvature, showing a maximum variation of about 2% with the downhill gradient case having slightly lower while the uphill gradient having slightly higher tolerable LCF values. But, the presence of cant excess significantly increases the tolerable LCF (~20%).

Table 12: Tolerable LCF values: Comparison between gradients (QGO buffer)

Configuration	Curve	m1e1 [kN]	m1e1_full [kN]
Horizontal	S190M10	1050	2687
Uphill (+10/mille) [kN]	S190M10	1118	2719
Downhill (-10/mille) [kN]	S190M10	986	2640
Uphill (+10/mille) [kN]	R300	6063	-
Downhill (-10/mille) [kN]	R300	5875	-
Cant excess	R300	7246	-

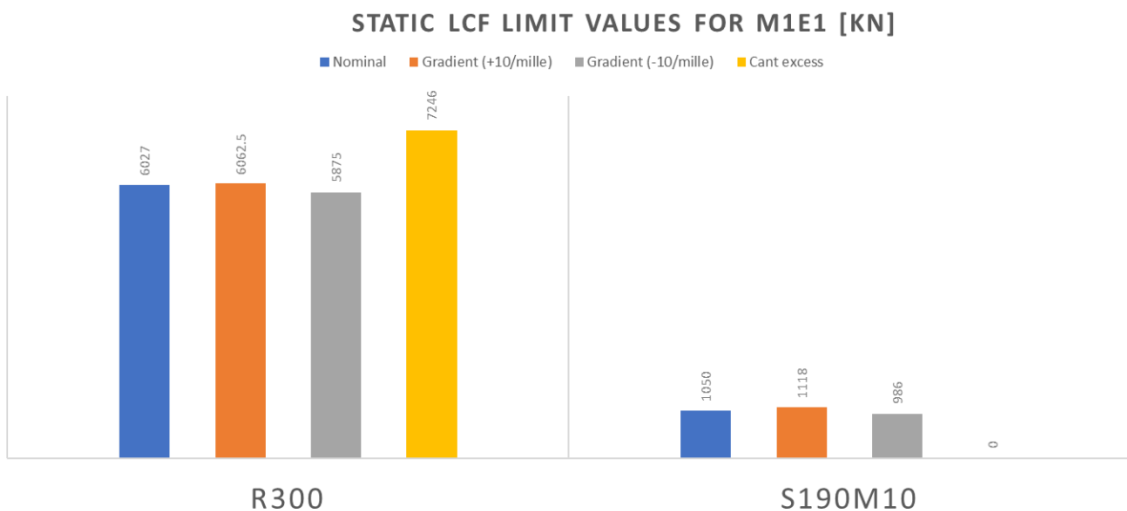


Figure 58: Tolerable LCF values: Comparison between gradients (QGO buffer)

Carbody torsional flexibility

In this step, carbody torsional flexibility is introduced. The torsional flexibility of the wagon is taken as 4×10^{10} kNm²/rad based on the 'Tds930' type wagons which have a similar carbody construction. Simulations were performed for S-curves with varying curvatures: S150M10, S170M10, S190M10, S200M10, S210M10 and S220M10 for the m0e0, m1e0, m0e1 and m1e1 cases. The results for the critically loaded cases are given in Table 13.

Table 13: Tolerable LCF values for critically loaded cases with torsionally flexible car bodies

Curve	Buffer	m0e0 [kN]	m1e0 [kN]	m0e1 [kN]	m1e1 [kN]
S150M10	QGO	367	343	352	336
S170M10	QGO	406	375	391	375
S190M10	QGO	460	430	445	421
S200M10	QGO	617	469	539	445
S210M10	QGO	875	609	727	594
S220M10	QGO	898	882	859	852
S150M10	KSB	414	-	-	797
S170M10	KSB	922	-	-	875
S190M10	KSB	1023	-	-	984

Similar simulations were also performed for the nominally loaded m0e0_full and m1e1_full cases (Table 14).

Table 14: Tolerable LCF values for nominally loaded cases with torsionally flexible car bodies

Curve	Buffer	m0e0_full [kN]	m1e1_full [kN]
S150M10	QGO	430	398
S170M10	QGO	508	461
S190M10	QGO	922	570
S220M10	QGO	1023	984

Tolerable LCF w.r.t buffer angle difference

For comparing the simulation cases with respect to coupler angles, two additional fictitious wagons were modelled, one shorter than FALNS 183 and the other FALNS 121. The tolerable LCF values for the rigid and the torsionally flexible cases are compared w.r.t. maximum buffer angle difference formed during the curve negotiation for S150M6 and S190M10. QGO buffers were used in this analysis. The simulation parameters and results are given in Table 15.

**Table 15: Comparing Tolerable LCF values of rigid and torsionally flexible carbody cases
(Cases 2 and 3 are FALNS183 and FALNS121 respectively)**

Case	Pivot distance [m]	Buffer to Buffer Distance [m]	S190-M10 (Rigid CB) [kN]	S190-M10 (Flexible CB) [kN]	S150-M6 (Rigid CB) [kN]	S150-M6 (Flexible CB) [kN]
1	6.4	12.04	2036	516	484	362
2	7.5	12.54	2422	640	438	426
3	7.7	13.04	1050	554	391	388
4	8	13.95	514	437	375	300

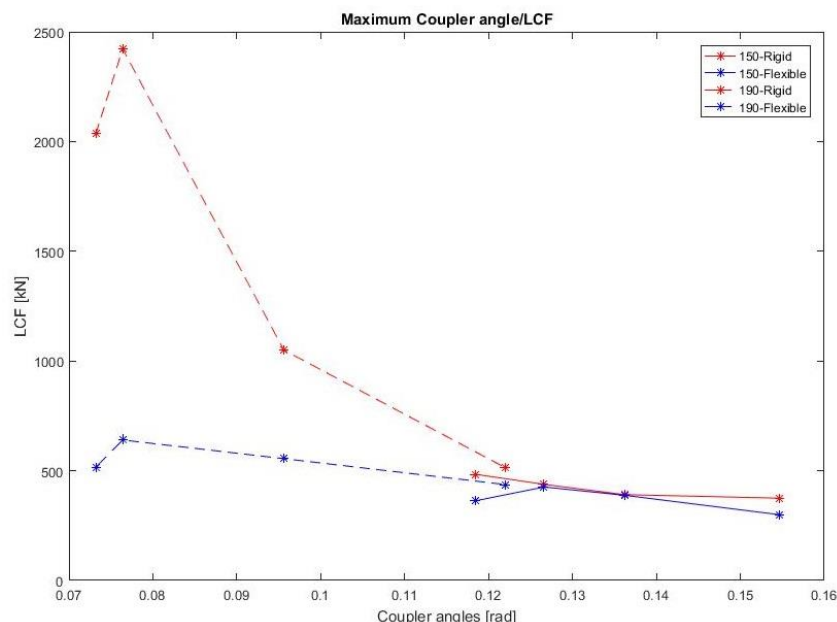


Figure 59: Comparison of Tolerable LCF between rigid and torsionally flexible wagon cases w.r.t maximum coupler angle (φ_{12max}): Red: rigid; Blue: flexible; Dashed line: S190M10; Solid line: S150M10.

As seen in Figure 59, the variation of tolerable LCF for the torsionally flexible carbody cases seems to be more steady as compared to the rigid carbody cases. More simulation cases were formulated and the trend between tolerable LCF and the maximum values of the coupler angle were checked. Different trendlines were constructed for the LCF values w.r.t buffer angle difference values for different buffers, wagon geometries and loading patterns as seen in Figure 60. The buffer angle is the angle between the centre lines of the adjacent wagons. The difference between the buffer angle on either side of the test

wagon gives the buffer angle difference which gives a measure of the yaw on the test wagon.

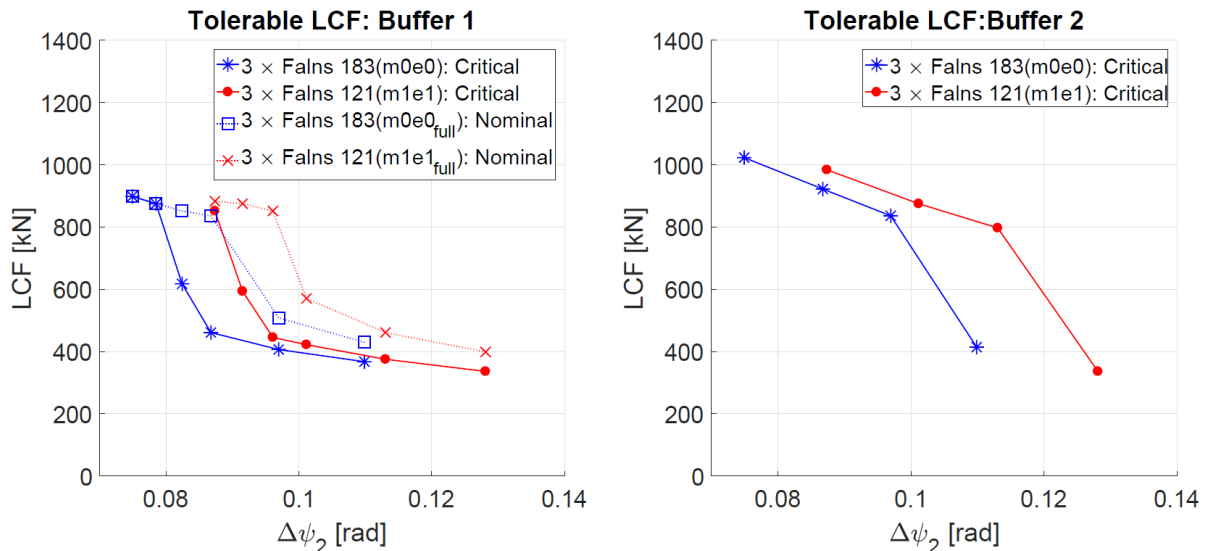


Figure 60: Tolerable LCF vs. buffer angle difference trends for m1e1 and m0e0 configurations. Buffer 1- QGO; Buffer 2- KSB

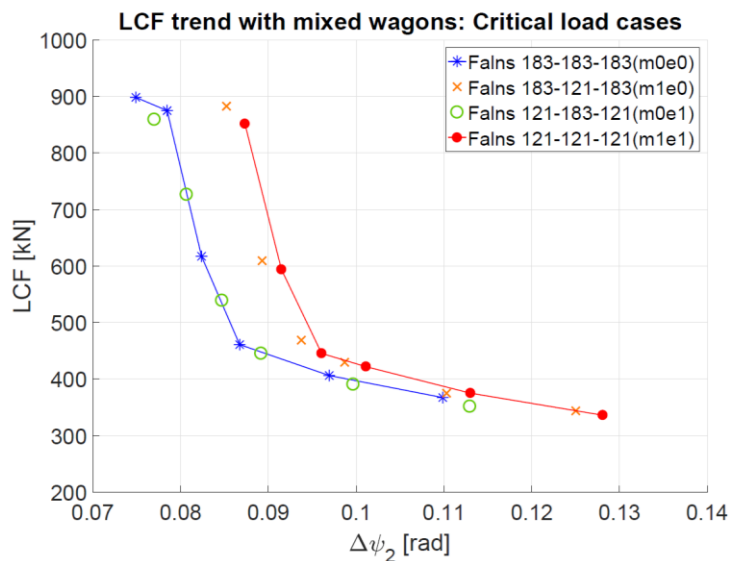


Figure 61: Tolerable LCF vs. buffer angle difference trends for mixed wagon configurations (m0e1 and m1e0).

Trendlines such as the ones seen in Figure 60 can be constructed for different wagon types so that the tolerable LCF values of mixed wagon configurations such as m1e0 and m0e1 can be calculated as well. The tolerable LCF values for the mixed configurations for the critically loaded cases with the QGO buffers super-imposed onto the m0e0 and m1e1 trends are given in Figure 61.

Derailment modes:

Over all, there is a decreasing trend for tolerable LCF with increasing bogie pivot lengths. The table below discusses more specific cases.

Table 16: Derailment mode examination

Curvature	Carbody (Length/Structural)	Derailment Mode
Very high (S150M6)	All/Both Flexible and Rigid	Happens due to wagon roll-over. The LCF is typically lower (~300-500 kN)
High (S190M10)	Short/Rigid	Happens due to empty wagon lift-off. The LCF is typically high (>1000 kN).
High (S190M10)	Long/Rigid	Happens in combination of wagon lift-off and roll-over. LCF is in medium range (<1000 kN)
High (S190M10)	Short and long/Flexible	Happens due to wagon roll-over. The LCF is typically lower (~400-600 kN)

3.5.3 Stochastic studies

Based on the assessment of the effect of individual heterogeneities in the previous section, a stochastic variation of different heterogeneities was formulated and 40 random train cases with different heterogeneities relating to wagon and operation were formulated. The 40 cases hence generated were all run on S-curves with radii 150 m, 190 m and 220 m respectively. Figure 62 represents the heterogeneities covered by the same.

The LCF values w.r.t. different loading patterns are shown in Figure 63. Despite all the introduced heterogeneities, it is demonstrated that the tolerable LCF values are high with homogeneous *distribution of payload in adjacent wagons* (Diagonal boxes). Strong effects of *torsional stiffness of the carbody and buffer characteristics* on the tolerable LCF values was also seen.

Wagons: Falns 121 and Falns 183	(2x2)	 									
Buffer:	(3)	QGO, KSB, KSB-QGO series									
Torsional stiffness	(3)	2.4e7, 4e7, 6.6e7									
Loading conditions	(3)	22.5 ton/axle 14.3 ton/axle 6 ton/axle									
Wagon arrangement (w.r.t payload)	(9)	<table border="1" data-bbox="858 713 1187 809"> <tr> <td>E-E-E</td> <td>E-H-E</td> <td>E-F-E</td> </tr> <tr> <td>H-E-H</td> <td>H-H-H</td> <td>H-F-H</td> </tr> <tr> <td>F-E-F</td> <td>F-H-F</td> <td>F-F-F</td> </tr> </table>	E-E-E	E-H-E	E-F-E	H-E-H	H-H-H	H-F-H	F-E-F	F-H-F	F-F-F
E-E-E	E-H-E	E-F-E									
H-E-H	H-H-H	H-F-H									
F-E-F	F-H-F	F-F-F									

Figure 62: Heterogeneities covered in stochastic simulations. (F- Fully loaded, H- Half loaded and E- Empty wagon)

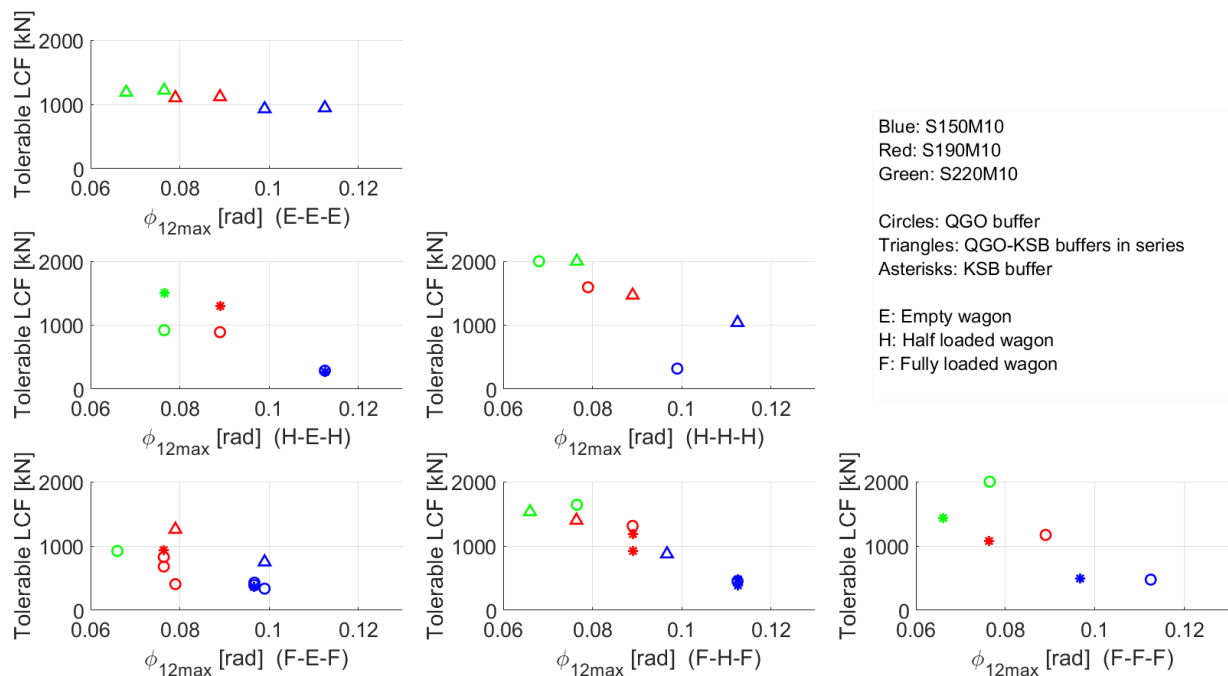


Figure 63: Results: Stochastic investigation sorted by payload distribution.

3.6 ACTUAL VS. TOLERABLE FORCES

Based on the plots seen in Figure 60 and the results obtained in Section 3.4, the actual forces for different scenarios were compared with the tolerable LCF values. In Figure 64 the yellow lines depict actual forces for nominal scenarios while the magenta lines depict the in-train forces for the degraded scenario. They are the maximum values of actual forces (LCF), filtered by a sliding 1s mean filter. The tolerable LCF curves correspond to the critical load cases where an empty wagon is surrounded by two fully loaded wagons. The nominal load case where all the wagons are fully loaded are not plotted since their tolerable LCF values do not exceed the maximum actual forces seen in Figure 64.

It can be seen that the maximum actual force values for nominal braking scenarios generally lie below the tolerable LCF values for all curvatures. However, there are some degraded braking scenarios where the simulated actual forces are more than the computed tolerable LCF values. For the maximum actual forces for the nominal and degraded scenarios, refer to Table 6 and Table 7. The critical scenario is the degraded scenario 202. It corresponds to emergency application of braking at the master locomotive with full traction and communication loss to the slave locomotive. The braking regime is LL.

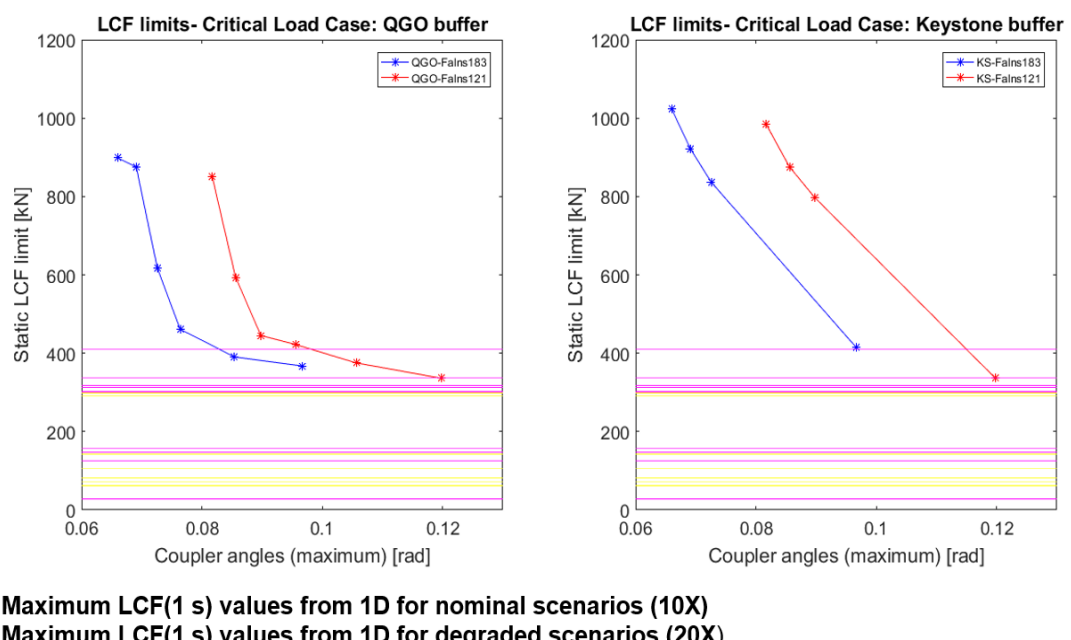


Figure 64: Actual vs. Tolerable forces - Demonstrator train

3.7 CONCLUSIONS AND SAFETY PRECAUTIONS

As far as the demonstrator train is concerned, the lowest tolerable LCF occurs at the tightest S-curve ($R = 150$ m). The limit value is 336 kN. This scenario occurs for the comparatively longer FALNS 121 train, compared to the 367 kN value for the corresponding case with FALNS 183 wagons. It should however be noted that the present demonstrator operation does not involve S-curves of radii less than 190 m along its route. Hence, it should be sufficient to consider the higher tolerable LCF values (see Table 13), corresponding to the S-curve with a radius of 190 m. For this curve, the train operation is safe even during degraded braking scenarios. In addition to this, modification of the second mechanism for traction cut-off in locomotives (see Section 3.4) is thus to be considered for other applications.

A general conclusion is that the present demonstrator train is safe if only the nominal braking/traction scenarios are considered but will still have derailment risks in case of a degraded braking scenario. This could be the case involving communication losses between the locomotives, further compounded by the effect of train attributes such as curvature, loading pattern, length, etc. As a precautionary measure, the positioning of critical wagon combinations along the train (w.r.t. payload) needs to be examined such that in case of a degraded braking scenario, it lies at a position with minimum actual force occurrence.

4. SECOND APPLICATION: TRAINS UP TO 1500 M LONG

4.1 INTRODUCTION

The demonstrator train described in Chapter 3 is one very special application for radio-controlled traction and braking. It is characterized by a train configuration that is very homogenous in many aspects. There is only one basic wagon type in the train (FALNS) where the train length is always 530 m and the wagons in the train are either all fully loaded or all empty. The only inhomogeneous aspects are the slight differences in length of the two subtypes of wagons (FALNS 121 13.04 m, FALNS 183 12.54 m), the different brake block materials, load devices and different buffer and draw gear types.

Several dozen simulations with varied parameters are necessary even for this comparatively homogeneous train in order to find critical scenarios and train configurations. Every variable parameter will lead to an exponentially growing number of possible train configurations. For example, if we consider one train with 50 wagons of the same type with 20 t of empty weight and only vary the payload in 10 t increments between 0 and 70 t for each wagon, we have $8^{50} = 1.4 * 10^{45}$ possible train configurations. Therefore, it is obvious that it is impossible to simulate each possible configuration of longer trains in a similar way as for the demonstrator.

These considerations lead to the development of the methodology that is used for the 1D dynamics analysis of longer trains. The basic idea is to make use of only a few discrete steps per variable parameter in order to keep the total number of necessary simulations manageable. At the same time, the explanatory power of the simulations should be as big and as universal as possible. Therefore, extreme characteristics (minimum and maximum values of ranges) and sometimes also intermediate values are used for the variations.

The next step is the identification of major influences and trends in the resulting data. Such major influences and trends can then possibly lead to inter- or extrapolation of results for the respective parameters. Additional variations for some selected cases with smaller discrete steps and therefore a larger number of variations help to check the relationship between the trains with a few extreme characteristics and more random trains.

The FALNS wagons used in the demonstrator train already tend to some extremes in parameters that should be accounted for in the analysis of long trains. They are among the shortest 4-axle wagons and they tend to be either fully loaded or completely empty. Furthermore, their car bodies have a high torsional stiffness value and the wagons are only used for bulk cargo.

Because this wagon was previously used for the simulations of the demonstrator train, it seems likely to model a wagon with parameters that are on the other end of the range.

Such a wagon is a SGGNNS80 wagon for container transport. Not only is the type of cargo and thus also the payload different from the FALNS wagon but also the wagon length. With 25.94 m, the SGGNNS80 wagon is almost twice as long as the FALNS wagon and thus among the longest wagons for freight. With a maximum total weight of 90 t for both wagons, the possible maximum weight per train length also differs by a factor of two between trains made up of the two wagon types. Furthermore, the torsional stiffness of the SGGNNS80 wagon is comparatively low. This would be further examined in detail in Section 4.4.

4.2 PNEUMATICS SIMULATIONS

Table 17 collects all the parameters considered for the analysis of trains longer than 500 m and characterized by operation with two locos. As far as the pneumatics is concerned, relevant parameters can be found in rows 1-6. In all the simulations it is assumed that the maximum pressure in braking cylinders is 3.8 bar. According to the loading status, braking forces developed by the vehicles will then be changed in 1D simulations.

Table 17: Parameters considered for simulations of trains longer than 500 m operating with two locos. (f= fully loaded, h= half loaded, e= empty)

Parameter	Value	Number of parameter values	Total number of variations
Number of locos	2	1	1
Brake regime	G	1	1
Wagon length	SGGNSS: 26 m FALNS: 13 m	2	2
Train length	750 m, 1000 m, 1250 m, 1500 m	4	8
Position of slave loco	1/4, 2/4, 3/4, 4/4	4	32
Scenarios	103,106,107,109, 202, 204, 205, 207	8	256
Loading status (front-rear)	f-f, f-h, f-e, h-f, h-h, h-e, e-f, e-h, e-e,	9	2305

Considering the data of Table 17, the variations of parameters should result in a total of 256 simulations for the pneumatic part. Actually, some of the scenarios considered are equivalent from the pneumatics point of view or do not involve pneumatics (underlined):

- 103: Emergency braking from master loco only
- 106: Emergency braking from master and slave loco (2s delay)
- 107: Pneumatics is not involved
- 109: Pneumatics identical to 106

- 202: Emergency braking from master + brake support from slave in communication loss mode
- 204: Pneumatics is identical to 202
- 205: Emergency braking from master and unexpected charging from slave
- 207: 2 subcases considering maximum-service or emergency braking from master loco as a consequence of unexpected emergency braking performed by slave loco.

Simulation 207 is divided into two subcases considering a different reaction from the master loco when a pressure drop in the main braking pipe is detected. Altogether, the pneumatics simulations are 198.

4.2.1 Train compositions and overall results

The train compositions were generated according to the data of Table 17. Looking at the schematic of Figure 65, the train is divided into two parts by the slave loco. The first part of the train is made up of the master loco followed by N1 wagons. The slave loco is then followed by N2 wagons.

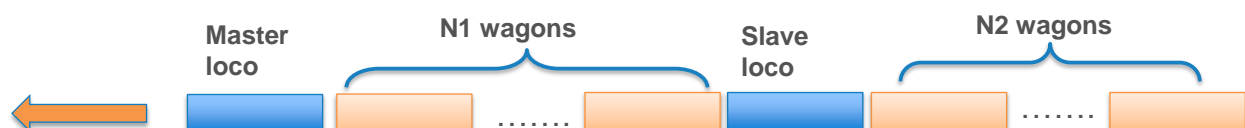


Figure 65: Schematic of a train with two locos

The compositions for the FALNS trains are reported in Table 18; As can be noticed, due to the finite length of the wagons, train lengths and positions of the slave loco are close but not equal to their nominal values. 750m-long and 1500m-long trains are made up of 57 and 114 vehicles respectively.

Table 18: Train compositions for trains with FALNS wagons

2nd loco	Train lenght [m]	ML position	N1	SL position	N2	N vehicles	Actual length [m]	SL position
25%	750	1	12	14	43	57	755,0	24,5%
	1000	1	17	19	57	76	1002,8	24,9%
	1250	1	22	24	71	95	1250,5	25,2%
	1500	1	27	29	85	114	1498,3	25,4%
50%	750	1	27	29	28	57	755,0	50,4%
	1000	1	36	38	38	76	1002,8	49,6%
	1250	1	46	48	47	95	1250,5	50,2%
	1500	1	55	57	57	114	1498,3	49,8%
75%	750	1	41	43	14	57	755,0	74,6%
	1000	1	55	57	19	76	1002,8	74,3%
	1250	1	70	72	23	95	1250,5	75,3%
	1500	1	84	86	28	114	1498,3	75,0%
100%	750	1	55	57	0	57	755,0	98,7%
	1000	1	74	76	0	76	1002,8	99,1%
	1250	1	93	95	0	95	1250,5	99,2%
	1500	1	112	114	0	114	1498,3	99,4%

Train compositions for SGGNSS wagons are shown in Table 19; these wagons are longer than FALNS and this explains why discrepancies between nominal and actual values of total length and slave-loco positions are larger.

Table 19: Train compositions for trains with SGGNSS wagons

2nd loco	Train lenght [m]	ML position	N1	SL position	N2	N vehicles	Actual length [m]	SL position
25%	750	1	6	8	21	29	738,2	24,9%
	1000	1	9	11	28	39	997,6	26,2%
	1250	1	11	13	36	49	1257,0	25,0%
	1500	1	13	15	43	58	1490,4	24,5%
50%	750	1	13	15	14	29	738,2	49,5%
	1000	1	18	20	19	39	997,6	49,6%
	1250	1	23	25	24	49	1257,0	49,7%
	1500	1	28	30	28	58	1490,4	50,6%
75%	750	1	21	23	6	29	738,2	77,6%
	1000	1	28	30	9	39	997,6	75,7%
	1250	1	35	37	12	49	1257,0	74,5%
	1500	1	42	44	14	58	1490,4	75,0%
100%	750	1	27	29	0	29	738,2	98,7%
	1000	1	37	39	0	39	997,6	99,1%
	1250	1	47	49	0	49	1257,0	99,2%
	1500	1	56	58	0	58	1490,4	99,4%

Overall results

196 simulations were performed to predict the dynamics of the pressure drop in the main braking pipe and pressure build-up in braking cylinders. Results of simulations for nominal operating conditions are reported in detail in Appendix B. Some synthetic results are described hereafter.

Focussing on FALNS wagons, Table 20 reports the time required to obtain a pressure drop of at least 1.5 bar in the main braking pipe in all the wagons; This pressure drop corresponds to the complete opening of distributor valves connecting the main reservoirs with the brake cylinders. The time values collected in the table thus indicate how fast the process of venting the main braking pipe is.

The analysis of scenarios 103 and 106 clearly points out the effectiveness of using two venting points; It is noteworthy that the fastest emptying times are obtained when the slave loco is at 75% of the total length.

The comparison between scenarios 106 and 202 allows evaluating the effect of communication loss on the venting process. In this case the slave loco regulates the venting according to the pressure drop generated in the main braking pipe by the emergency braking commanded by the front loco.

Data relevant to scenario 205 reveal the dramatic increase in the time required to complete the venting process when the slave loco refills the main braking pipe while the master loco is performing an emergency braking.

Finally, the columns relevant to scenarios 207E and 207MS put into evidence the difference in venting times when emergency braking or maximum service braking is activated on the master loco as a consequence of unexpected venting of the main braking pipe from the slave.

Table 20: Time required to complete a pressure drop of at least 1.5 bar in MBP in all wagons [s]; trains with FALNS wagons.

Train	Scenario					
	103	106	202	205	207E	207MS
750-25	21,4	16,3	21,4	27,2	15,0	15,5
750-50	21,4	11,2	17,9	35,5	8,8	8,7
750-75	21,4	6,8	16,0	49,3	6,4	10,0
750-100	21,4	8,7	16,0	77,2	9,9	14,2
1000-25	32,6	24,1	32,6	44,2	22,4	23,2
1000-50	32,6	16,0	26,8	62,0	13,2	13,0
1000-75	32,7	9,5	23,7	105,0	10,0	14,7
1000-100	32,6	12,6	24,1	110,0	13,8	20,1
1250-25	45,5	32,8	43,0	65,4	30,8	31,7
1250-50	45,5	20,9	36,8	103,9	17,7	17,4
1250-75	45,6	12,7	32,0	138,0	13,1	19,5
1250-100	45,5	17,0	33,5	138,0	19,4	27,1
1500-25	59,9	42,4	56,1	22,2	39,9	41,2
1500-50	59,9	26,7	48,1	165,0	23,0	22,7
1500-75	60,0	16,0	41,3	165,0	16,3	24,1
1500-100	59,9	21,9	44,3	165,0	24,3	34,0

Data is reported in Table 20 the chart in Figure 66 for a more immediate evaluation of results.

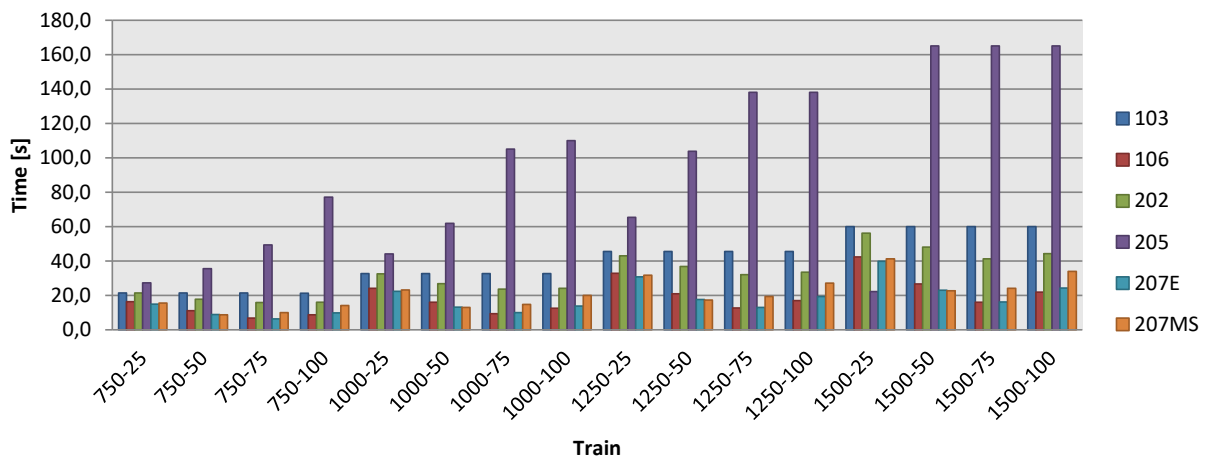


Figure 66: Time required to complete a pressure drop of at least 1.5 bar in MBP in all wagons [s]; trains with FALNS wagons.

Data collected in Table 21 represent the time required to reach at least 99% of the maximum force in all the braking cylinders. This time is in part associated with the venting process of the main braking pipe and in part with the delay due to the G braking regime. In most cases, delays associated with braking regime G tend to mitigate the differences due to faster/slower venting processes (see Figure 67).

Table 21: Time required to reach at least 99% of maximum pressure in braking cylinders of all wagons [s]; trains with FALNS wagons.

Train	Scenario					
	103	106	202	205	207E	207MS
750-25	28,3	27,8	28,3	28,8	26,5	26,4
750-50	28,3	27,0	27,7	36,3	24,7	24,7
750-75	28,4	27,0	27,0	49,5	25,9	25,9
750-100	28,2	26,7	27,0	75,9	27,3	27,4
1000-25	33,9	30,1	33,9	44,8	28,2	27,6
1000-50	33,9	28,5	29,8	62,0	25,4	25,0
1000-75	33,9	27,4	28,4	102,8	26,7	26,8
1000-100	33,9	27,1	29,9	110,0	28,3	21,4
1250-25	46,4	34,2	43,9	65,5	32,1	33,0
1250-50	46,4	29,5	38,0	102,6	26,6	25,8
1250-75	46,5	27,6	33,9	138,0	27,3	27,6
1250-100	46,4	27,7	36,4	138,0	30,5	30,9
1500-25	60,5	43,4	56,7	22,2	40,9	42,2
1500-50	60,5	30,9	49,0	165,0	27,7	26,9
1500-75	60,6	27,8	42,5	165,0	27,9	28,6
1500-100	60,5	29,0	45,6	165,0	31,8	35,2

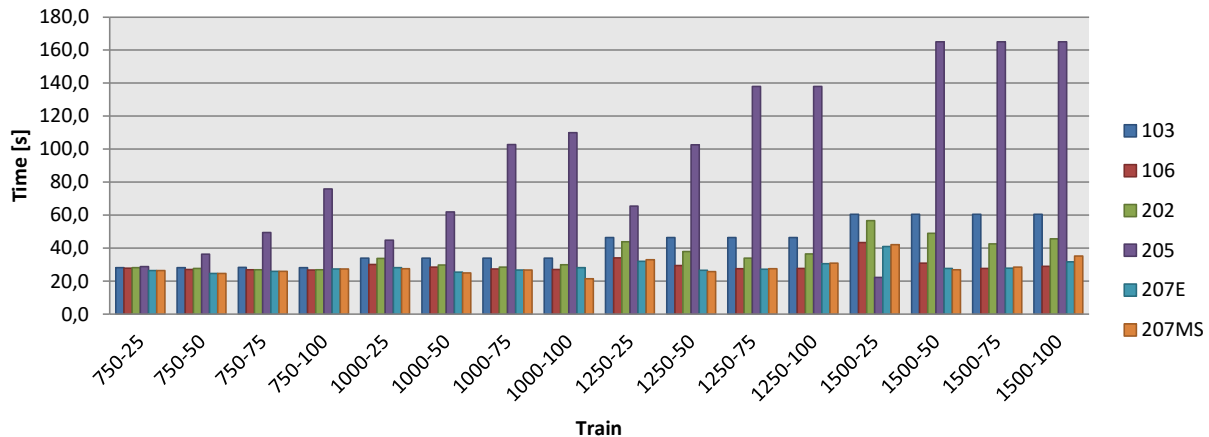


Figure 67: Time required to reach at least 99% of maximum pressure in braking cylinders of all wagons [s]; trains with FALNS wagons.

Table 22 reports the time required to obtain a pressure drop of at least 1.5 bar in the main braking pipe in all the wagons, this time referred to SGGNSS wagons. Conclusions that can be made are similar to those for FALNS wagons.

Table 22: Time required to complete a pressure drop of at least 1.5 bar in MBP in all wagons [s]; trains with SGGNSS wagons.

Train	Scenario					
	103	106	202	205	207E	207MS
750-25	21,6	16,4	21,2	27,5	15,0	15,7
750-50	21,6	11,5	18,9	34,5	9,2	9,1
750-75	21,6	7,2	16,0	49,0	8,0	11,3
750-100	21,6	8,8	16,2	70,4	9,9	14,3
1000-25	33,9	24,4	32,2	46,2	22,6	23,5
1000-50	33,8	16,5	27,8	62,1	13,8	13,6
1000-75	33,8	10,0	24,3	105,1	10,6	15,7
1000-100	33,9	13,0	24,8	110,0	14,6	21,3
1250-25	48,0	34,5	45,4	68,2	32,6	33,6
1250-50	48,0	22,2	38,7	104,1	18,9	18,6
1250-75	47,9	13,2	33,7	138,0	13,9	20,4
1250-100	47,9	17,9	34,8	138,0	20,2	28,6
1500-25	62,1	44,4	58,5	92,4	41,9	43,4
1500-50	62,1	27,1	49,4	165,0	23,3	23,0
1500-75	62,1	16,6	42,6	165,0	17,8	25,7
1500-100	62,0	22,8	45,4	165,0	25,6	35,9

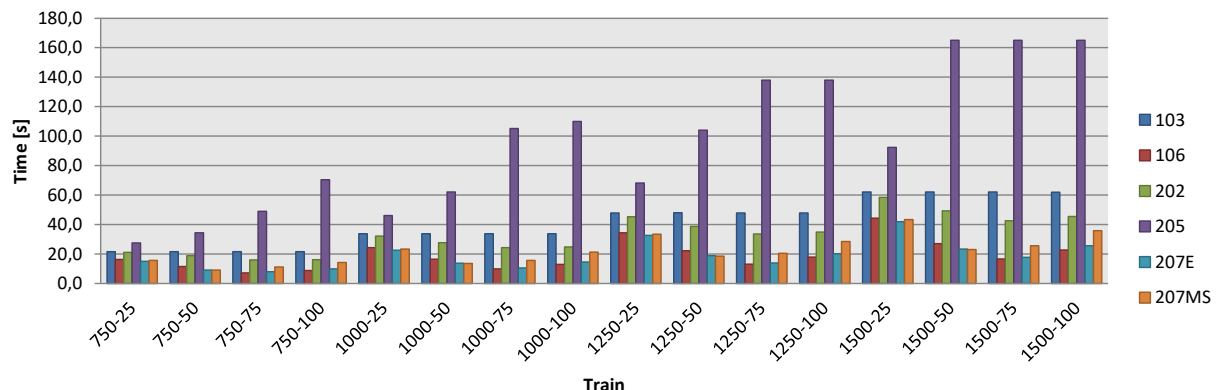


Figure 68: Time required to complete a pressure drop of at least 1.5 bar in MBP in all wagons [s]; trains with SGGNNS wagons.

Table 23: Time required to reach at least 99% of maximum pressure in the braking cylinders of all wagons [s]; trains with SGGNNS wagons.

Train	Scenario					
	103	106	202	205	207E	207MS
750-25	29,1	28,4	29,3	29,7	27,0	26,8
750-50	29,1	27,6	29,0	35,3	25,2	25,1
750-75	29,1	27,0	27,7	49,1	26,9	27,0
750-100	29,4	27,3	27,9	69,6	27,9	28,2
1000-25	35,1	31,6	33,5	46,8	29,2	28,7
1000-50	35,1	29,0	31,0	62,1	26,3	25,8
1000-75	35,1	27,5	29,4	103,0	27,6	28,0
1000-100	35,2	28,1	29,9	110,0	29,9	30,3
1250-25	48,9	35,9	46,3	68,4	34,0	34,8
1250-50	48,9	30,5	39,9	103,0	27,5	26,9
1250-75	48,9	27,9	35,6	138,0	29,0	29,3
1250-100	48,8	29,2	37,8	138,0	32,0	32,8
1500-25	62,7	45,5	59,2	92,2	43,0	44,3
1500-50	62,7	32,0	50,3	165,0	28,6	27,8
1500-75	62,7	28,8	43,9	165,0	30,3	31,9
1500-100	62,6	30,6	46,8	165,0	34,0	37,1

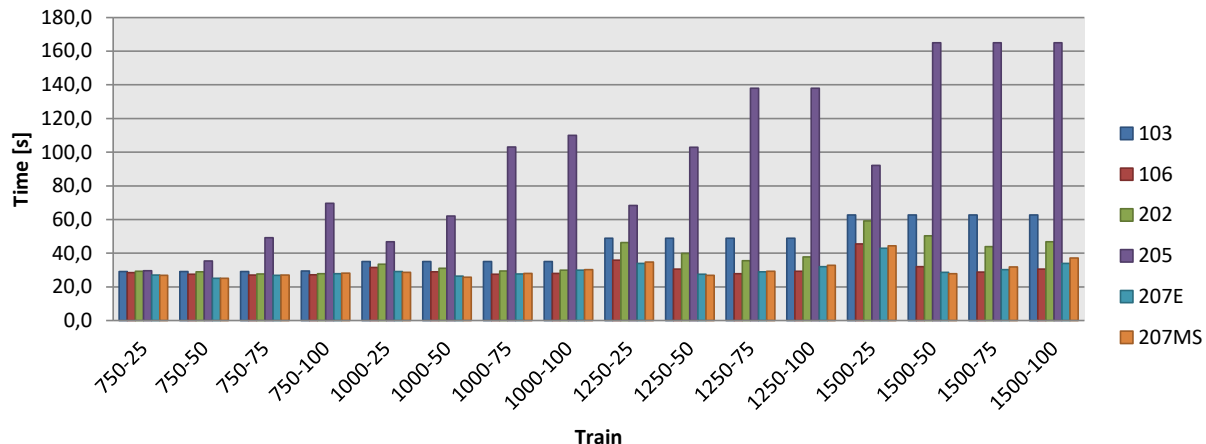


Figure 69: Time required to reach at least 99% of maximum pressure in braking cylinders of all wagons [s]; trains with SGGNSS wagons.

4.2.2 Results for scenario 202

Scenario 202 considers an emergency braking performed by the master loco with a simultaneous communication loss. This means that the slave loco does not copy the same command with a given delay. The slave loco supports the braking by monitoring the pressure drop in main braking pipe according to the logic described.

While performing simulations referred to this scenario, a possible issue appeared when the master and the slave locos are quite close to each other. In particular, this logic is triggered by a pressure drop with a given gradient; typically this is associated with a pressure drop wave that is transmitted through the pipe during the first instants of the braking.

Since in scenario 202 the slave loco stays in “stand-by” mode for 1 second after the communication loss (according to the logic proposed by Faiveley Transport the slave loco should not react for 1 s), when the locos are close to each other, the pressure drop wave crosses the slave loco when this last is inactive. As a consequence, the braking-support logic does not activate in certain cases.

Figure 70 clarifies the situation. Figure 70a reports the time histories of pressure drop in the main braking pipe determined by an emergency braking commanded from the master loco after 2 s. Figure 70b shows the time history of the pressure gradient in the main braking pipe at the slave loco; the negative peak of gradient that shoud trigger the braking-support logic occurs between 2 and 3 seconds. As a consequence the same logic does not activate.

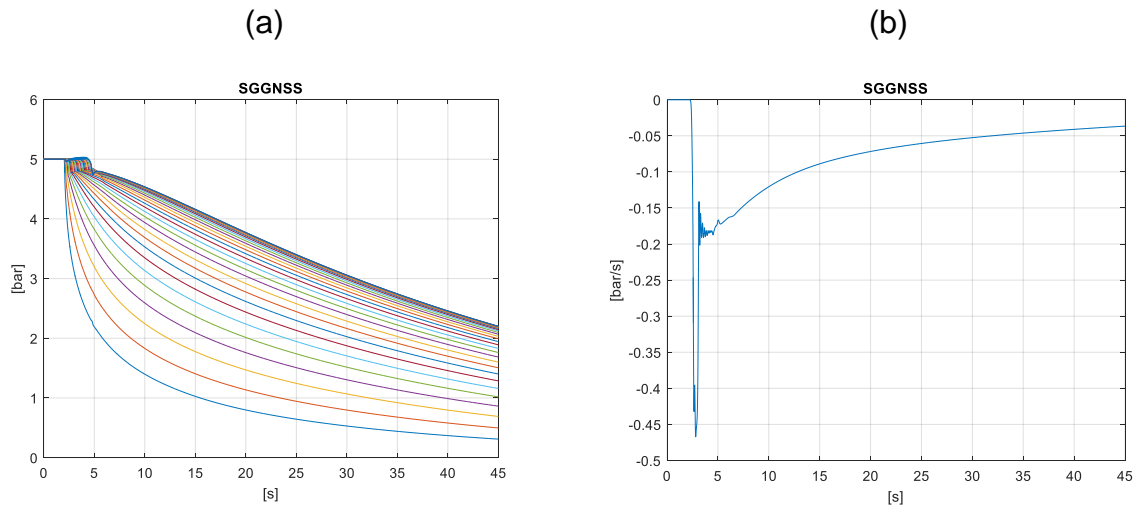


Figure 70: 750m-long train (SGGNSS), slave loco 25%, scenario 202. Time histories of pressure drop in the main braking pipe (a); time history of pressure gradient in the main braking pipe for the slave loco (b).

4.2.3 Simulations with two slave locos

Additional simulations were performed for trains with two slave locos; This line of research was developed considering that only a few configurations with 750 m long trains with one slave loco were able to satisfy the requirements in terms of maximum longitudinal forces (as reported in the following sections on 1D and 3D analyses). The presence of two slave locos is expected to reduce the longitudinal forces associated to delays in propagation of braking command.

Table 24: Parameter considered for simulations of trains longer than 750 m operating with three locos. f= fully loaded, h= half loaded, e= empty.

Parameter	Value	Number of parameter values	Total number of variations
Number of locos	3	1	1
Brake regime	G	1	1
Wagon length	SGGNSS: 26 m FALNS: 13 m	2	2
Train length	1000 m, 1250 m, 1500 m	3	6
Position of slave loco	$\frac{1}{2}, 1$	1	6
Scenarios	103,106,107,109	4	24
Loading status (front-rear)	f-f, f-h, f-e, h-f, h-h, h-e, e-f, e-h, e-e	9	216

Simulations with two locos were focused on trains with lengths between 1000 and 1500 m. Due to the limited time left for completing the DYNAFREIGHT project, the analysis was performed considering only normal operating condition (i.e. no degraded operation mode) with the second loco in the train centre.

Considering that scenario 107 does not involve pneumatics and that scenario 109 is identical to 106 from the pneumatics point of view, a total of 12 simulations was performed.



Figure 71: Schematic of a train with three locos.

Figure 71 shows the schematic of a train with three locos. Considering that the first slave loco is at 50% of the train length, the position of wagons are reported in Table 25 and Table 26 for FALNS and SGGNNS wagons respectively.

Table 25: Train compositions for trains with FALNS wagons.

Train lenght [m]	ML position	N1	SL position	N2	N vehicles	Actual length [m]	SL position
1000	1	36	38	36	75	995,6	50,0%
1250	1	46	48	46	95	1256,4	50,0%
1500	1	55	57	56	114	1504,1	49,6%

Table 26: Train compositions for trains with SGGNSS wagons.

Train lenght [m]	ML position	N1	SL position	N2	N vehicles	Actual length [m]	SL position
1000	1	18	20	18	39	990,5	50,0%
1250	1	23	25	23	49	1249,9	50,0%
1500	1	28	30	28	59	1509,3	50,0%

Overall results

Pneumatics simulations with three locos were performed assuming the same delay (i.e. 2 s) in the propagation of radio command from the master loco.

To get an idea of the benefits achievable with adding one slave loco, it is useful to compare the results reported in Figure 72 and Figure 73. Data are referred to a 1500 m long train (FALNS wagons) and scenario 109, i.e. an emergency braking commanded from master loco with the same command copied by the slave loco(s) after 2 s. Figure 72 refers to the case with one slave loco positioned at the train center.

Looking at the left pictures allows to notice how faster the pressure drop in MBP and the pressure build-up in BC become. The comparison of the graphs on the right part clearly put into evidence how the rear part of the train reacts faster; the blue line indicates the time required to complete a pressure drop of 1.5 bar in MBP. When one slave loco is used, the “slowest” wagon (the last one in this case) requires 26 s to complete the pressure drop. Adding a slave loco at the train end significantly speeds-up the process: the slowest wagon (approximately at 75% of the train length) requires now 11 s.

The time required to reach 99% of the maximum pressure in BCs is also influenced by the presence of the second slave loco. With the 2-loco configuration (1 master + 1 slave), the first wagon develops 99% of the maximum pressure after 24.5 s, while the slowest wagon requires 31 s. This 6.5 s delay is associated with non-uniform brake forces which negatively affect the maximum levels of LCF and LTF.

When a second slave loco is added the slowest wagon requires 27.5 s to reach 99% of the maximum pressure; This means that the difference between the first wagon and the slowest one is within 3 s. This is expected to produce clear benefits on maximum LCF and LTF.

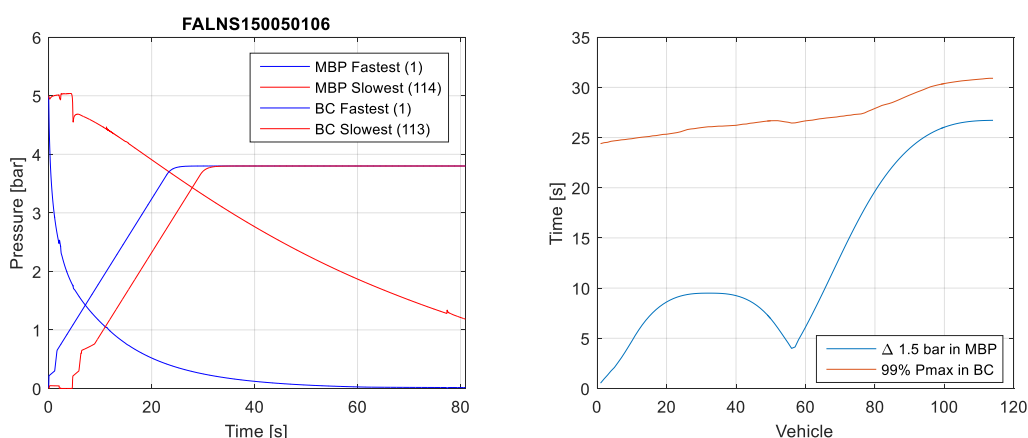


Figure 72: 1000 m FALNS train with one slave loco: time histories of pressure drop in MBP and pressure build-up in BC for the slowest and fastest wagon (a); time required to obtain a pressure drop of 1.5 bar in MBP and to reach 99% of maximum pressure in BC.

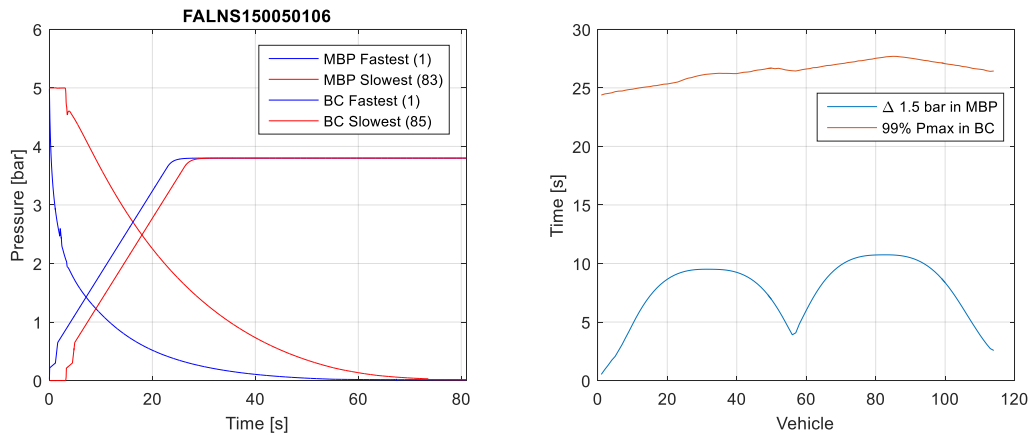


Figure 73: 1000 m FALNS train with two slave locos: time histories of pressure drop in MBP and pressure build-up in BC for the slowest and fastest wagon (a); time required to obtain a pressure drop of 1.5 bar in MBP and to reach 99% of maximum pressure in BC.

To get a complete picture of the results of pneumatics simulations, Figure 74 replots the time required to complete a pressure drop of 1.5 bar in MBP (Figure 74a) for FALNS wagons. Figure 74b refers to the time required to reach 99% of the maximum pressure in BCs for the same wagons. Figure 75 displays the same information for SGGNSS trains.

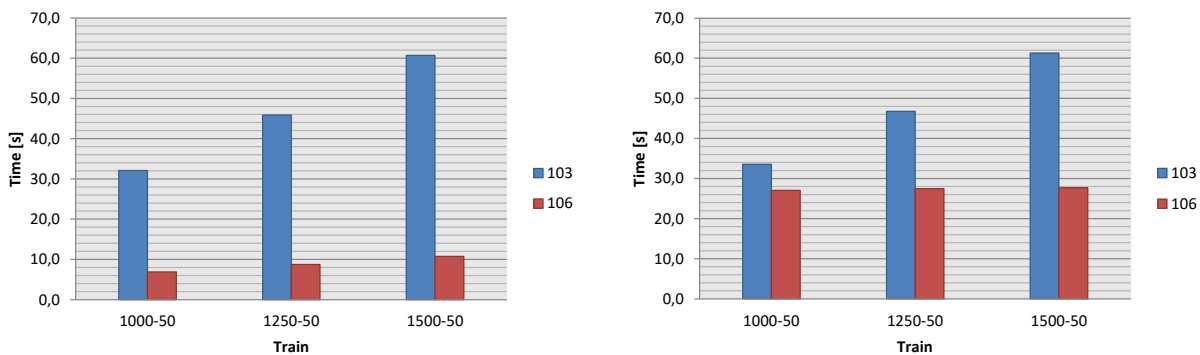


Figure 74: FALNS wagons: time required to complete a pressure drop of 1.5 bar in MBP and time required to reach 99% of the maximum pressure in BC (b).

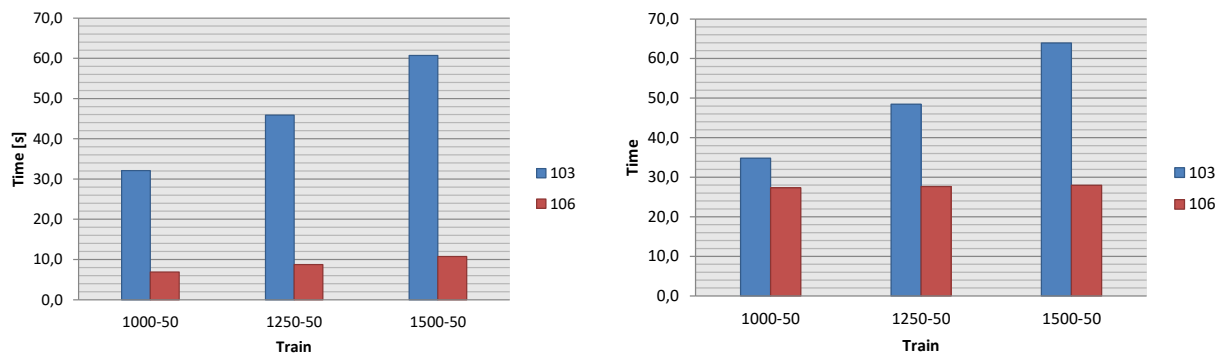


Figure 75: SGGNNS wagons: time required to complete a pressure drop of 1.5 bar in MBP and time required to reach 99% of the maximum pressure in BC (b).

4.3 1D SIMULATIONS (ACTUAL FORCES)

4.3.1 Modelling of the SGGNNS80 wagon

The standard SGGNNS 80 wagon is equipped with a brake system that allows for running speeds of 120 km/h in the fully loaded state. This is indicated by the trailing “ss” in the classification letters. This is not implemented in the model used in the 1D simulations of longer trains for two reasons. Firstly, this would add another varied parameter, which would make it more complex to compare between effects due to different wagon lengths and those due to a different brake performance. Secondly, there was no detailed data sheet for the brake performance of the SGGNNS 80 available as it was available for the FALNS wagons. Therefore, the wagon was modelled with a brake system that is typically used for wagons that can run with 100 km/h in the loaded state, indicated with the trailing single “s”. This means that the wagon should be referred to as Sggns to be according to UIC nomenclature. However, to indicate which real wagon was taken as a basis for the simulation model, the wagon will always be referred to as SGGNNS in the following. Accordingly, the other wagon will be referred to as FALNS.

4.3.2 Methodology of the result analysis

It was mentioned in the introduction of this chapter that the 1D simulations of longer trains should be used to identify major influences and trends. The overall plausibility of results can be checked in parallel. To be able to perform such an analysis, the results of all variations or at least a large subset of variations must be visible on one figure. At the same time, the markers indicating the values must be in a way that they allow for a unique attribution to the parameters used for this specific result value.

Two different methods are used for the present analysis. The first method is primarily to check the results for overall plausibility and to identify trends. The second method is to check whether the results are below the respective limit values or above.

The first method works with different marker types and colours at the same position to uniquely attribute the relevant parameters. A large bold circle or x indicate the wagon type, a midsized triangle, square, diamond or circle indicate the slave locomotive position, the colour filling of this marker indicates the train length and a small inner marker with different colours indicates the loading status of the train. The operational cases are indicated on the vertical axis. The result values are indicated on the horizontal axis. These are especially the instantaneous LCF and LCF values with the 1 s filter and the stopping distance. Figure 76 shows an example of the first method.

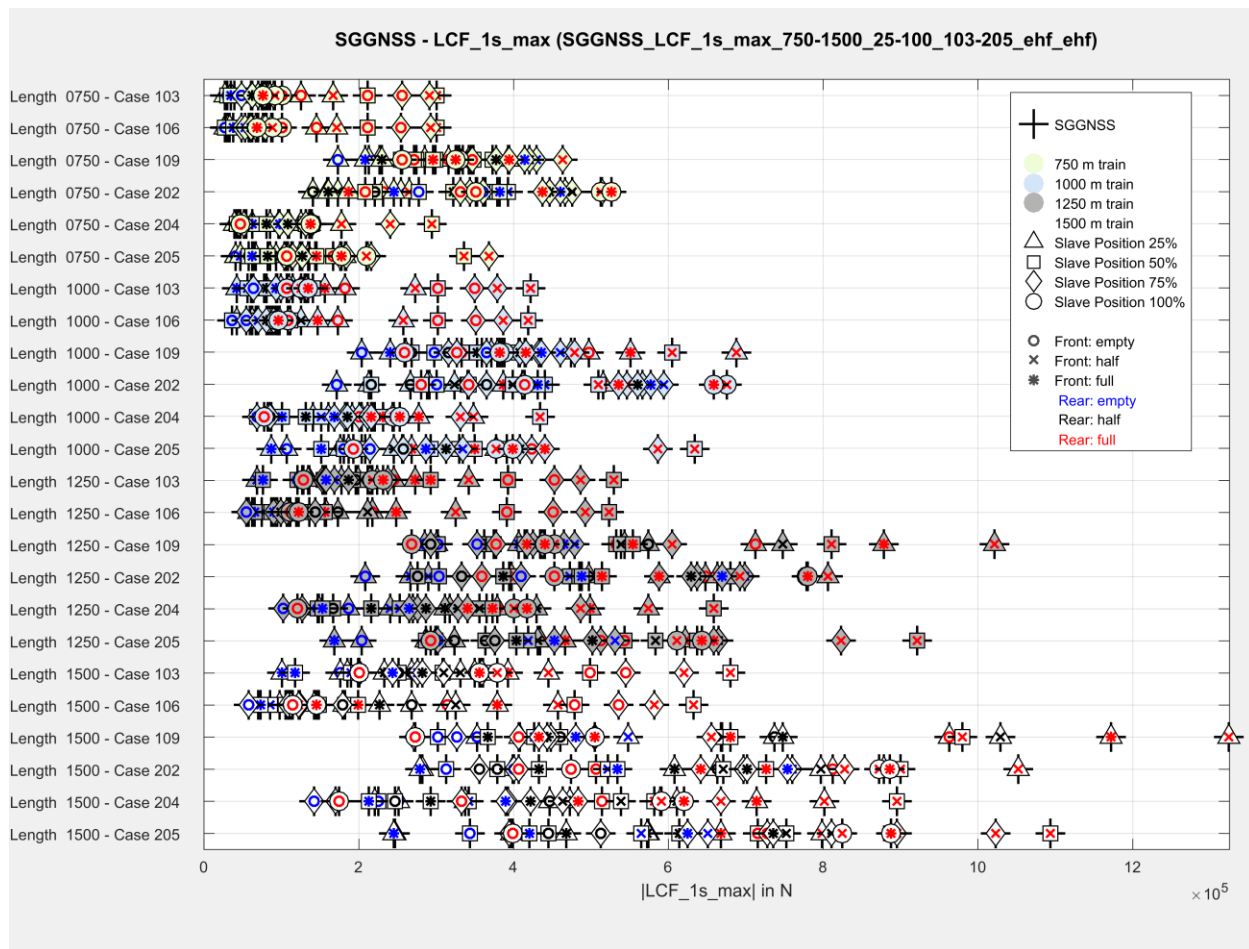


Figure 76: Exemplary LCF analysis - method 1

The second way, which is used to check results against limits, uses normalized bar plots. The entire figure consists of a $2n * 9$ matrix of bar plots, where n is the number of slave locomotive positions (indicated on the vertical axis) and 9 is the number of different load statuses (indicated on the horizontal axis). There are always two bar plots per slave locomotive position and load status. One bar plot is for LCF values with a white background and the other one for LTF values with a grey background. Each bar plot has the same number of bars representing the operational cases, indicated on the vertical

axis. The values are normalized with their respective limit value. The letters "e", "h" and "f" indicate the relevant limit value. There are two basic scenarios of relevant limit values. The first variant assumes that there might be single empty wagons in loaded or half-loaded trains. Therefore, the relevant limit value is empty for each load status. The second variant assumes that there is no load status of a single wagon lower than the lowest load status of the two train parts. For example, there is no empty wagon in a train with the load status "half-full". The lowest load status in this case is "half".

A bar value below one means that the value is below the limit, the bar is green in this case. A value above one means that the value is above the limit, the bar is red in this case. A vertical black line indicates the position of the respective limit. Orange bars indicate LTF values, which are below the limit but may be in a range where fatigue might occur. Furthermore, a green or an yellow frame around a set of LCF and LTF bar plots summarizes the results. A green frame means that all bars for all operational scenarios of a specific combination of load status and slave locomotive position are below the limit. An orange frame means that the bars of the four nominal operational cases (103, 106, 107, and 109) of a specific combination of load status and slave locomotive position are below the limit. However, at least one degraded case exceeds a limit when the combination has an yellow frame.

There is no information about absolute values in the figure except for the relevant limit values, which are given in the bottom of the figure. These limit values are obtained from the 3D analysis (see Section 4.4). Figure 78 shows an example of the second LCF analysis method

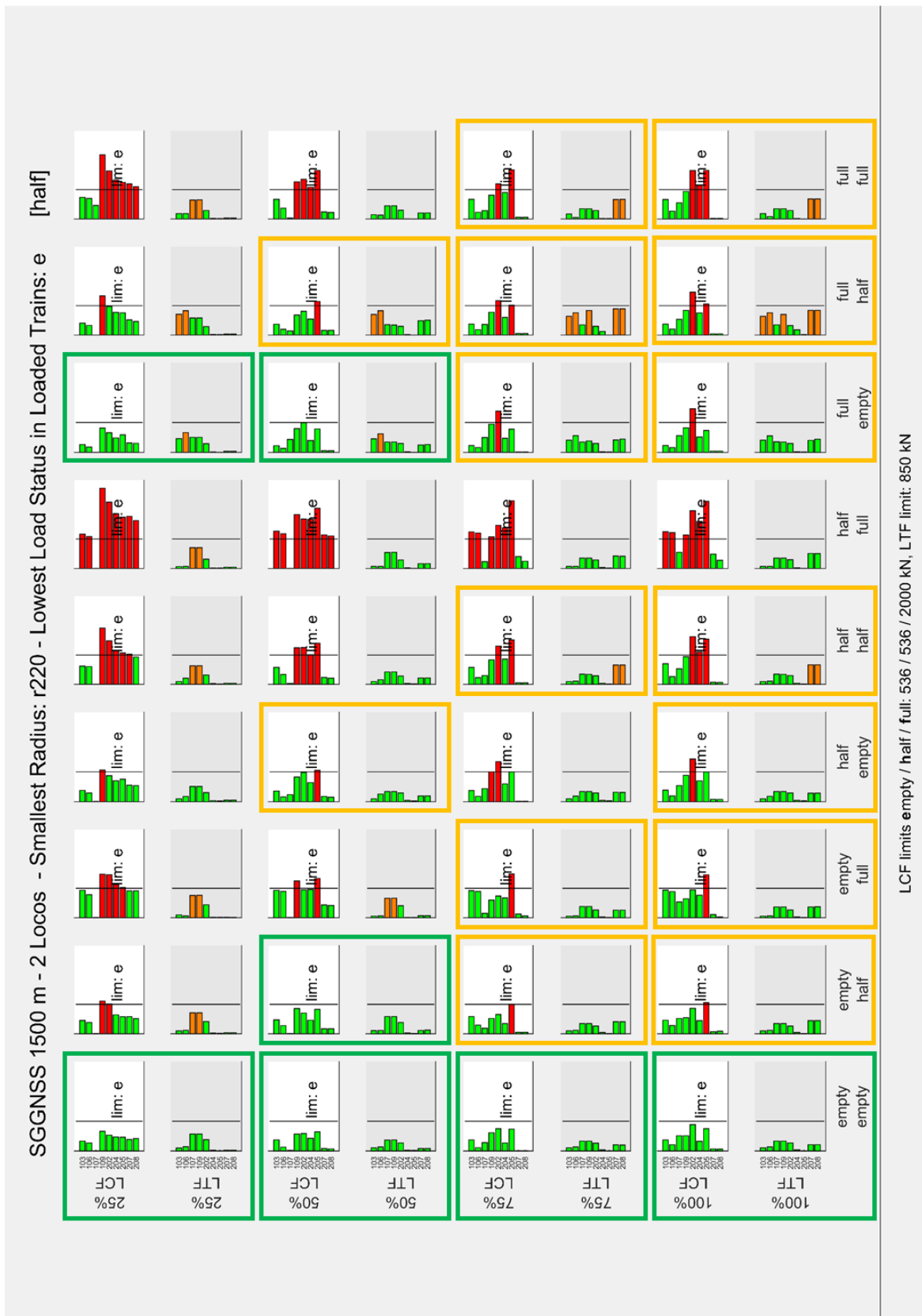


Figure 1: Exemplary LCF analysis – method 2

4.3.3 Assessment of stopping distances

Figure 78 shows the stopping distances for all simulated trains in cases 103 and 106. The initial velocity in both cases is 100 km/h. The upper four lines represent case 103 (without venting of the MBP by the slave locomotive) separated by the slave locomotive position. The lower four lines show the same for case 106 (with venting of the MBP by the slave locomotive).

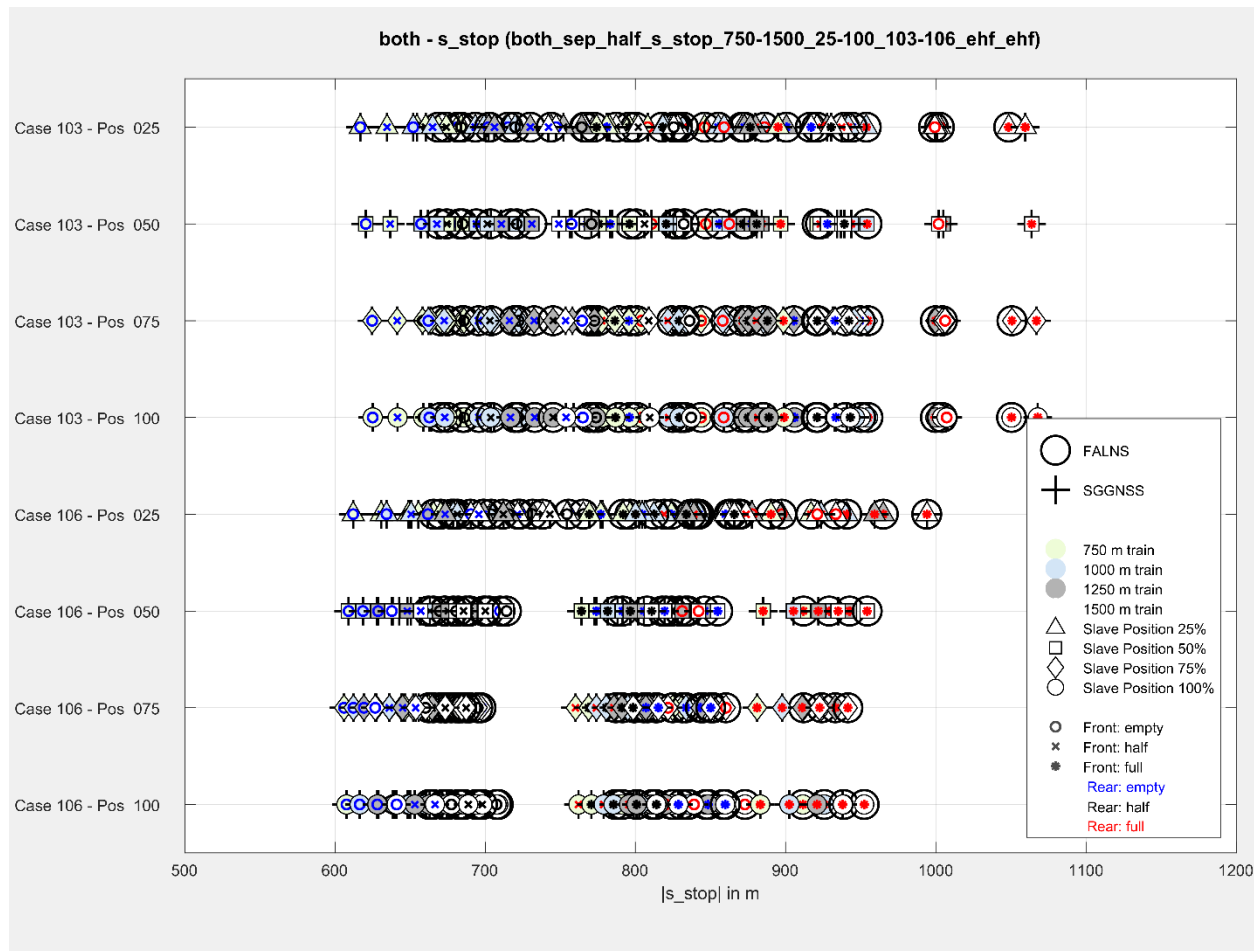


Figure 78: Stopping distances from 100 km/h in cases 103 and 106

All stopping distances range from approx. 600 m to approx. 1070 m. Empty trains are on the left (blue circles), fully loaded trains are on the right (red stars). The positive effect of the MBP venting by the slave locomotive is clearly visible as the stopping distances of all trains are below 1000 m in case 106. The 75 % slave position leads to the shortest stopping distances in case 106 followed by 100 % and 50 %. The stopping distances for the 25 % position is longer than for the other three positions. The difference in stopping distance of a 750 m train and a 1500 m train with the same loading status and the same slave locomotive position might be 150 m or more in case 103. It is clearly below 100 m

in case 106, except for the 25 % position. There are only minor differences between the FALNS and SGGNSS trains.

4.3.4 General trends of LCF and LTF results

Figure 79 shows the maximum LCF values of all trains with regard to the total train mass. The operational cases cannot be distinguished in this figure.

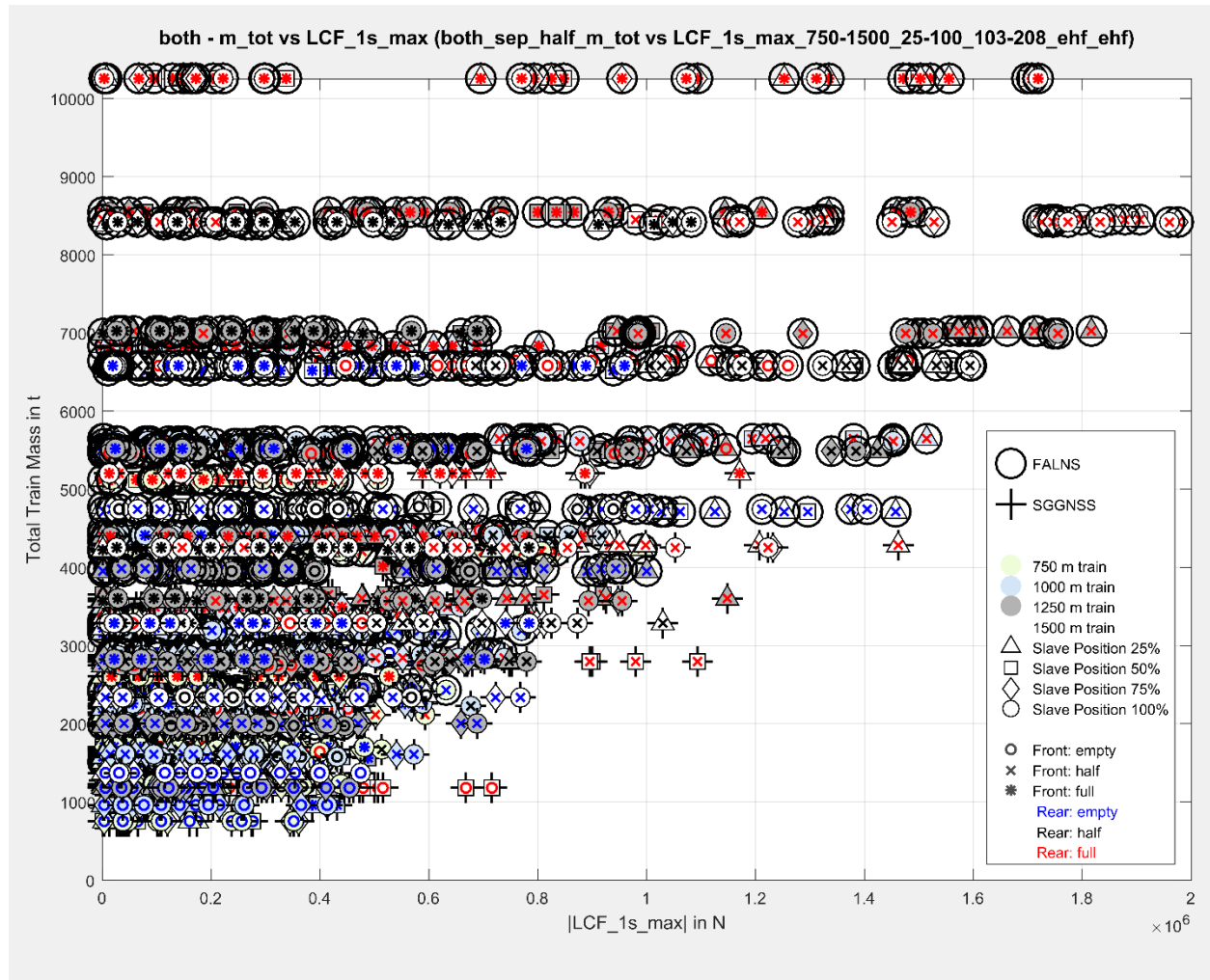


Figure 79: Maximum LCF values vs. total train mass

The lightest (and shortest) trains with a total mass under 1000 t have maximum LCF values below 400 kN. The heaviest (and longest) trains with a total mass over 10,000 t reach maximum LCF values of 1,700 kN. The highest LCF values of 2,000 kN occur at a total mass of approx. 8,500 t. These trains are 1500 m FALNS trains with the load status "half-full". The highest LCF values at a specific mass occur when the front part of the train is half-loaded (indicated by an x). The load status "half-full" (red crosses) clearly

dominates the rightmost values. The values on the right form a straight line by approximation. This indicates a linear correlation between total mass (and thus also length) and maximum LCF values.

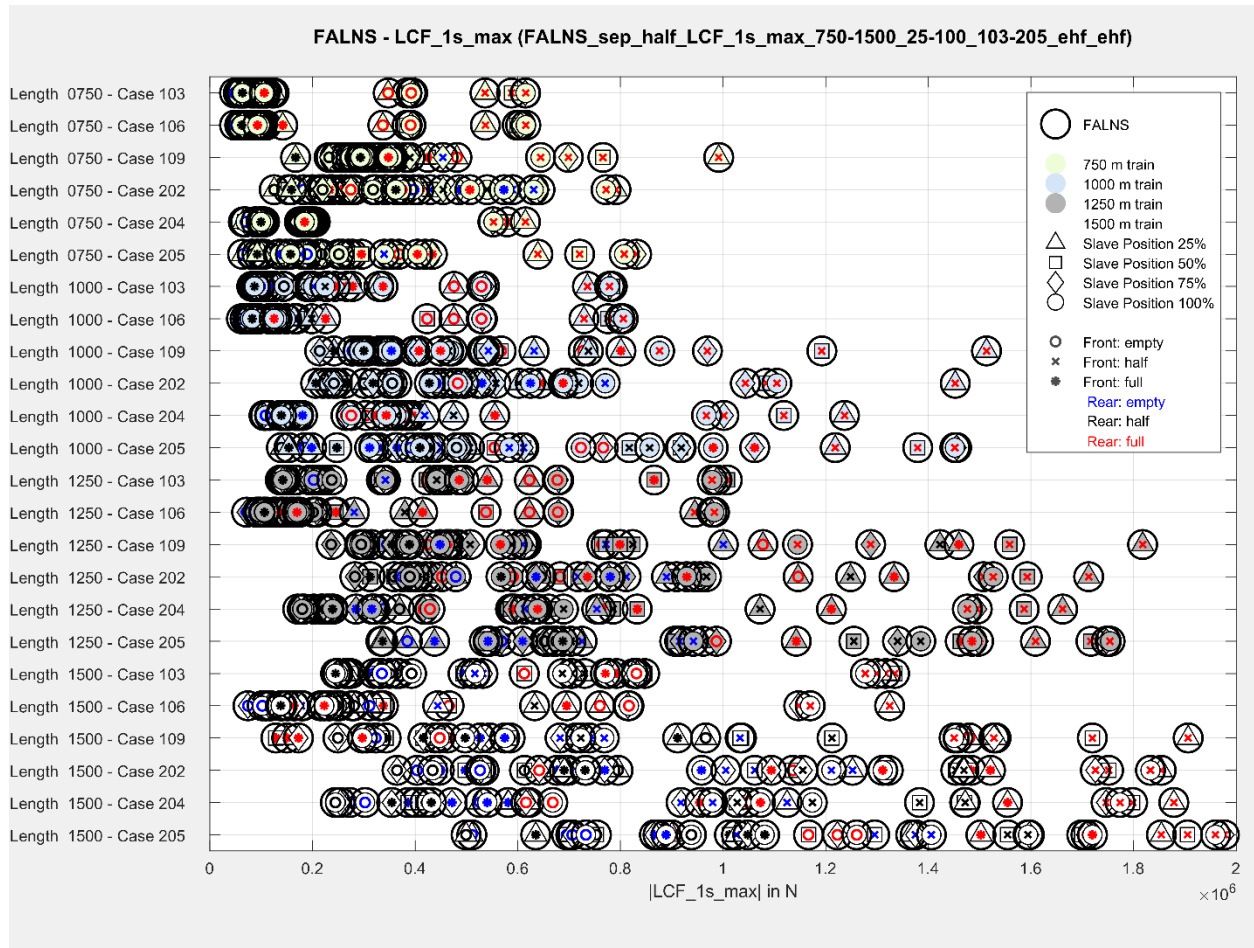


Figure 80: Maximum LCF values for FALNS trains

Figure 80 shows the results for the FALNS trains separated by length and case. An approximately linear correlation between train length and maximum LCF values is visible on the right. The highest values of all length-case combinations belong to the load status "half-full" (red crosses). Case 109 (emergency brake application after full traction) with slave position 25 % (triangle) stands out at every train length. Generally, case 109 is the most critical nominal case.

Figure 81 shows the same analysis for the SGGNSS trains. The results are completely analogous. The most significant difference are the generally lower values.

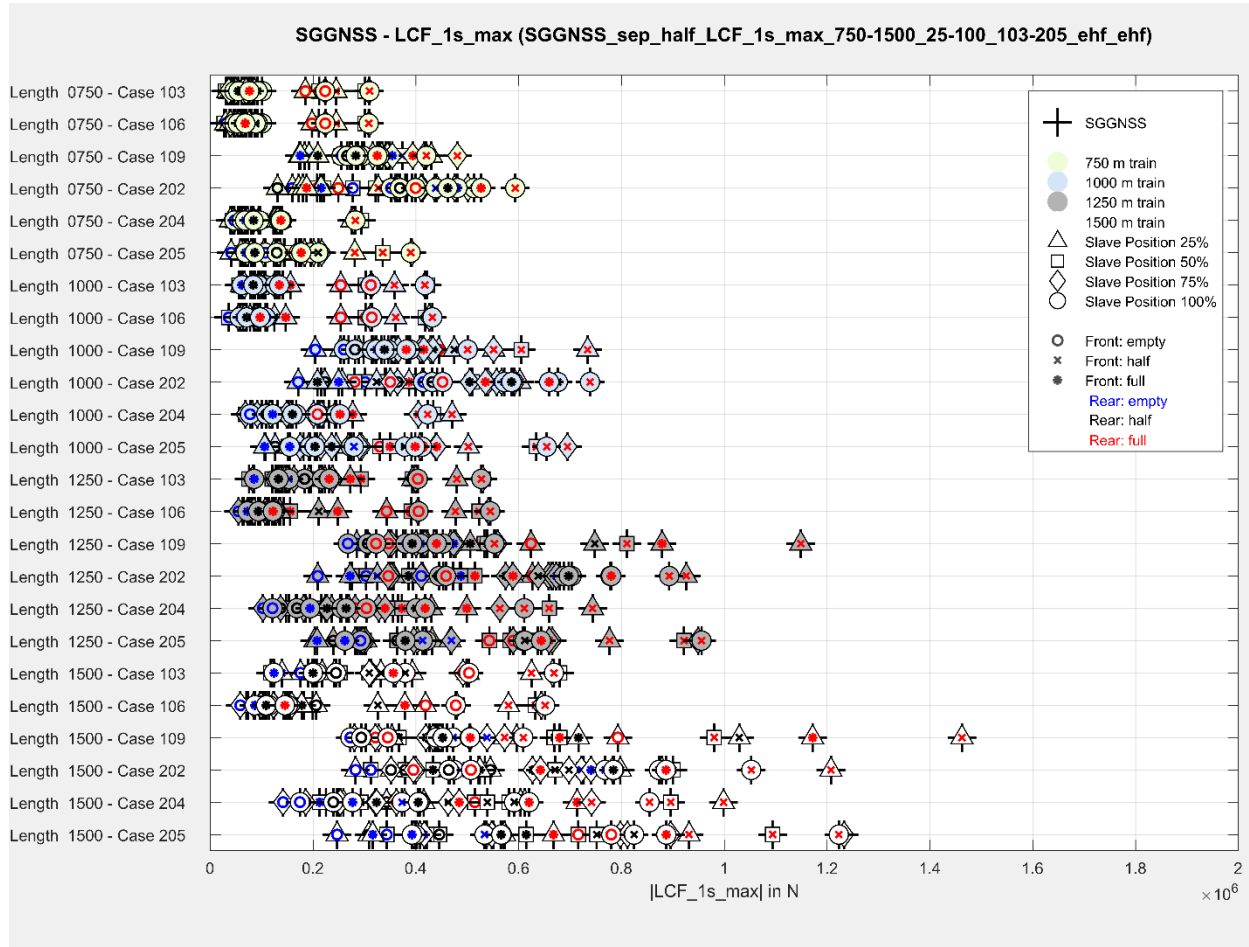


Figure 81: Maximum LCF values for SGGNSS trains

4.3.5 LCF and LTF results of trains with random individual load statuses

The analysis of longer trains makes use of nine discrete load statuses in order to reduce computational effort (cf. Section 4.1). Furthermore, all wagons have the same type of draw gear and buffers.

To check the validity of such “artificial” load statuses and to check the influence of different buffer and draw gear characteristics, a number of parameter variations was performed. The previous analysis identified case 109 as most critical nominal case. Therefore, this case was chosen to perform the parameter variations. Trains with 1000 m and 1250 m length and 50 % and 100 % slave locomotive positions are considered. There are two different cases of variations. In the first case, only the wagon mass is varied. Each wagon can have a random mass between empty weight and maximum weight. In the second case, wagon mass, buffer type and draw gear type are changed at the same time. There

are 500 variations for each case and for each train length / slave locomotive combination. Figure 82 shows the maximum LCF values of the 1250 m SGGNNS train. Green crosses indicate the results of the 500 mass variations. Pink crosses indicate the results of the 500 combined mass/buffer/draw gear variations.

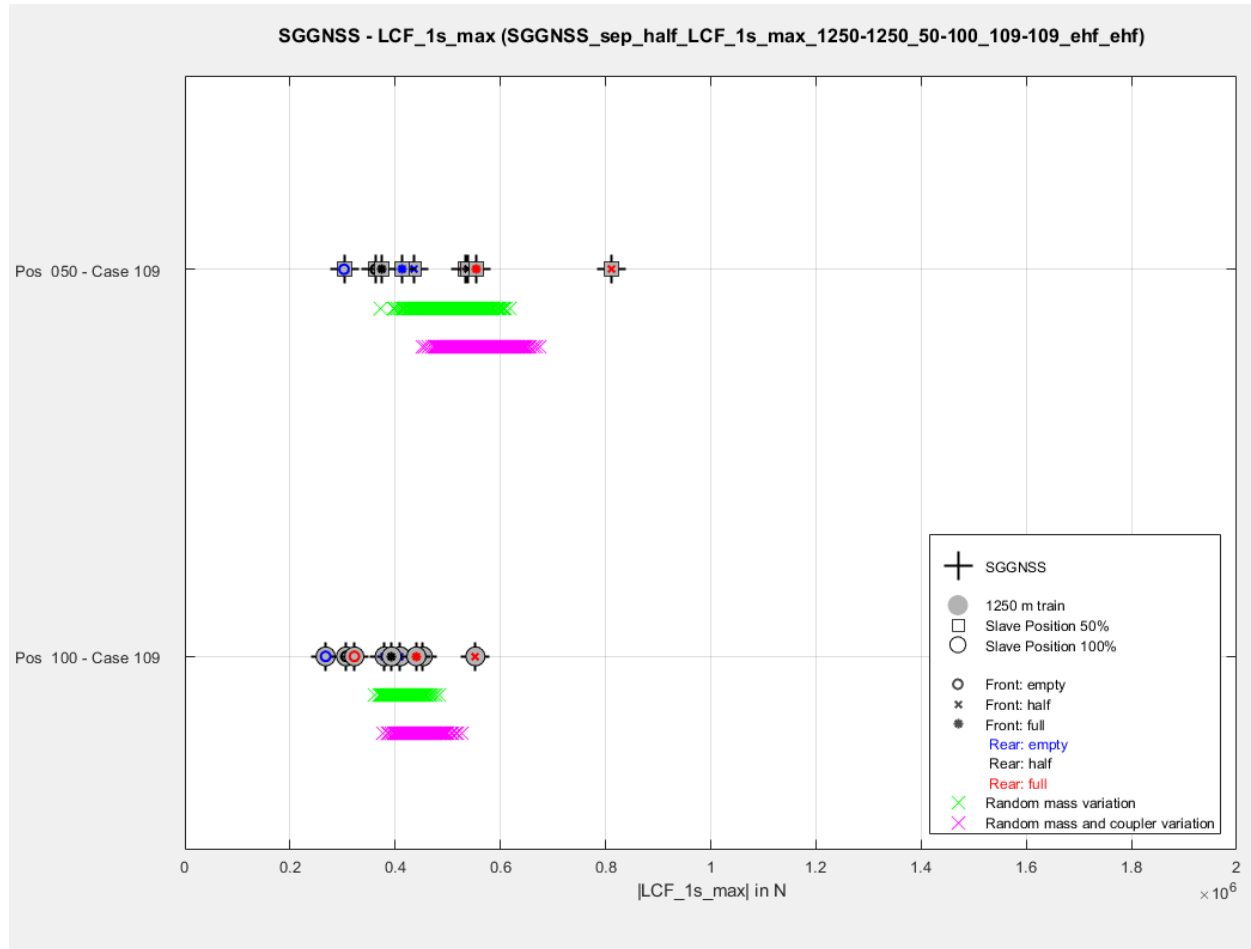


Figure 82: LCF values of mass and buffer/draw gear variations for the SGGNNS train

All of the variations are within the range defined by the “artificial” load statuses. The majority of the variation results lies in the middle of this range. The results of the combined variations are slightly shifted to higher values. Figure 83 shows the same analysis for LTF values. The results are very similar. The results for the 100 % slave position are very close to each other. This matches the “artificial” load statuses, where the results are also very close to each other, except for the maximum value.

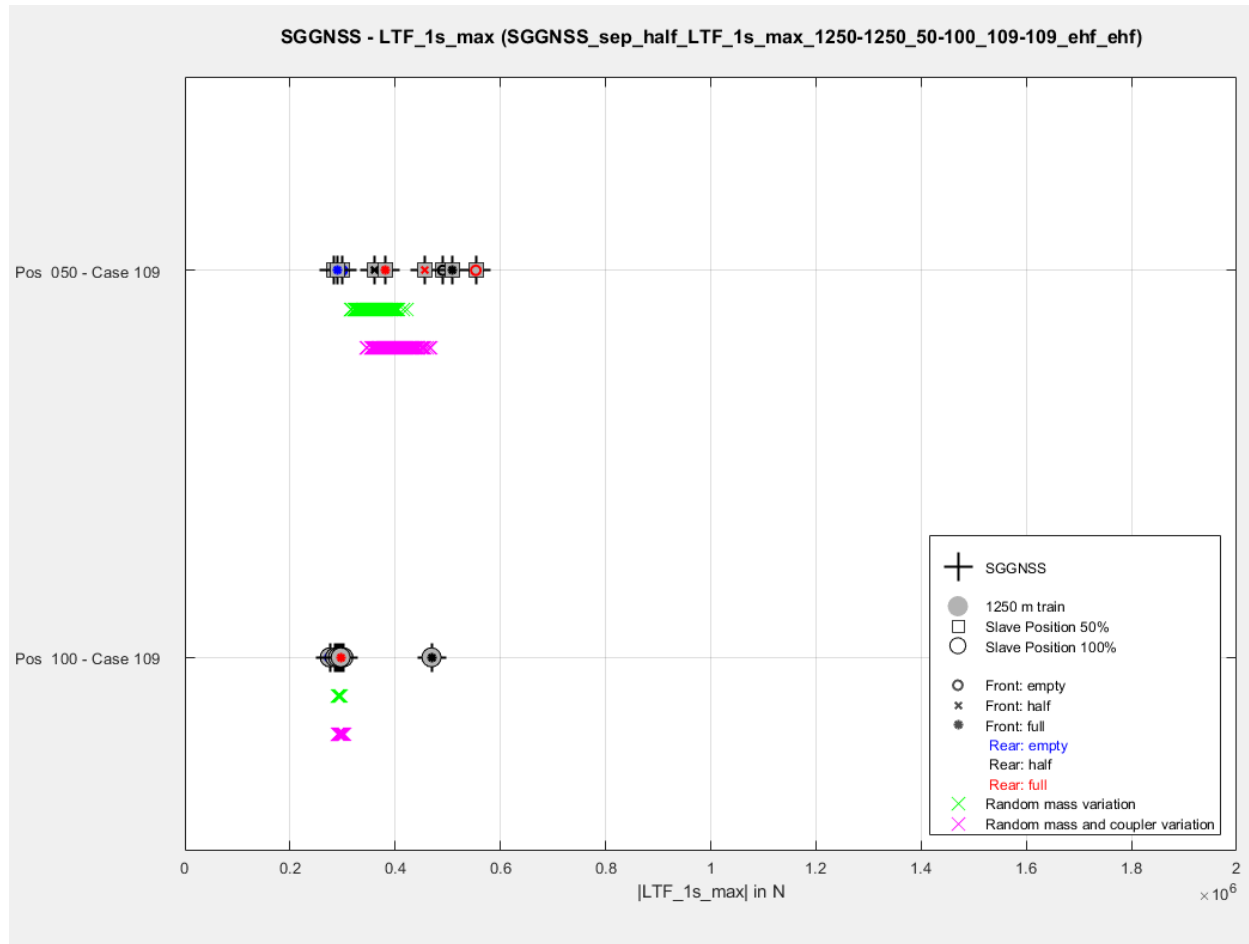


Figure 83: LTF values of mass and buffer/draw gear variations for the SGGNSS train

The results of the FALNS trains are completely analogue to the SGGNSS trains. 8000 variations were simulated in total. All result values are within the range defined by the “artificial” load statuses. This shows that these “artificial” load statuses are a valid method to evaluate the entire possible range of results. Furthermore, it shows again that the load status “half-full” is very critical. However, that does not imply that this “artificial” load status is unrealistic. The variations consider the load status of a single wagon as entirely random. Train building processes are not entirely random though. In fact, the load status “half-full” does not appear as unrealistic at all when the front part of the train is a loaded container train (containers with medium-heavy goods) and the second part is a fully loaded bulk train.

4.3.6 Comparison of 1D simulations results with 3D limit values (SGGNSS)

The comparison of 1D results with the limit values from the 3D analysis (see Section 4.4) shows that there is no train length above 750 m where every combination of slave locomotive position and load status is possible. The configuration with the most possible combinations is the 1000 m train of SGGNSS wagons with no empty wagons in loaded trains and an S-curve radius of 220 m (Figure 84). However, even in this case there is no slave locomotive position where all load statuses of the train are possible. The 100 % slave locomotive position is possible for each load status when degraded cases are not considered. Load statuses where at least one part of the train is half-loaded are the most critical. The load status “half-full” is especially critical as previously mentioned.

The analogue configuration with a length of 1250 m, shown in Figure 85, offers less possible combinations. Combinations of full and empty train parts become critical here, too. The load statuses “empty-empty”, “empty-half” and “full-full” are possible for each slave locomotive position. There is no slave locomotive position where every load status is possible, even only in nominal condition.

The longest train with 1500 m in length shows even less possible combinations. Only “empty-empty” and “full-full” are possible for each slave locomotive position.

The number of possible combinations further decreases when there might be empty wagons within loaded trains or when the tightest S-curve radius is 190 m. The worst case is obviously the combination of both. Figure 86 shows these results for the 1000 m train. The general trend is that the number of possible combinations per configuration (S-curve radius + lowest load status) decreases with increasing train length. Possible combinations move more and more towards the left and right side of the diagram. This means that load statuses “empty-empty”, “empty-half”, “full-half” and “full-full” are most likely to be possible. As long as only nominal cases are considered, the 100 % slave locomotive position seems to be most favorable, followed by the 75 % position. Again, there is no slave locomotive position that works for each load status even if only 1000 m trains are considered.

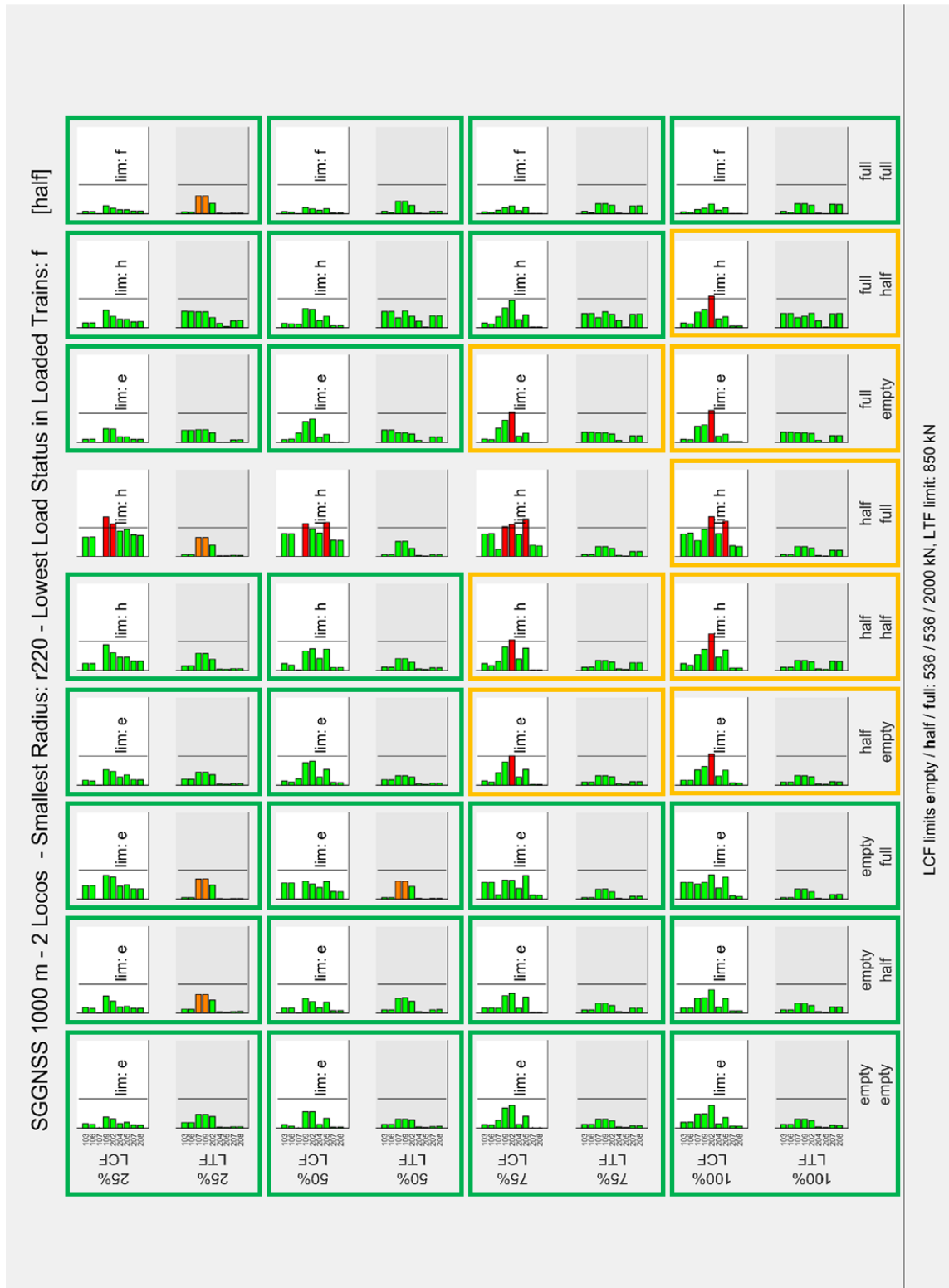


Figure 2: LCF/LTF values of 1000 m SGGNSS train with 220 m S-curve radius and without empty wagon in loaded trains



Figure 3: LCF/LTF values of 1250 m SGGNSS train with 220 m S-curve radius and without empty wagon in loaded trains



Figure 4: LCF/LTF values of 1000 m SGGNSS train with 190 m S-curve radius and empty wagon in loaded trains

4.3.7 Comparison of 1D simulations results with 3D limit values (FALNS)

The comparison of the results for the FALNS trains with the respective limit values generally show the same trends as the one for the SGGNSS wagons. Figure 87 shows the configuration with the most possible combinations. The most significant difference here is that the degraded case 205 exceeds limits in the “full-full” load status. This is because of two reasons. Firstly, the total train weight of fully loaded FALNS wagons is much higher than that of fully loaded SGGNSS trains, because the FALNS wagons are much shorter. Secondly, the LCF limit value for loaded FALNS wagons is 883 kN for the 220 m S-curve, whereas the limit value for the SGGNSS wagon is above 2000 kN. Another difference between FALNS trains and SGGNSS trains is the high number of high LTF values, which are very close to the limit value, even for the 1000 m train. In fact, some longer trains exceed LTF limits especially with the “full-half” load status.

The load statuses, which are most likely to be possible in the case of the FALNS train, are “empty-empty”, “empty-half”, “full-empty” and “full-half”. However, the latter three become increasingly critical with increasing train length. Figure 88 shows the analogue configuration as above with a train length of 1250 m.

When considering the most critical scenario of 190 m S-curve radius and the possibility of empty wagons within loaded trains, there are only seven fully possible combinations. These combinations are all for the 1000 m train (Figure 89). There are no fully possible combinations for trains longer than 1000 m. Even when only considering nominal cases there are very few possible combinations for train lengths of 1250 m and 1500 m.

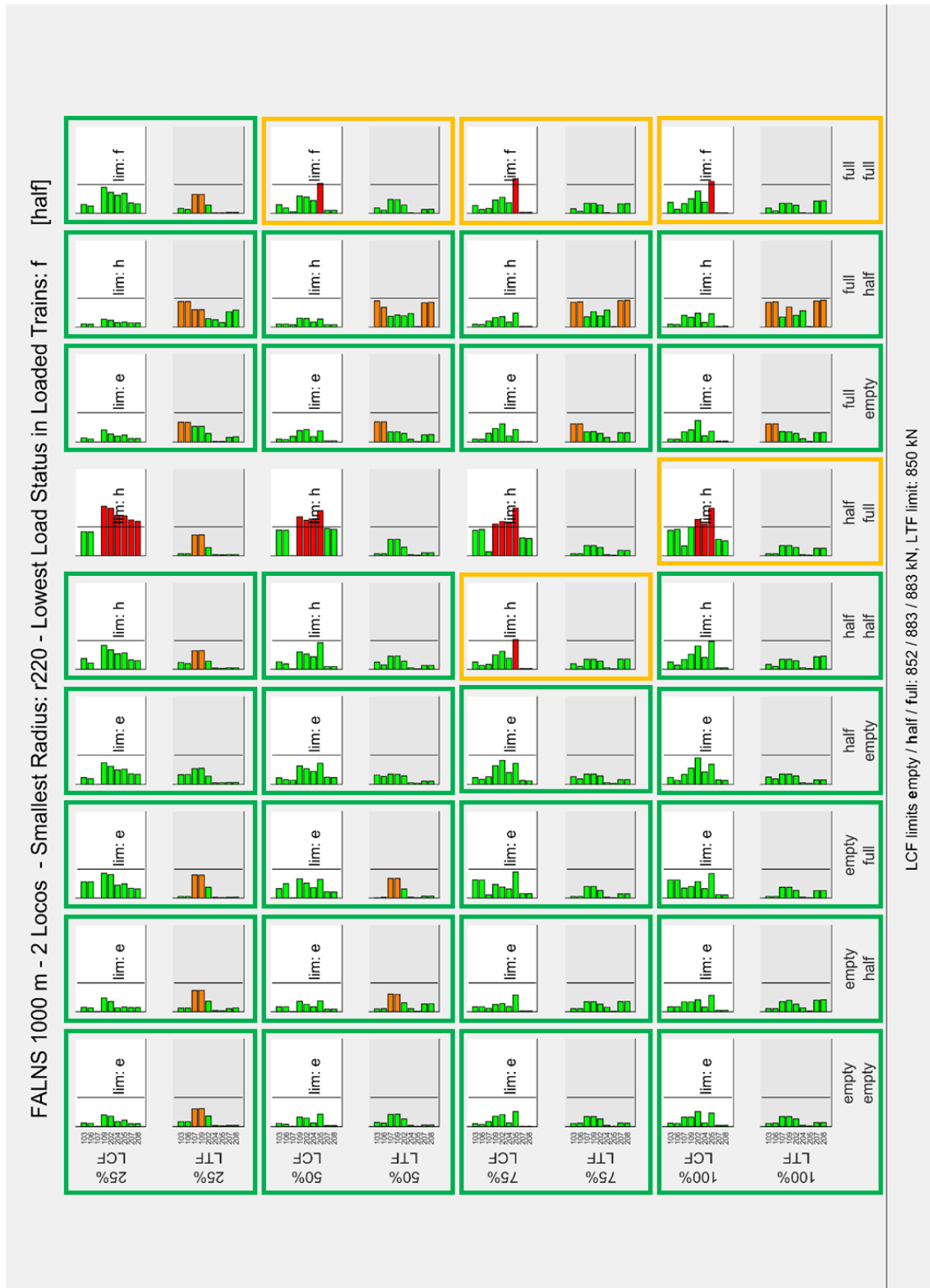


Figure 5: LCF/LTF values of 1000 m FALNS train with 220 m S-curve radius and no empty wagon in loaded trains

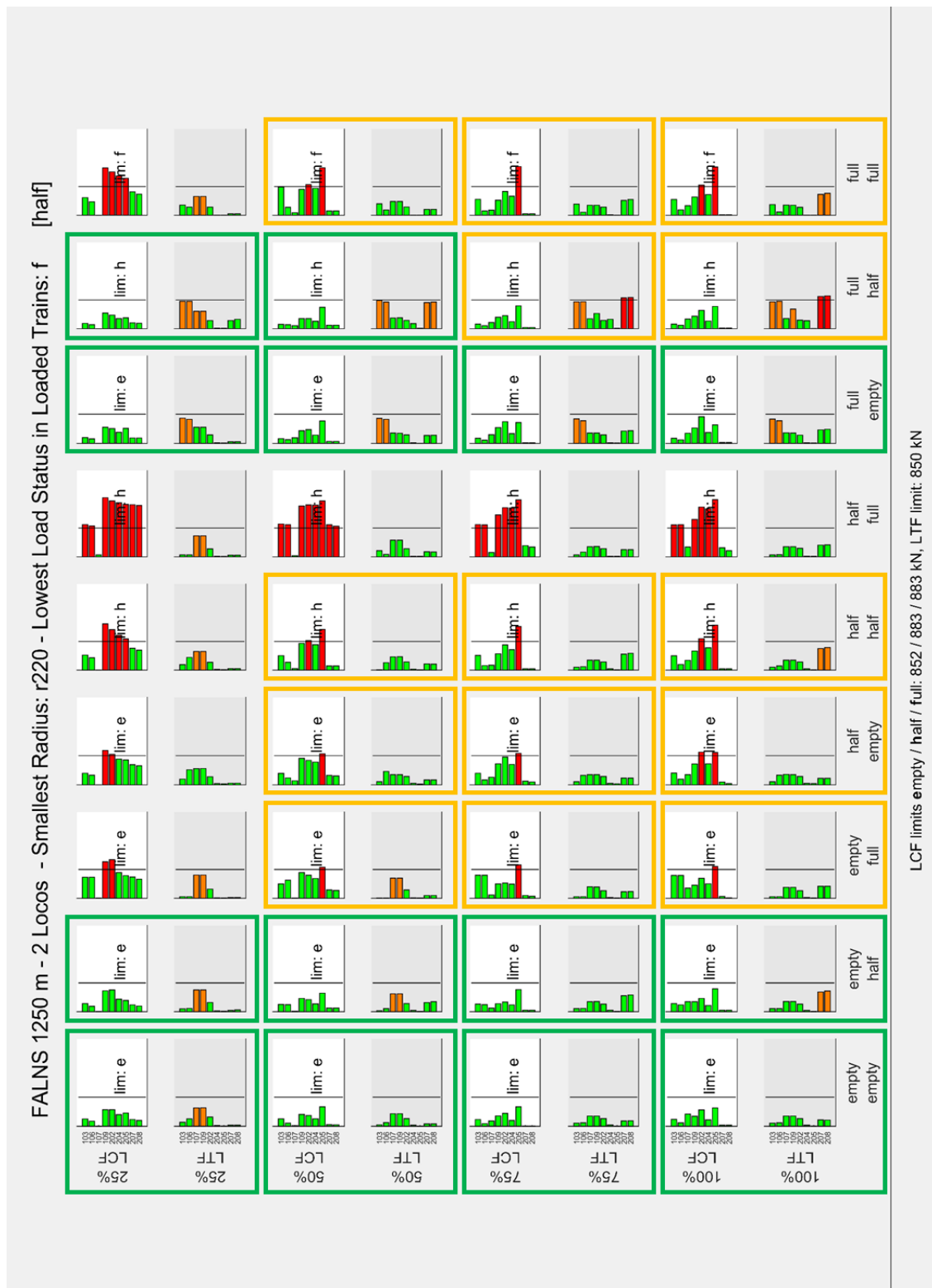


Figure 6: LCF/LTF values of 1250 m FALNS train with 220 m S-curve radius and no empty wagon in loaded trains



Figure 7: LCF/LTF values of 1000 m FALNS train with 190 m S-curve radius and empty wagon in loaded trains

4.3.8 Simulations with two slave locomotives

The 1D-simulation results of trains with one master locomotive at the front and one slave locomotive at various positions along the train show that there is no slave locomotive position that works for every load status even when the train is only 1000 m long. Load statuses where one part of the train is half-loaded are very critical. The load status “half-full” is especially critical.

The inevitable question then is: Can a second slave locomotive within the train improve the situation? The assumption is that it does, because every position in the train where the main brake pipe pressure is influenced helps to homogenize the brake cylinder pressure build up. The ideal situation in this context would be a control device in each vehicle. This would correspond to an electro-pneumatic brake control. It is obvious that this solution is very extensive. Adding a second slave locomotive, however, is a step in this direction, which might already be sufficient, and at the same time be economically feasible. To answer the question whether a second slave locomotive is sufficient, corresponding pneumatic and 1D simulations were performed (also see Section 4.2.3). In order to reduce the simulation effort, these simulations were performed for a train configuration with the master locomotive in the front, the first slave locomotive at the 50 % position and the second slave locomotive in the back. The trains have lengths of 1000 m, 1250 m, and 1500 m and consider the nominal cases 103, 106, 107, and 109.

Figure 90 shows the results for the 1000 m SGGNSS trains with empty wagons in loaded trains in the 220 m S-curve and Figure 91 shows the analogue results of the FALNS trains. Both trains are possible in each load status. With the addition of a second slave locomotive at the back of the train, the studied simulations show that with 1000 m trains all cases are possible; however, for the 1250 and 1500 m trains the “half-full” load status case is exceeding the limits with both types of wagons. The 1500 m trains further exceed some other limits. Figure 92 and Figure 93 show the exemplary results of the 1250 and the 1500 m SGGNSS train.

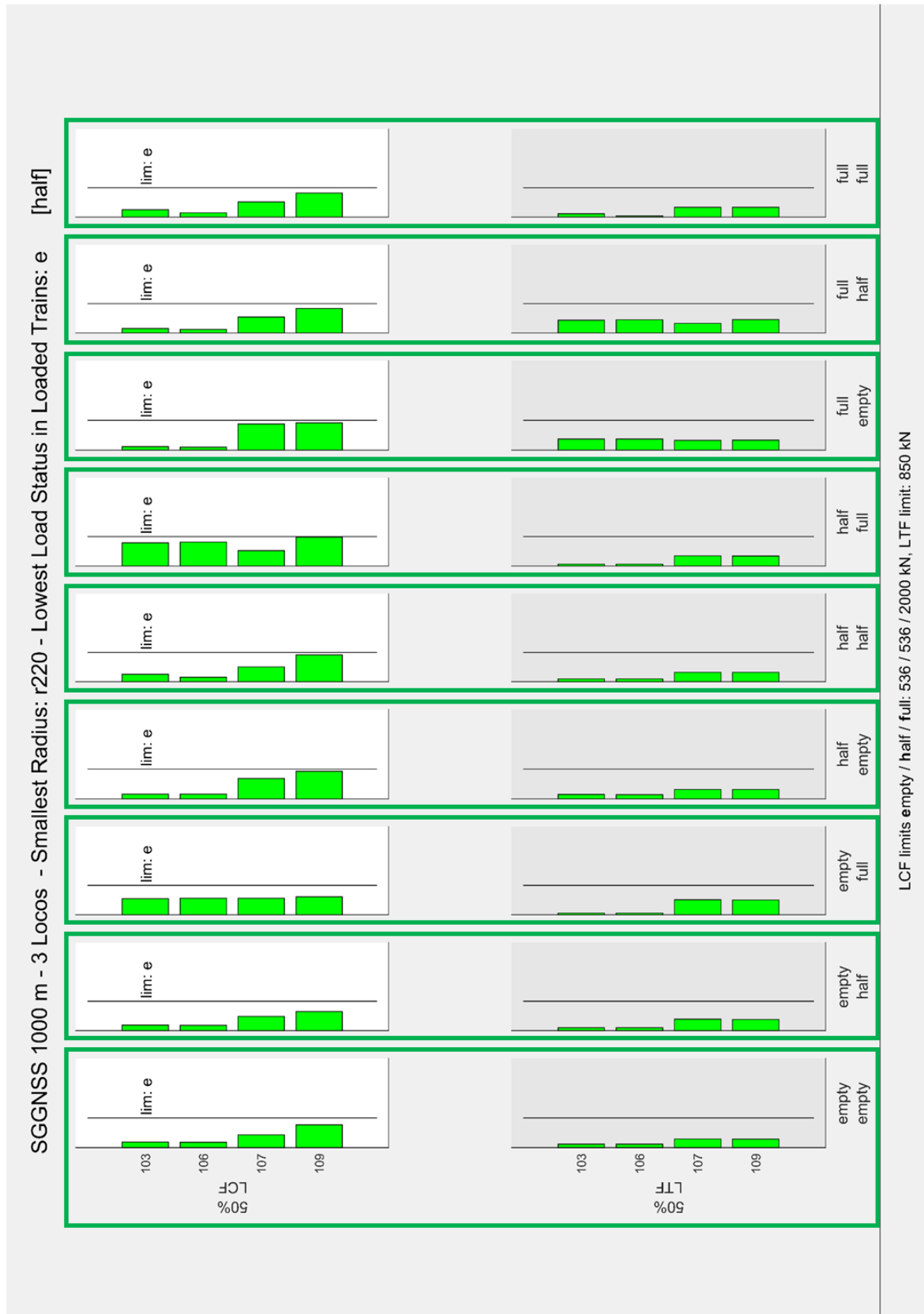


Figure 8: LCF/LTF values of 1000 m SGGNSS train with two slave locomotives, 220 m S-curve radius and empty wagon in loaded trains

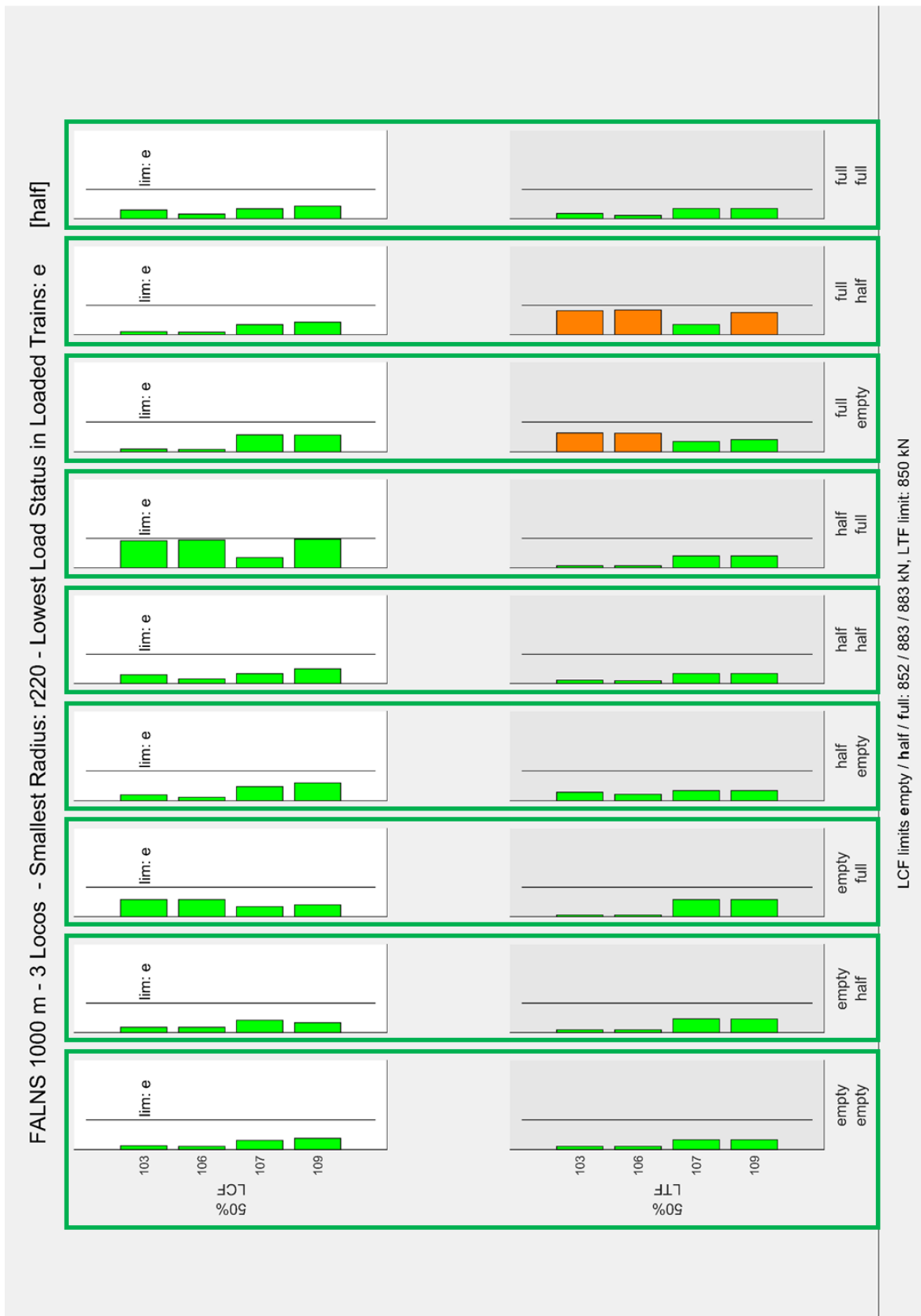


Figure 9: LCF/LTF values of 1000 m FALNS train with two slave locomotives, 220 m S-curve radius and empty wagon in loaded trains

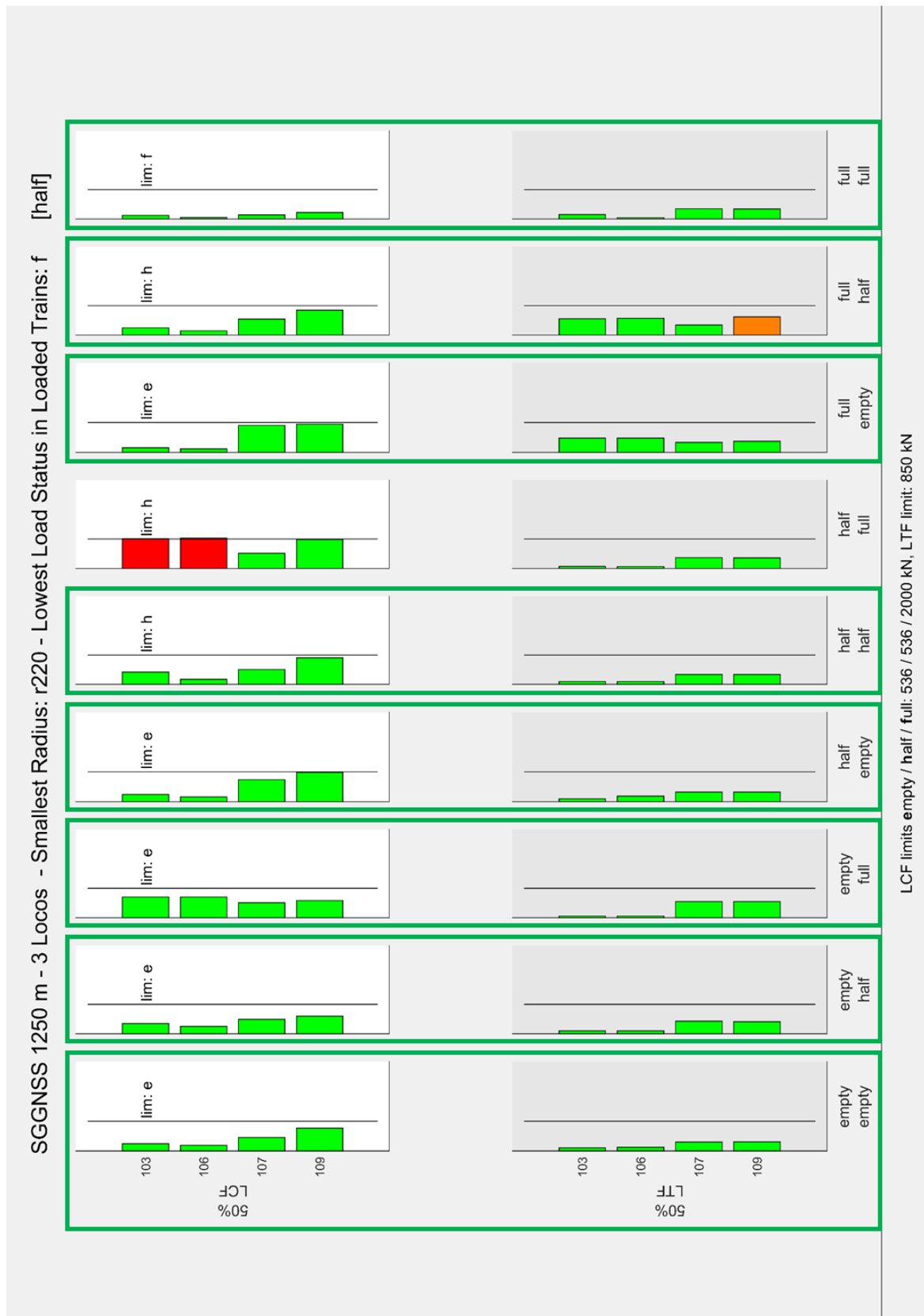


Figure 10: LCF/LTF values of 1250 m FALNS train with two slave locomotives, 220 m S-curve radius and without empty wagon in loaded trains

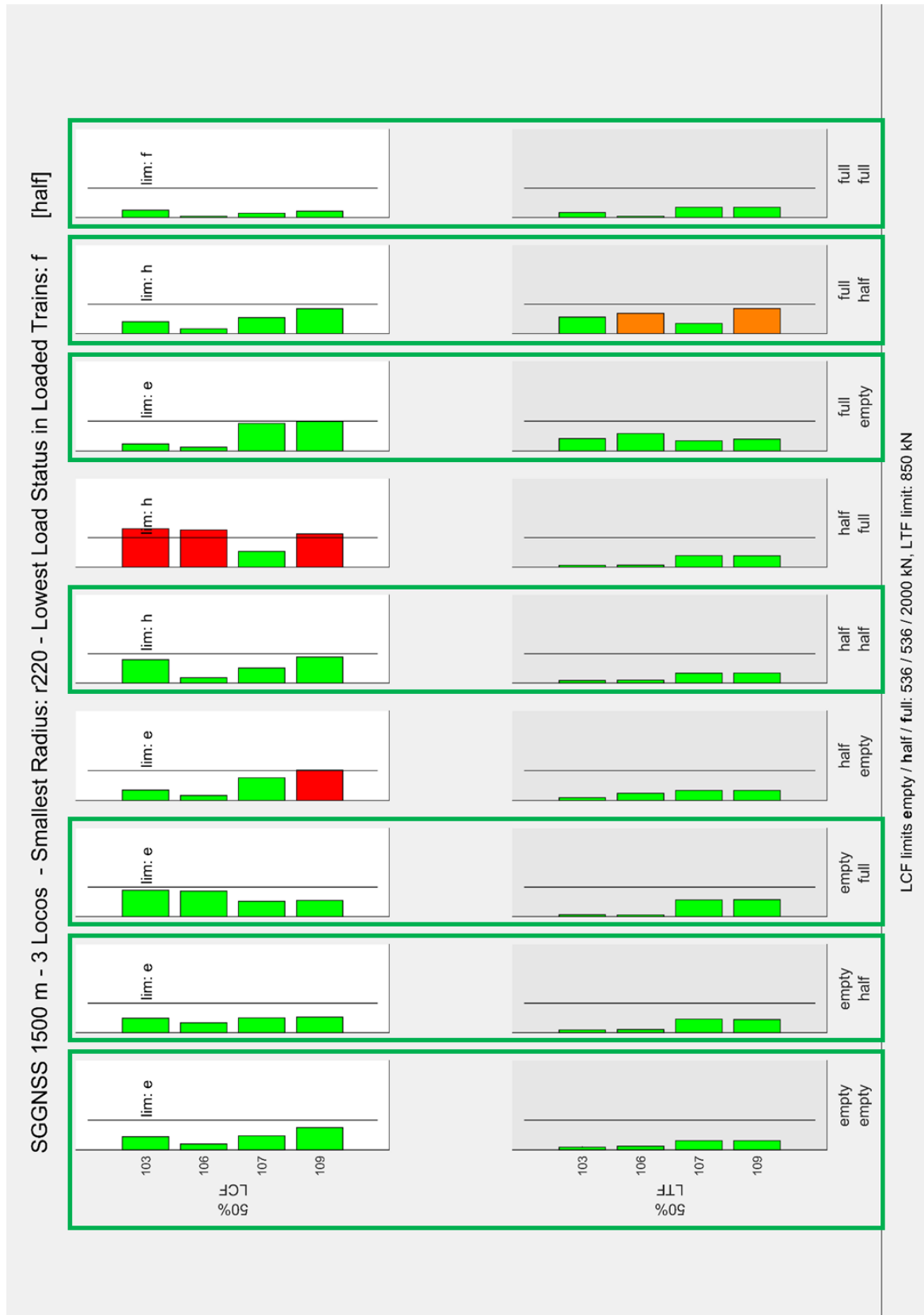


Figure 11: LCF/LTF values of 1500 m FALNS train with two slave locomotives, 220 m S-curve radius and without empty wagon in loaded trains

4.3.9 Further analysis of simulation results with two slave locomotives

The obtained results contradict the expectation that more slave locomotives would lead to lower forces because of a more homogenous brake force build-up. Figure 94 shows the main brake pipe pressure and the resulting brake cylinder pressure of a 1000 m FALNS train with load status “half-full” when the venting of the main brake pipe takes place at the master locomotive only (case 103).

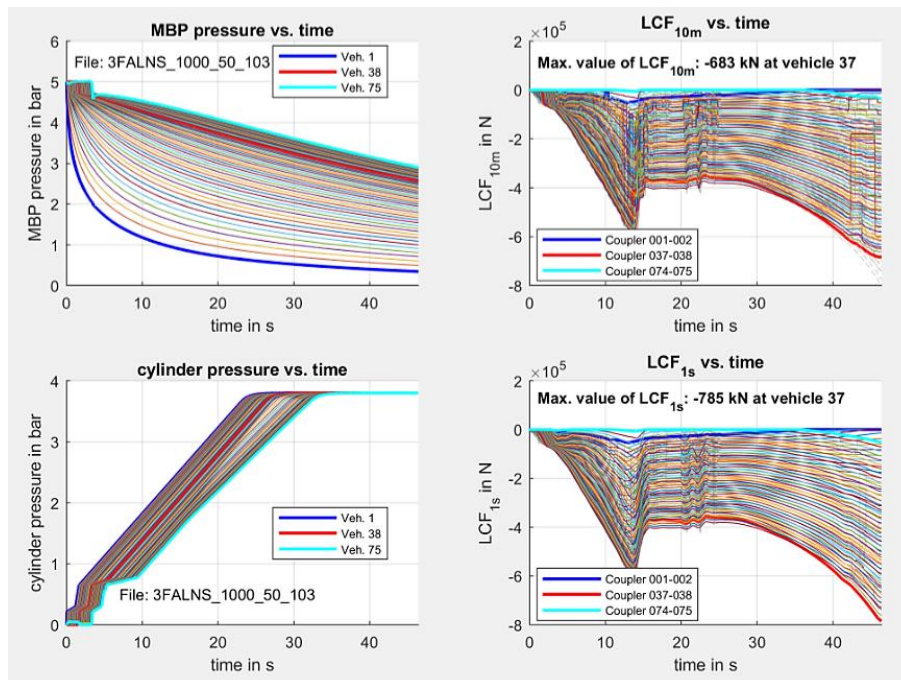


Figure 94: MBP pressure, brake cylinder pressure, and LCF values for 1000 m FALNS train with two slave locomotives in case 103

The large differences in the main brake pipe pressure and the resulting differences between the brake cylinder pressures are clearly visible. The resulting LCF values are visible on the right. There is a peak of LCF around 12 seconds. However, the maximum values of LCF are not reached during this peak but towards the end of the stopping process. There is a steady increase of LCF. Figure 95 shows the same train but now in case 106 where all three locomotives in the train vent the main brake pipe. The results are much lower differences between the main brake pipe pressures at each wagon and

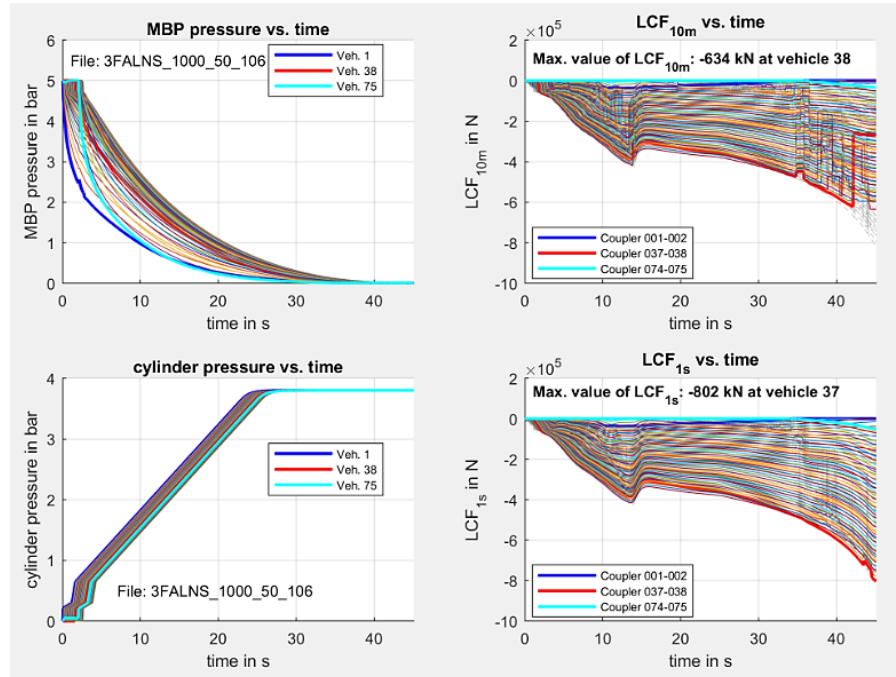


Figure 95: MBP pressure, brake cylinder pressure, and LCF values for 1000 m FALNS train with two slave locomotives in case 106

even smaller differences between the brake cylinder pressures. This clearly shows that the intended effect of multiple venting points within the train works. However, the resulting LCF values on the right have not changed much. The peak around 12 seconds has decreased but the maximum value at the end of the stopping process has not decreased. It has even increased.

The consequence of these results is that the reason for the high forces towards the end of the stopping process is not dynamics in the train that are induced but an inhomogeneous brake force build-up. The remaining reasons are the differences in total mass of the two train parts and the effective brake forces. Figure 96 shows a primitive model of the train with two different load statuses of the front and the rear part.

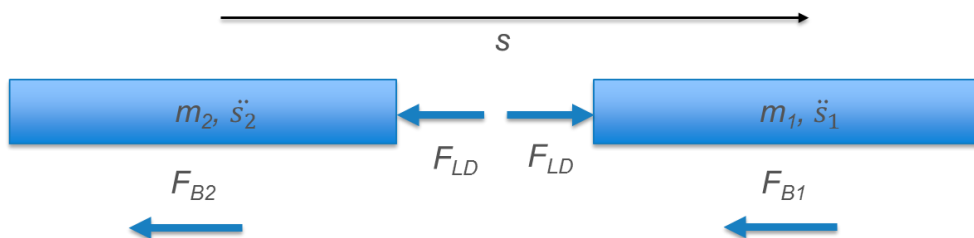


Figure 96: Primitive model of the train with two different load statuses of the front and the rear part

The mass m_1 resembles the first part of the train in front of the first slave locomotive. The mass m_2 resembles the second part of the train behind the first slave locomotive. The equilibrium of forces leads to:

$$m_1 \ddot{s}_1 - F_{B1} + F_{LD} = 0 \quad (27)$$

$$m_2 \ddot{s}_2 - F_{B2} + F_{LD} = 0 \quad (28)$$

When we neglect the locomotives for reasons of simplicity, there are 36 FALNS wagons with a mass of 57.25 t each in the first part. The maximum brake force at the end of the stopping process is approx. 100 kN per wagon. The second part of the train also has 36 FALNS wagons. Their total mass is 90 t each. Their maximum brake force is almost the same as for the front wagons because the auto-continuous device keeps the brake force constant from 58 t (= 65 % of 90 t) on (also see Section 2.4). This means:

$$F_{B1} \approx F_{B2} = F_B \quad (29)$$

Equations (27) to (29) and transposition lead to:

$$F_{LD} = \frac{F_B(m_2 - m_1)}{m_2 + m_1} \quad (30)$$

Finally, filling in the actual values for the train gives:

$$F_{LD} = \frac{36 * 100 \text{ kN} * 36 * (90 \text{ t} - 57,25 \text{ t})}{36 * (90 \text{ t} + 57,25 \text{ t})} = 800.7 \text{ kN} \quad (31)$$

The force value of 800.7 kN is almost exactly the same value as in Figure 95. It shows that effects of mass and brake force distribution may lead to high LCF/LTF values, independent of pneumatic effects. Furthermore, it shows a linear dependence with the number of wagons in the train (2×36 in this case). This means that the effect becomes more significant for longer trains.

4.3.10 Stretch braking

It is obvious that high LCF values occur when a train is being compressed. Effects that lead to a stretching of the train therefore reduce the LCF values. Of course, too much stretching can lead to high LTF values.

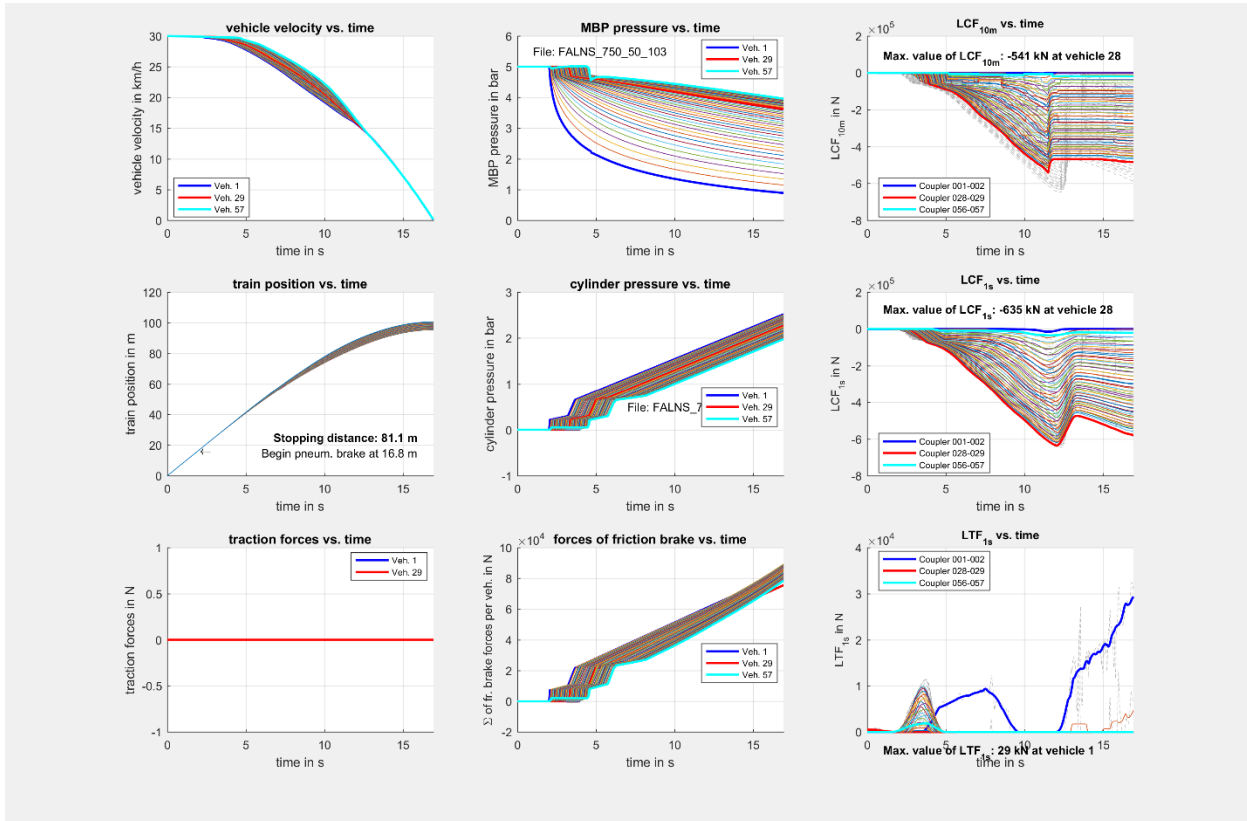


Figure 97: Emergency brake application of a 750 m FALNS train with load status “half-loaded” and an initial velocity of 30 km/h

Applying traction forces from the master locomotive while the rest of the train is braking effectively stretches the train. This procedure is called “stretch braking” and used for service brake applications at North American freight railroads [20]. Figure 97 shows an emergency brake application of a 750 m FALNS train with load status “half-loaded” and an initial velocity of 30 km/h. The stopping distance is 81.1 m, the maximum LTF value is 29 kN, and the maximum LCF value is 635 kN. Figure 98 shows the same train with disabled pneumatic locomotive brake and with a traction force build-up to 300 kN within 10 s instead. In this case, the stopping distance has increased by 5.5 m (6.8 %), the maximum LTF value has increased to 402 kN (1386.2 %), and the maximum LCF value has decreased to 338 kN (53.2 %). This shows how compressive forces are converted into tension forces. However, 402 kN of LCF are still within the normal operational limits. Stretch braking could therefore significantly decrease LCF values without extending the stopping distance too much and without creating the risk of a train disruption. The application of such a method could be limited to emergency brake applications from low speeds, as they are most critical. Further work should investigate the possibility to use stretch braking for the operation of longer trains.

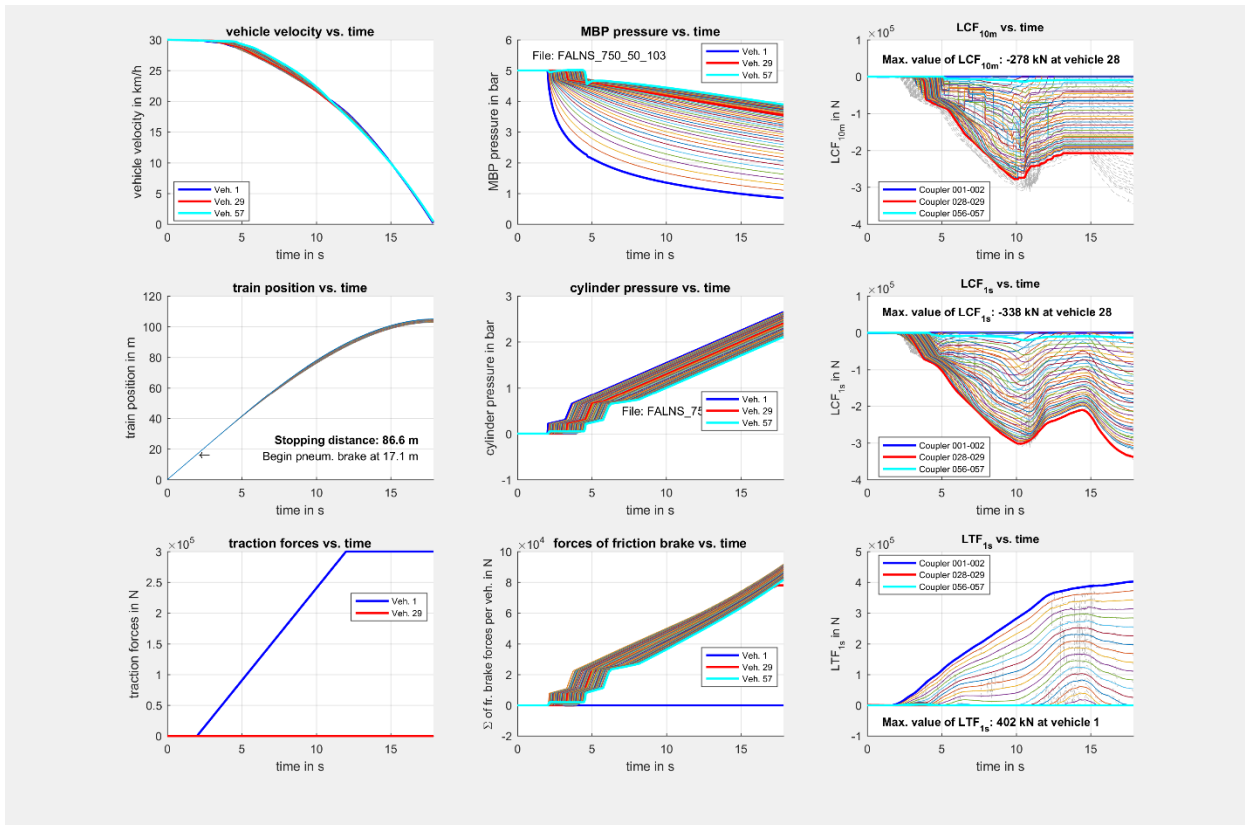


Figure 98: Emergency brake application of a 750 m FALNS train with load status “half-loaded” and an initial velocity of 30 km/h with ‘stretch braking’

4.4 3D SIMULATIONS (TOLERABLE FORCES)

In the previous chapter in the application of shorter train cases, the tolerable LCF for FALNS type wagons were examined (Section 3.5). In this section, the tolerable LCF values for a contrasting type of wagon, SGGNSS80 is presented and discussed. Further, simulations with the trains of mixed wagon configurations i.e. (FALNS and SGGNSS) are also performed and the results are discussed.

4.4.1 Flat wagons: SGGNSS80

The SGGNSS80 is a long flat wagon with low torsional carbody flexibility that are used as container wagons (see Figure 99). It is a modified version of the model used in the MARATHON project [1].

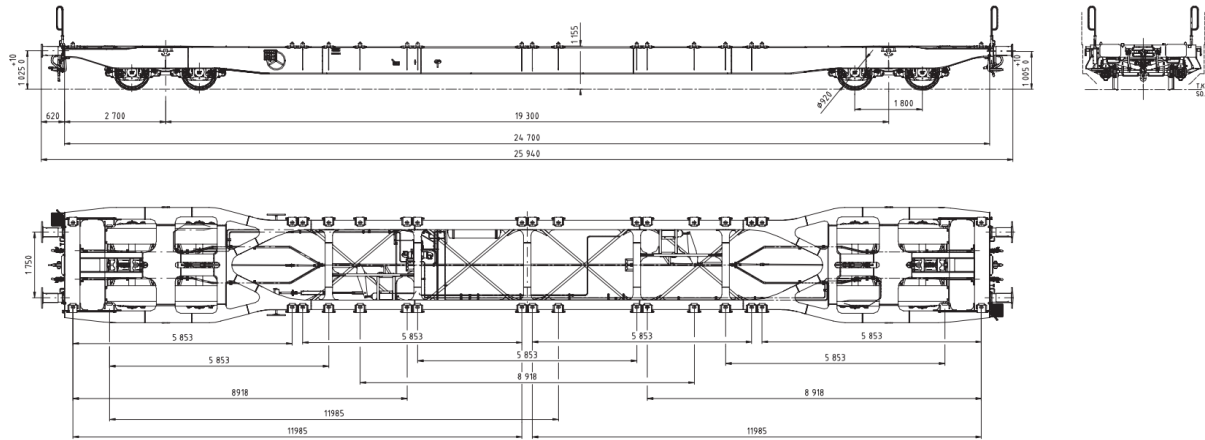


Figure 99: SGGNNS80 [22]

Some of the important attributes of the wagon concerning the three dimensional simulation model is given in Table 27.

Table 27: SGGNNS80 attributes

Attribute	Values
Bogie pivot length (a_{cb}) [m]	19.3
Length over buffers (L) [m]	25.94
Length of the buffers (l_{buff}) [m]	0.62
Wheelbase length (a_b) [m]	1.8
Wheel radius (r_o) [m]	0.46
Carbody torsional flexibility (c_t^*) [Nm^2/rad]	5.5×10^6
Running gear	Y25

4.4.2 Flat wagons - Tolerable LCF

The simulation model for the SGGNNS80 wagons can be seen in Figure 100.

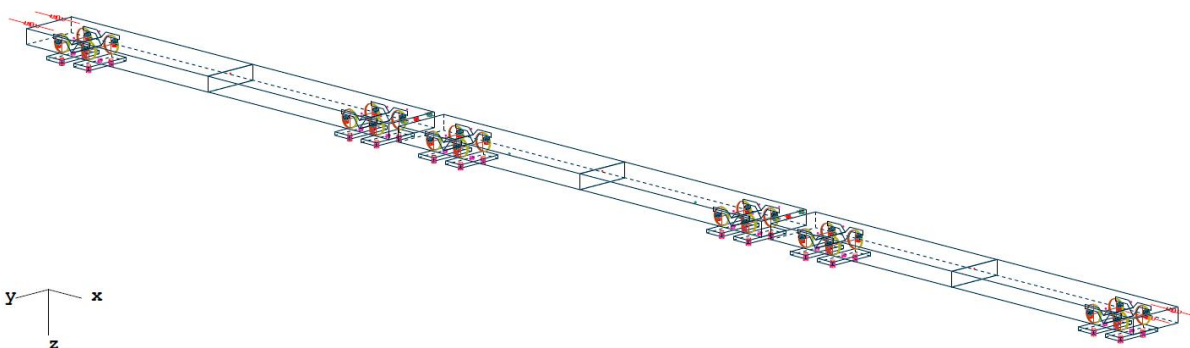


Figure 100: Simulation model for SGGNSS80

The model consists of three wagons connected for testing as described in the methodology in Section 2.5. The tolerable LCF is calculated accordingly. The concept of heterogeneities is extended further here with an additional running gear (Y25) as well. The simulations were performed and the corresponding Tolerable LCF values are presented in Table(s) below. The range of LCF values checked in the simulations is 0-2000 kN. Critically loaded wagon cases refer to three wagons with the middle one empty and others fully loaded. Nominally loaded wagon cases refer to all three wagons fully loaded.

**Table 28: Tolerable LCF for critically loaded wagon cases with QGO buffers
 (SGGNSS80x3)**

Sno.	Wagon(s)	Track	Tolerable LCF [kN]
1	SGGNSS80-SGGNSS80-SGGNSS80	S150M10	331
2	SGGNSS80-SGGNSS80-SGGNSS80	S170M10	388
3	SGGNSS80-SGGNSS80-SGGNSS80	S190M10	456
4	SGGNSS80-SGGNSS80-SGGNSS80	S200M10	488
5	SGGNSS80-SGGNSS80-SGGNSS80	S210M10	504
6	SGGNSS80-SGGNSS80-SGGNSS80	S220M10	536

**Table 29: Tolerable LCF for critically loaded wagon cases with Keystone buffers
(SGGNSS80x3)**

Sno.	Wagons	Track	Tolerable LCF [kN]
1	SGGNSS80-SGGNSS80-SGGNSS80	S150M10	318
2	SGGNSS80-SGGNSS80-SGGNSS80	S170M10	392
3	SGGNSS80-SGGNSS80-SGGNSS80	S190M10	395
4	SGGNSS80-SGGNSS80-SGGNSS80	S200M10	441
5	SGGNSS80-SGGNSS80-SGGNSS80	S210M10	463
6	SGGNSS80-SGGNSS80-SGGNSS80	S220M10	554

**Table 30: Tolerable LCF for nominally loaded wagon cases with QGO buffers
(SGGNSS80x3)**

Sno.	Wagon(s)	Track	Tolerable LCF [kN]
1	SGGNSS80-SGGNSS80-SGGNSS80	S150M10	1338
2	SGGNSS80-SGGNSS80-SGGNSS80	S170M10	1544
3	SGGNSS80-SGGNSS80-SGGNSS80	S190M10	1832
4	SGGNSS80-SGGNSS80-SGGNSS80	S200M10	>2000
5	SGGNSS80-SGGNSS80-SGGNSS80	S210M10	>2000
6	SGGNSS80-SGGNSS80-SGGNSS80	S220M10	>2000

Table 31: Tolerable LCF for nominally loaded wagon cases with Keystone buffers (SGGNSS80x3)

Sno.	Wagon(s)	Track	Tolerable LCF [kN]
1	SGGNSS80-SGGNSS80-SGGNSS80	S150M10	1368
2	SGGNSS80-SGGNSS80-SGGNSS80	S170M10	1566
3	SGGNSS80-SGGNSS80-SGGNSS80	S190M10	1821
4	SGGNSS80-SGGNSS80-SGGNSS80	S200M10	>2000
5	SGGNSS80-SGGNSS80-SGGNSS80	S210M10	>2000
6	SGGNSS80-SGGNSS80-SGGNSS80	S220M10	>2000

It can be seen from these values that while the tolerable LCF values are low for the nominally loaded cases, they can be quite high for highly loaded cases.

4.4.3 FALNS121-SGGNSS80-FALNS121

In a case of further heterogeneity, the barrier wagons are replaced by more rigid and shorter wagons as seen in Figure 101.

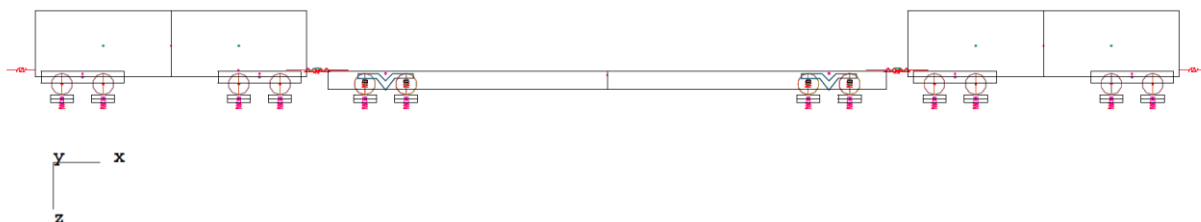


Figure 101: Heterogeneity (Barrier wagons: FALNS121)

The test wagon is kept as SGGNSS80 but the barrier wagons are replaced with the FALNS 121 type wagons seen in Section 3.5. The tolerable LCF of this mixed configuration, critically loaded and for different buffer types are listed in Table 32 and Table 33.

Table 32: Tolerable LCF for critically loaded wagon cases with QGO buffers (FALNS121-SGGNSS80-FALNS121)

Sno.	Wagon(s)	Track	Tolerable LCF [kN]
1	FALNS121-SGGNSS80- FALNS121	S150M10	200
2	FALNS121-SGGNSS80- FALNS121	S170M10	232
3	FALNS121-SGGNSS80- FALNS121	S190M10	240
4	FALNS121-SGGNSS80- FALNS121	S200M10	240
5	FALNS121-SGGNSS80- FALNS121	S210M10	248
6	FALNS121-SGGNSS80- FALNS121	S220M10	248

Table 33: Tolerable LCF for critically loaded wagon cases with Keystone buffers (FALNS121-SGGNSS80-FALNS121)

Sno.	Wagon(s)	Track	Tolerable LCF [kN]
1	FALNS121-SGGNSS80- FALNS121	S150M10	200
2	FALNS121-SGGNSS80- FALNS121	S170M10	208
3	FALNS121-SGGNSS80- FALNS121	S190M10	232
4	FALNS121-SGGNSS80- FALNS121	S200M10	248
5	FALNS121-SGGNSS80- FALNS121	S210M10	248
6	FALNS121-SGGNSS80- FALNS121	S220M10	256

It can be seen from the tolerable LCF values that the barrier wagons have a profound effect on the tolerable LCF of the SGGNSS wagons, decreasing the tolerable LCF by 44% in average. The tolerable LCF of the nominally loaded cases for different buffer types are listed out in Table 34 and Table 35. It can be seen that the nominally loaded mixed

wagon cases also exhibit lower forces, only slightly higher than the critically loaded cases compared to the homogeneous cases.

Table 34: Tolerable LCF for nominally loaded wagon cases with QGO buffers (FALNS121-SGGNSS80-FALNS121)

Sno.	Wagon(s)	Track	Tolerable LCF [kN]
1	FALNS121-SGGNSS80- FALNS121	S150M10	216
2	FALNS121-SGGNSS80- FALNS121	S170M10	272
3	FALNS121-SGGNSS80- FALNS121	S190M10	280
4	FALNS121-SGGNSS80- FALNS121	S200M10	288
5	FALNS121-SGGNSS80- FALNS121	S210M10	288
6	FALNS121-SGGNSS80- FALNS121	S220M10	320

Table 35: Tolerable LCF for nominally loaded wagon cases with Keystone buffers (FALNS121-SGGNSS80-FALNS121)

Sno.	Wagon(s)	Track	Tolerable LCF [kN]
1	FALNS121-SGGNSS80- FALNS121	S150M10	216
2	FALNS121-SGGNSS80- FALNS121	S170M10	224
3	FALNS121-SGGNSS80- FALNS121	S190M10	288
4	FALNS121-SGGNSS80- FALNS121	S200M10	304
5	FALNS121-SGGNSS80- FALNS121	S210M10	304
6	FALNS121-SGGNSS80- FALNS121	S220M10	304

4.4.4 SGGNSS80-FALNS121-SGGNSS80

Checking the effect of placing the flat wagons as the barrier wagons to the stiffer and shorter FALNS test wagon gives interesting results. The MBS model can be seen in Figure 102. This configuration results in higher values of tolerable LCF as the softer barrier wagons lifts-off instead of the test wagons.

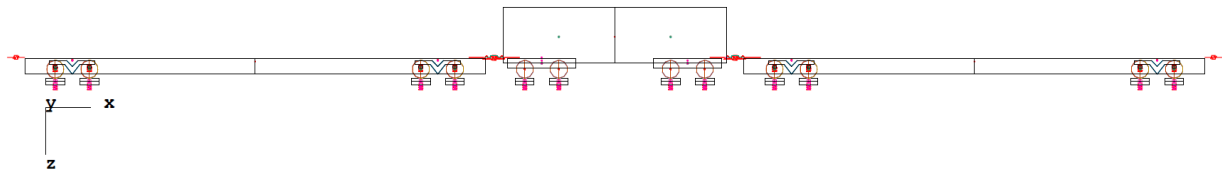


Figure 102: Heterogeneity (Barrier wagons: SGGNSS80)

The tolerable LCF values of this mixed configuration, critically loaded and for the QGO buffer are listed out in Table 36.

Table 36: Tolerable LCF for critically loaded wagon cases with QGO buffers (SGGNSS80-FALNS121-SGGNSS80)

Sno.	Wagon(s)	Track	Tolerable LCF [kN]
1	SGGNSS80-FALNS121-SGGNSS80	S150M10	528
2	SGGNSS80-FALNS121-SGGNSS80	S170M10	608
3	SGGNSS80-FALNS121-SGGNSS80	S190M10	712
4	SGGNSS80-FALNS121-SGGNSS80	S200M10	784
5	SGGNSS80-FALNS121-SGGNSS80	S210M10	832
6	SGGNSS80-FALNS121-SGGNSS80	S220M10	888

The tolerable LCF values of this mixed configuration, nominally loaded and for the QGO buffer are listed in Table 37.

**Table 37: Tolerable LCF for nominally loaded wagon cases with QGO buffers
 (SGGNSS80-FALNS121-SGGNSS80)**

Sno.	Wagon(s)	Track	Tolerable LCF [kN]
1	SGGNSS80-FALNS121-SGGNSS80	S150M10	544
2	SGGNSS80-FALNS121-SGGNSS80	S170M10	608
3	SGGNSS80-FALNS121-SGGNSS80	S190M10	712
4	SGGNSS80-FALNS121-SGGNSS80	S200M10	800
5	SGGNSS80-FALNS121-SGGNSS80	S210M10	840
6	SGGNSS80-FALNS121-SGGNSS80	S220M10	896

4.4.5 Effect of adjacent wagons

In the previous section, the tolerable LCF of the SGGNSS wagons and its combination with contrastingly different wagons were seen. The effect of the wagon type w.r.t. difference in buffer angle difference can be seen in Figure 103. It can be seen that contrasting wagons with vastly different torsional stiffness values do not follow the buffer angle trend listed in Figure 61 in Section 3.5. This can be explained due to the fact that the two wagons FALNS121 and FALNS183 were similar with a small difference in their torsional stiffness, while the same is not the case here. This highlights the sensitivity of carbody torsional stiffness on the tolerable LCF values of the wagons.

Figure 103 can be interpreted as giving the train operator the critical combination to check when two contrasting types of wagons are used. The blue and red lines represent the cases where a single wagon model was used for all the three wagons in the test train. While green and magenta lines show the combinations with different test and barrier wagons. The change in trend is highlighted by the arrows. From this plot, it can be concluded that critically loaded cases where the longer and flexible empty wagon is surrounded by two fully loaded, short and rigid wagons present the most critical combination as far as tolerable LCF of a wagon combination is concerned.

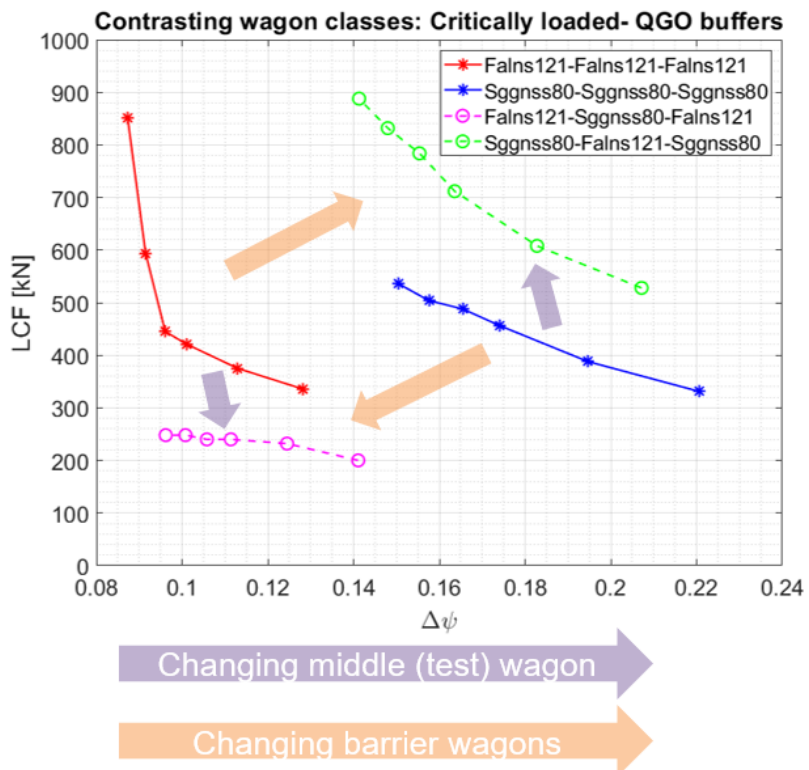


Figure 103: Tolerable LCF: Combination of contrasting wagon classes.

It should be noted here though, that a similar trend is not visible in the nominally loaded wagons.

4.5 CONCLUSIONS AND PRECAUTIONS

Longer trains, especially composed of long and flexible wagons increase the complexity of the operation. The effect of the resulting dynamics between the wagons are clearly pronounced in the actual longitudinal forces obtained from 1D simulations done in Section 4.3. It results in high in-train forces for various braking scenarios as described in Sections 4.3.6 and 4.3.7.

A lot of the work done for longer trains so far, was focussed on the vehicle/train attributes. There is a need to also consider the possibility of altering the infrastructure bottlenecks such as the radius of the S-curves and the length of sidings, that can increase the tolerable LCF values as well.

In case of operation of longer freight trains (>1000 m) equipped with the traditional pneumatic braking systems, the presence of an additional slave locomotive (one master, two slave locomotives) does not improve the situation much in terms of the actual forces. Stretch braking (see Section 4.3.10) could significantly decrease LCF values without increasing the stopping distance too much and without creating the risk of a train

disruption. The application of such a method could be limited to emergency brake applications from low speeds, as they are the most critical. Further work should investigate the possibility to use stretch braking for the operation of longer trains.

Coming to the tolerable LCF calculation (Section 4.4), longer and flexible flat wagons (SGGNSS80) exhibit higher derailment risks. Coupling them with contrastingly different type of wagons (FALNS), also changes the running behaviour and can influence the tolerable LCF. The critically loaded cases where the longer and flexible empty wagon is surrounded by fully loaded, short and rigid wagons present the most critical combination. This should be the first combination to be checked for derailment risk in a train with mixed wagon types and loading patterns.

From the overall analysis carried out for the different wagon types in Section 3.5 and Section 4.4, it can be concluded that while the buffer angle difference might serve as a useful indicator for finding the tolerable LCF of combinations of wagons of similar type (specifically the torsional stiffness), it might not be the case for contrasting wagon classes. In such cases, the sensitivity of carbody torsional stiffness plays a major role in addition to the buffer angles.

5. OVERALL CONCLUSIONS AND SAFETY PRECAUTIONS

Overall, the complex nature of Longitudinal Train Dynamics and the various attributes that influence the operation of long freight trains in a European context was studied extensively by the project partners, together with FFL4E partners, and presented in the current work. A bottom-up approach was adopted in conducting the study. The engineering models were constructed for different subtasks involved and in the end, linked together to provide a simulation-based platform that can be used to judge the feasibility of the long freight train for the given set of wagons and track route.

The different issues and heterogenities were studied in detail in different parts by the project partners. Based on these, some of the following precautions are to be drawn:

- From the pneumatics point of view, the goal is to obtain a pressure build-up in BCs as uniform as possible along the train. With one slave loco operation, pneumatics simulations suggest that positioning the slave loco at 75% the train length generally allows more uniform pressure build-up.
- Operation with two slave locos significantly improves the situation guaranteeing faster venting and uniform pressure build-up. However, the actual longitudinal forces still remain high for longer trains.
- Automatic activation of emergency/maximum service braking in communication-loss mode (loss of radio signal) based on monitoring of pressure in MBP may be by-passed if the two locos are too close to each other. Thresholds of these activation logics should be properly tuned according to distance between locos.
- The loading pattern in which the front part of the train is half-loaded and the rear fully loaded is very critical in the operation of very long trains.
- Two slave locomotives improve the situation for trains up to 1000 m long, but are not very effective for the trains beyond this length.
- Some load statuses may lead to very high forces independently of pneumatics/number of slave locomotives. This effect linearly increases with train length.
- Freight wagons with different load statuses exhibit disparate deceleration behaviour due to characteristics of load devices. Therefore, replacement of the current load devices might be necessary.
- Active stretching ('stretch braking') may significantly reduce LCF values but increase LTF values (see Section 4.3.10).
- The general approach adopted in the three-dimensional simulation methodology could be built up to include similar look-up charts for different types of wagons that could effectively provide operation-based tolerable LCF values. The tolerable LCF values calculated from the current methodology provides higher values for some cases which would otherwise be lower, calculated according to the UIC 530-2 methodology.

- The carbody torsional stiffness plays a major role in the running behaviour of wagons in tight S-curves. This effect combined with a longer wagon length could increase the derailment risks.
- The presence of an empty wagon surrounded by two fully loaded wagons form the most critical case in terms of derailment as already seen in the testing procedure. But the derailment risk increases further if the empty middle wagon is longer and flexible and is surrounded by two fully loaded, short and stiff wagons.
- In a mixed train configuration, critical wagon combinations as the one stated above should be avoided, or placed at a position with minimum actual force occurrence.
- Apart from the carbodytorsional stiffness, the critical attributes concerning the three-dimensional LTD behaviour are:
 - Buffer angle difference (Curvature+wagon geometry).
 - Loading pattern.
 - Buffer type.

REFERENCES

- [1] Deliverable 3.3 of MARATHON project; 2013.
- [2] Deliverable 3.1: Functional requirements of radio controlled traction and braking; DYNAFREIGHT project; 2018
- [3] Carello M., Ivanov A., Mazza A., Pressure drop in pipe lines for compressed air: comparison between experimental and theoretical analysis, transactions on Engineering Sciences vol 18, 1998, WIT Press, ISSN 1743-3533.
- [4] UIC Code 541-4: Brakes - Brakes with composite brake blocks - General conditions for certification of composite brake blocks (4th edition), International Union of Railways (UIC); 2010.
- [5] EN 16452: Railway Applications - Braking - Brake Blocks; 2015
- [6] UIC Code 541-3: Brakes - Disc brakes and their application - General conditions for the certification of brake pads (7th edition), International Union of Railways (UIC); 2010.
- [7] UIC Code 541-04: Brakes - Regulations concerning the manufacture of brake components - Self-adjusting load-proportional braking system and automatic "empty-loaded" control device (3rd edition), International Union of Railways (UIC); 2006.
- [8] UIC Code 544-1: Brakes - Braking performance (5th edition), International Union of Railways (UIC); 2013.
- [9] Persson I, Gensys software, DEsolver AB, www.gensys.se; 2017.
- [10] Krishna V.V. Longitudinal Train Dynamics for Freight Wagons passing through an S-curve, Conference proceedings. The First International Railway Symposium Aachen; 2017.
- [11] UIC. UIC Code 530-2: Wagons - Running safety, International Union of Railways (UIC);2008.
- [12] Cantone L. TrainDy: The new Union Internationale des Chemins de Fer software for freight train interoperability. Proceedings of the Institution of Mechanical Engineers, Part F: Journal of Rail and Rapid Transit, 225(1):57-70; 2011.
- [13] Wu Q, Spiriyagin M and Cole C. Longitudinal train dynamics: an overview, Vehicle System Dynamics, 54:12, 1688-1714, DOI: 10.1080/00423114.2016.1228988; 2016.
- [14] Wu Q, Spiriyagin M, Cole C, Chang C, Guo G, Sakalo A, Wei W, Zhao X, Burgelman N, Wiersma P, Chollet H, Sebes M, Shamdani A, Melzi S, Cheli F, Galleonardo E, Bosso N, Zampieri N, Luo S, Wu H and Kaza G. International benchmarking of longitudinal train dynamics simulators: results, Vehicle System Dynamics, 56:3, 343-365, DOI: 10.1080/00423114.2017.1377840; 2018.
- [15] Andersson E, Berg M and Stichel S. Rail Vehicle Dynamics, Division of Rail Vehicles, Department of Aeronautical and Vehicle Engineering, Kungliga Tekniska Högskolan (KTH), Stockholm. ISBN 978-91-7595-420-2; 2014.

- [16] Simson S. Three axle locomotive bogie steering, simulation of powered curving performance passive and active steering bogies [doctoral thesis]. Rockhampton: CQUniversity; 2009.
- [17] Cole C, Spiriyagin M and Sun Y Q. Assessing wagon stability in complex train systems. International Journal of Rail Transportation, 1:4, 193-217, DOI: 10.1080/23248378.2013.836396; 2013.
- [18] Deutsche Bahn; Güterwagenkatalog;
https://gueterwagenkatalog.dbcargo.com/de/gueterwagenkatalog/detail/detail/bauart/121/?tx_cyzkatalog_katalog%5Bsearch%5D%5BselectedBranche%5D=15&tx_cyzkatalog_katalog%5Bsearch%5D%5BselectedProduktart%5D=19&cHash=cb829f1b33779fdc8178100d45cc5afc; 2018
- [19] Jönsson P A, Stichel S and Persson I. New simulation model for freight wagons with UIC link suspension, Vehicle System Dynamics, 46:S1, 695-704, DOI:10.1080/00423110802036976; 2008.
- [20] BNSF Railway: Air Brake and Train Handling Rules, No. 5; 2010. Online: <http://1405.utu.org/Files/I48891BNSF-AirBrake-TrainHandle-updated.pdf>
- [21] Jönsson P A. Dynamic Vehicle-Track Interaction of European Standard Freight Wagons with Link Suspension, Doctoral Thesis, Rail Vehicles, KTH, TRITA AVE 2007:36, ISBN 978-91-7178-727-9, Stockholm, Sweden; 2007.
- [22] Poprad, T. "http://tatravagonka.sk/wagons/SGGNSS-80/?lang=en," Tatravagonka Poprad, 2012. [Online].

APPENDIX A: PNEUMATICS VALIDATION

MODEL VALIDATION

The model for the pneumatics was validated against several experimental results provided by Faiveley Transport. Tests were performed by Faiveley in 2008 using an indoor test facility where a pneumatic brake system for a train, including main braking pipe and distributors, was set-up in laboratory. Trains up to 1500 m long were considered. Data of pressure drop inside the main braking pipe and of pressure build-up in the brake distributors were recorded in 9 positions along the pipe.

Emergency braking

The following figures report results of comparisons for emergency braking. Subfigures on the left show the time histories of both pressure drop and pressure build-up for the first and last vehicle of the train overlapping numerical and experimental results. Subfigures on the right display the time history of pressure build-up in the 9 vehicles. In all the cases, results indicate a good agreement between experimental and numerical data. Some discrepancies are present in the pressure build-up time history, though they are due more to the dispersion of the response of distributors with respect to the nominal value. Direct comparison of time histories gives a good accuracy in all the phases of braking.

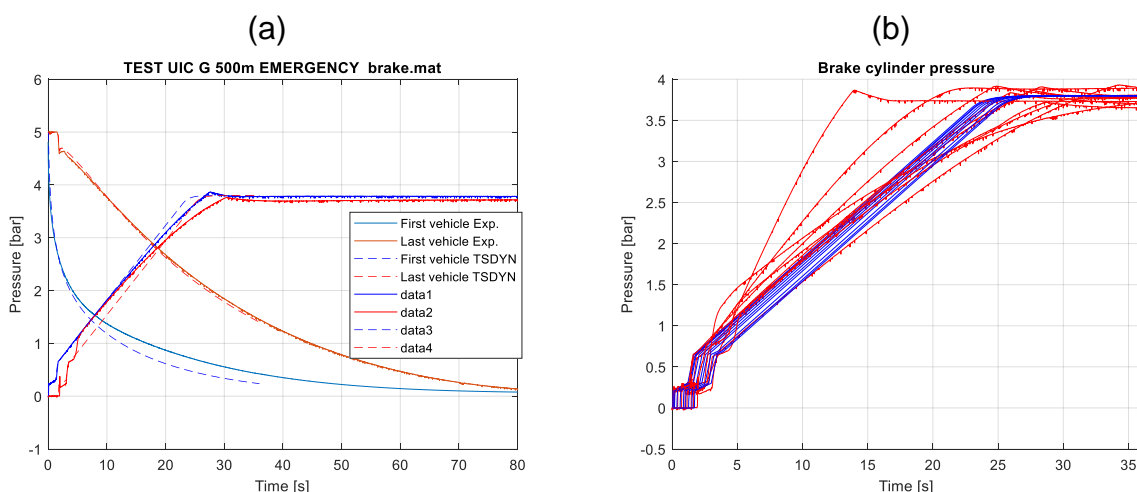
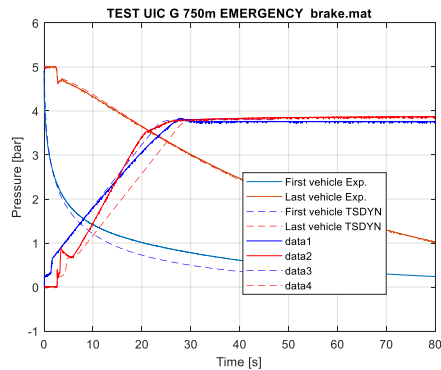


Figure 104: 500m-long train, emergency braking; (a): time histories of pressure drop in the main braking pipe and pressure build-up in the braking cylinders for first and last vehicle; (b) time histories of pressure build-up in 9 braking cylinders along the train.

(a)



(b)

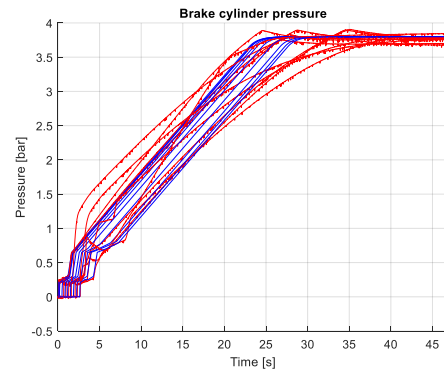
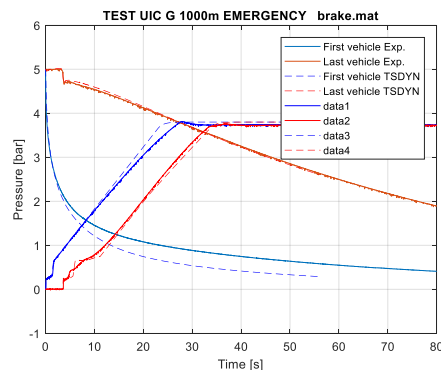


Figure 105: 750m-long train, emergency braking; (a): time histories of pressure drop in the main braking pipe and pressure build-up in the braking cylinders for first and last vehicle; (b) time histories of pressure build-up in 9 braking cylinders along the train.

(a)



(b)

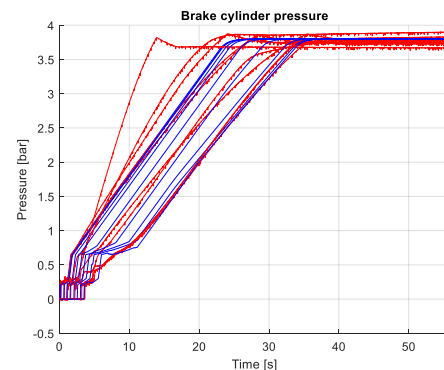


Figure 106: 1000m-long train, emergency braking; (a): time histories of pressure drop in the main braking pipe and pressure build-up in the braking cylinders for first and last vehicle; (b) time histories of pressure build-up in 9 braking cylinders along the train.

(a)

(b)

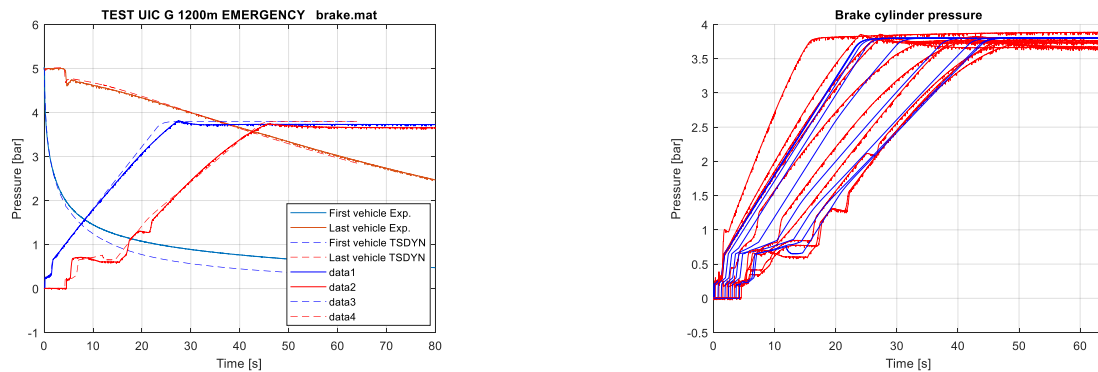


Figure 107: 1200m-long train, emergency braking; (a): time histories of pressure drop in the main braking pipe and pressure build-up in the braking cylinders for first and last vehicle; (b) time histories of pressure build-up in 9 braking cylinders along the train.

Maximum service braking

The following figures report results of comparisons for maximum service braking. Subfigures on the left show the time histories of both pressure drop and pressure build-up for the first and last vehicle of the train overlapping numerical and experimental results. Subfigures on the right display the time history of pressure build-up in the 9 vehicles. Also in this case, comparisons point out good agreement between measurements and numerical results.

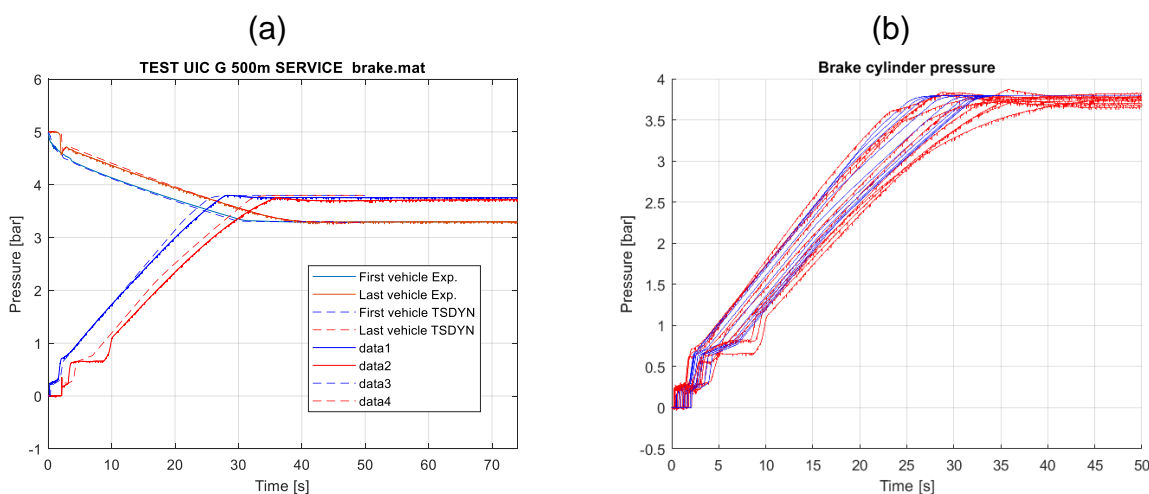


Figure 108: 500m-long train, maximum service braking; (a): time histories of pressure drop in the main braking pipe and pressure build-up in the braking cylinders for first and last vehicle; (b) time histories of pressure build-up in 9 braking cylinders along the train.

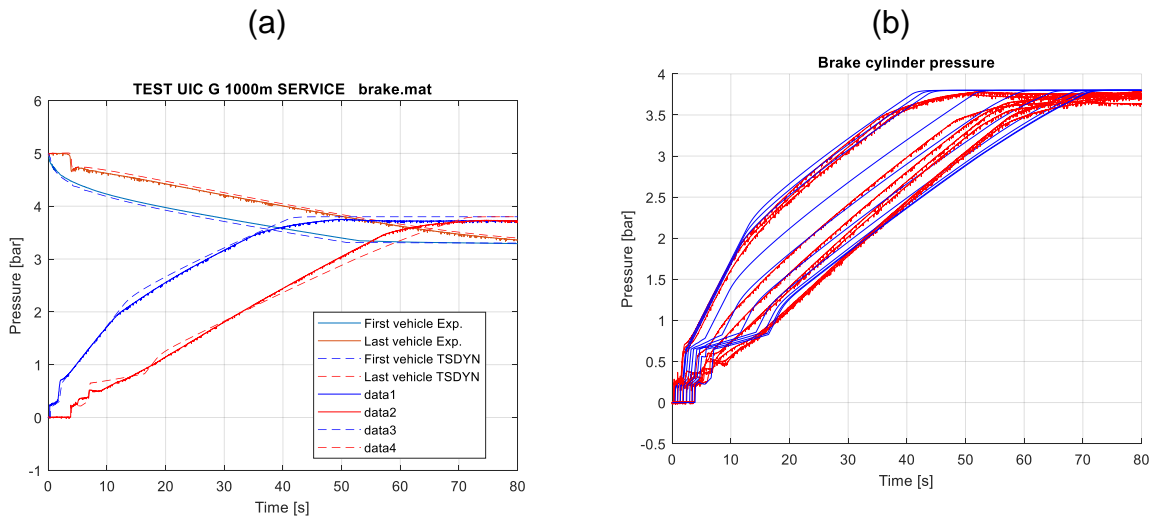


Figure 109: 1000m-long train, maximum service braking; (a): time histories of pressure drop in the main braking pipe and pressure build-up in the braking cylinders for first and last vehicle; (b) time histories of pressure build-up in 9 braking cylinders along the train.

Venting of main braking pipe from different positions

As very long freight trains are operated with more than one loco, it is important to reproduce the behaviour of compressed air inside the main braking pipe also when it is vented from different positions simultaneously. Experimental tests relevant to this operating conditions were performed. The same condition was simulated with the brake model and the results were compared. Results of Figure 110 refer to a 1500m-long train. Figure 110a reports the time histories of the DBV for the leading loco (master) and the 2nd loco (slave) located in the train centre: both the locos perform a maximum service braking; the command of the slave loco is delayed by nearly 2s. Figure 110b reports the comparisons between the time histories of pressure drop in the main braking pipe recorded during the experiments and obtained through the model. Also in this case results are in good agreement, showing the capability of the model of reproducing venting of the main braking pipe from different positions.

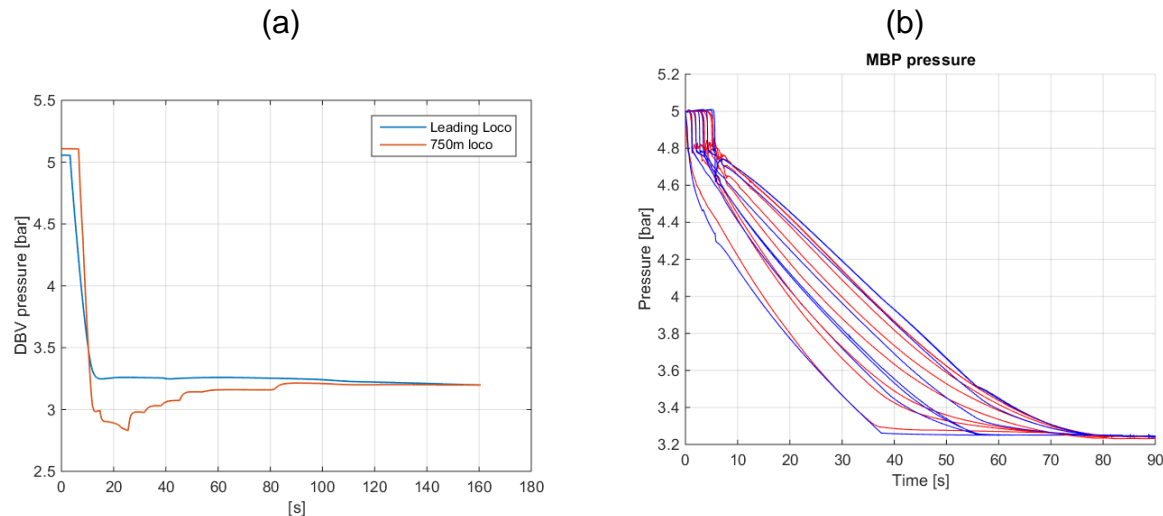


Figure 110: 1500m-long train, maximum service braking commanded by two locos; (a): time histories of pressure DBV controls; (b) time histories of pressure drop in MBP in several positions along the train.

Refilling of main braking pipe

Simulating refilling of the main braking pipe is another challenging operating condition, especially when different commands are set by master and slave locos. Experimental tests were carried out to reproduce this condition. As shown in Figure 111a, both the locos activate refilling of braking pipe at about 0 s; also in this case a delay of 2 s is present on the slave loco. After approximately 18 s, maximum service braking is commanded by the master loco while the slave loco continues trying to refill the main braking pipe. Figure 111b presents the comparisons between experimental and numerical results: time histories of the pressure drop in main braking pipe are shown. Also in this case the agreement is good, especially in the refilling phase (0-18s). When the two locos are operating with conflicting targets, comparison can still be considered good, with a maximum difference of about 0.5 bar after 40 s.

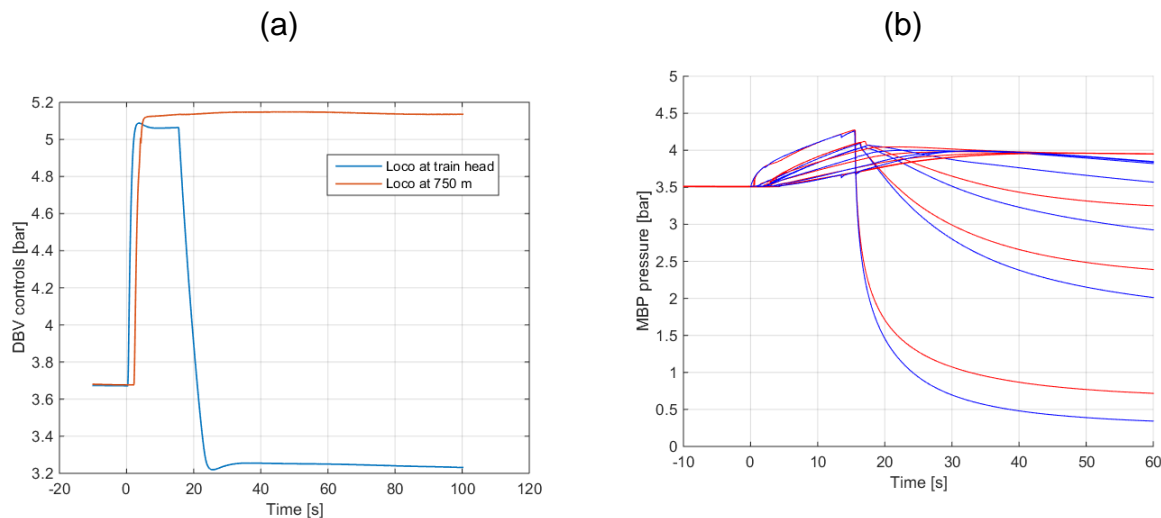


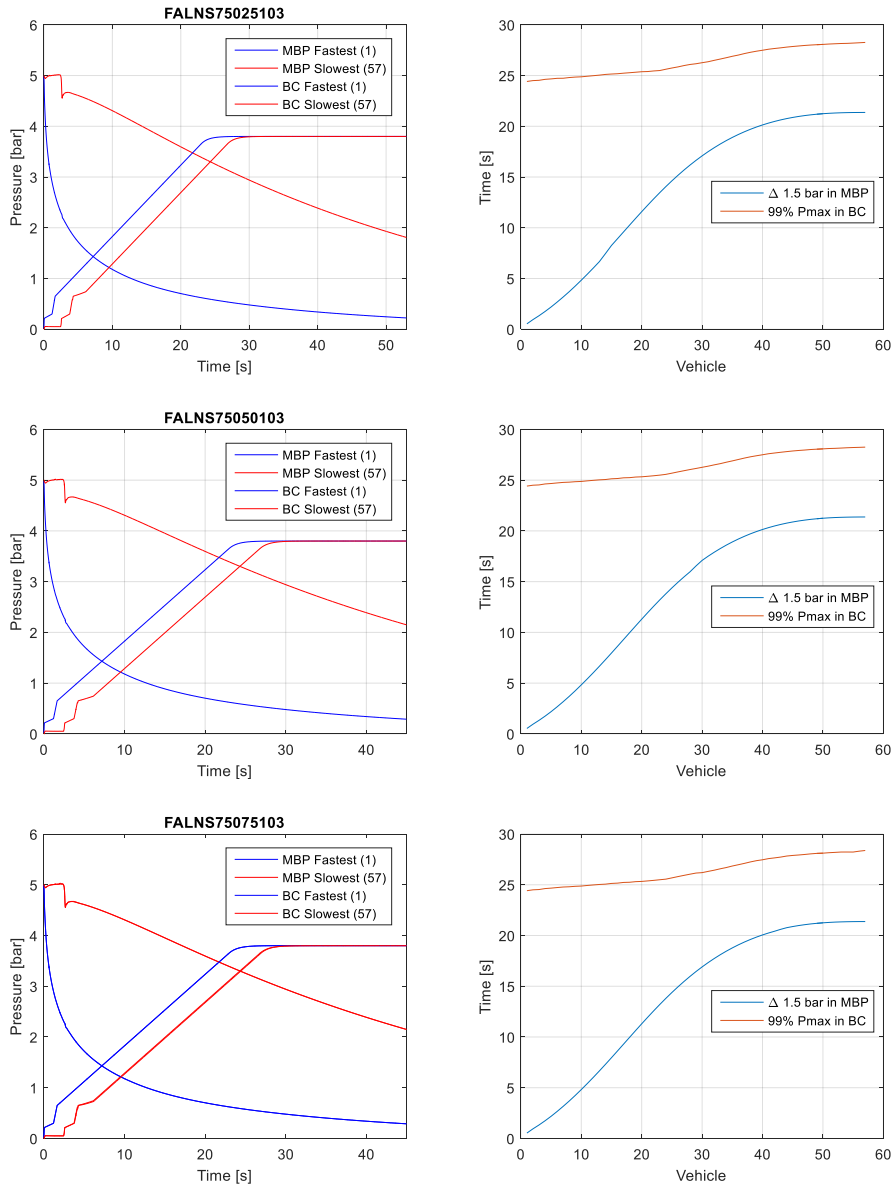
Figure 111: 1500m-long train, refilling of the braking pipe; (a): time histories of pressure DBV controls; (b) time histories of pressure drop in MBP in several positions along the train.

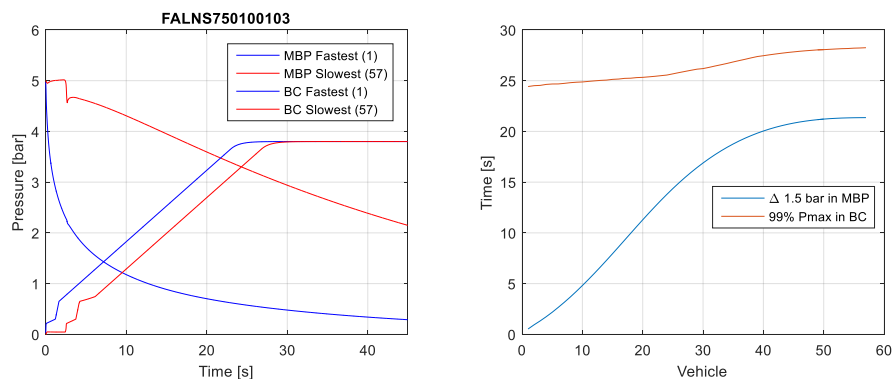
APPENDIX B: RESULTS OF PNEUMATICS FOR TRAINS UP TO 1500 M

This appendix collects the main results of pneumatics simulations for freight trains with lengths between 750 and 1500m, operating in nominal conditions.

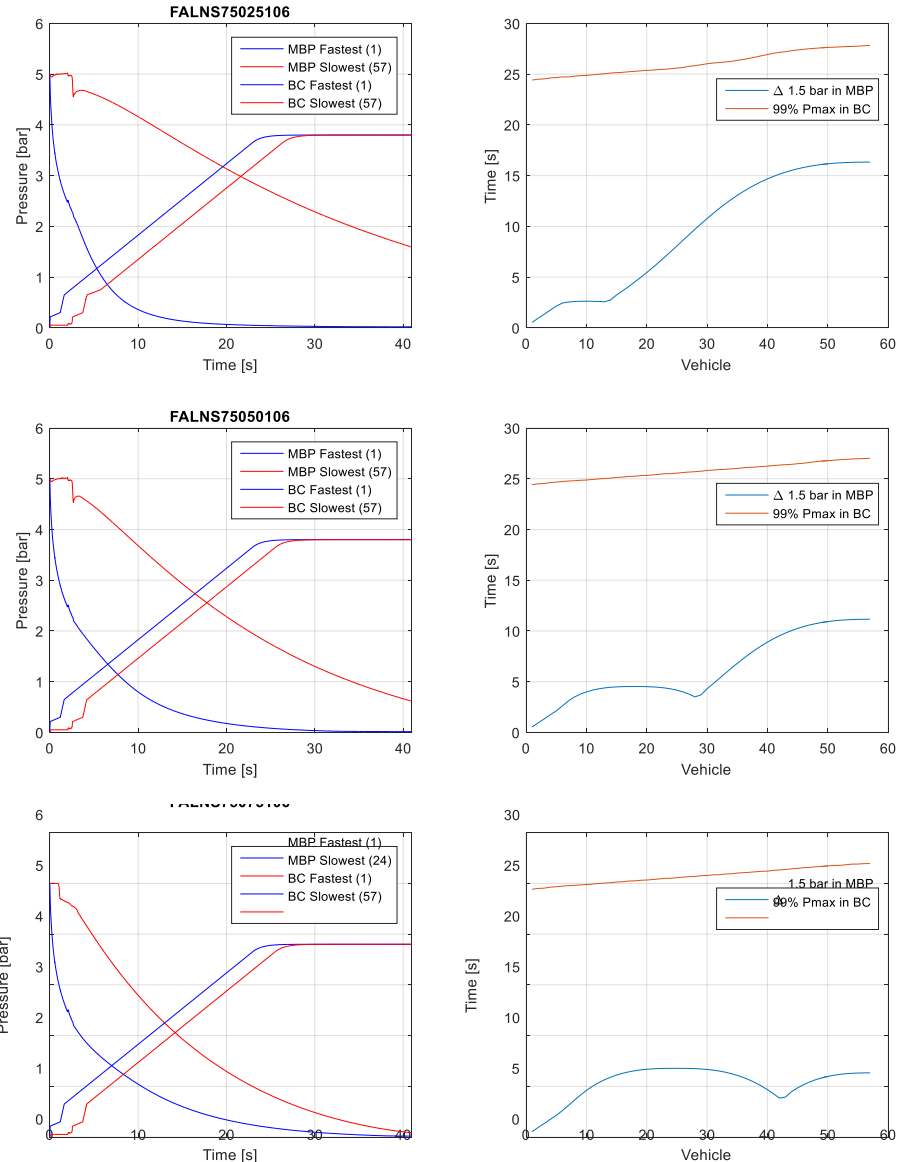
FALNS WITH TWO LOCOS

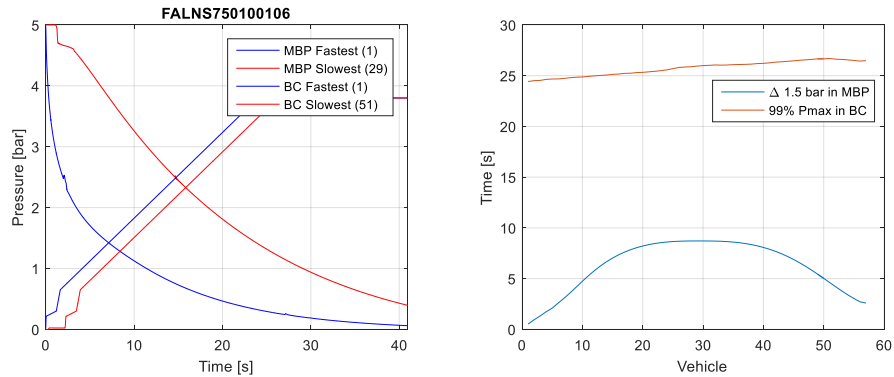
FALNS 750 m, scenario 103



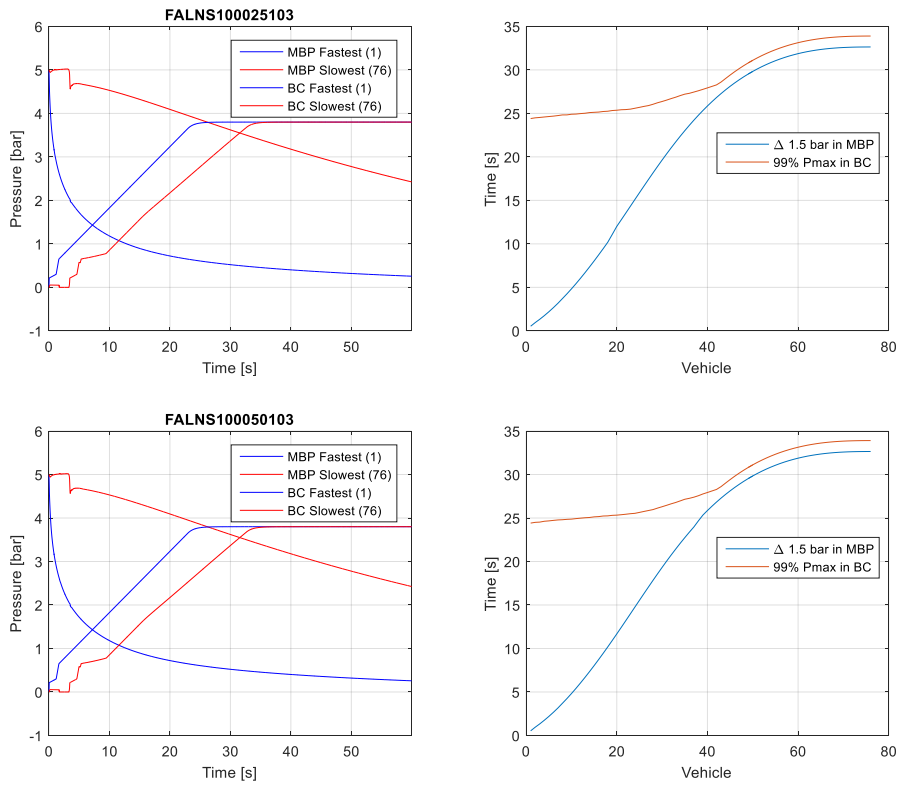


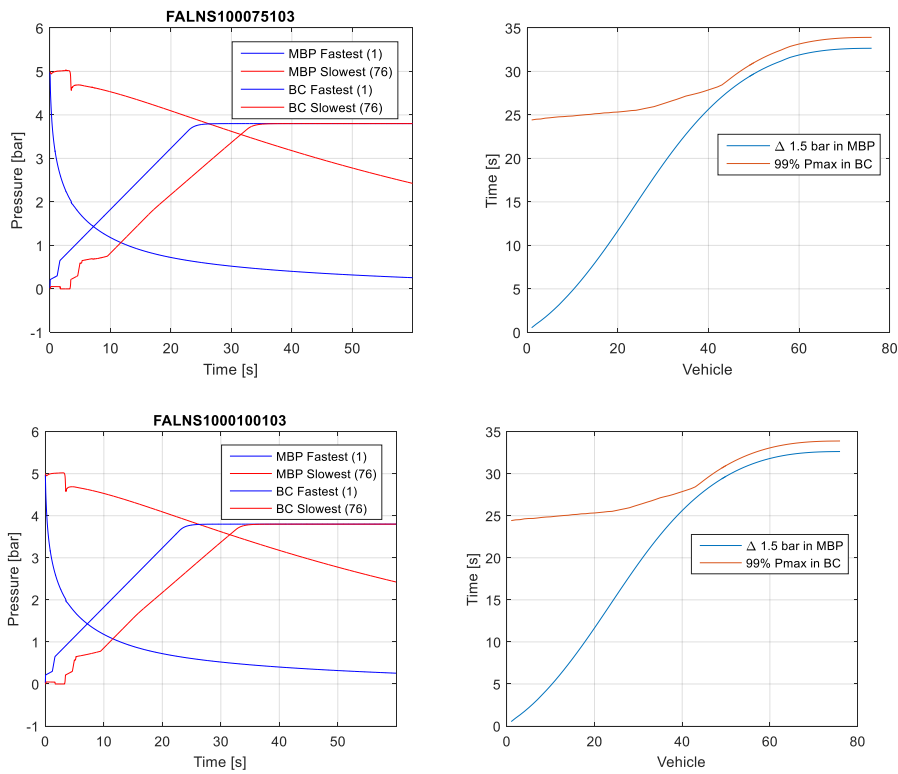
FALNS 750 m, scenario 106



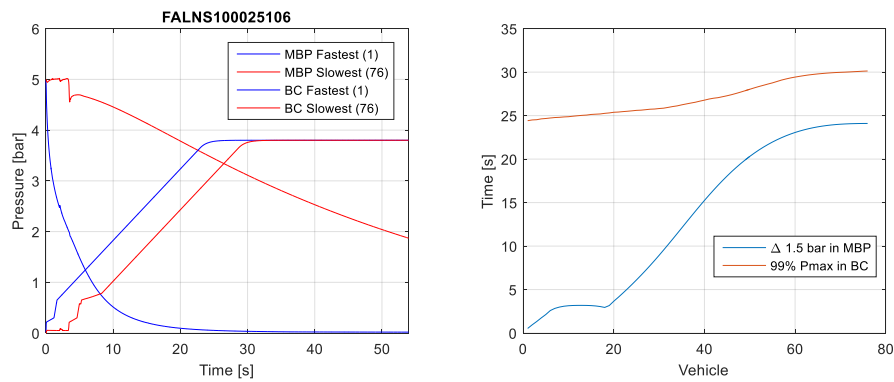


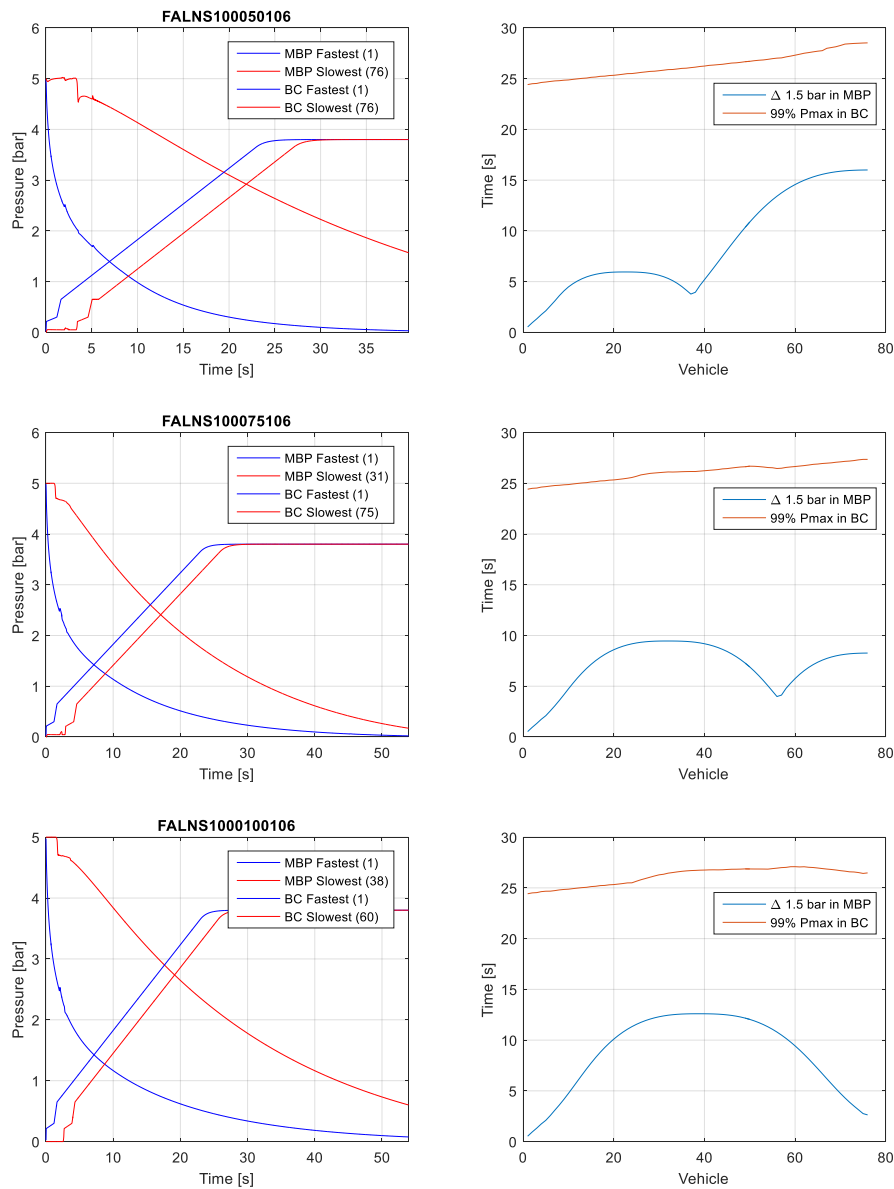
FALNS 1000 m, scenario 103



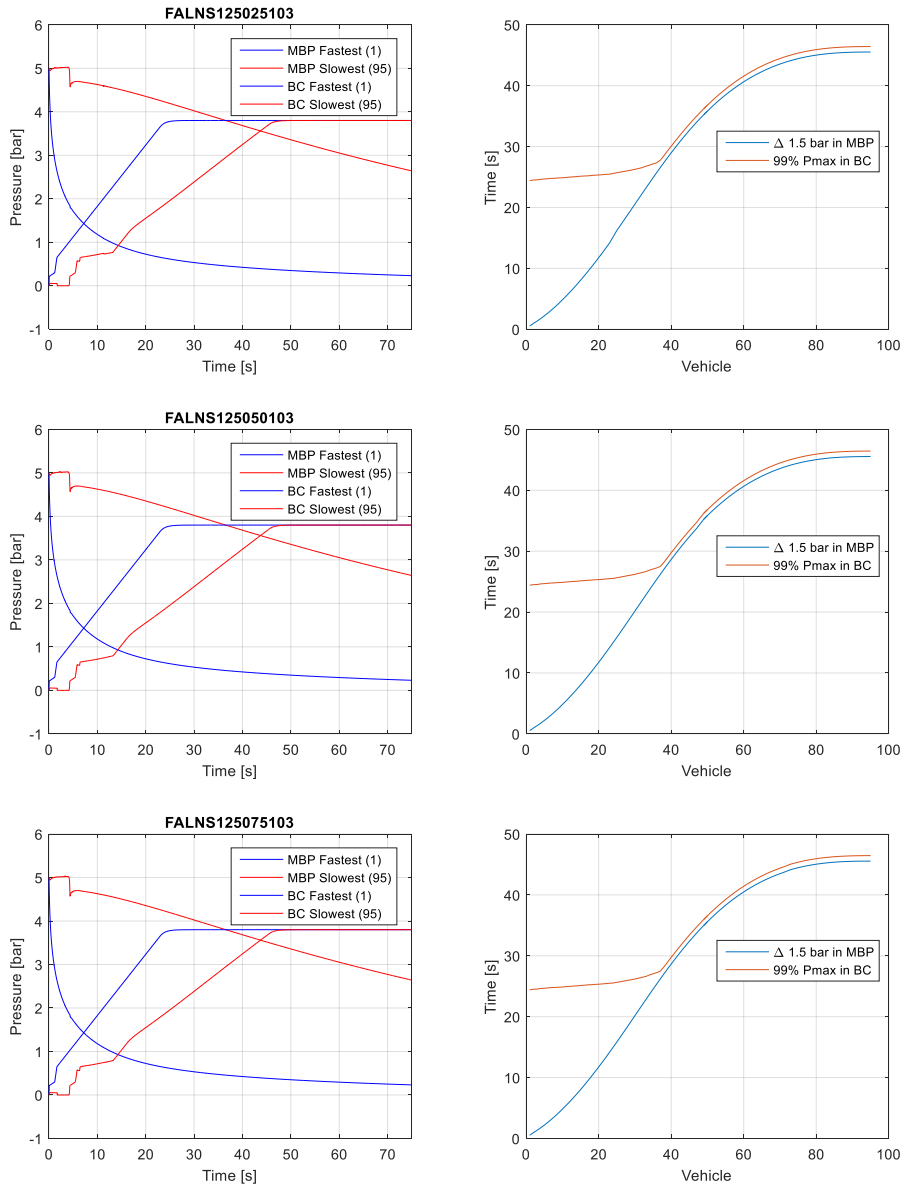


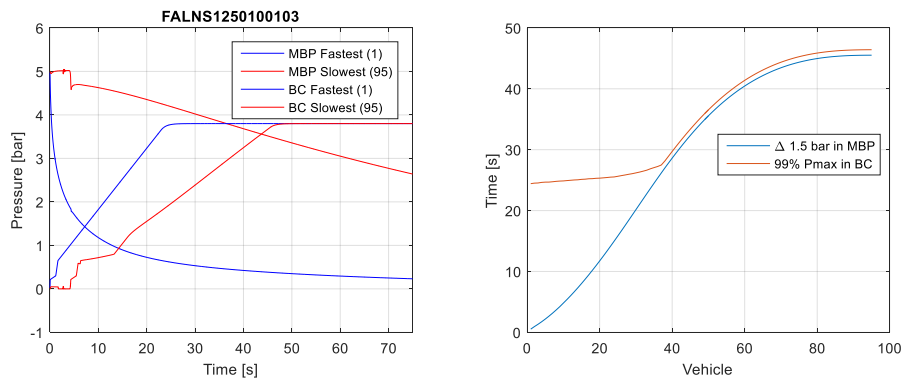
FALNS 1000 m, scenario 106



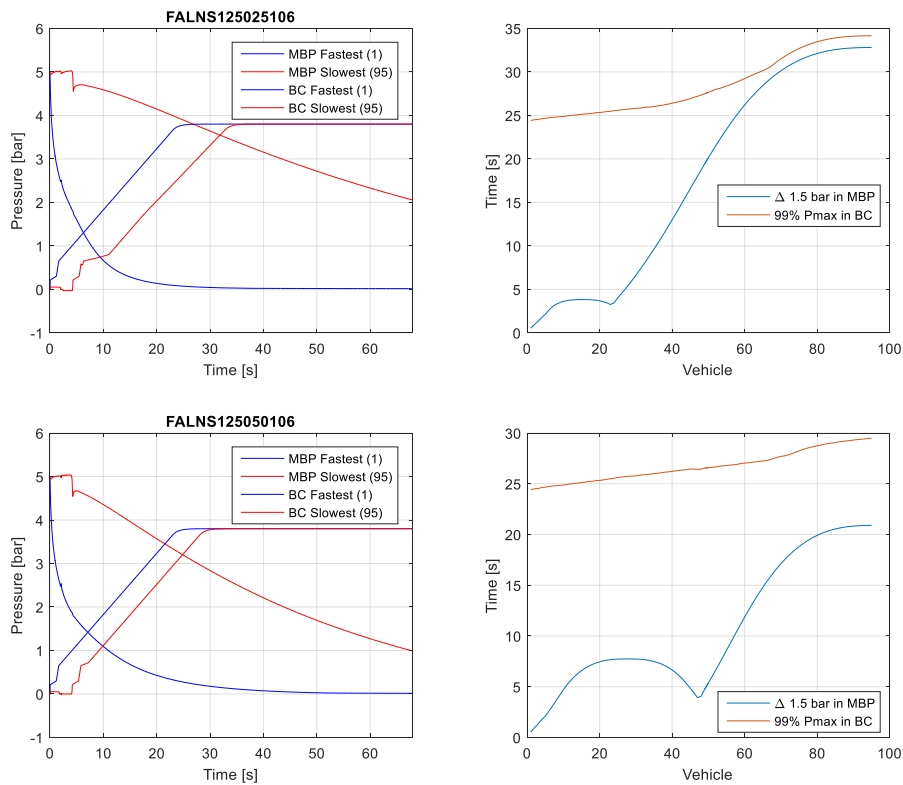


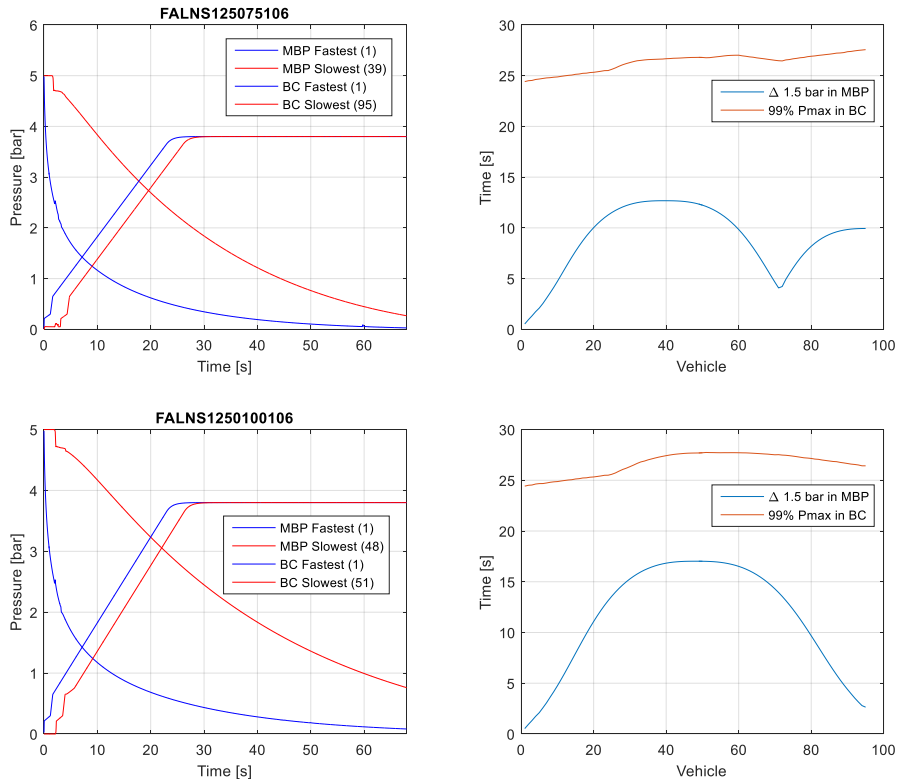
FALNS 1250 m, scenario 103



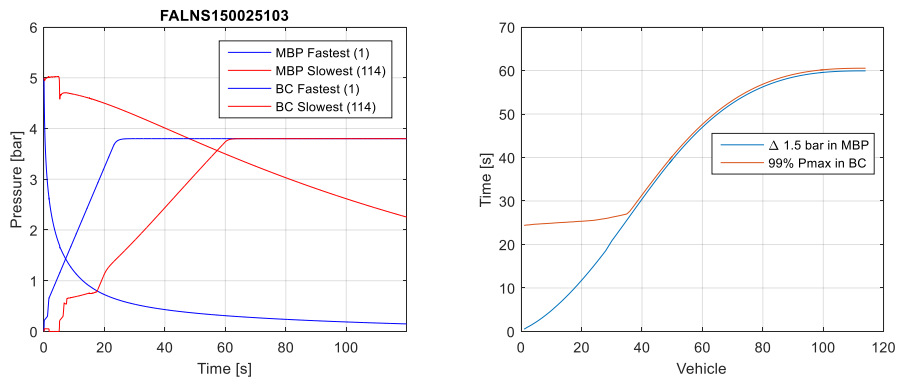


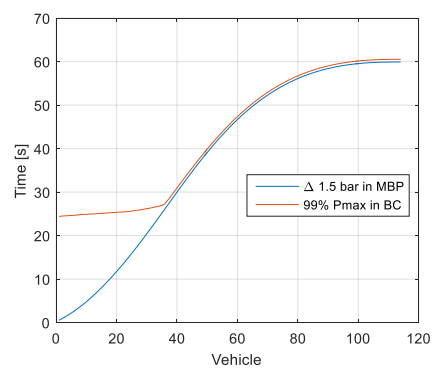
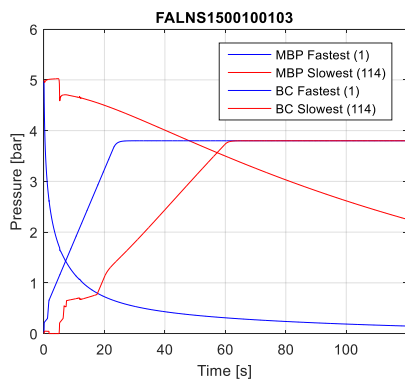
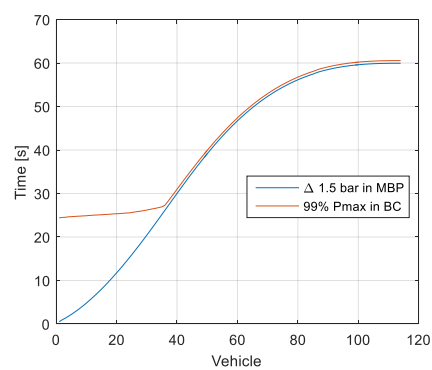
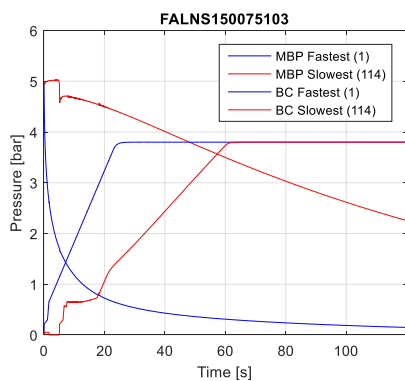
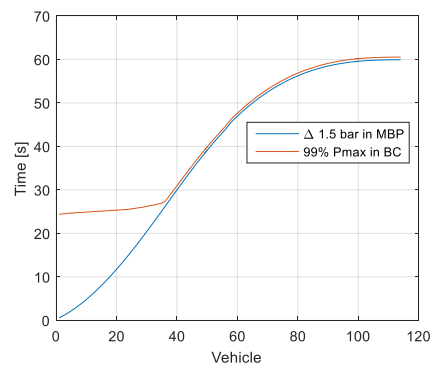
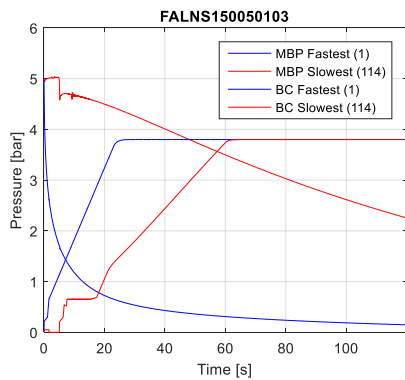
FALNS 1250 m, scenario 106



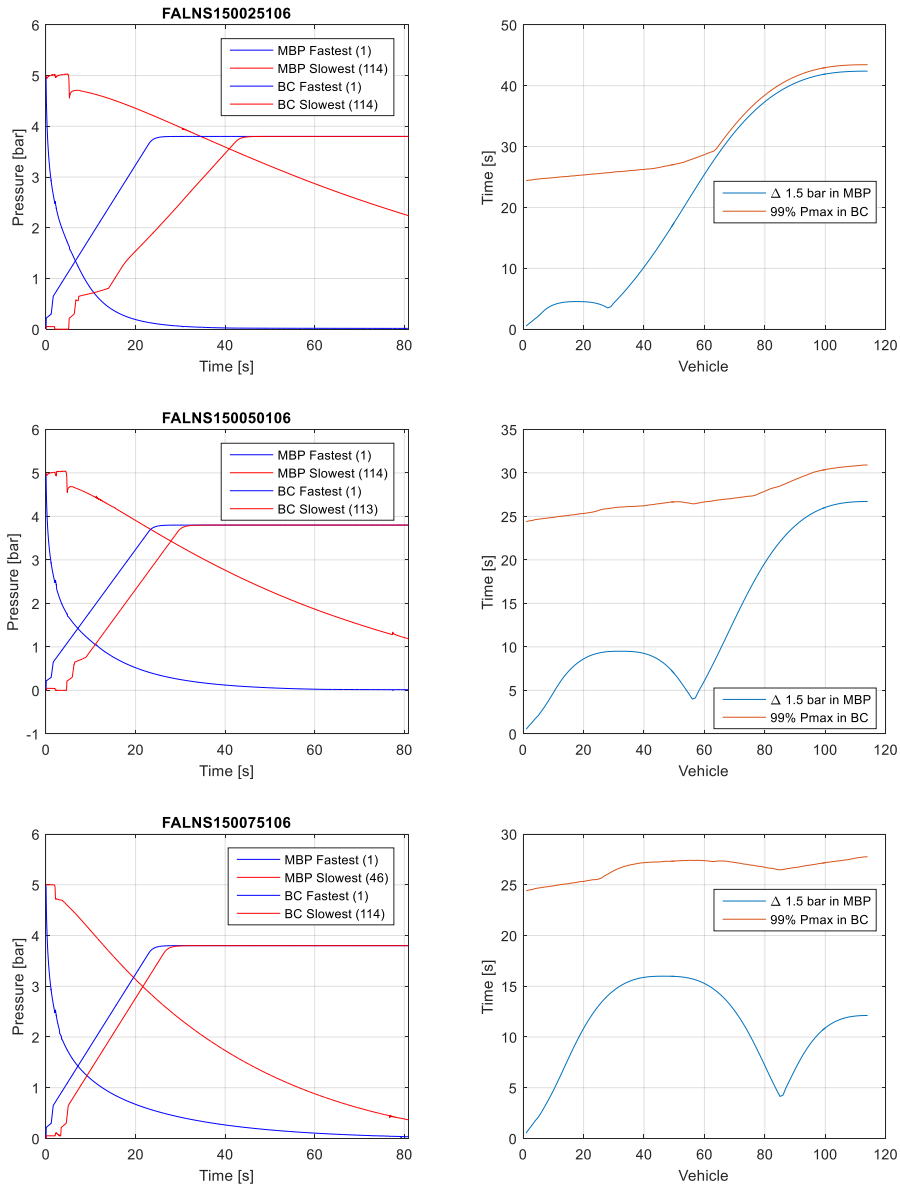


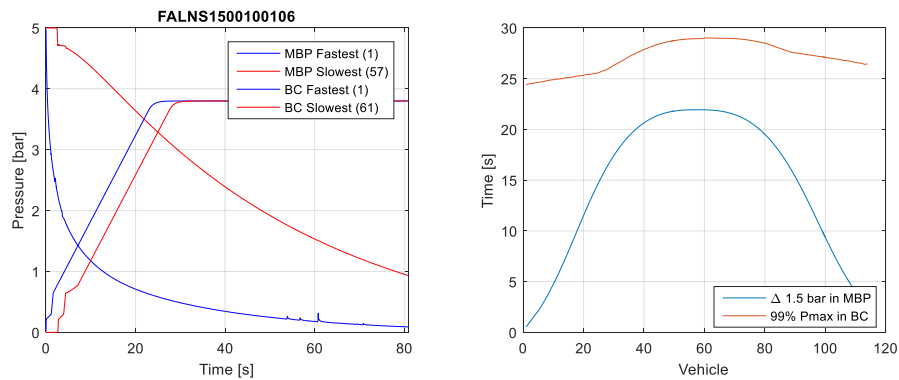
FALNS 1500 m, scenario 103





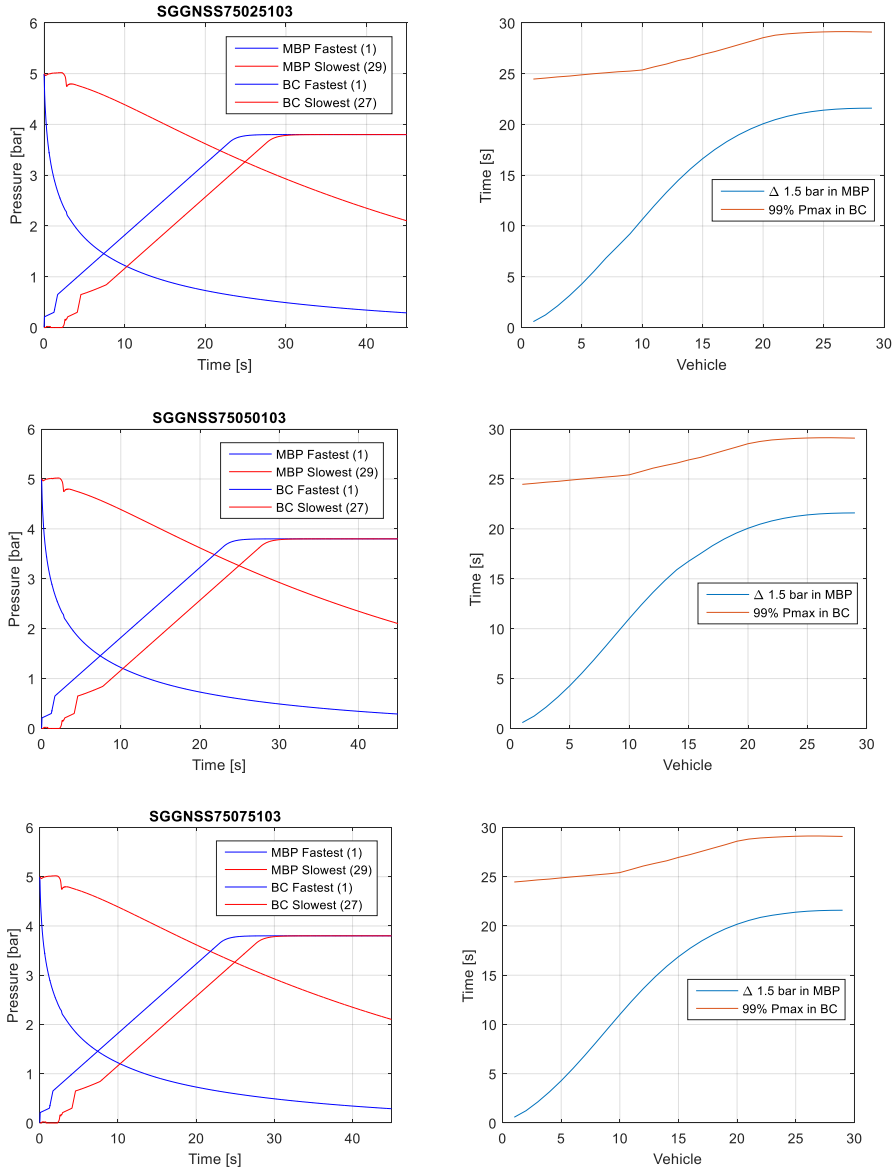
FALNS 1500 m, scenario 106

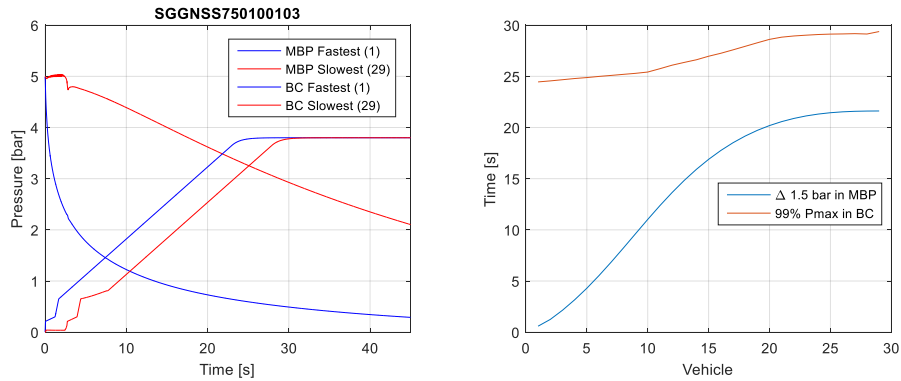




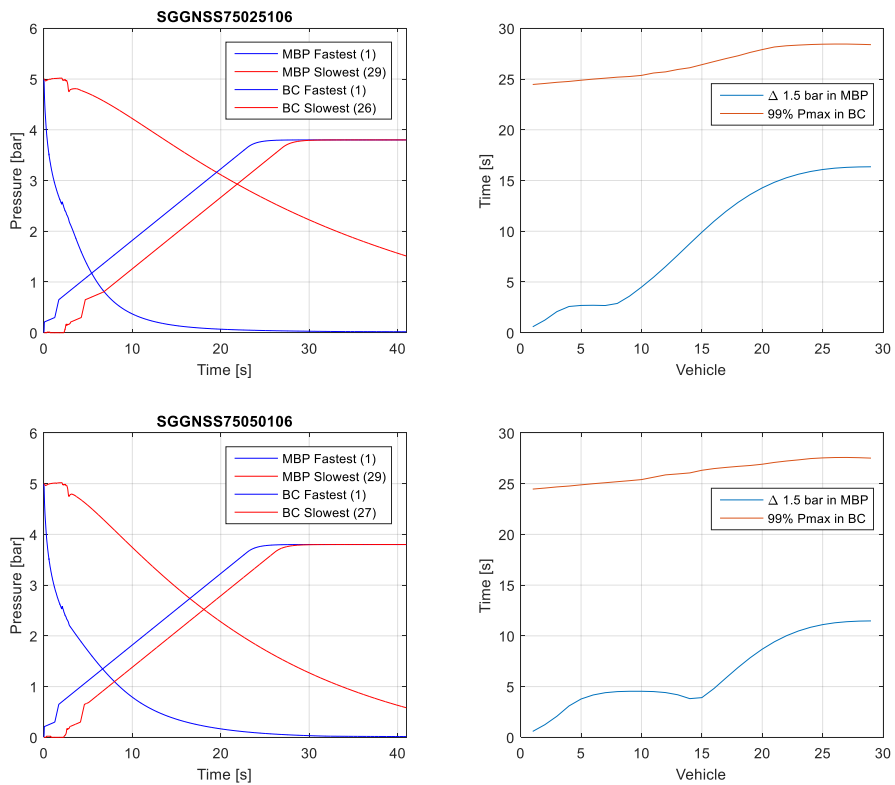
SGGNSS WITH TWO LOCOS

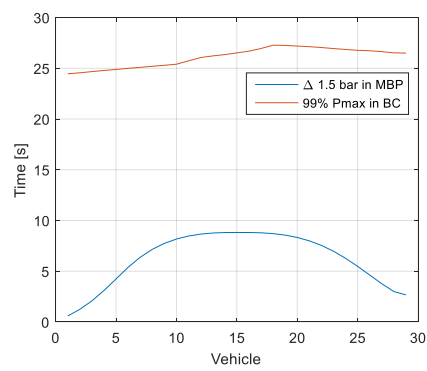
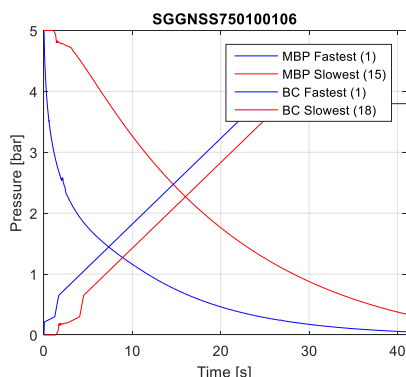
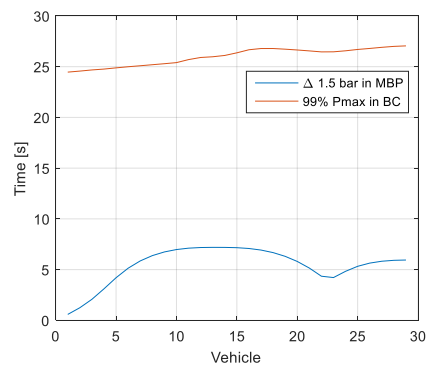
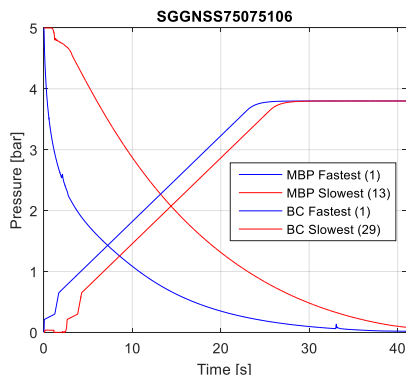
SGGNSS 750 m, scenario 103



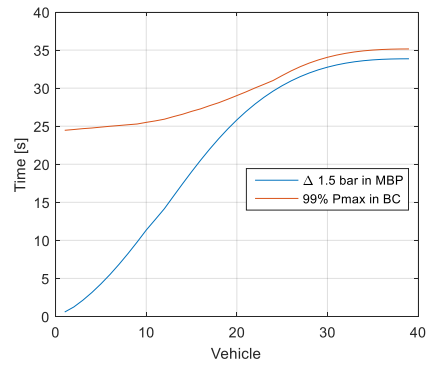
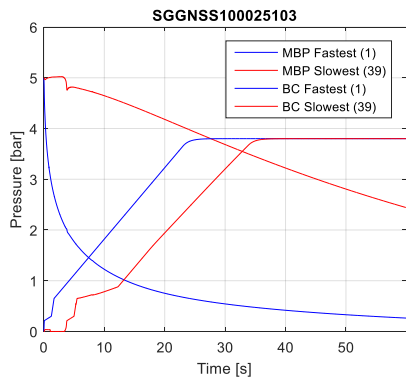


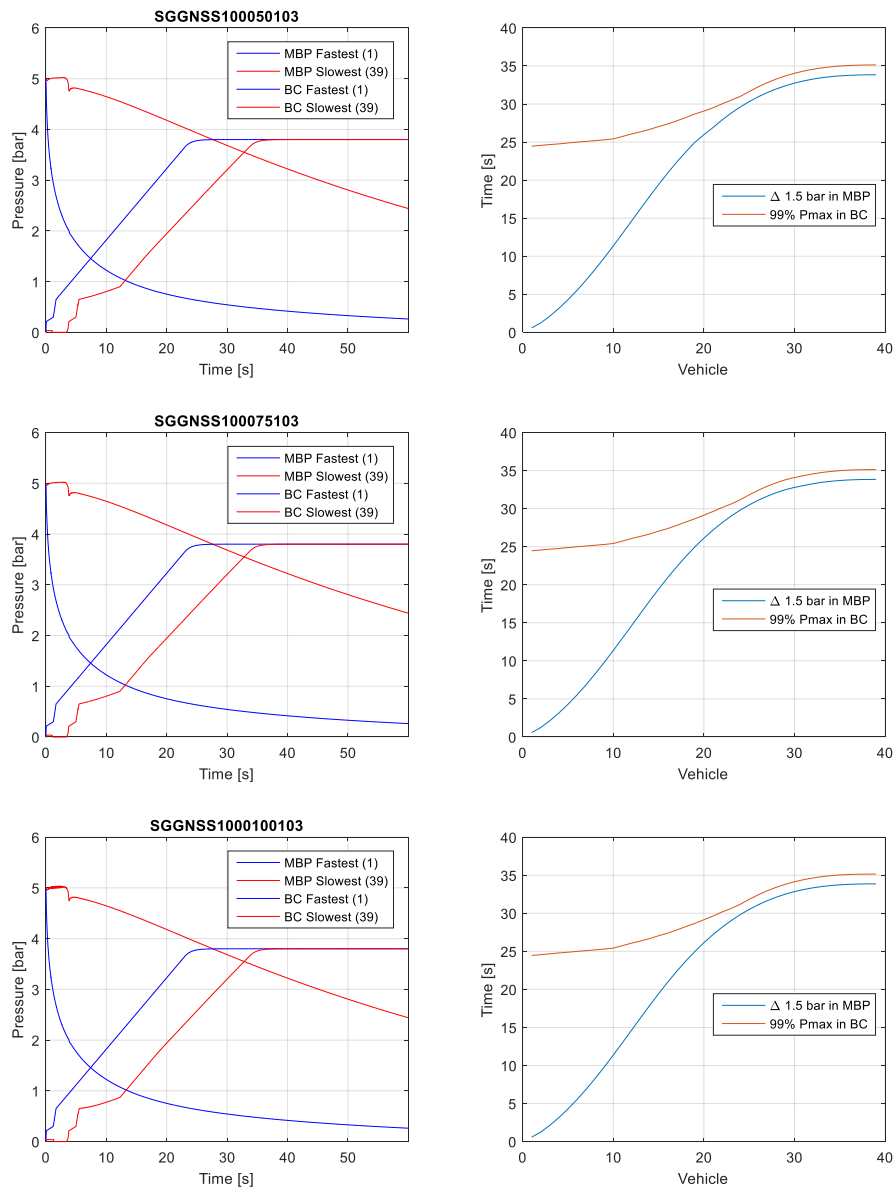
SGGNSS 750 m, scenario 106



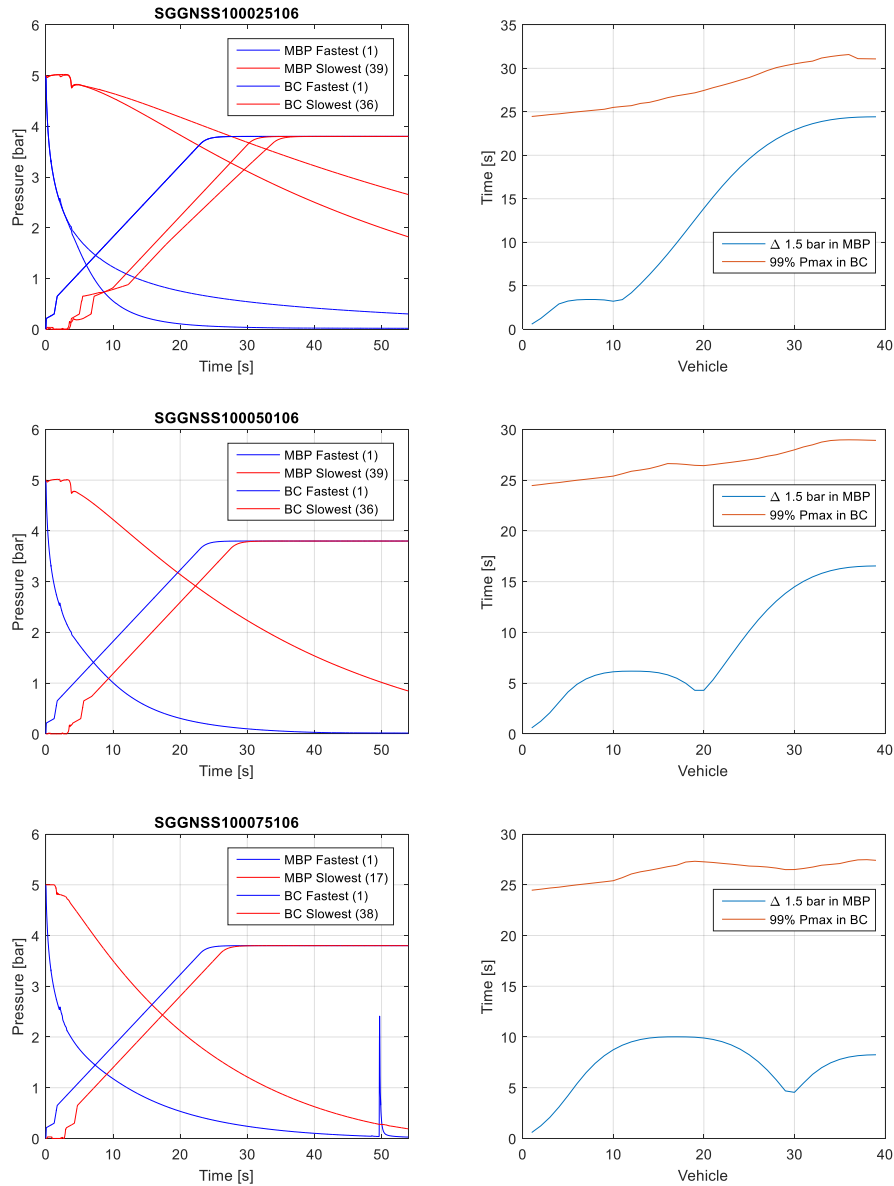


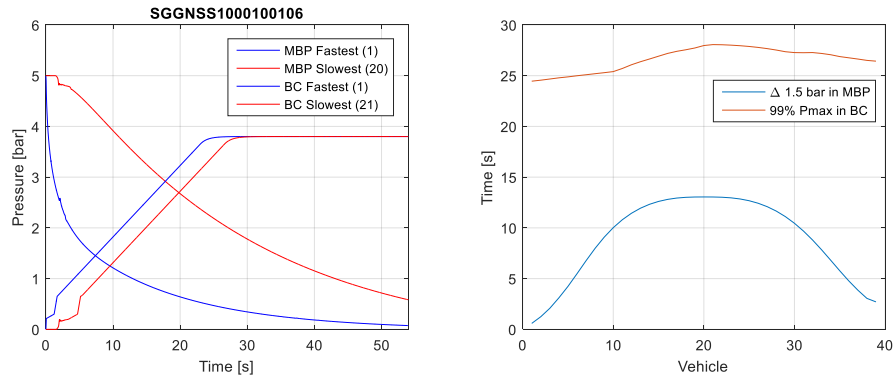
SGGNSS 1000 m, scenario 103



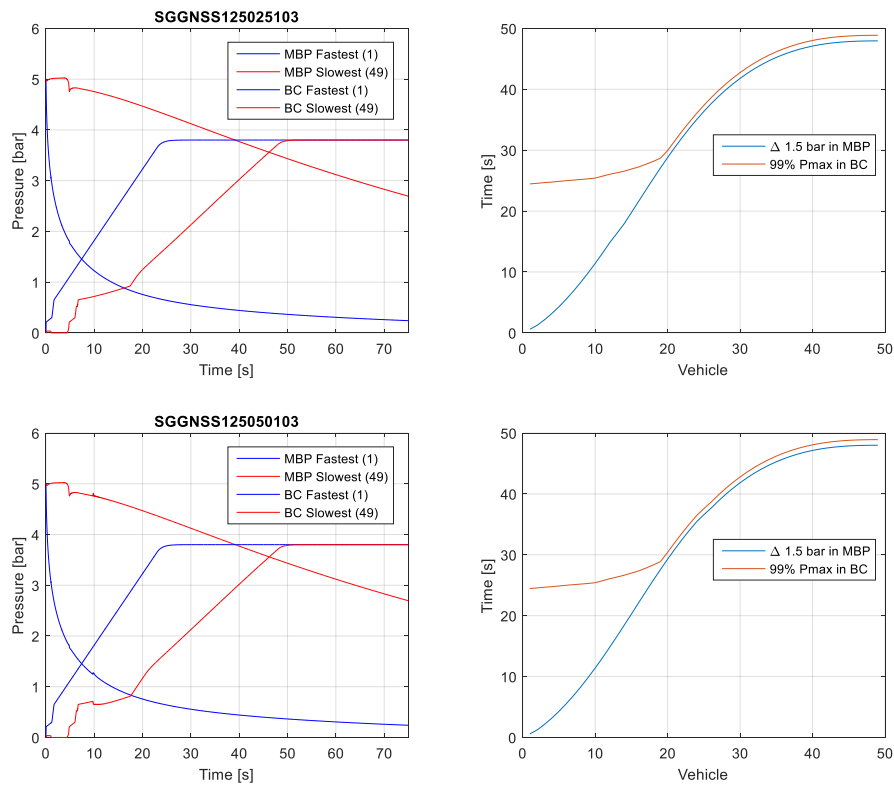


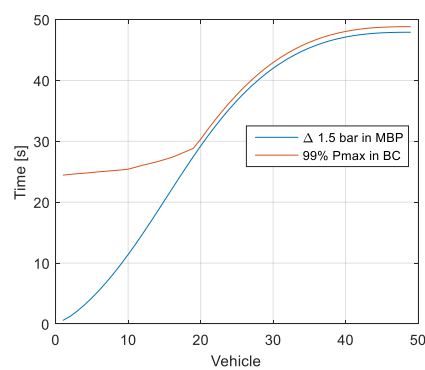
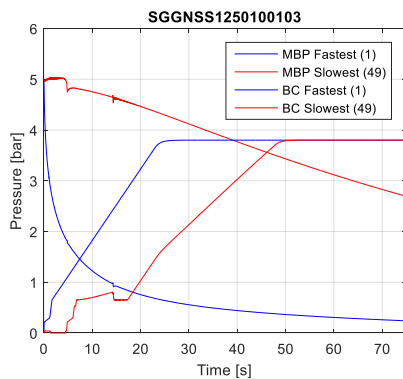
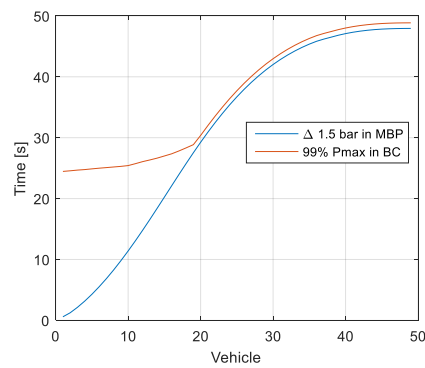
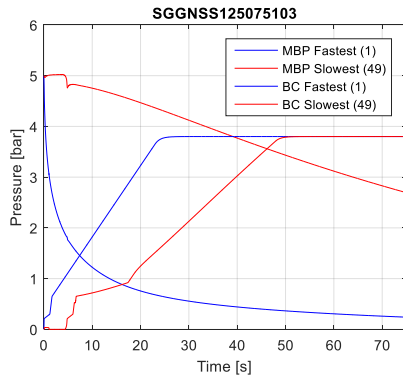
SGGNSS 1000 m, scenario 106



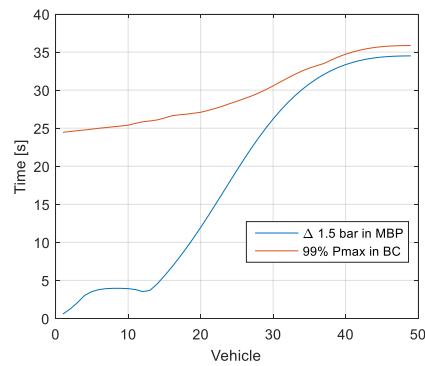
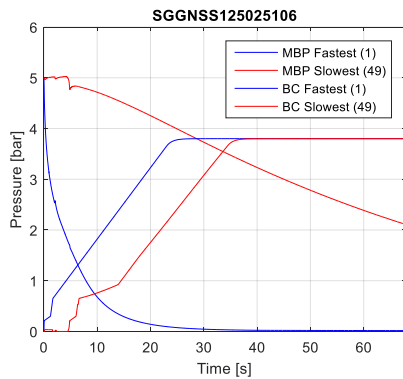


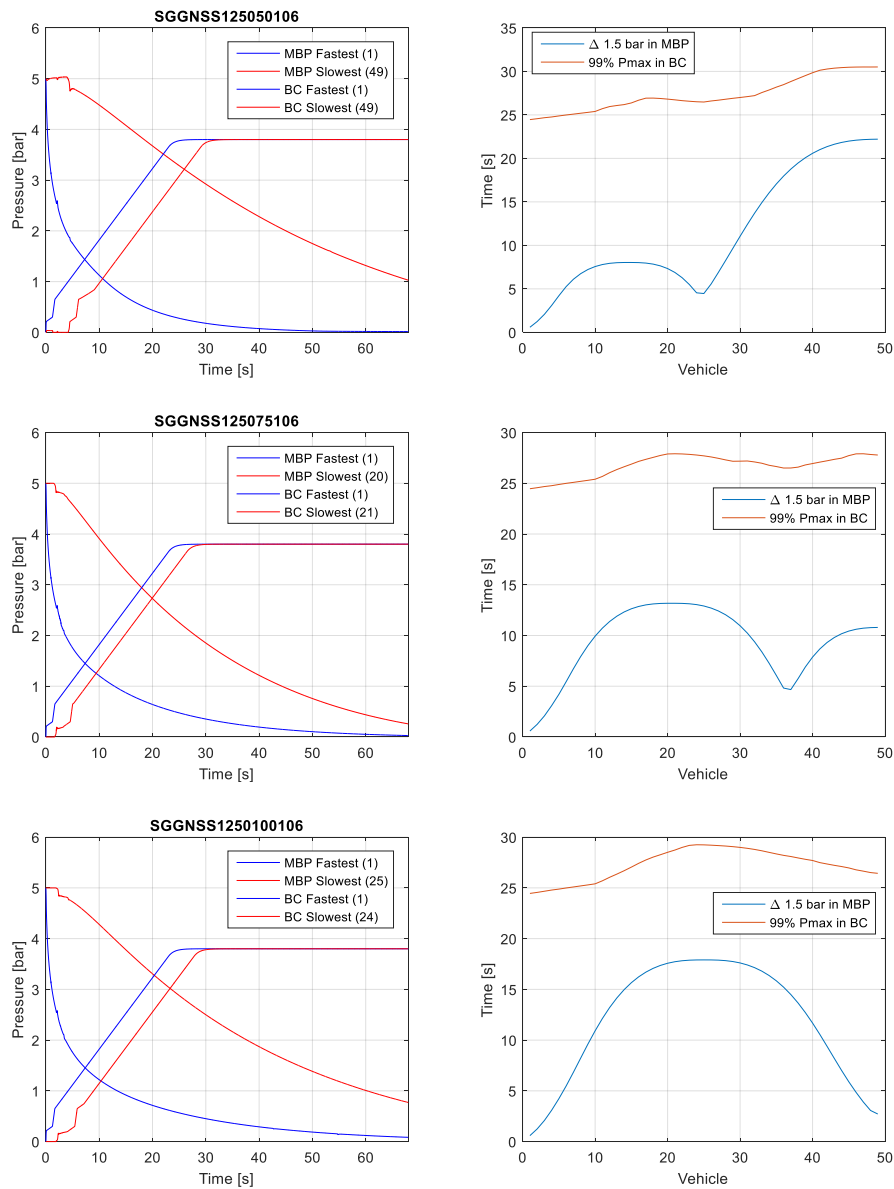
SGGNSS 1250 m, scenario 103



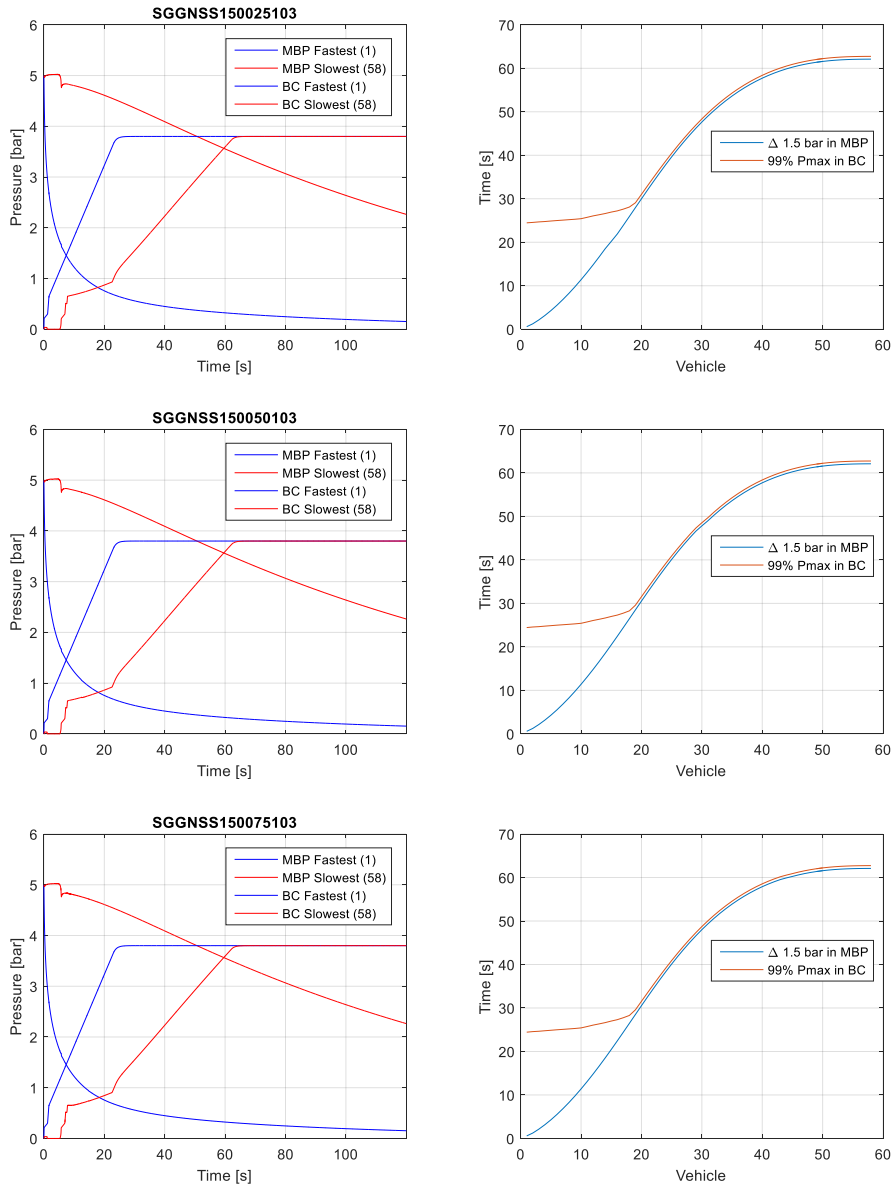


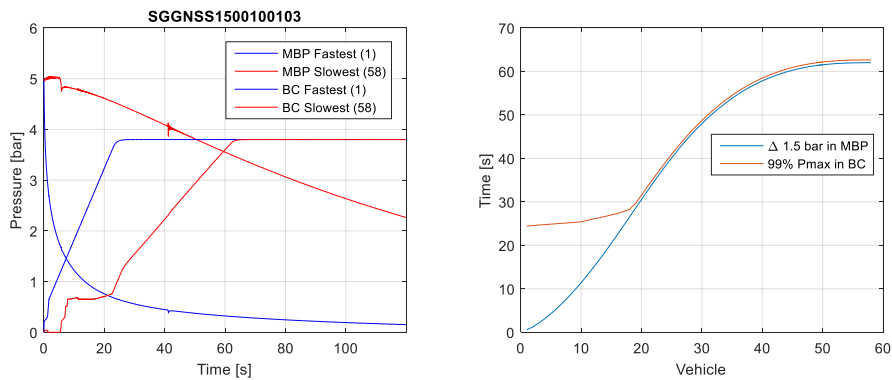
SGGNSS 1250 m, scenario 106



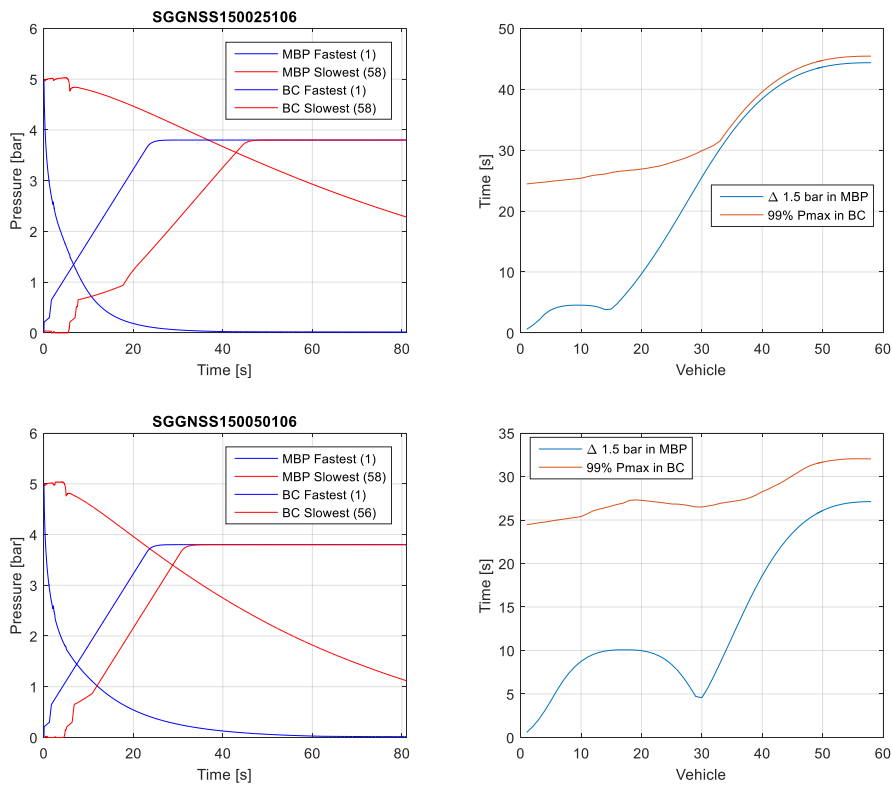


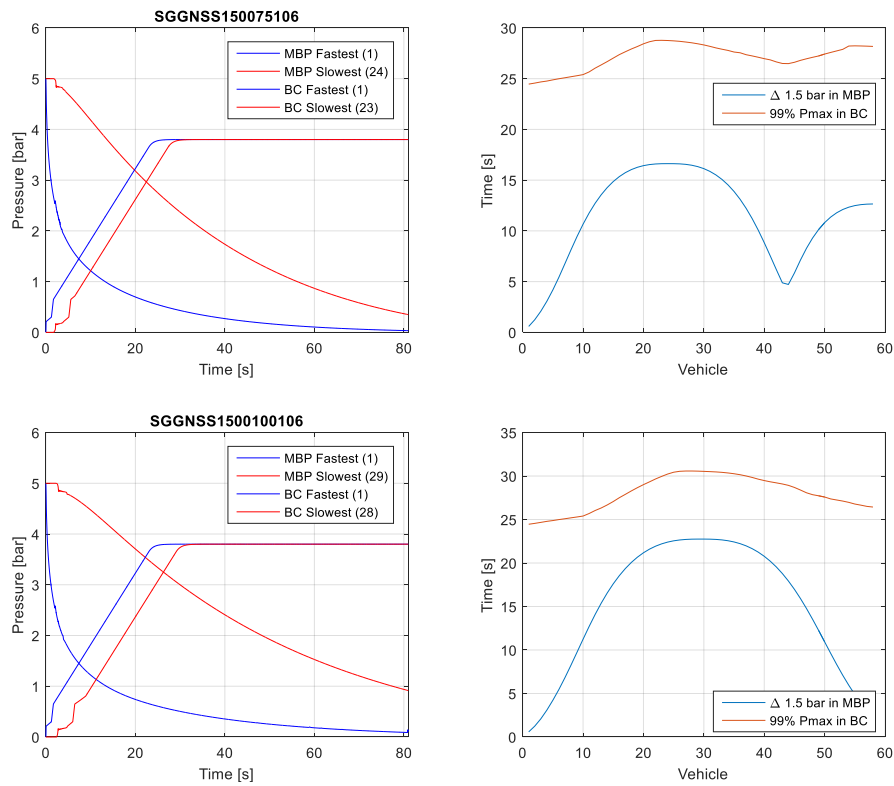
SGGNSS 1500 m, scenario 103





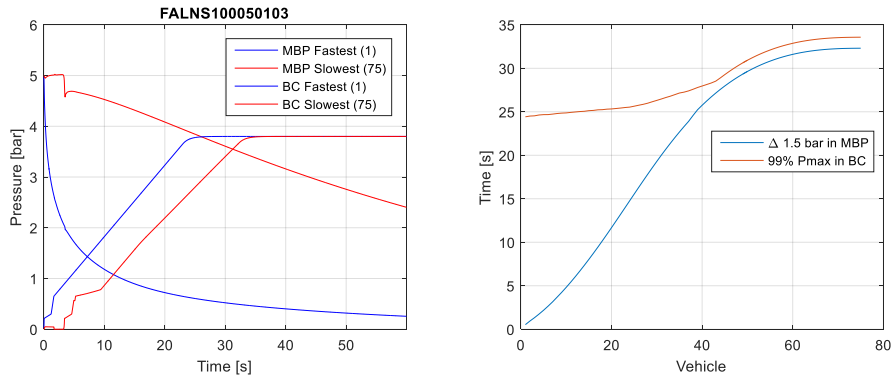
SGGNSS 1500 m, scenario 106



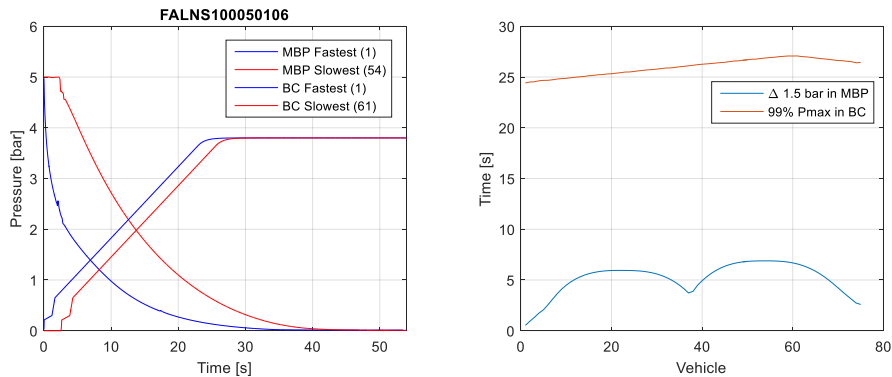


FALNS WITH THREE LOCOS

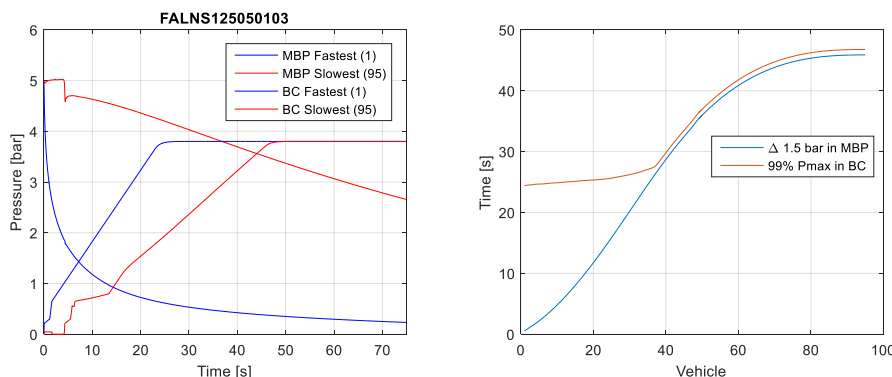
FALNS 1000 m, scenario 103



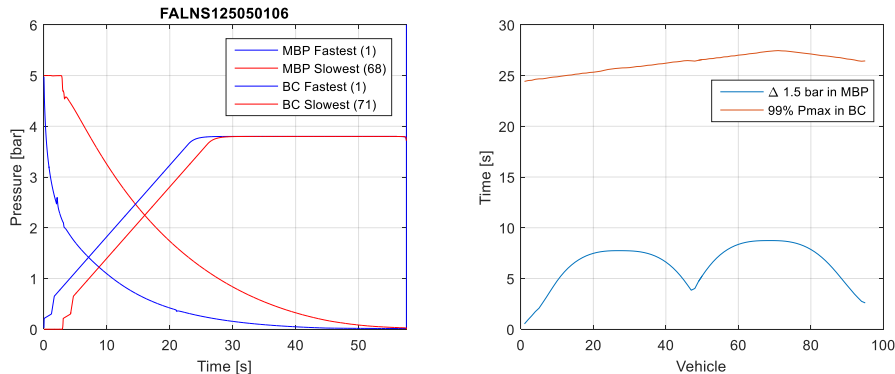
FALNS 1000 m, scenario 106



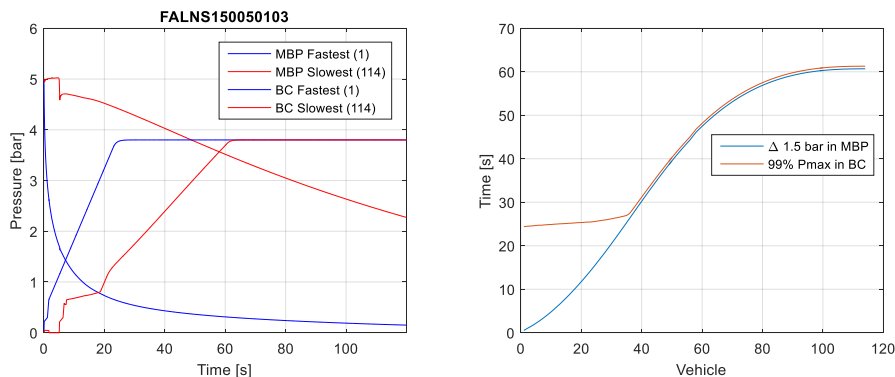
FALNS 1250 m, scenario 103



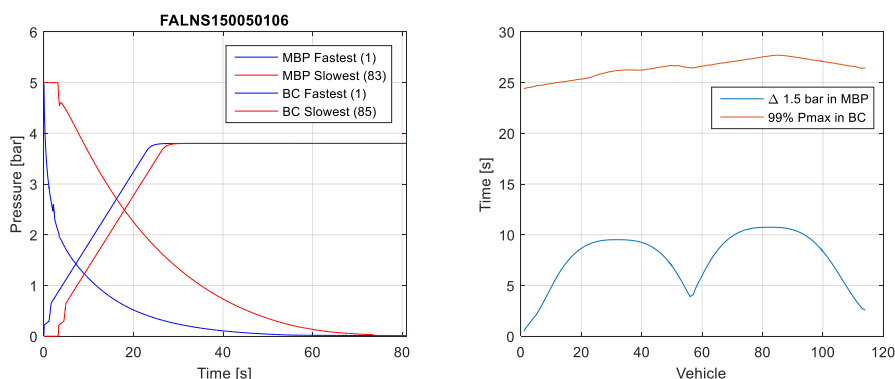
FALNS 1250 m, scenario 106



FLANS 1500 m, scenario 103

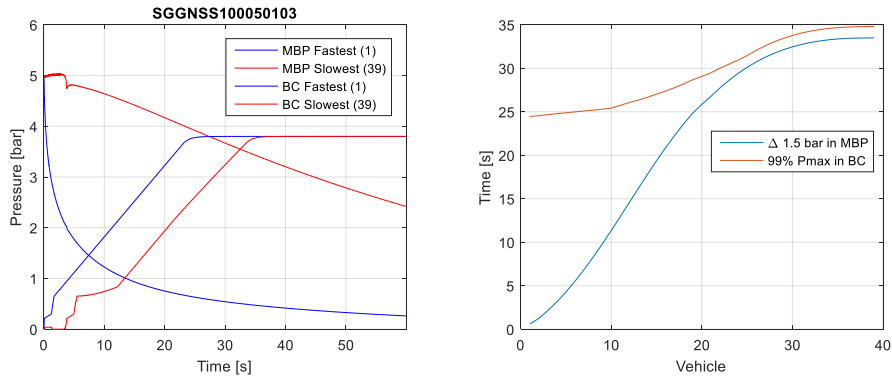


FALNS 1500 m, scenario 106

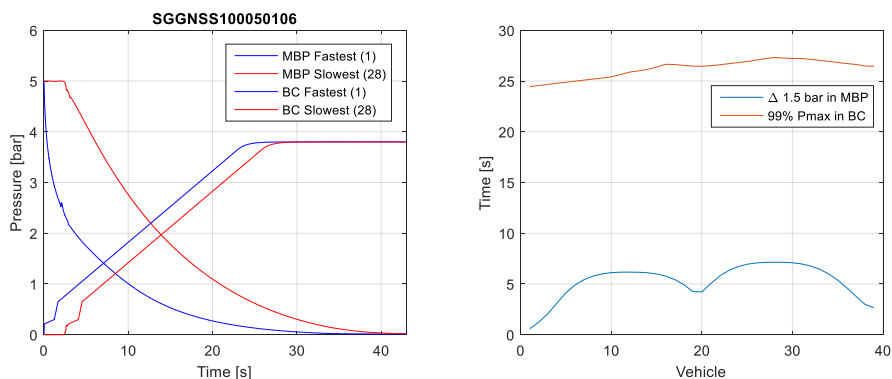


SGGNSS WITH THREE LOCOS

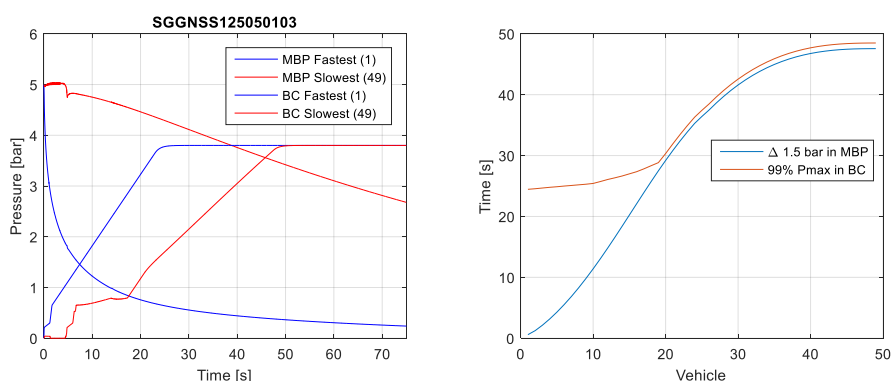
SGGNSS 1000 m, scenario 103



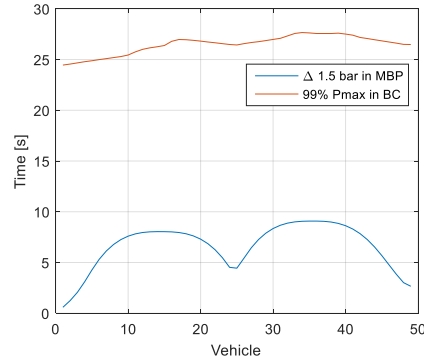
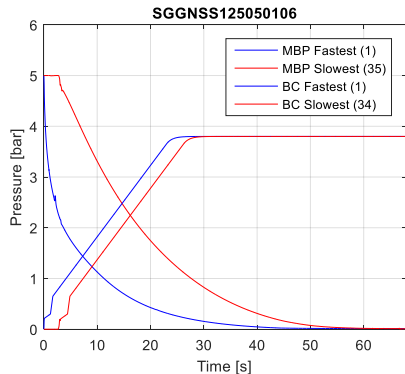
SGGNSS 1000 m, scenario 106



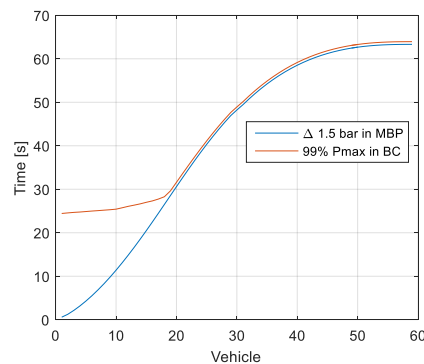
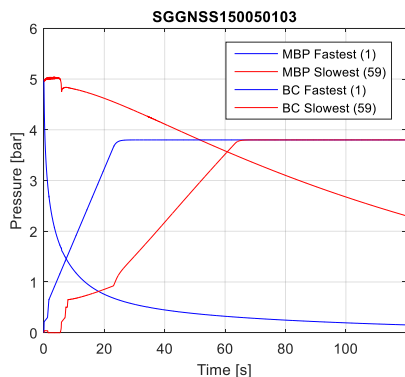
SGGNSS 1250 m, scenario 103



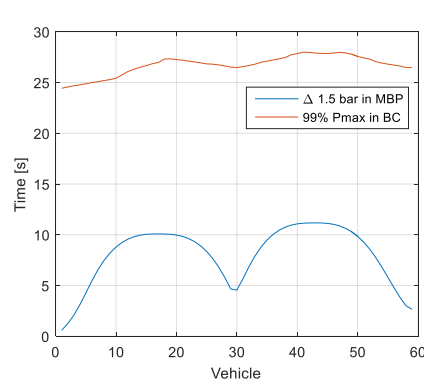
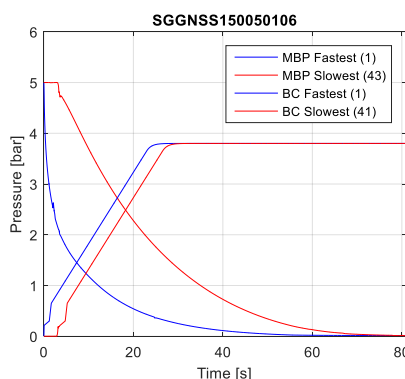
SGGNSS 1250 m, scenario 106



SGGNSS 1500 m, scenario 103

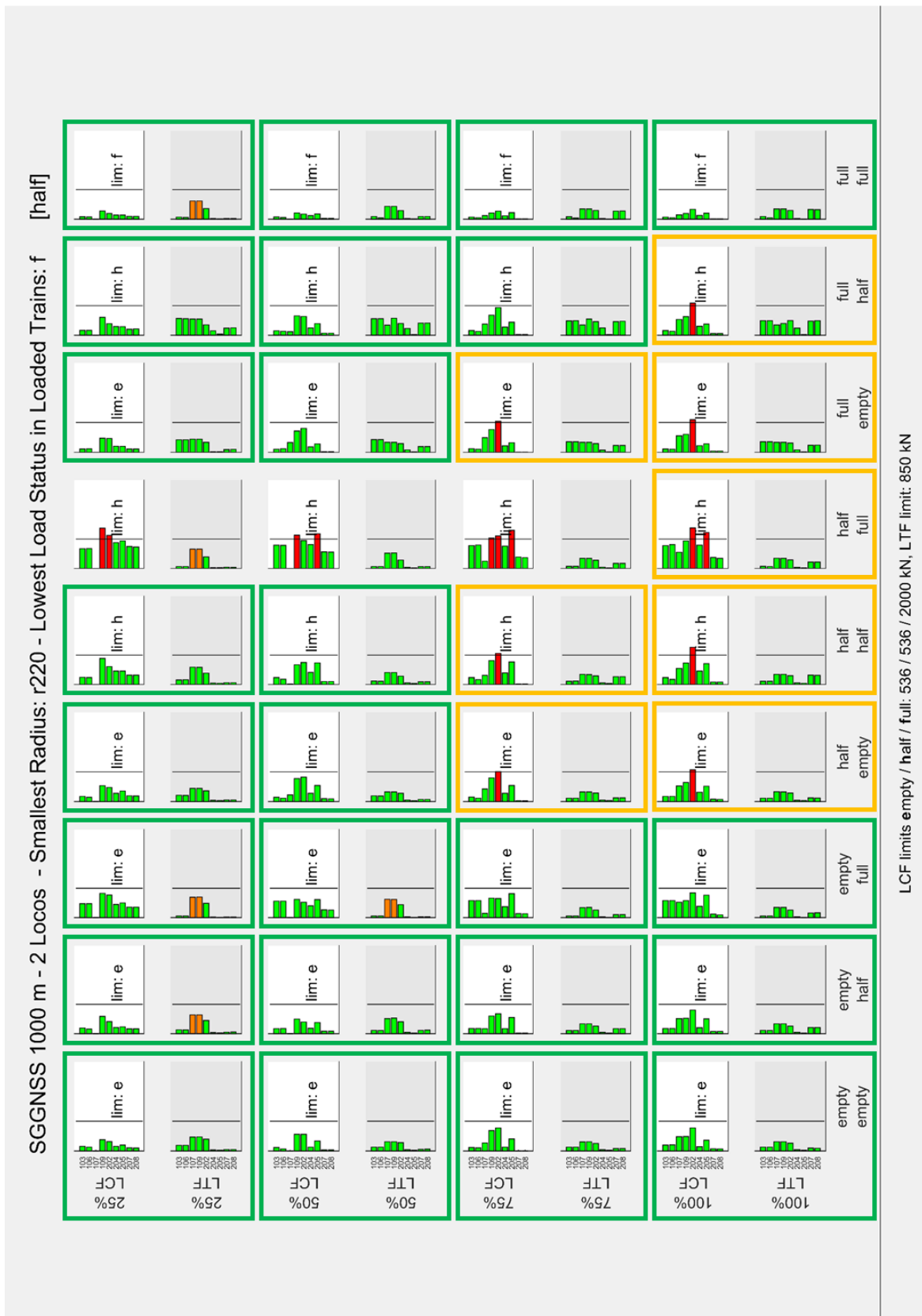


SGGNSS 1500 m, scenario 106

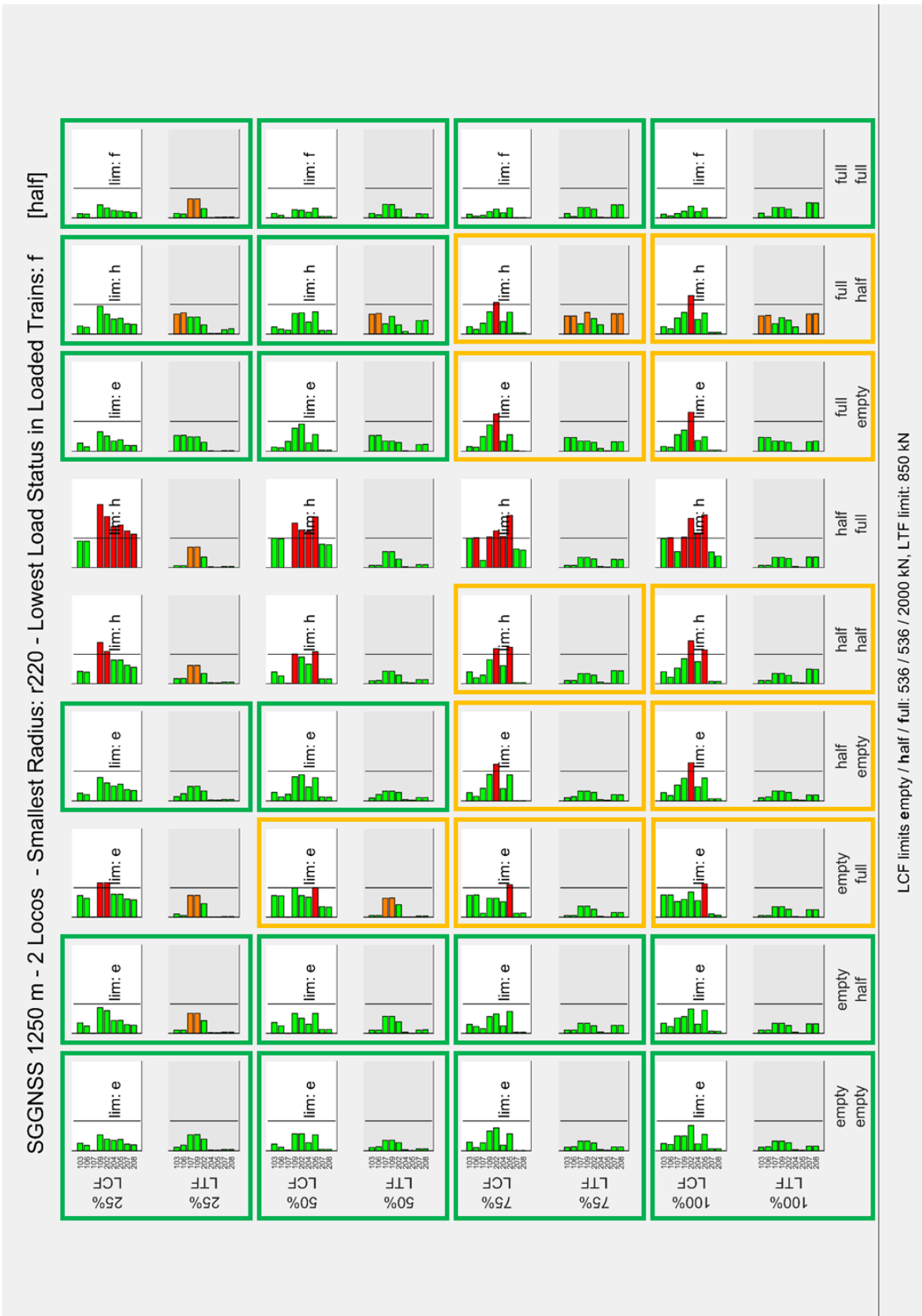


APPENDIX C: COMPARISON OF 1D SIMULATION RESULTS WITH LIMIT VALUES

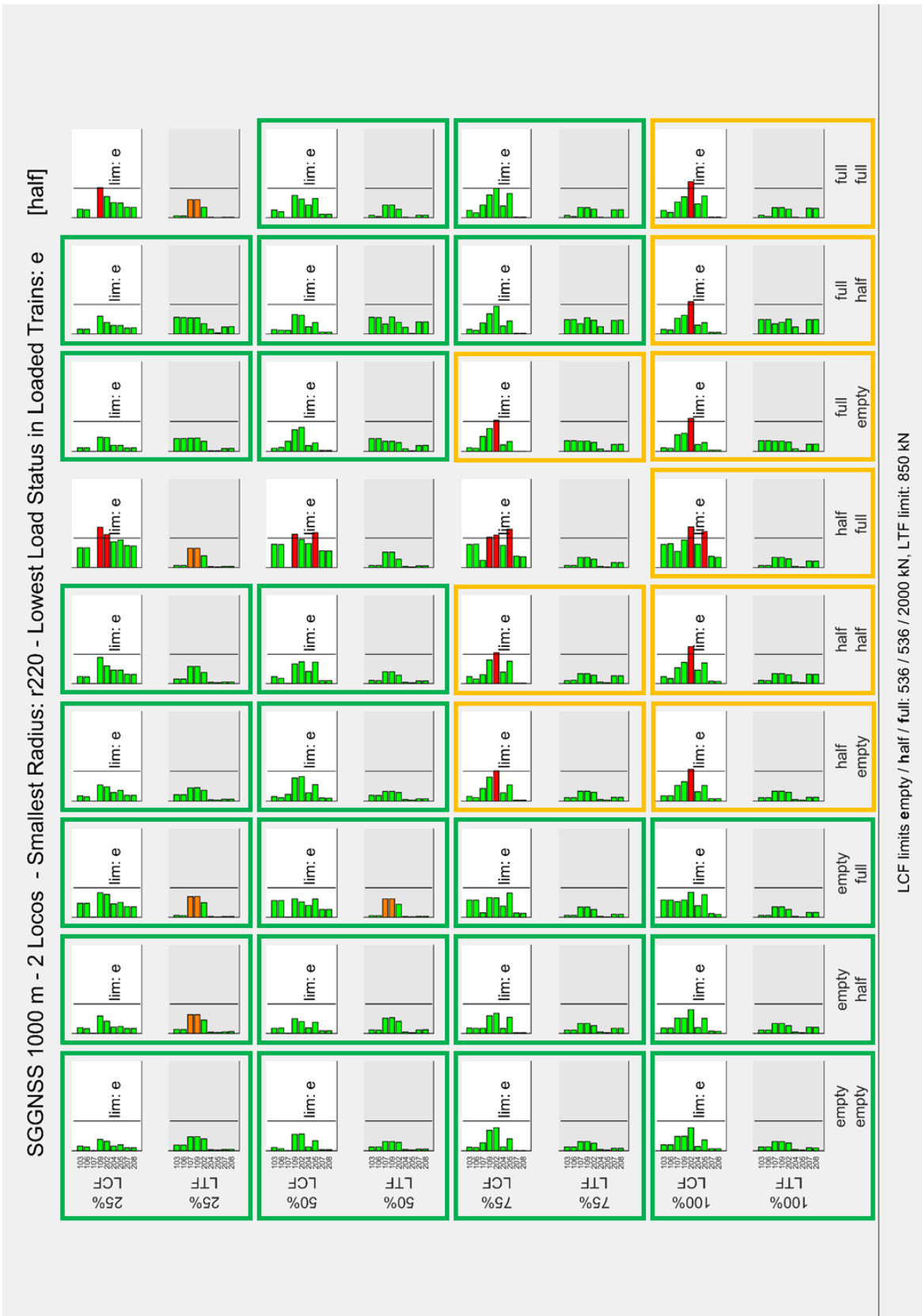
This appendix collects all comparisons of 1D simulation results with limit values.



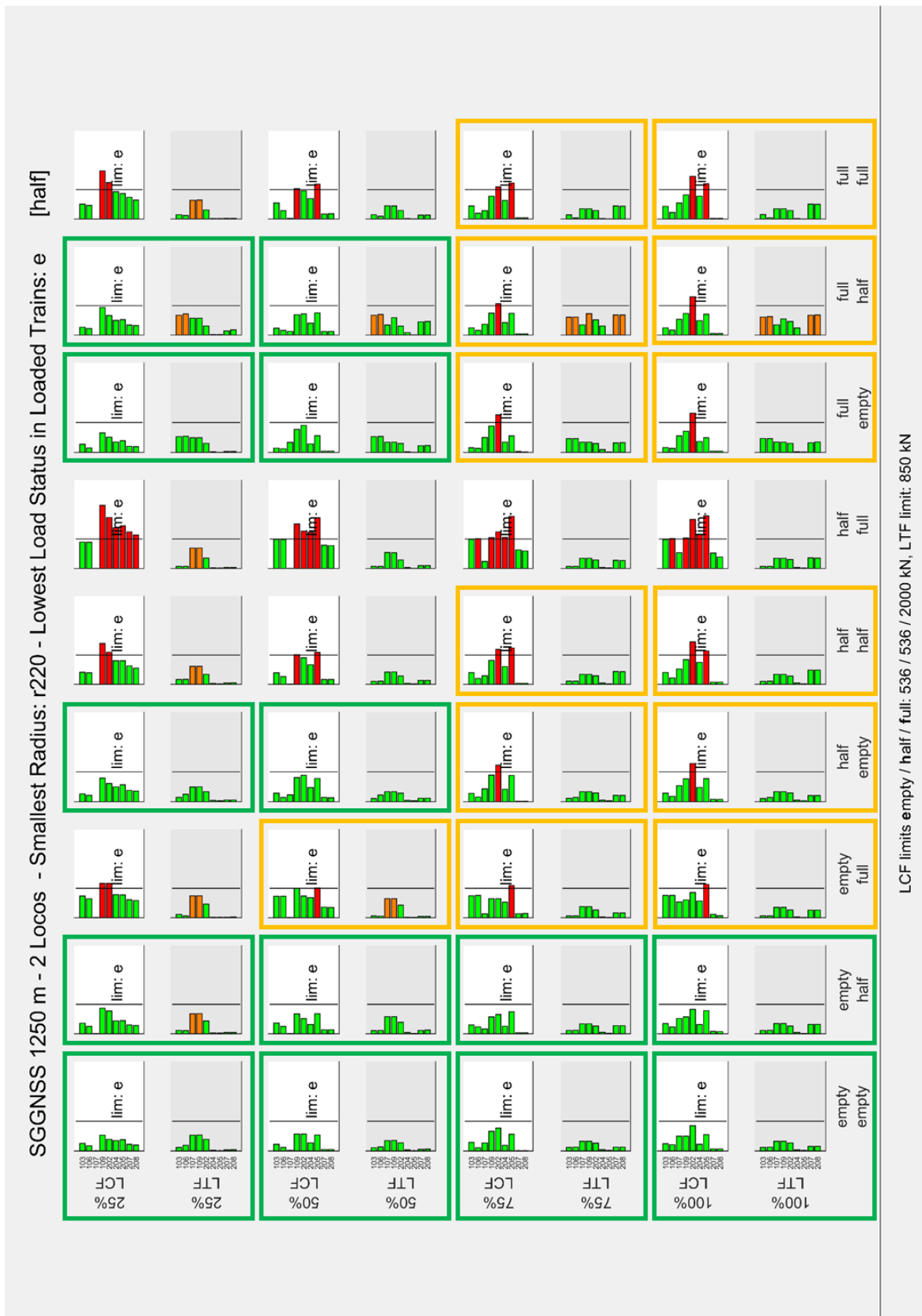
LCF limits empty / half / full: 536 / 536 / 2000 kN, LTF limit: 850 kN

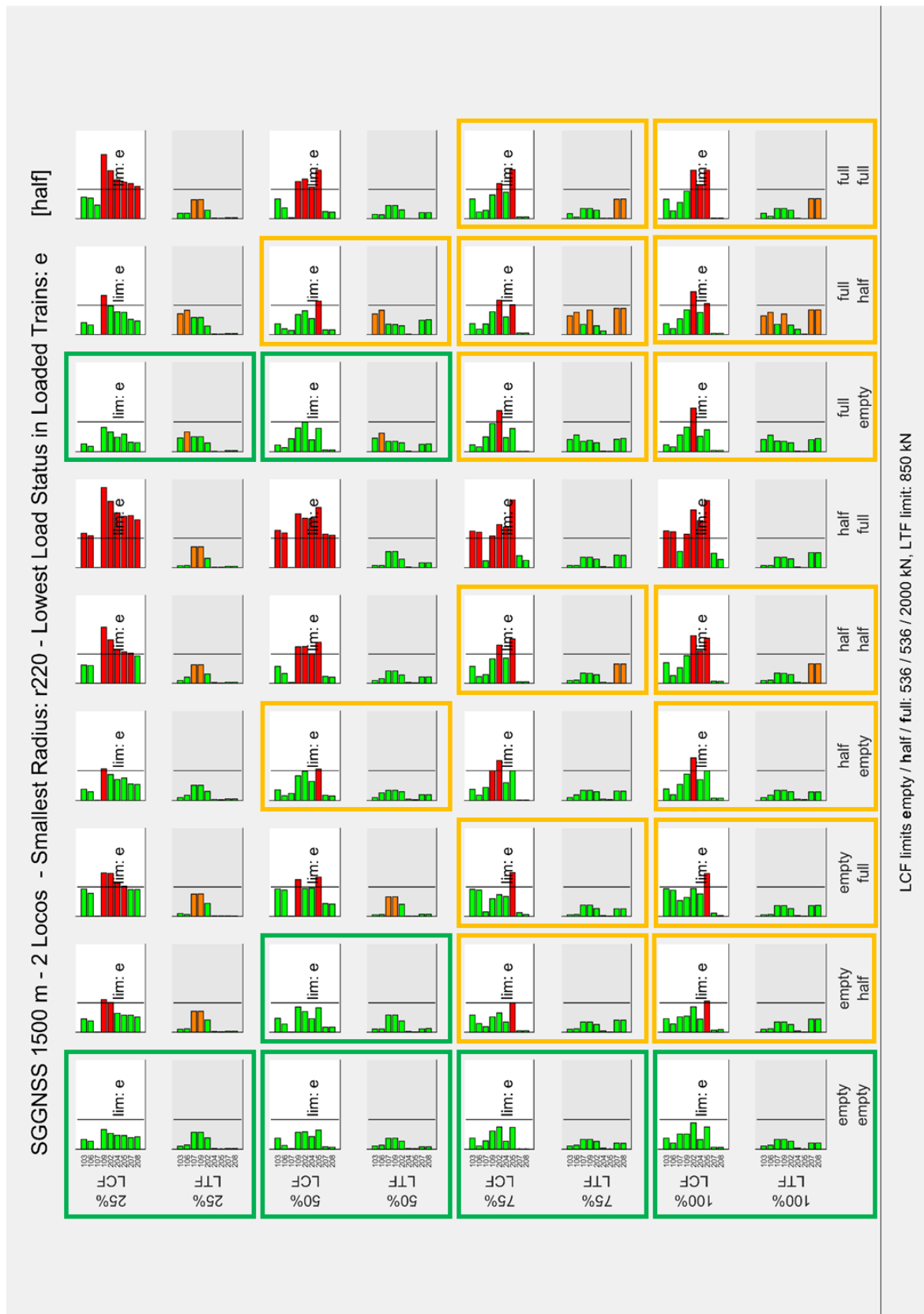




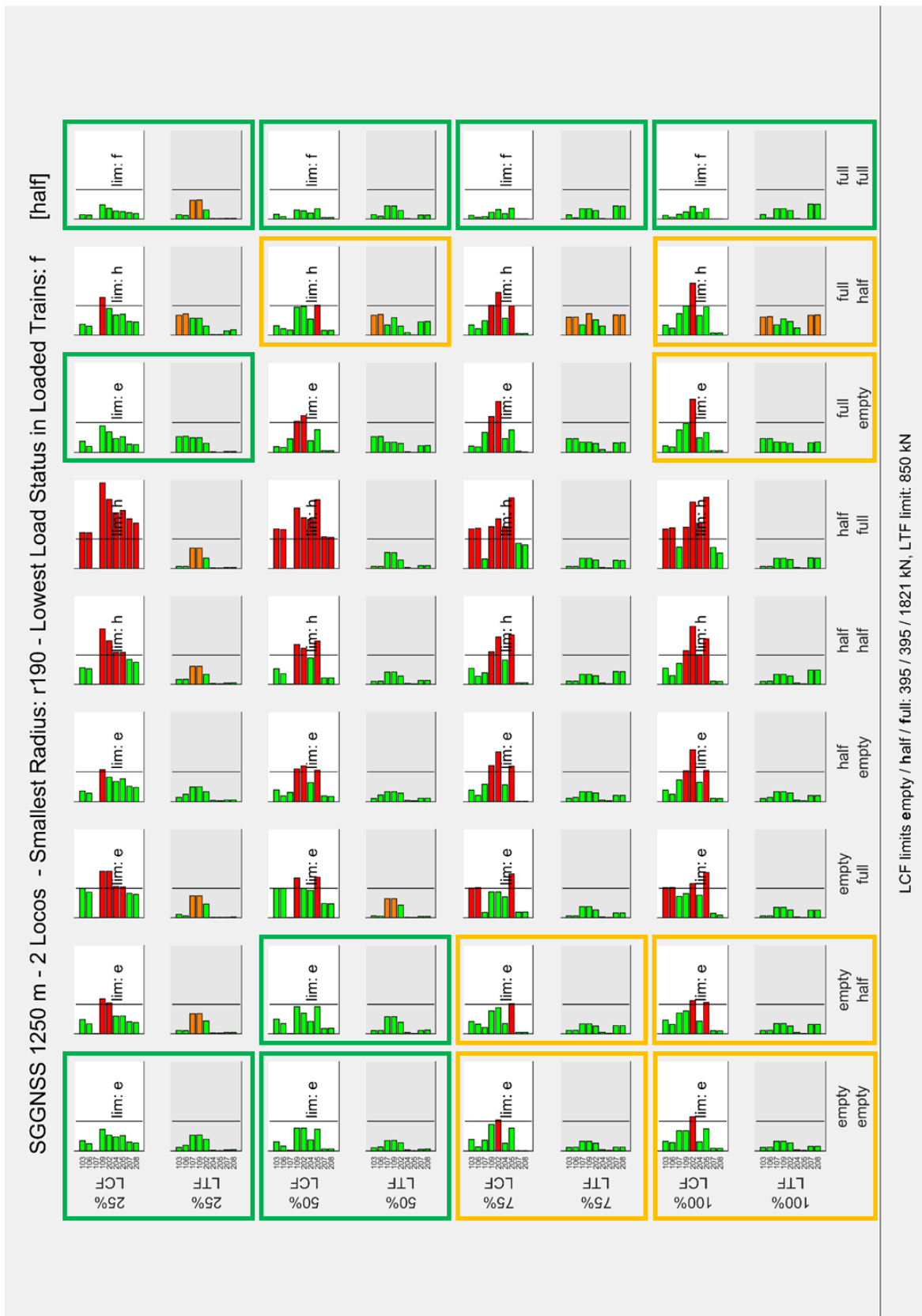


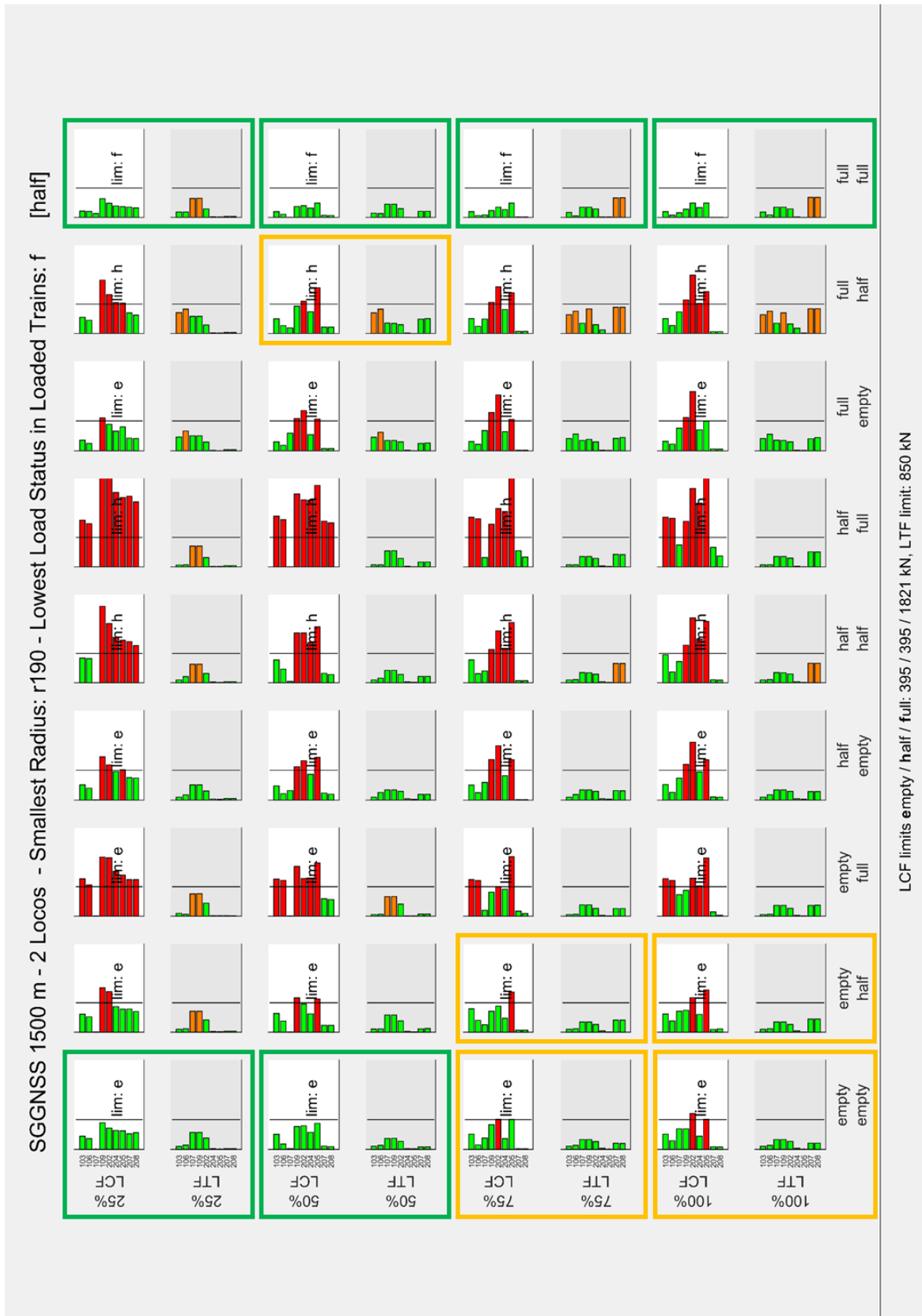
LCF limits empty / half / full / full: 536 / 536 / 2000 kN, LTF limit: 850 kN

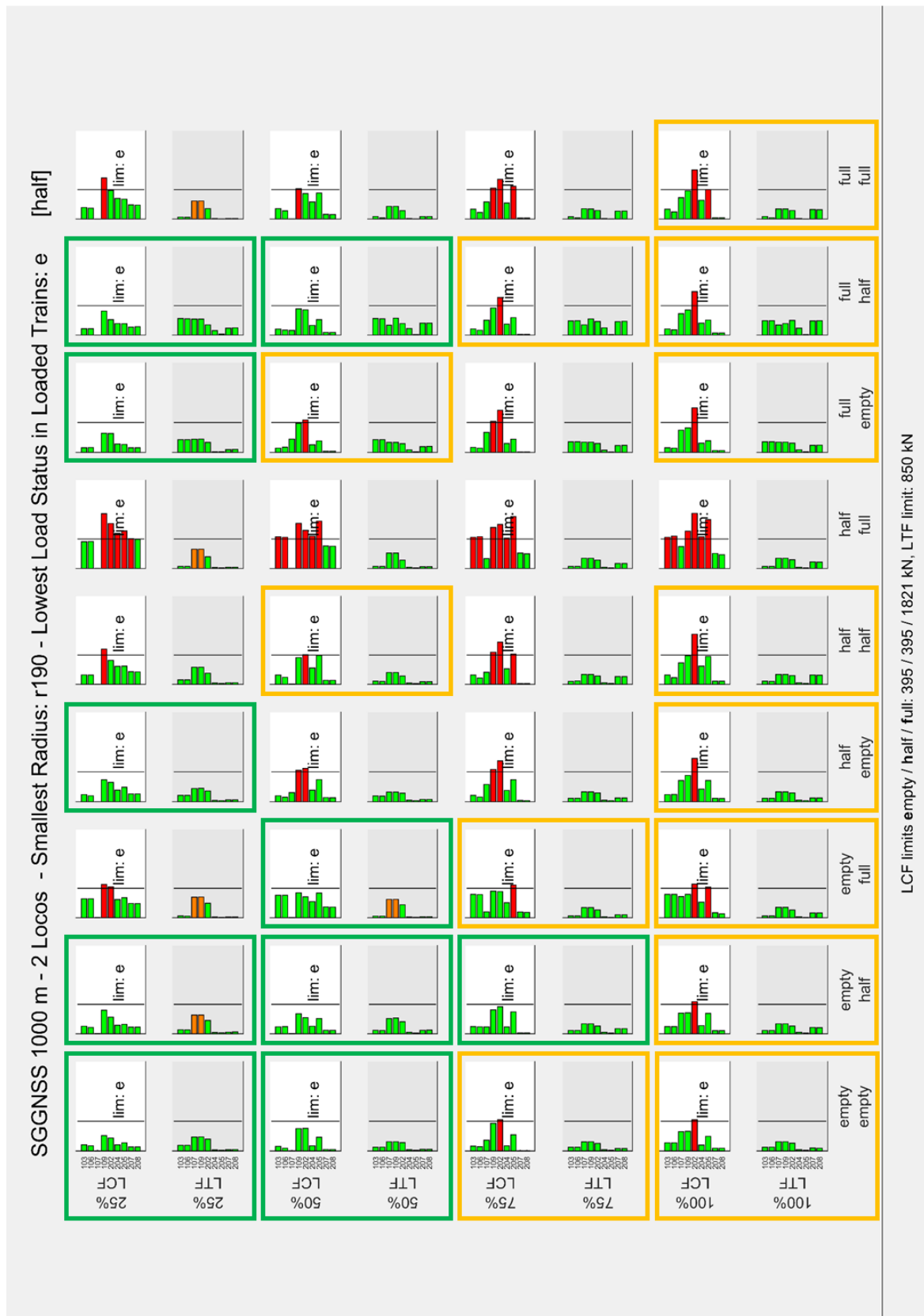


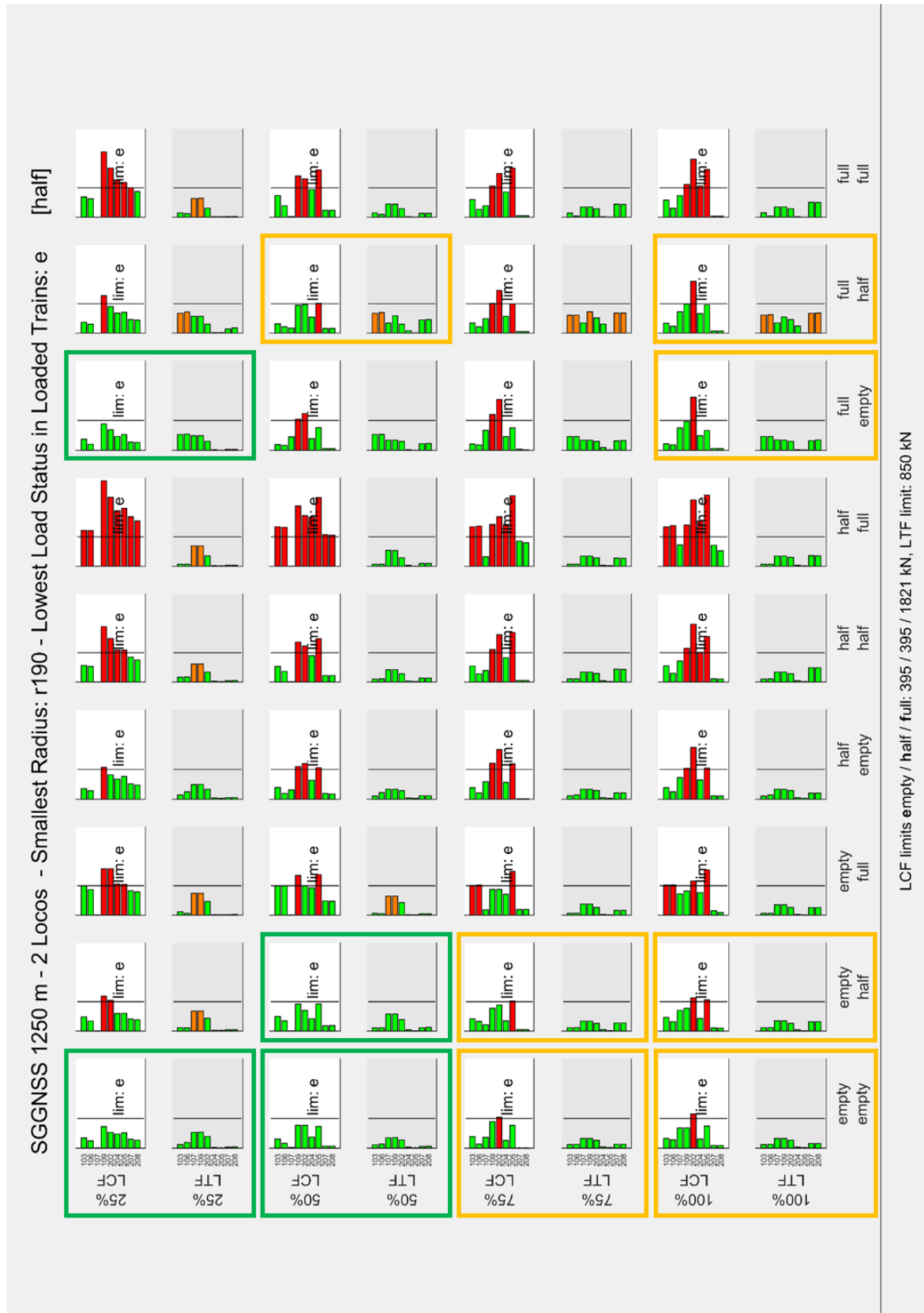


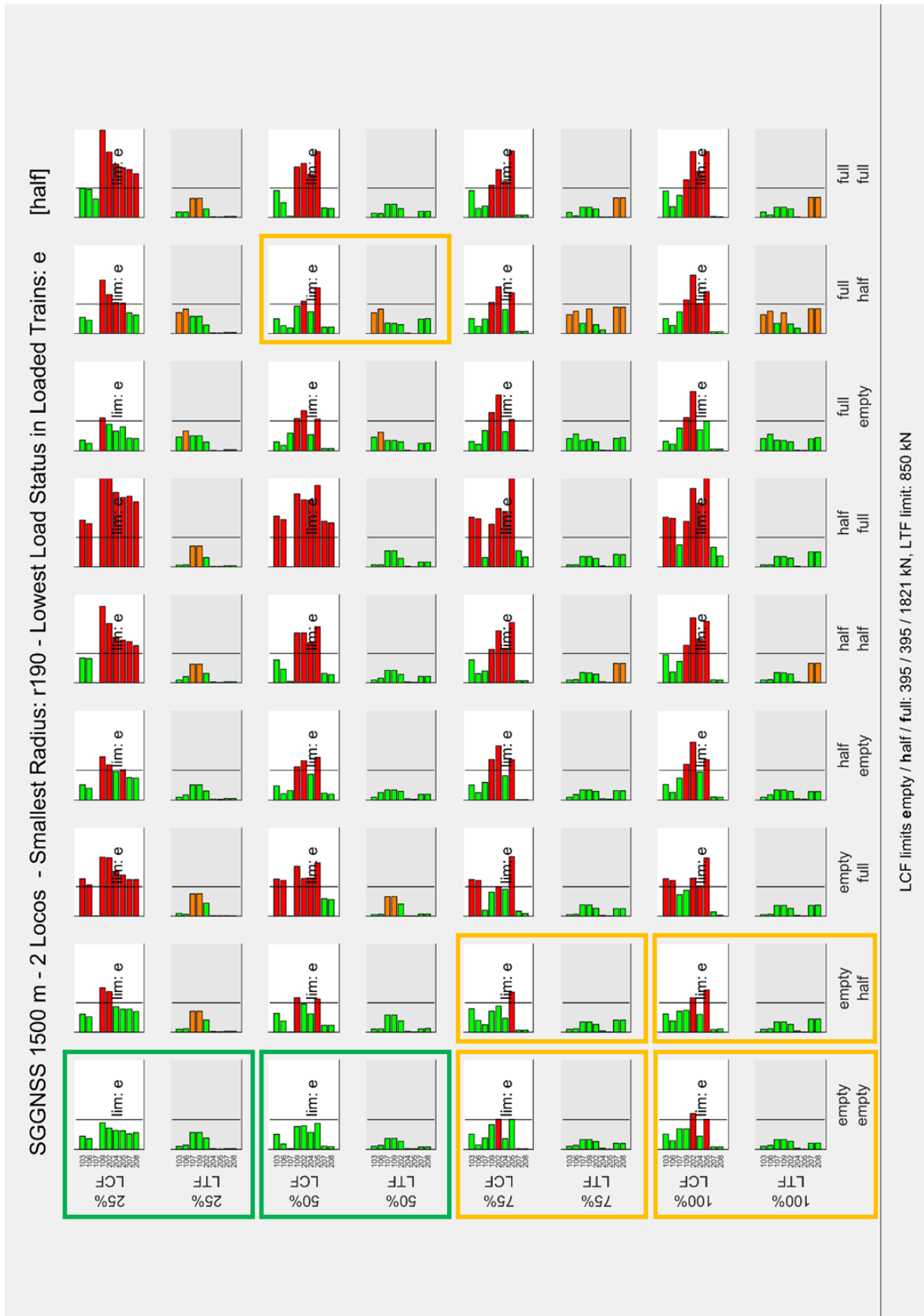


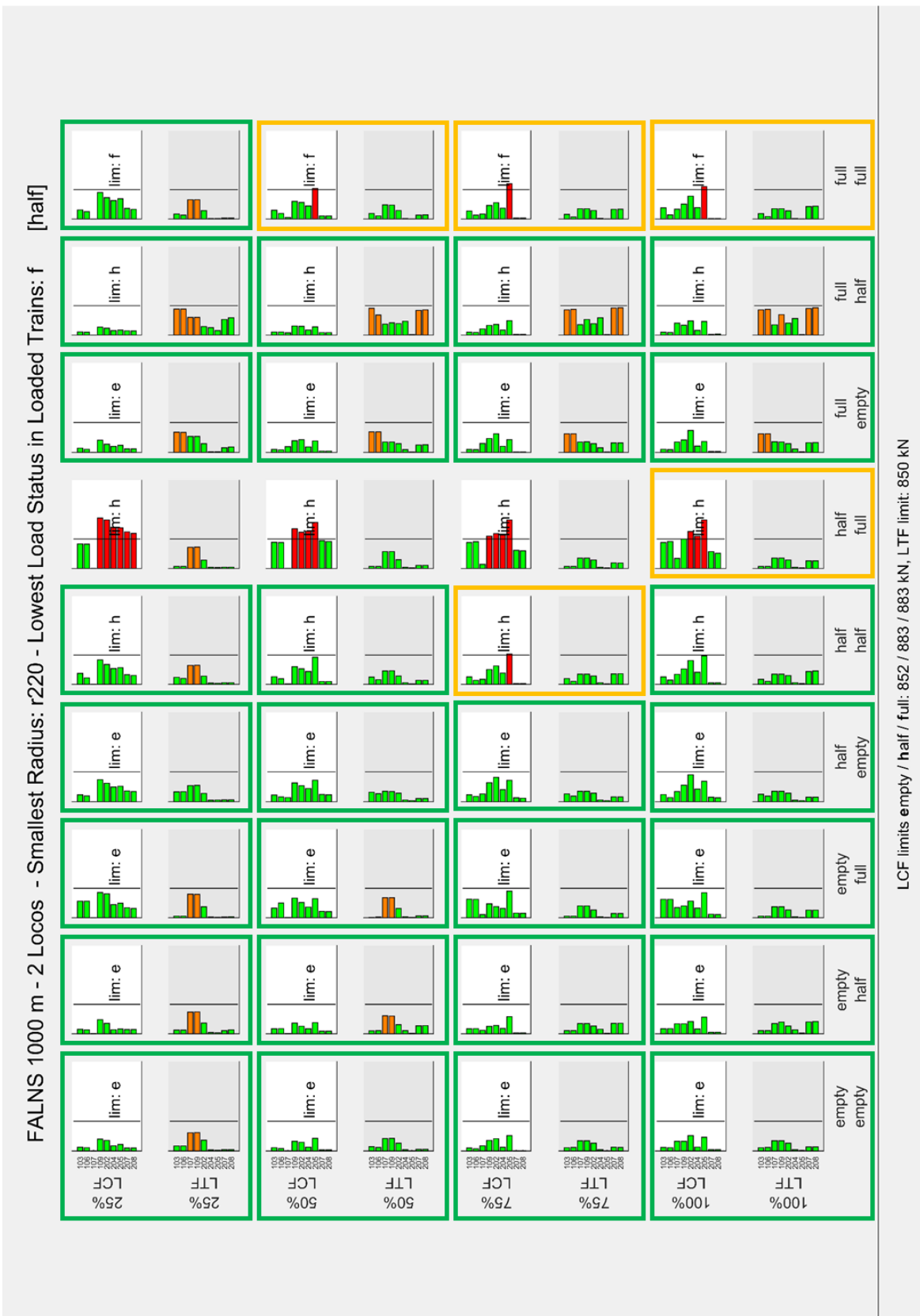


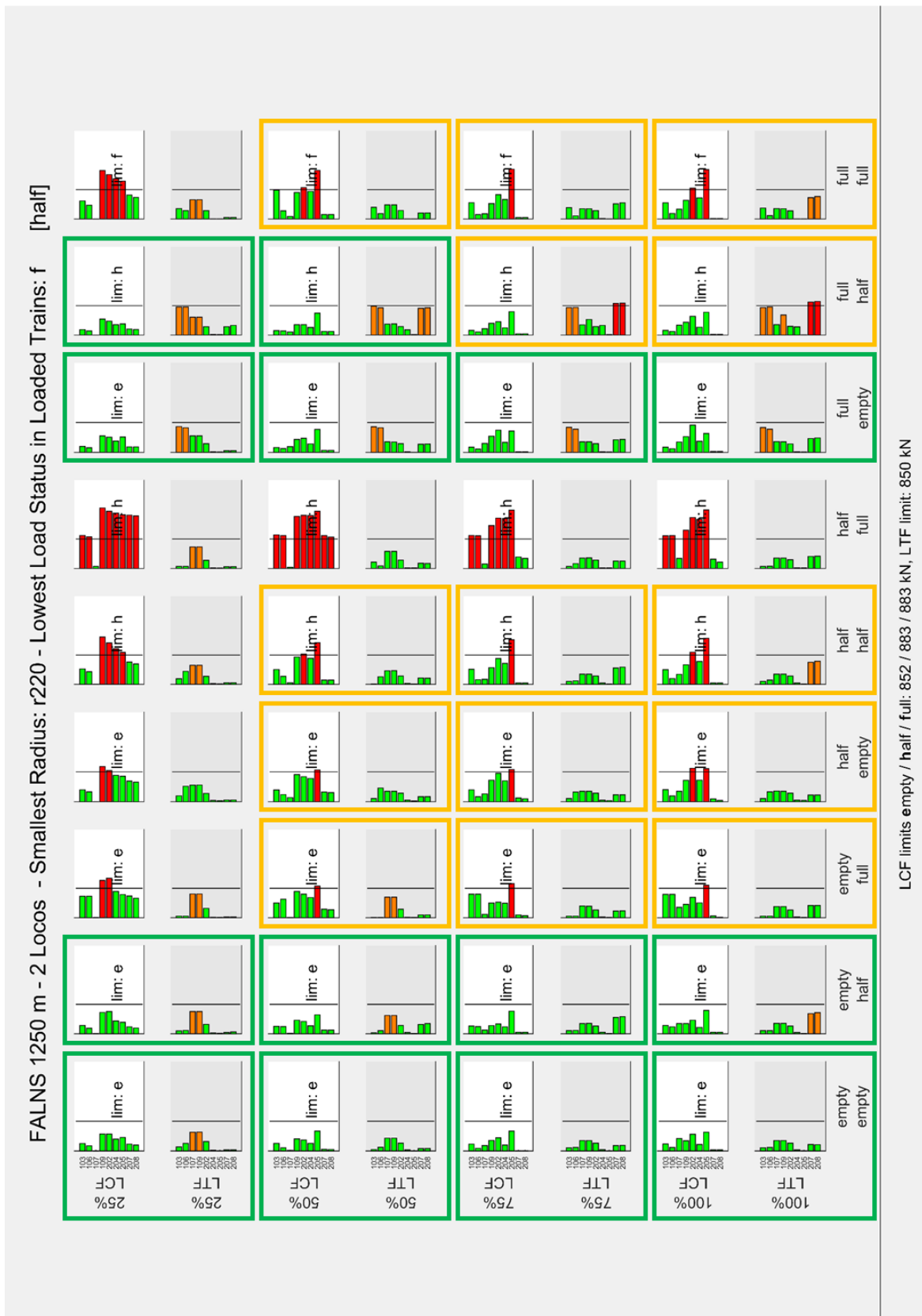












LCF limits empty / half / full: 852 / 883 / 883 kN, LTF limit: 850 kN

